Assessing Platelet RNA as a Potential Biomarker for Prostate Cancer Detection

Submitted in partial fulfilment of the requirements of the Degree of Doctor of Philosophy

Xueke Wang

Primary Supervisor: Yongjie Lu

Secondary Supervisor: Gunnel Hallden

Queen Mary University of London,
London, United Kingdom

Statement of Originality

I, Xueke Wang, confirm that the research included within this thesis is my own work or that where it has been carried out in collaboration with, or supported by others, that this is duly acknowledged below and my contribution indicated.

I attest that I have exercised reasonable care to ensure that the work is original and does not to the best of my knowledge break any UK law, infringe any third party's copyright or other Intellectual Property Right, or contain any confidential material.

Miss Edwina Burke, Dr Tianyu Guo, Xueying Mao, Elzbieta Stankiewicz Rachel Lawrence, Caitlin Rachel Davies, Alistar Grey, Karen Tipples and Tarek Al-Hammouri and Professor Greg Shaw provided invaluable assistance in collecting and processing a significant proportion of the clinical samples used in this study. Dr Jiaying Lu aided in the extraction of platelet RNA, while Dr Tianyu Guo contributed to the first Fluidigm of 68 PCa and 27 non-Ca patients. Dr Xueying Mao, Elzbieta Stankiewicz, and Miss Edwina Burke carried out all the immunofluorescence staining of CTC samples, and Dr Glenda Scandura, Ms Sakunthala Kudahetti and Professor Daniel Berney facilitated the collection of clinical information for recruited patients. Dr Jiayu Gu and Professor Ninghan Feng conducted

the Chinese sample collection and provided the small RNA sequencing data. Professor Lili Jiang facilitated the modification of platelet collection. Dr Wai Yiu Tse helped the revision of the thesis draft. Lastly, Dr Faraz Khan provided indispensable assistance in performing bioinformatics analysis of the mRNA sequencing data.

I accept that the College has the right to use plagiarism detection software to check the electronic version of the thesis.

I confirm that this thesis has not been previously submitted for the award of a degree by this or any other university. The copyright of this thesis rests with the author and no quotation from it or information derived from it may be published without the prior written consent of the author.

Xueke Wang

Date: 27/09/2023

Covid 19 Impact Statement

The completion of this project was notably impacted and delayed by the unforeseen circumstances of the COVID-19 pandemic. The first lockdown in the UK (from March 18th, 2020, to June 26th, 2020) prevented access to laboratory facilities and the oncology clinic at Barts Hospital. This interruption significantly hindered the collection of new samples and data during the second year of my PhD studies. Upon resuming work at Barts Cancer Institute on June 29th, 2020, new operational protocols were introduced due to the ongoing pandemic. We adopted rotational shifts of four hours per day, which considerably limited my ability to generate data. Not until March 30th 2021 was I was permitted full-day access to the laboratory. As the result, certain experiments could not be performed due to the time limitation and social distancing.

Furthermore, the impact of clinical sample collection has been significant. The patient consenting rate experienced a substantial decline from the beginning of 2020, ceasing prior to the UK national lockdown. Although it reopened in the summer of 2021, the process was subject to numerous restrictions, and the recruitment numbers and rates never returned to pre-pandemic levels.

In summary, the COVID-19 pandemic has significantly affected the

progression and completion of this thesis and the research detailed within.

Acknowledgement

I would like to express my profound gratitude to my advisors, Prof. Yong-Jie Lu and Dr Gunnel Hallden, for allowing me to undertake my PhD studies. Their invaluable support and mentorship have been instrumental throughout the course of my academic journey.

I extend my thanks to our dedicated team members and all my esteemed colleagues (Professor Yongjie Lu, Dr Gunnel Hallden, Tianyu Guo, Xueying Mao, Elzbieta Stankiewicz, Rachel Lawrence, Caitlin Rachel Davies and Miss Edwina Burke) at Barts Cancer Institute. Their generosity in offering guidance and advice has been a pillar of support for my laboratory work and my life in the UK.

Lastly, a special acknowledgement goes to my wife, Yu-Ping Liu, my daughters, An-Sin Wang & Wen-Xin Wang, my parents, Mr Liu-Jun Wang & Ms Ming Zhang, my mother-in-law Lihsueh Rao, sister-in-law Yu-Hui Liu and other family members. The acknowledgment is also extended to my late father-in-law, Dai-Zhong Liu. Their unwavering support and encouragement have been my guiding light, and their faith in me is a constant source of motivation.

Abstract

Prostate cancer (PCa) is a major carcinoma among Western men. The current prostate-specific antigen (PSA) test has limited sensitivity and specificity, necessitating the exploration of alternative non-invasive diagnostic markers. Recent studies indicate platelet RNAs, particularly mRNA and microRNA (miRNA), might serve as potential PCa indicators, based on the premise that PCa alters platelet RNA expression.

An initial study on platelet miRNAs used small-RNA sequencing on samples from a Chinese cohort, followed by validation in a British cohort. Key findings revealed certain miRNAs, especially miR627 and miR22, displayed significant potential as diagnostic markers. Their combined detection yielded an area under the curve (AUC) value surpassing that of PSA. Including circulating tumour cell (CTC) data further improved diagnostic accuracy. For detecting clinically significant PCa, miR190 was the standout miRNA, potentially targeting the HMGA2 gene.

Platelet mRNA sequencing from a British cohort failed to reveal differential mRNA expression, which could be due to actual absence or technical issues. Concerns arose regarding white blood cell (WBC) contamination in platelet samples, potentially affecting RNA data. Evidence from DAPI nucleus staining and mRNA-seq data supported this suspicion. Only 25%

of the samples met purity standards for platelet RNA analysis. To address this, I introduced several modifications of the platelet collection.

The research suggests PCa might influence platelet RNAs, potentially positioning them as additions to a diagnostic panel alongside other biomarkers. However, this requires further exploration and methodological optimisation.

Abbreviations

ADT - Androgen deprivation therapy

AJCC - American Joint Committee on Cancer

APC - Antigen presenting cell

AR - Androgen receptor

AS - Active surveillance

ASR - Age-standardized rate

AUC - Area under the curve

BPH - Benign prostatic hyperplasia

bFGF - Basic fibroblast growth factor

cDNA - Complementary DNA

cfDNA - Cell-free DNA

CK - Cytokeratin

CRUK - Cancer Research UK

CTC - Circulating tumour cell

CT-PET - Computed tomography-positron emission tomography

DAPI - 4′,6-diamidino-2-phenylindole

DHT - Dihydrotestosterone

DLX1 - Distal-less homeobox 1

DRE - Digital rectal examination

EAU - European Association of Urology

EMT - Epithelial-to-mesenchymal transition

ERBT - External beam radiotherapy

EV - Extracellular vesicle

FDR - False discovery rate

HCC - Hepatocellular carcinoma

HMGA2 - High mobility group AT-hook 2

IFC - Integrated fluidic circuit

IGRT - Image-guided radiation therapy

IL-6 - Interleukin 6

IMRT - Intensity-modulated radiation therapy

ISUP - International Society of Urological Pathology

KIF2A - Kinesin family member 2A

LHRH - Luteinizing hormone releasing hormone

LNA - Locked nucleic acid

lncRNA - Long noncoding RNA

MiPS - Michigan prostate score

miRDB - MicroRNA database

MiRNA - MicroRNA

MMP - Matrix metalloproteinase

MRI - Magnetic resonance imaging

mRNA - Messenger RNA

NA - Not available

NF-κB - Nuclear factor kappa B

NK - Natural killer

OR - Odds ratio

PAGE - Polyacrylamide gel electrophoresis

PCA3 - Prostate cancer antigen 3

PCR - Polymerase chain reaction

PDGF - Platelet derived growth factor

PIN - Prostatic intraepithelial neoplasia

pri-miRNA - Primary microRNA

PRP - Platelet-rich plasma

pre-miRNA - Precursor microRNA

PSA - Prostate specific antigen

qRT-PCR - Quantitative reverse transcription polymerase chain reaction

RBC - Red blood cell

RIN - RNA integrity number

RISC - RNA-induced silencing complex

RNA - Ribonucleic acid

RNase - Ribonuclease

ROC - Receiver operating characteristic

RP - Radical prostatectomy

RPE - RNA purification elution

RT - Reverse transcription

SD - Standard deviation

SRT - Salvage radiotherapy

SSV4 - Switching mechanism at 5′ ends of RNA template V4

TGF-β - Transforming growth factor beta

TF - Tissue factor

TMPRSS2 - Transmembrane serine protease 2

TNM – Tumour node metastasis

TXA2 - Thromboxane A2

UICC - Union for International Cancer Control

UK - United Kingdom

UGS - Urogenital sinus

USPSTF - US Preventive Services Task Force

UTR - Untranslated region

VEGF - Vascular endothelial growth factor

VIM - Vimentin

vWF - von Willebrand factor

WBC - White blood cell

WHO - World Health Organization

Contents

List of Figures

List of Tables

Chapter I: Introduction and Aims

1. Anatomy and Development of the Prostate

1.1 Location and Structure

The prostate gland is a pyramid-shaped component of the male reproductive system, located below the bladder and in front of the rectum, surrounding the urethra [1]. It averages 15-20 g in weight. Histologically, it is divided into peripheral, transition, and central zones, where the peripheral zone is most prone to cancer [2] [3].

1.2 Prostate Formation and Growth

The prostate forms from the urogenital sinus (UGS) during the 10th to 12th weeks of fetal development, influenced by androgens [4, 5]. Postnatally, the gland grows gradually without significant enlargement after puberty, maintaining a stable size in adults. Prostatic diseases typically increase with age and reduced serum androgen levels [6].

2. Prostate Histology and Cancer: From Hormonal Influence to Disease Progression

2.1 Histology of Prostate

The prostate's histological structure includes a fibromuscular stroma

surrounding prostatic glands with ducts [7-9]. These glands produce secretions like PSA in response to 5-α-DHT, influencing various cell types including luminal, basal, and intermediate cells [10]. Luminal cells are primary secretory cells, basal cells support structure and are less dependent on androgens, and intermediate cells are a mix of the two [10].

2.2 Role of Hormones in Prostate Development

DHT, derived from testosterone via 5-alpha reductase, is crucial for prostate development, affecting tissue growth from embryonic stages to adult size [11]. This growth is tightly regulated until puberty, when increased testosterone and DHT levels cause significant enlargement [12].

2.3 Prostate Cancer Progression

The precise origin of PCa cells is still under investigation, with both stem and differentiated cells exhibiting tumorigenic potential [13]. Both luminal [14, 15] and basal [16, 17] phenotypes have been discovered in PCa. Intermediate cells, due to their similarity to PCa stem cells, are also speculated to be involved in neoplastic transformation [18, 19].

The malignant transformation of cells encompasses a progression from benign to malignant phenotypes. This process initiates with prostatic intraepithelial neoplasia (PIN), marked by luminal cell proliferation with dysplasia along the ducts. High-grade PIN, considered a precancerous

lesion, exhibits large, hyperchromatic nuclei with prominent nucleoli [20]. Subsequently, PIN progresses to localized prostate adenocarcinoma, which can evolve into invasive carcinoma upon the degradation of the basal cell layer and invasion through the basal lamina. Locally advanced prostate cancer can metastasise via the lymphatic and circulation system to distant organs such as the bones, liver, brain, and lungs. Bone metastasis is the most prevalent [7] [9].

3. Epidemiology

3.1 Global Prevalence of PCa

PCa is the second most commonly diagnosed cancer in men worldwide [21]. In 2020, about 1.4 million new cases were diagnosed worldwide [21]. In England, 41,201 new cases were identified out of 48,588 across the UK in 2017, according to Cancer Research UK's statistics.

An autopsy study-based systematic review reported a 5% prevalence of PCa in men under the age of 30, increasing to 59% in men over the age of 79, with an odds ratio (OR) of 1.7 (1.6–1.8) per decade [22]. These figures correspond with CRUK data, indicating that 35% of diagnoses were in individuals aged 75 and over, compared to a mere 2% in those under 50 years, between 2015 and 2017 (Cancer Research UK https://www.cancerresearchuk.org/ Accessed [09][2023]).

3.2 Geographical Variations in PCa Incidence

Geographical differences in PCa incidence are stark. The highest age-standardised rates (ASRs) per 100,000 are found in Australia, New Zealand and Northern America, standing at 111.6 and 97.2 respectively, whereas Eastern and South-Central Asia report the lowest rates, with ASRs of 10.5 and 4.5 [23]. Discrepancies are also observed within Europe, with Western and Northern regions having higher ASRs (94.9 and 85 respectively) than Eastern and Southern regions (34.0 and 35.9 respectively) [24]. The low ASRs was explained to be associated to a diet high in antioxidants from grains, vegetables, olive oil, and etc. [25].

3.3 Racial Disparities in PCa Diagnosis

Racial disparities also exist in PCa incidence rates. Asian men, particularly those from China, Japan, and India, exhibit the lowest rates [31]. In contrast, African men are most affected, displaying a risk three times higher than Caucasian men [24]. In fact, one in four African men are likely to develop PCa at some point in their lives [26]. Moreover, African American men are often diagnosed with more advanced diseases and have poorer prognoses compared to white men [27]. Potential reasons behind these disparities, such as genetic predisposition should be considered [27-30]. Interestingly, as Japanese men who have a lower risk

of PCa moved to California where there was a higher PCa incidence rate, those Japanese risks of PCa were found higher, close to the figure of local American men [31]. This study implied the role of environmental or dietary factors in PCa development [32, 33].

4. Aetiology

4.1 Germline mutations

Studies have reported an association between various genetic mutations and the risk of developing PCa. For example, genome-wide association studies have identified more than 200 susceptibility loci that contribute to PCa risk [34-37]. Furthermore, clinical cohort studies have indicated that 15% to 17% of germline mutations exist in PCa [38, 39].

Among numerous findings which have reported germline mutations associated with PCa, breast cancer gene family (BRCA family of BRCA1 and BRCA2) has shown its importance in the development and progression of PCa. PCa with germline BRCA1/2 mutations more frequently exhibited aggressive features compared to non-carriers [40]. Another study reported that men with BRCA1 and BRCA2 mutations had a significantly higher incidence of malignant disease, and the rate of PCa among BRCA1 carriers was more than twice as high compared to the general population [41]. Furthermore, the combined BRCA1/2 and ATM

mutation carrier rate was significantly higher in lethal PCa patients (6.07%) than in localized PCa patients (1.44%) [42].

More interest has been taken in BRCA2, mutations in which have been found to be associated with aggressive PCa [43]. Similarly, another study demonstrated that BRCA2 mutation carriers had a higher incidence of PCa, a younger age at diagnosis, and more clinically significant tumours compared with non-carriers [44].

4.2 Role of Hormones in the Aetiology of PCa

Androgens, including both testosterone and DHT, are believed to play a role in the development of prostate cancer. Prostate cells continue to be sensitive to androgens throughout life, and it is thought that androgens may promote the growth of cancerous cells in the prostate [45].

Research has suggested that high levels of androgens may increase the risk of prostate cancer, but the relationship is complex [12]. Once prostate cancer has developed, it is often initially sensitive to androgens, and one common treatment approach is to reduce androgen levels or block their activity, a treatment known as androgen deprivation therapy [46].

On a genetic level, mutations or alterations in the androgen receptor gene have been implicated in the progression of prostate cancer, mainly after hormone therapy [47, 48]. Some prostate cancer patients have been

found to have increased expression of AR transcripts that activate AR-target genes, potentially promoting the growth of cancer cells [49].

4.3 Risk factors

There are a large number of exogenous/environmental factors which may be related to the risk of developing PCa. Hypertension, waist circumference, and metabolic syndrome were reported to be associated with a greater risk of PCa [50, 51]. Interestingly, obesity was shown to be affiliated with lower risk of low-grade PCa, but higher risk of high-grade cancer which might be due to the environmental determinants [52, 53]. Regarding dietary factors, a dose-response relationship between alcohol intake and PCa was published [54]. Coffee was shown to reduce the risk of PCa [55], and a similar association was found with soy products (phytoestrogens) [56].

5. Early Detection of Cancer and Diagnostic Evaluation of Prostate Cancer

In many scientific and medical contexts, the term “cancer early detection” refers to the discovery of cancer before the manifestation of symptoms and progression of the disease. Screening refers to the administration of simple tests across a healthy population to identify individuals who,

although asymptomatic, may have the disease. The primary goal of screening is to detect the disease at an early stage, where treatment is most effective. However, the balance of benefits and potential harm from screening is a critical consideration [57]. Therefore, cancer early detection may enhance the likelihood of successful treatment (before the tumour has spread), lowering morbidity and improving survival [58].

The conventional diagnostic pathway for PCa Involves checking for abnormal PSA levels and/or conducting a digital rectal examination (DRE) [59]. If these tests suggest abnormalities, a random systematic transrectal ultrasound-guided prostate biopsy (TRUS) may follow [60]. However, the reliability of standard TRUS is questionable [61], and additional biopsies of hypoechoic lesions have limited diagnostic value [62]. Reports showed that using MRI led to more diagnoses of clinically significant cancers, without increasing biopsy recommendations or overdiagnosing insignificant cancers [63, 64]. Therefore, according to the European Association of Urology (EAU) guidelines, an MRI scan, noted for its high sensitivity in detecting aggressive PCa, is recommended before performing a biopsy [65, 66].

6. Classification and Staging of Prostate Cancer

6.1 Gleason Score and International Society of Urological Pathology 2014

Grade

In PCa, the Gleason grading system, a classic histopathological tool, differentiates between indolent and aggressive forms of PCa based on comparative tissue architecture. In the original system, the Gleason score (GS) ranges from 1 to 5, with a higher score indicating greater abnormality in the tissue [67]. The International Society of Urological Pathology (ISUP) modified the GS in 2005, which now includes the Gleason grade of the most extensive (primary) pattern, plus the second most common (secondary) pattern [68]. Clinically, pathologists rarely assign scores of 2-5. In 2014, GS grades 1 and 2 were eliminated from ISUP [68, 69]. Hence, Gleason scores range from 6 to 10, with a score of 6 as the lowest grade of cancer (**Table 1**) [69]. Cancer with a higher GS is more aggressive, suggesting a worse prognosis [70].

Table 1. International Society of Urological Pathology 2014 grade (group) system [69]**.**

Gleason score	ISUP grade
≤6	1
7 (3+4)	2
7 (4+3)	3
8 (4+4 or 3+5 or 5+3)	4
9-10	5

ISUP: international society of urological pathology.

6.2 Clinical Tumour Node Metastasis (TNM) classification and EAU Risk Group Classification of PCa

The aim of a tumour classification system is to group patients with similar prognoses. The TNM system, provided by the American Joint Commission on Cancer (AJCC) and the Union for International Cancer Control (UICC), serves this purpose (**Table 2**) [71]. Classification systems like the TNM has been used to stratify patients in clinical trials.

Table 2. Definitions of American Joint Committee on PCa TNM criteria.

Clinical (cT)		
T category	TX	Primary tumour cannot be assessed
	T0	No evidence of primary tumour
	T1	Clinically inapparent tumour that is not palpable
	T1a	Tumour incidental histologic finding in 5% or less of tissue resected
	T1b	Tumour incidental histologic finding in more than 5% of tissue resected
	T1c	Tumour identified by needle biopsy found in one or both sides, but not palpable
	T2	Tumour is palpable and confined within prostate
	T2a	Tumour involves one-half of one side or less
	T2b	Tumour involves more than one-half of one side but not both sides
	T2c	Tumour involves both sides
	T3	Extraprostatic tumour that is not fixed or does not invade adjacent structures
	T3a	Extraprostatic extension (unilateral or bilateral)
	T3b	Tumour invades seminal vesicle(s)
	T4	Tumour is fixed or invades adjacent structures other than seminal vesicles, such as external sphincter, rectum, bladder, levator muscles, and/or pelvic wall
Pathologic (pT)		
T category	T2	Organ confined
	T3	Extraprostatic extension
	T3a	Extraprostatic extension (unilateral or bilateral) or microscopic invasion of bladder neck
	T3b	Tumour invades seminal vesicle(s)
	T4	Tumour is fixed or invades adjacent structures other than seminal vesicles, such as external sphincter, rectum, bladder, levator muscles, and/or pelvic wall
N category	NX	Regional lymph nodes were not assessed
	N0	No positive regional lymph nodes
	N1	Metastases in regional lymph node(s)
M category	M0	No distant metastasis
	M1	Distant metastasis
	M1a	Non-regional lymph node(s)
	M1b	Bone(s)
	M1c	Other site(s) with or without bone disease

T: tumour, cT: clinical tumour, pT: pathologic tumour, N: lymph node, M: metastasis (*Adapted from [71]*)

The EAU risk group classification system is designed to categorise patients with localised PCa who have a similar risk of biochemical recurrence after receiving treatment like radical prostatectomy and external beam radiotherapy [72]. While categorizing the risk groups,

factors like PSA, Gleason score, International Society for urological pathology grade system (ISUP), and TNM criteria are taken into account in each risk group (**Table 3**).

Table 3. Risk stratification for biochemical recurrence of localised and locally advanced PCa.

Definition			
Low-risk	**Intermediate-risk**	**High-risk**	
PSA < 10 ng/mL and GS < 7 (ISUP grade 1) and cT1-2a	PSA 10-20 ng/mL or GS 7 (ISUP grade 2/3) or cT2b	PSA > 20 ng/mL or GS > 7 (ISUP grade 4/5) or cT2c	any PSA any GS (any ISUP grade) cT3-4 or cN+
Localised			**Locally advanced**

GS = Gleason score; ISUP = International Society for Urological Pathology; PSA = prostate-specific antigen.

(Adapted from [73].)

6.3 Clinically Significant PCa

The term 'clinically significant' prostate cancer primarily differentiates between PCa that may cause morbidity or mortality and 'insignificant' PCa that might not cause harm but could potentially lead to overtreatment [22], a major drawback of PSA screening [73]. The clinical focus is now shifting to accurately detecting clinically significant PCa in order to reduce overdiagnosis [74].

In contrast to easier identification of ISUP grade 1 as ‘insignificant’ because of its rare extraprostatic extension and seminal vesicle invasion [75, 76], the definition of ‘clinically significant’ remains controversial. The previous systems classifies Gleason score 7 as intermediate-risk PCa without distinguishing between Gleason 3+4 and 4+3 [69]. Furthermore, studies have used varying definitions, such as ISUP grade 2 (Gleason 3+4) and above or ISUP grade 3 (Gleason 4+3) and above, underscoring the

lack of a universally accepted definition [62, 77-79].

Recent data shows that PCa with ISUP grade 2 is often undetected during a man's lifetime [80] or upgraded [81]. Reports showed that the outcomes of ISUP grade 2 may be closer to ISUP grade 1 concerning cause-specific survival and early metastasis development [82, 83]. Hence, diagnosis of ISUP grade 2 could potentially lead to overtreatment.

According to the EAU's recent guidelines, ISUP grade 3 has a close association with poor prognosis, while patients with ISUP grade 2 (Gleason 3+4) tend to have a good prognosis with less metastasis. Therefore, this project will consider 'clinically significant' PCa as ISUP grade 3 (Gleason 4+3), and above in the biomarker study, to better group patients with poor prognosis. Detecting patients with ‘clinically significant’ PCa becomes another aim in my study.

7. Treatments of Prostate Cancer

7.1 Treatment of Low-risk disease

Active Surveillance (AS) involves regular monitoring without immediate treatment, suitable for low-risk cancers unlikely to spread. MRI is key for identifying aggressive cancers in this group [84, 85]. Changes in PSA levels during AS warrant a repeat MRI and biopsy before initiating active

treatment [86].

7.2 Treatments of Intermediate-risk PCa

Treatments include Radical Prostatectomy (RP) [87, 88] and radiotherapy, possibly combined with ADT, offering improved survival and disease control. Low-volume intermediate-risk patients might qualify for AS, with treatment adjustments based on biopsy results [86].

7.3 Treatments of Non-metastatic, High-risk PCa

Recommended treatments include RP [89-91] with lymph node dissection [92, 93], followed by radiotherapy or ADT [94-96]. Other options involve advanced radiotherapy techniques combined with long-term ADT [97-101].

7.4 Treatments of Metastatic PCa

Treatment primarily consists of ADT, with CT and bone scans for diagnosis [102]. It's often combined with systemic therapies like docetaxel for symptom management and complication reduction [103, 104].

In terms of ‘volume of disease’ – referring to the amount or size of diseased tissue or lesions within a patient – it’s an important factor in treatment planning. In the CHAARTED (Chemo-hormonal Therapy versus Androgen Ablation Randomized Trial for Extensive Disease in Prostate Cancer) trial, ‘volume’ of PCa has proven to be a valuable predictor of

treatment benefits (**Table 4**) [105-108]. For patients with low-volume PCa according to CHARRTED criteria, ADT with prostate radiotherapy (RT) is recommended by the STAMPEDE study [108].

In summary, the clinical focus of prostate cancer treatment primarily centers on part of intermediate (ISUP>2) and higher-risk diseases, leaving room for further research in the field of cancer detection.

Table 4. Definition of high- and low-volume risk in CHAARTED.

High	Low
>4 Bone metastasis including >1 outside vertebral column or pelvis OR Visceral metastasis	Not high

8. Biomarkers for Prostate Cancer diagnosis

8.1 Introduction of Biomarkers

A biomarker is a biological molecule found in blood, other body fluids, or tissues that serves as an indicator of a normal or abnormal process, disease, or condition [109]. A biomarker is defined as “a characteristic that is objectively measured and evaluated as an indicator of normal biologic processes, pathogenic processes or pharmacologic responses to a therapeutic intervention” by the official National Institutes of Health in 2001. This definition encompasses the clinical applications of diagnostic biomarkers, including their role in population screening and disease diagnosis.

Biomarkers can be derived from various sources and have different components, such as proteins, nucleic acids, gene expressions, antibodies, peptides, or certain cell types such as circulating tumour cells (CTCs) [109]. The presence of biomarkers in locations like the circulation,

excretions, or secretions makes them accessible through non-invasive methods, leading particular interest to the concept of "liquid biopsies" [109].

Currently, various cancer biomarkers are endorsed for clinical application, predominantly for monitoring treatment responses in advanced disease stages, rather than for initial cancer detection [109]. However, screening guidelines for many disorders are debated and change over time, with tests often misaligned with evidence, significant shifts in detection criteria and disease definitions, and changes by health organizations [110].

There also might be a disparity in how therapeutics and diagnostic biomarkers are perceived. Treatments offering slight enhancements in survival are often viewed as 'successful.' In contrast, diagnostic biomarkers offering similar advancements in disease detection or prognosis might be deemed 'failures.'

For a diagnostic biomarker to be genuinely effective, it should excel in both sensitivity and specificity. A commendable positive predictive value of over 10% mandates both a high sensitivity (>80%) for early and asymptomatic disease detection and an unparalleled specificity (⩾99.5%) [111]. Yet, balancing sensitivity and specificity is crucial in real-world applications. A biomarker is a biological molecule found in blood, other

body fluids, or tissues that serves as an indicator of a normal or abnormal process, disease, or condition [109].

8.2 Psychological Impact on Patients Who Receive an Early Cancer Diagnosis

The psychological impact on patients is a considerable concern. Early detection can undoubtedly be beneficial in terms of improving treatment outcomes, but it can also lead to stress and anxiety, particularly if a patient is identified as high-risk but does not yet have a definitive cancer diagnosis. This "waiting game" can have a significant psychological toll [112].

For patients who do receive a cancer diagnosis, the information that these tests provide about their prognosis may also have significant psychological effects. Some patients may prefer not to know this information, while others may want to use it to inform their treatment decisions and plan for their future. Moreover, potential false-positive or false-negative results can lead to undue stress or a false sense of security, respectively. This uncertainty underscores the importance of further improving the accuracy and reliability of these early detection methods. To improve the predictive value of the discovered biomarkers, in this study, I conducted additional trials aimed at combining different biomarker

candidates.

8.3 Prostate Specific Antigen (PSA)

8.3.1 Origin of PSA

PSA, a serine protease produced by the prostate epithelia, primarily functions in semen gel dissolution by proteolyzing the major gel-forming proteins such as semenogelin I, semenogelin II, and fibronectin [113]. Though typically present in low levels in the blood, PSA concentrations can rise in the presence of PCa [113]. However, elevated PSA levels are not solely indicative of cancer and may also result from benign prostatic hypertrophy (BPH), prostatitis, or other non-malignant conditions Interestingly, studies have identified PSA expression in breast cancer [114]. This phenomenon might be partly attributed to the shared expression of BROCA-2 in both cancers, which are hormonally influenced [115].

8.3.2 PSA Testing: Specificity, Sensitivity, and Implications

Based on a recent meta-analysis, at the cutoff of 4ng/ml, PSA provides a sensitivity of 92% and a specificity of 16% [116]. Here, the specificity refers to PSA ability to correctly identify those without PCa (true negative rate). Low specificity means that PSA incorrectly identifies many individuals as having PCa when they do not, leading to false positive results. PSA has

low specificity because PSA is not tumour-specific and the PSA level can be elevated due to some non-malignant reasons, such as benign prostatic hypertrophy (BPH), prostatitis, urinary tract infection and ejaculation [117, 118]. Consequently, the low specificity of the test can lead to unnecessary and invasive tissue biopsies in individuals without cancer [119, 120]. Despite its lack of specificity, PSA testing revolutionized PCa diagnosis [121] and led to decreases in mortality according to American national screening results [122]. The utility of PSA testing has been confirmed by studies such as European Randomized Study of Screening for PCa, which reported modest PCa survival benefits from PSA testing [123].

8.3.3 Controversies Surrounding PSA Testing: Overdiagnosis, Overtreatment and Detection Limitations

However, the controversy surrounding PSA testing stems from concerns of overdiagnosis and overtreatment due to the limitation of PSA in differentiating aggressive PCa from indolent tumour [124]. It has been found that over half of the patients diagnosed with early-stage PCa via PSA testing have an indolent form of the disease, suggesting that these patients may not die of cancer even without treatment [73]. When a potentially non-harmful (indolent) tumour is detected (overdiagnosis), it might then lead to unnecessary treatments (overtreatment). Several trials

found no significant differences in mortality rates between PSA screened and unscreened groups [125, 126]. Therefore, the risks and harms associated with PSA testing led to initial recommendations against PSA-based screening by the US Preventive Services Task Force (USPSTF) [73] and AUA guidelines [127]. However, this stance has been contested by clinicians, citing increased diagnoses of advanced PCa in the absence of PSA screening [128-131] and gradual increases in PCa-related mortality [132]. Additionally, a 16-year randomised trial in Europe also found the value of PSA in reducing PCa associated mortality [133].

Given these conflicting data, it is clear that while systemic screening may not be ideal, there is a growing need for individualised early detection strategies for PCa. Thus, PSA testing has been re-evaluated and upgraded from a grade ‘D’ (Discourage the use of this service.)[134] to a grade 'C' (Offer or provide this service for selected patients depending on individual circumstances.) [135, 136] recommendation, implying that PSA testing should be individualised [135]. As such, the EAU’s guidelines continue to list PSA as a crucial biomarker for PCa detection.

In summary, while PSA remains a valuable tool in PCa detection, its limitations underscore the need for the development of more accurate diagnostic tools. Further research on refining existing biomarkers and or

exploring novel ones to enhance early detection is needed to reduce overdiagnosis and overtreatment of PCa.

8.4 Alternative Biomarkers for PCa Detection

Given the limitations of PSA screening, several other biomarkers have been developed to improve diagnostic accuracy. Blood-based biomarkers such as the Prostate Health Index (PHI) (free, total PSA, and the pro-PSA isoform) and the four kallikreins (4K) (free, intact, total PSA and kallikrein-like peptidase with age, DRE and prior biopsy status) score have been reported to improve the prediction of clinically significant PCa in patients with PSA levels ranging from 2 to 10 ng/ml [137-139].

In the field of urinary biomarkers, prostate cancer gene 3 (*PCA3*), a long non-coding RNA (lncRNA), has shown promise in detecting PCa in men with elevated PSA levels [26, 140, 141], although its ability to independently detect ISUP grade remains uncertain [142]. Combination tests such as the Michigan Prostate Score (MiPS), which uses *PCA3*, serum PSA, and the *TMPRSS2-ERG* fusion gene [143], have been developed to improve detection [144]. The SelectMDX test, which measures *HOXC6* and *DLX1* mRNA levels, has also shown efficacy in detecting high-risk PCa [145] and reducing unnecessary biopsies [146].

Emerging techniques such as the use of exosomes released from cancer

cells (ExoDx prostate intelliscore) have also shown promise in reducing unnecessary biopsies [147]. However, further validation is necessary to confirm the efficacy of these newer markers [148].

In the future, the role of artificial intelligence and machine learning in predicting cancer based on biomarkers could provide an interesting angle [149]. In particular, these technologies can be used to analyse a vast array of biomarkers and clinical data to create predictive models for PCa, improving the accuracy of diagnosis [150, 151].

9. Emerging Circulating Biomarkers in Liquid Biopsies for Cancer Detection

Having reviewed common biomarkers like PSA and PSA-based biomarker panels in PCa detection, I next examined other biomarkers, which aim to address some of the challenges around early cancer detection.

In clinical practice, when the patient is suspected has cancer, the next step typically involves a tissue biopsy to confirm the diagnosis. However, tissue biopsy has several limitations. For instance, the procedure is invasive and often requires surgical involvement, limiting its applicability. Patients undergoing long-term treatments face not only the physical burden of repeated biopsies but also mental stress and an increased risk

of complications. In the case of PCa, these may include bleeding, infections, and even sepsis [152]. Additionally, due to intra-tumour heterogeneity, spatial variations can result in incomplete or inaccurate biopsy results when only a limited number of procedures are performed [153-155]. Finally, inaccessible or multiple cancer sites can further complicate biopsy results.

An alternative to tissue biopsy is liquid biopsy, which is less invasive and less costly. Liquid biopsies involve simple body fluid sampling, such as peripheral blood, and enable real-time and repeatable biomarker analysis. For cancer detection, blood is one of the most frequently used resources for biomarker analysis. This encompasses cell-free nucleic acid, circulating tumour cells (CTCs), exosomes, and platelets, all of which are either already in clinical use or being developed.

9.1 Cell-free Nucleic Acid

Cell-free DNAs (cfDNAs) are DNAs freely in peripheral blood, albeit at low concentrations [156]. cfDNAs include a majority of DNAs from normal cells and a minority from cancer cells, termed circulating tumour DNAs (ctDNAs) [157]. Their presence in plasma or serum was first detected in patients with nasopharyngeal cancer [158] and melanoma [159]. The US Food and Drug Administration (FDA) has approved several ctDNA-based diagnostic

tests to ensure the safe and efficacious application of targeted therapies [160]. One such test is the Cobas EGFR Mutation Test V.2, designed to detect EGFR exon 19 deletions or exon 21 L858R mutations. This test aids in selecting non-small cell lung cancer (NSCLC) patients for treatment with specific EGFR tyrosine kinase inhibitors. Another notable test is the therascreen PIK3CA RGQ PCR Kit, which identifies 11 PIK3CA mutations in ctDNA. This is used to guide the treatment of breast cancer patients with alpesilib [160].

First reported in the late 1980s, ctDNAs originate from malignant cells and enter the bloodstream via cell death processes such as necrosis and apoptosis [161]. Detectable in blood (serum or plasma), ctDNAs contain mutation information [162, 163], and are increasingly used as cancer biomarkers [164-167]. Currently, there is limited evidence supporting the clinical validity and utility of ctDNA assays in the context of early-stage cancer [168]. As for the value of tumour early detection, a prospective study on breast cancer showed that ctDNAs can detect mutant *PIK3CA* molecules preoperatively in early-stage (stage I–III) patients with a sensitivity of 93.3% and a specificity of 100% [169]. Regarding PCa, DNA methylation—a common early tumorigenesis event—can serve as a diagnostic marker [170, 171]. Different panels of DNA methylation

markers have been developed for early detection with high accuracies, such as the hypermethylation of *ST6GALNAC3* [172], *CCDC181* [172], and *HAPLN3* [172] and promoter methylation of *APC* [173], *FOXA1* [173], and *GSTP1* [173].

RNA analysis offers a “real-time” snapshot of which genes are being actively expressed at any given moment, helping to understand transcriptional activity. Although RNAs are conventionally much less stable [174-176]. MicroRNAs (miRNA) display better stability than messenger RNAs when exposed to RNase in circulation [177]. This stability is linked to either the miRNA structure [177] or its microparticle carriers in circulation [178, 179]. With this protection from degradation, extracellular vesicle-incorporated cell-free miRNA analysis has become a primary focus of circulating tumour RNA (ctRNA) research. The presence of circulating miRNA in cancer was first reported in 2008 [180], with elevated levels of miRNA-155, miRNA-210, and miR-21 found in patients with lymphoma [180]. Furthermore, Mitchell *et al*. reported that detection of tumor-deritumouriR141 could distinguish PCa patients from healthy controls [181]. Subsequent studies have linked other miRNAs to the presence of PCa, including the downregulation of miR-125b, miR-221/222, Let-7b, and the upregulation of miR-25 and miR-93 [182, 183].

Studying cell-free nucleic acid analysis is not without its challenges. The conditions of sample collection, such as plasma volume, storage temperature, and the time from blood collection to plasma isolation, can influence the results [184]. Moreover, different centrifugation protocols and purification methods may yield varied results. Extracellular vesicle-incorporated miRNAs have been reported to carry different information compared to peripheral cell-free miRNAs [185]. Furthermore, the short half-life of cfRNAs after clinical collection can negatively impact their concentration for analysis [186]. In early-stage cancers, the typically low level of mutant cfDNA presents a significant challenge for distinguishing it from non-cancerous cfDNA variants [160, 187]. Lastly, a limited number of standardized methods have gained widespread acceptance and application [188].

9.2 Circulating Tumour Cells

9.2.1 Definition

Circulating tumour cells (CTCs) were first reported in the blood of cancer patients by the Australian physician Thomas Ashworth in 1869 [189]. These are tumour cells that have escaped from primary tumours or metastases into the peripheral blood [190]. Unlike other biomarker sources, CTCs offer the unique possibility of examining live cancer cells

[191].

As tumour cells proliferate and invade surrounding tissues, they release matrix metalloproteinases to degrade the basement membrane, allowing them to migrate via blood or lymphatic vessels to distant locations [192]. Once there, they can adapt to the new microenvironment and establish new colonies, a process known as metastasis [192].

Epithelial-to-mesenchymal transition (EMT) is critical for this process. Before becoming CTCs, tumour cells can down-regulate epithelial markers such as E-cadherin and Cytokeratin (CK), while up-regulating mesenchymal markers like N-cadherin and Vimentin (VIM) [193]. This transition enhances the cells' ability to detach from the initial tumour invade the bloodstream, boosting their metastatic potential and survival [194]. Alternatively, CTCs can infiltrate passively without undergoing EMT transition due to mechanisms such as centrosome amplification-triggered invasion or external forces [195], retaining their epithelial phenotype [196].

CTCs can also form clusters with fibroblasts, leukocytes, endothelial cells, or platelets and other CTCs, which potentially enhance their metastatic potential and survival compared to individual CTCs [197]. As a heterogeneous population, CTC clusters may provide new insights into tumour heterogeneity [198].

9.2.2 Landmark Studies and Clinical Significance of CTCs

In 2004, a landmark study titled "Circulating tumour cells, disease progression, and survival in metastatic breast cancer" represented a major advancement in the field of CTCs [199]. The study demonstrated that the number of CTCs could predict progression-free survival and overall survival in patients with metastatic breast cancer. It opened the door for extensive research into the utility of CTCs as a marker in various cancers [199]. The FDA approved the Parsortix system for clinical use to forecast the prognosis of advanced breast [200], and colorectal cancer [201], while CellSearch was approved by the FDA in predicting the outcomes of metastatic breast cancer [202] and metastatic castration-resistant PCa [203].

Most studies have focused on CTC's value as a reliable biomarker for treatment response and prognosis in advanced cancer patients [204, 205]. Whether CTCs could be used as a diagnostic marker remains under investigation.

In a mouse model, CTCs were found in the early stage of breast cancer [206, 207]. In a 130-patient study of breast cancer from Tis to T1-4 stages, Jin *et al* reported CTC detection rates were 50% (Tis), 81.67% (T1), 91.07% (T2), 100% (T3), and 100% (T4) respectively [208]. In lung cancer, 3% of

patients with chronic obstructive pulmonary disease had positive CTC results. The follow-up showed that all CTC-positive patients were found to develop lung cancers within four years [209]. In non-small cell lung cancer, 49% and 48% of patients in pTNM stage I and II respectively had positive CTC findings [210]. In colorectal cancer, a single medical center reported a CTC accuracy of 88% for all stages of cancer in 620 patients [211]. This study team also found a similar result in 667 patients with a specificity of 86% and AUC of 0.940 for colorectal cancer detection [212]. Another study based on 88 cases showed that CTCs could detect colorectal cancer with a sensitivity of 75% sensitivity and a specificity of 100% [213]. However, these results were from a single centre which may need further validation by other independent centers. In hepatocellular carcinoma, a cut-off value of mesenchymal CTCs ≥ 1 was reported as meaningful for detecting late-stage cases [214]. In pancreatic cancer, EMT-mediated CTC invasion was found at an early stage before clear malignancy was confirmed by histology [215]. Additionally, mesenchymal CTCs were observed in 76% of patients with pancreatic cancer from a 100-case study [216].

Traditional clinical imaging can only detect tumours comprised of over 10^9 cells [217]. Thus, for the aggressive subtypes of a cancer, early diagnosis becomes crucial**.** Whether metastatic dissemination of CTCs appears

early or not during tumour development is also in debatable, the discovery of CTCs has been reported in patients with solid tumours before the identification of distant metastasis [218-221], implying its potential for identifying aggressive cancer types. From the above findings in different cancers, CTCs demonstrated to be more promising in identifying the aggressive types of different cancers at early stage.

Regarding PCa, CTCs have also shown its potential of early detection. A study from our research team showed that, in asymptomatic PCa patients with a family history of cancer or advanced age (>50 years), positive CTC counts (0.2-50 CTC/ml) were reported in half of the total patients [222]. Regarding clinically significant PCa, the AUC of clinically significant PCa prediction was 0.927 with the combination of CTCs, PSA, and a CTC gene panels, showing the value of CTCs in detecting this cancer type [223]. However, other studies using different CTC isolation methods have cast doubt on the diagnostic performance of CTCs in early cancer detection [224]. CTC was reported an accuracy of 53.2% with a sensitivity of 40.0% [225]. A study of 50 patients with clinically localized prostate cancer revealed a 50% positive rate for CTC, but no correlation with other factors such as PSA, TNM, and Gleason classifications [226]. In summary, the value of CTC in the early detection of PCa shows to be promising but

under investigation.

Despite their potential, CTCs pose several challenges for cancer diagnosis. Firstly, their rarity in circulation makes detection difficult, even in metastatic stages, where there may be less than one CTC in 1ml of blood [227]. Since the correlation between the CTCs number and the tumour volume remains unclear, this makes the detection of early-stage cancers difficult [228-231]. A low detectable rate of CTCs in patients with early-stage cancer or with an advanced stage was reported in PCa. Helo *et al.* reported that there was a low frequency of CTCs in patients with localized disease [232], which was consistent with Davis's result of only 3.1% of patients having 3 or more CTCs in 22.5ml whole blood [233] and Loh's finding of 14% in non-metastatic PCa by using the CellSearch assay [234].

Furthermore, the results of CTC tests can vary greatly depending on the methods used. For example, differences were reported in the positive rates of CTC tests using CellSearch, CellCollector, and EPISPOT assay, with rates of 37.4%, 54.9%, and 58.7% respectively [220]. The comparison of CellSearch, Dual fluoro-EPISPOT, and CellCollector CANCER01 in another study showed CTC detection rates of 23.9%, 52%, and 57.7% respectively [235]. From the above results, CellSearch has

shown a relatively lower detection rate of CTC.

There is a clear need for more efficient CTC isolation methods to improve detection sensitivity [217]. Recent developments, such as enhancing the specificity of CTC isolation using prostate cancer antigen expression, show promise [236]. For example, expression of AR in PCa tissue was reported to be significantly associated with the presence of CTCs in the blood. Diagnosis of PCa using CTCs combined with positive AR has a 14.2% sensitivity and a 78.4% specificity [237]. Beside this, further research on how to improve molecular analyses of CTCs and their translation to clinical practice are needed [238].

9.3 Exosomes

Exosomes are small, extracellular vesicles characterized by a lipid bilayer. Ranging from 40 to 150 nm in diameter, these vesicles are expelled from cells, including cancer cells [239]. They carry a host of tumour-derived materials such as DNA, RNA, proteins (including oncoproteins, tumour suppressor proteins, and transcriptional regulators), and peptides, which serve to facilitate intercellular communication. Moreover, antigens of exosomes have been reported to offer valuable information about the originating cancer [240-242].

Exosomes act as biological messengers used by cancer cells to

encourage tumour growth in an autocrine manner [243]. By activating the autocrine pathway, exosomes can control cell polarity and movement, stimulating cancer cell invasion [244]. These vesicles also facilitate the transfer of oncogenic traits between primary tumours and recipient cells, effectively modulating the tumour microenvironment [245-247].

Given their stability in plasma and urine and their role in the disease process, exosomes offer a promising avenue for cancer detection [248].

A comprehensive analysis of exosome levels in different body fluids and their potential role as tumour markers was published in 2017, showing the promise of using exosomes to overcome the limits of current tumour biomarkers [249]. Recent studies in PCa [250, 251], pancreatic [252], and breast cancer [253] have underscored their potential as a clinically relevant circulating biomarker.

In the case of PCa, exosomes derived from cancer cells were found to be rich in prostate-specific antigen (PSA), thus mirroring the features of the originating PCa cells [251]. Additionally, exosomal RNA has been identified as a key player in intercellular communication within PCa [254]. Clinical studies have demonstrated that plasma exosomal miRNAs hold high diagnostic value for PCa, boasting a sensitivity of 86% and a specificity of 89% [255]. Another panel of 36 exosomal miRNAs has been

identified as potential biomarker candidates for PCa [256].

There are several challenges associated with the use of exosomes in cancer detection. The isolation and purification techniques for exosomes are still being refined [257-259]. With regard to isolation, the presence of components in biological fluids such as lipoprotein, chylomicrons, and other microvesicles that their size is similar to exosomes complicates the process [258, 260]. As for purification methods, while ultracentrifugation is a common and efficient way to purify exosomes from cell culture [261], its effectiveness decreases when applied to urine [262] and serum [261, 263]. Microfluidics-based methods have been reported to yield better outcomes [264-267].

10. Platelets

10.1 Overview

Platelets was first described by Max Schultze in 1865. They are an essential part of our blood [268]. Originally recommended for ‘those concerned with the in-depth study of the blood of humans’ [268], these minute elements, second only to red blood cells in abundance, are indeed vital to our health [269, 270].

Named ‘piastrine,’ or ‘small plates,’ in Italian by Bizzozero 17 years after

their initial discovery [268], these 1.5-3 μm [271] discoid-shaped cells were reported to maintain a resting status without being activated, but play a crucial role in coagulation and thrombosis [272]. They bind to the walls of damaged blood vessels [273], and are activated in adhesion, aggregation, and clot formation [271]. Furthermore, their role extends beyond hemostasis. They are involved in several pathophysiological processes, including infection [274, 275], atherosclerosis [276, 277], and even cancer development [278-280].

Common cytoplasmic structures, such as lysosomes and mitochondria are found in platelets, while special granules which include alpha and dense types have also been discovered [281-284]. The alpha granules contain a variety of substances that play important roles in platelet activation, such as PF4, vWF, fibrinogen, PDGF, PF5, and thrombospondin [281, 283]. When platelets are activated, the alpha granules fuse with the plasma membrane and release their contents into the surrounding area. Alternatively, the special surface-connecting tubular system in platelets [285] may also provide a passage for the exchange in activation and other interactions [286]. This activation also causes platelets to undergo morphological and other biochemical changes [287], including a change in shape from a discoid to a spherical shape, which

allows for better adherence, as well as the synthesis and release of prostaglandin and other markers of platelet activation, such as P-selectin [283, 288, 289]. Additionally, there is a special membrane system in a platelet, allowing different types of communication to continue flexibly via both passing through the membrane directly [290, 291] and indirect vesicle transfer [292]. Therefore, activation of platelets causes not only the granules to fuse with the plasma membrane, but also triggers morphological and biochemical changes in platelets, enabling them to function more effectively.

Originating primarily from megakaryocytes (MKs) in the bone marrow, and to a lesser extent, the lungs [290, 355], platelets reflect the functional subpopulations of their parent MKs [356, 357]. Notably, research suggests that specific markers could indicate differences in megakaryocyte differentiation and platelet formation, a topic of ongoing investigation. Platelets may primarily come from the platelet generating MK, a subgroup that are positive for the marker ARNTL, while immune MK, another subgroup of CD53 and LSP1 positive MKs primarily contribute to immunity [357]. Platelet-producing MKs only occupy a small percentage of total MK cells with larger size and slower migration velocity, suggesting their inability to be involved in immune response [357]. Understandably, in front

of cancer, platelet producing MKs may not firstly and directly interact with cancer, leaving their following platelet content remain stable. Finally, the lifespan of platelets ranges from 7 to 10 days, after which they are removed by the spleen [289].

10.2 Protein Synthesis, Composition and Intricate RNA Profile in Platelets

Additionally, the protein content of platelets, while not fully understood, is believed to be derived largely from the cytoplasm during the maturation of megakaryocytes and from plasma [293]. Interestingly, evidence of de novo protein synthesis [293-295] in platelets has been reported, suggesting potential RNA changes within platelets [296, 297]. Biomarkers associated with PCa, including kallikrein-related peptidase-2 and -3, folate hydrolase 1, and neuropeptide-Y, have been reported to be exclusive to the platelets of PCa patients and absent in those from healthy donors [298]. Another study observed increased expressions of TGF-β, NF-κβ, VEGF and decreased expressions of AKT and PI3K in the platelets from hepatocellular carcinoma patients. Notably, AKT and PI3K appeared particularly useful in detecting early-stage HCC [299]. However, there is a limited sample size of only 20 cancer patients and 10 controls which necessitates further validation.

While Bizzozero observed that platelets are anucleate [273], meaning

they lack a nucleus and hence a significant amount of DNA, they are not devoid of functional biomolecules [300]. Platelets contain functional ribosomes, signaling proteins, and various types of RNAs, parts of which can be remnant of the originating megakaryocytes [273, 301, 302]. Therefore, the transcriptome of platelets is largely reflective of megakaryocytes, representing about 70-90% of platelet profile [303, 304]. However, the RNA expression in platelets may be different from that in MKs. Interestingly, megakaryocytes were shown to differentially express mRNAs that subsequently manifest in varied RNA expressions within the platelets they produce. This phenomenon has been observed in conditions like lung cancer [305]. Another example is that matrix metalloproteinases and their tissue inhibitors were reported to be selectively sorted into platelets [306]. This mechanism makes the origin of platelet RNA contents non-uniform. Moreover, the abnormalities in the medullary and/or extra medullary megakaryocyte niche could influence transcriptional profile of platelets [307]. The genomic mutations in megakaryocyte could result in the change of the platelet profile [307, 308]. Upon stimulation, megakaryocyte-derived pre-mRNA transcripts in platelets were reported to be differentially spliced into mature mRNA differently [309].

After platelets are formed, they are capable of actively responding to different external stimuli via changing their RNAs. The RNA content of platelets can change in response to various stimuli, with and without activation. In the thrombin-mediated activation, mRNA formation by pre-mRNA-splicing was shown that platelets accurately remove introns from interleukin-1beta pre-mRNA, yielding a mature message [309]. Similar finding was also reported that by the stimuli of endotoxin, platelets expressed TLR4, binding Lipopolysaccharide to induce splicing of unprocessed IL-1beta RNA [310]. Finally, it has been reported that platelets can directly take up RNA from other vascular cells [311] and tumour cells [312]. Report showed that platelets from both glioma and prostate cancer patients carry cancer-specific RNA like EGFRvIII and PCA3 respectively [312].

Thus, the different constitutions and possible changes of the RNAs in platelets make them potential candidates for further study.

10.3 Crosstalk between Tumours and Platelets

Platelets, traditionally implicated in haemostasis and thrombosis [313], have been associated with solid tumours for over 150 years, with early reports documenting thrombosis in malignancy [314, 315]. In the present day, thrombosis is acknowledged as a common manifestation in the

relationship between cancer and platelets. However, the complex and bidirectional interactions between tumours and platelets extend beyond thrombosis and warrant further exploration for their potential implications in cancer progression and treatment [279]. This bidirectional reaction will be introduced in the following paragraph separately.

10.3.1 How Do Tumours Affect Platelets?

In addition to modifying platelet activity, tumours can enhance platelet production, a process known as thrombocytosis. Thrombocytosis, characterized by an elevated platelet count, has been reported in various solid cancers including lung [316], kidney [317], stomach [318], colon, breast, uterine [319] and ovary cancers [280]. Tumour cells can stimulate the bone marrow to produce more megakaryocytes – the precursors to platelets – through various factors. A clear example is seen in ovarian cancer, where tumours secrete cytokines such as interleukin-6 that stimulate hepatic thrombopoietin production. This process promotes the expansion and maturation of megakaryocytes in the bone marrow, leading to an increased production of platelets [320].

Tumours could activate platelets and this education process of tumour-induced platelet activation occurs through two primary mechanisms: direct and indirect tumour cell-induced platelet activation [273, 321].

Direct activation is facilitated through physical contact between cancer cells and platelets. By using surface receptors/ligands, tumour cells directly bind and activate platelets [322]. Molecules present on the surface of cancer cells such as P-selectin [278, 323-327], integrins [328-330], and glycoproteins [331-333] facilitate the binding of platelets to cancer cells.

Cancer cells can also indirectly ‘educate’ platelets by releasing various factors into the bloodstream, triggering platelet activation [334]. These factors, such as proteinase [335-337], TF [338, 339], adenosine diphosphate [336, 340, 341], matrix metalloproteinases (MMP) [342, 343], TXA2 [344-346] and so on, can stimulate platelet activation and aggregation, potentially leading to thrombosis. For example, in pancreatic [347, 348], brain [349], and breast cancer [347], tumour cells can release TF through microparticles, which is a potent initiator of blood clotting [339]. By this way, tumours could also ‘educate’ platelets at an early stage in cancer development, making platelets themselves a potential resource for early cancer detection.

Based on the preceding discussion, tumour cells can activate platelets via both direct and indirect mechanisms. An interesting example can be observed in CTCs. Both the direct mechanism (through interactions with glycoproteins, integrins, and P-selectin) and the indirect method (involves

a ligand-receptor approach, encompassing P2Y receptors, PAR, and TXR) were reported and shown in [321].

As a result of these interactions, the concept of “tumour-educated platelets (TEPs)” has emerged [350-352], suggesting a role for platelets that extends beyond traditional functions and has implications for cancer biology.

10.3.2 How Do Platelets Effect Tumour Cells?

The interplay between cancer cells and platelets is bidirectional [353], with platelets implicated in various phases of cancer progression [273]. Platelets promote tumour angiogenesis.

10.3.2.1 Platelets Involve Angiogenesis

A critical role of platelets in cancer involves the promotion of angiogenesis – the process of forming new blood vessels that provide tumours with essential nutrients and oxygen. Platelets facilitate tumorigenesis through several mechanisms. Firstly, platelets secrete angiogenic factors. Platelets secrete various growth factors, including vascular endothelial growth factor (VEGF) [323, 354-357], platelet-derived growth factor (PDGF) [356, 358-360], and basic fibroblast growth factor (bFGF) [357, 360], which stimulate the formation of new blood vessels by binding to endothelial cell receptors. Secondly, platelets also house proteases like

matrix metalloproteinases (MMPs) and plasminogen activators that can degrade the extracellular matrix, facilitating the migration of endothelial cells and the creation of new blood vessels [361, 362]. Thirdly, platelets can directly adhere to tumour vasculature through the interaction between tissue factor (TF) and thrombin, thereby enhancing endothelial cell proliferation [363]. The formation of platelet aggregates triggers coagulation, leading to microthrombi that can occlude blood vessels and create hypoxic regions, a common characteristic of solid tumour [364, 365]. Therefore, platelets aid in promoting the survival and proliferation of tumor vessels [366]. Finally, platelets can also release anti-permeability factors like angiopoietin-1 and serotonin, which help stabilize tumour blood vessels, preventing intra-tumoral bleeding and facilitating tumour grow [367].

10.3.2.2 Platelets Promote Tumour Proliferation

During the initial stages of tumour growth (typically less than a few millimeters in size), tumour not require a blood supply for continued growth [368], which means platelets might not have a direct impact during this period. However, several studies indicate that platelets could indirectly influence tumor proliferation even at this stage. For instance, *in vitro* studies have demonstrated that platelets can release transforming growth

factor-beta1 (TGF-β1) without direct contact, thereby stimulating the proliferation of ovarian cancer cells [369]. A study conducted on the lung cancer cell line A549 indicated that platelet-derived microvesicles enhanced cancer proliferation by increasing cyclin2 expression [370]. Further, in clear cell renal cell carcinoma, suppression of the platelet isoform of phosphofructokinase led to altered glycolysis, which resulted in cell cycle arrest [371].

10.3.2.3 Platelets Enhance Tumour Invasion

Platelets contribute to cancer cell invasion via several mechanisms. Platelets are a major reservoir for transforming growth factor β (TGFβ) [372], which has been reported to induce and maintain tumour invasion [373, 374]. Platelets also contribute to the degradation of the extracellular matrix (ECM) by secreting proteases such as matrix metalloproteinases (MMPs) and plasminogen activators. These enzymes can degrade the ECM, thereby enabling cancer cells to invade surrounding tissues. For instance, MMP7 has been reported to enhance the invasion of chondrosarcoma cells [375]. Platelets can stimulate the production of MMPs in breast cancer cells, reinforcing cancer invasion [376]. Furthermore, platelets assist in tumour extravasation, which is the movement of cancer cells from blood vessels into surrounding tissues.

Platelets proximal to tumours can regulate vascular permeability by releasing substances such as TXA2 [377], 12-HETE [377], and ATP [378, 379]. This regulatory action can lead to the retraction of endothelial cells, exposing the basement membrane and facilitating cancer cell extravasation.

10.3.2.4 Platelets Assist Metastasis

Platelets contribute to metastasis through several mechanisms. Firstly, platelets induce epithelial-mesenchymal transition (EMT), a crucial process whereby cancer cells acquire a more invasive and motile phenotype [380]. Platelet-derived factors, like TGF-β, induce EMT by suppressing cell adhesion molecules and upregulating mesenchymal markers. The activation of the TGFβ/SMAD and NF-κB pathways, by platelet-derived TGF-β and direct platelet-tumour cell contacts, initiates a shift to an invasive mesenchymal-like phenotype, thereby promoting metastasis, especially in lung cancer [381]. Platelets promote anoikis resistance. Anoikis is a specialized form of programmed cell death triggered when cells lose their connection to the extracellular matrix [382]. For tumour cells to metastasize, platelets help tumour cells gain resistance to anoikis by several pathways [383]. Platelet-derived Autotaxin plays a role in this resistance [384]. ATX transforms

lysophosphatidylcholine into lysophosphatidic acid [384]. When LPA binds to the LPAR-1 receptor on circulating tumour cells (CTCs), it activates the RhoA-Gα12/13-YAP-1 signaling pathway, promoting anoikis resistance in CTCs [385]. By triggering the RhoA-MYPT1-PP1 pathway that leads to YAP1 dephosphorylation and its subsequent nuclear translocation, platelets inhibit tumour cell apoptosis and enhance the expression of genes associated with cell survival [386]. Platelet-derived growth factor-BB was reported to suppress anoikis through the Hippo/YAP signaling pathway in pancreatic cancer [387].

Secondly, platelets assist CTC survival in circulation. Platelets can adhere to cancer cells, promoting their movement through the bloodstream [388]. Circulating tumour cells (CTCs) are susceptible to immune attacks and mechanical stress. Platelets, utilizing P-selectin, bind to the mucin on tumours, creating a physical barrier [326]. This shields CTCs from immune system attacks, including tumor necrosis factor-α (TNF-α) [389] and natural killer (NK) cell-induced cell death [390]. Platelets not only offer physical protection but may also inhibit the ability of NK cells to detect cancer cells. Platelets mask CTCs by shifting ‘pseudonormal’ major histocompatibility class I molecules on cancer cell surfaces, dampening the anti-tumor response tumour cells [391]. Moreover, platelet-derived

TGF-β inhibits the activity of NK cells by downregulating NKG2D [392].

Platelets play a crucial role in helping CTCs adhere successfully to the epithelium at a distant site [393]. Platelet-derived ATP can disrupt the endothelial barrier to create gaps by activating endothelial P2Y2, thus enabling CTC transmigration and extravasation [378].

On the contrary, reports suggest that platelets may also impede tumour development. Mouse platelets have been shown to inhibit the growth of prostate cancer cells in vitro [394]. Similar observations were made in co-cultures of human platelets with melanoma and renal cell cancer cells, where increasing platelet density led to cancer cell cytotoxicity [395]. The inhibition effect has also been reported in leukemia [396, 397], lung cancer [396], cervical cancer [398], melanoma, and adenocarcinoma [399]. The multifaceted Interactions between platelets and tumours reflect the complexities. Further research is required to tease apart these complexities and determine under what conditions platelets inhibit versus promote tumour progression.

10.3.3 The Clinical Potential of Platelets in Cancer Treatment

Notably, the role of platelets becomes increasingly pronounced in advanced stages of cancer, especially in the metastatic phase. Studies have reported significant increases in agonist-induced and spontaneous

platelet aggregation [334, 400, 401], implying the platelet's potential to monitor cancer advancement. However, this phenomenon is not universal across all cancer types, as some studies have reported no change in platelet activity in ovarian cancer [402] and even decreased reactivity in other cancers [403].

Interestingly, a study shows that tumour cell-induced platelet activation can protect tumours from natural killer cell-mediated lysis, suggesting platelet as a potential therapeutic target [391]. Based on the above mechanism, cancer treatment could be considered by disrupting the adhesion of platelets to tumour cells, theoretically limiting tumour progression based on cancer-induced platelet activation. For instance, certain integrin blockers have been reported to inhibit platelet-tumor cell interactions [404].

Thrombocytosis has been reported to be associated with poor prognosis in patients with ovarian [320], oesophageal [405], pancreatic ductal adenocarcinoma [406] and liver carcinoma [407]. Existing literature offers limited data on the correlation between thrombocytosis and prostate cancer. One report showed that there was minimal or no link between elevated platelet counts and prostate cancer [408]. On the other hand, another author observed a higher platelet count correlated with an

increased chance of a prostate cancer diagnosis but without a connection with poor prognosis [409].

10.3.4 Platelets in the Early Detection of Cancer

Historically, studies have primarily concentrated on the correlations between platelet count and cancer progression and prognosis. These studies indicate that patients with elevated platelet counts often exhibit shorter disease-specific survival rates across various types of cancer, including lung, colon, breast, pancreatic, kidney, and gynecologic cancers [278]. However, recent investigations suggest that platelets could serve as potential biomarkers for the early detection of cancer. Research has highlighted thrombocytosis as an indicator of increased risk for early-stage lung and colorectal cancers [410-412]. Additionally, one study found that platelet counts and mean platelet volume were elevated in patients with early-stage lung cancer compared to healthy individuals [413]. A long-term, ten-year study further established that ovarian and stomach cancer patients also had higher platelet counts six months before their cancer diagnoses [412].

A study comprising 298 patients suspected of having cancer (126 with benign prostatic hyperplasia and 172 with PCa), revealed that the platelet-to-lymphocyte ratio could be a valuable predictor of prostate cancer [414],

a finding echoed in a subsequent study [415]. These investigations suggest that certain platelet parameters could contribute to the development of a non-invasive blood test for early cancer detection [416]. However, these parameters are subject to significant fluctuations and can be influenced by inflammation-associated factors, which presents a potential challenge [417, 418].

10.3.5 Potential of Platelet RNAs in Cancer Detection

The alteration of RNA profiles in platelets has been previously reported during activation [419, 420]. The ongoing interaction between tumour cells and platelets could also result in alterations in platelet RNA profiles [352, 421, 422]. These changes can occur through multiple mechanisms. Mechanism included the absorption of extracellular molecules released by tumour cells or direct cell-to-cell contact [311, 312]. Tumours can package their RNAs into extracellular vesicles (EVs) and transfer these RNAs to platelets [273, 312]. One study identified two cancer-specific biomarkers – EGFRvIII and PCA3, from glioma and PCa respectively – transferred to platelets via tumour membrane vesicles [312]. Alternatively, cancer cells can directly transfer RNA to platelets through cell-cell contact [273]. The mechanisms behind this RNA transfer still require further investigation. Another mechanism could involve post-transcriptional

regulation such as pre-mRNA splicing. Despite the absence of direct evidence linking this mechanism to tumour-platelet interactions, functional spliceosomes in platelets have been reported to splice pre-mRNA differently based on specific stimuli [309, 423, 424].

Platelets, shown to participate in cancer development and progression, have raised interest as potential biomarkers for early cancer detection, particularly with regards to alterations in platelet mRNAs.

Preliminary studies using microarray technology indicated that as many as one third of all human genes are present at the mRNA level in platelets [300, 304, 425]. Moreover, human platelets contain the fundamental components of the mRNA translation apparatus which respond to physiological stimuli through biosynthetic processes, highlighting their active and dynamic role in cellular responses [296, 426, 427].

An Initial study In 2015 demonstrated that, among 228 patients with varying cancers (lung, colorectal, glioblastoma, pancreatic, hepatobiliary, and breast) and 55 healthy participants, platelet mRNA could identify cancer with a diagnostic accuracy of 96% and locate the primary cancer site with 71% accuracy [352]. In a follow-up study, the researchers utilized the ThromboSeq pipeline which incorporates particle-swarm optimization algorithms to generate biomarker panels of platelet RNAs. This method

detected early-stage non-small-cell lung cancer with an 81% accuracy rate [351]. By refining this method [428], the authors later achieved diagnostic accuracies of 95% and 87% for glioblastoma [429] and sarcoma [430] respectively, using platelet mRNA profiles. Nevertheless, potential contamination from leukocytes during initial platelet isolation could influence these sequencing results [352, 428].

Another research group identified seven mRNA (RSL24D1, IFI27, CRYM, HBD, IFITM3, FCGR2A, and KLHDC8B) from the platelet RNA profile as potential biomarkers, further validated by RT-PCR [431]. Of these, RSL24D1 demonstrated a sensitivity of 71.8% and a specificity of 64.3% for early pan-cancer detection [431]. However, these results require further validation. These studies collectively indicate that platelets could serve as a source of potential biomarkers for early cancer detection. Platelet mRNAs, given their dynamic response to tumour presence, could correspondingly change, making them a promising focus area. While no studies have reported on platelet mRNAs in detecting PCa, as of my knowledge cutoff, the potential for platelets to aid in early PCa diagnosis is eagerly to be investigated.

MiRNAs, noncoding single-stranded RNA molecules of about 18-22 nucleotides (nt) in length, are developmentally preserved and play a

significant role in the posttranscriptional regulation of genes [432]. They begin as long primary transcripts (pri-miRNAs), produced in the nucleus by RNA polymerase II or III [432]. The microprocessor complex, made up of the RNase III enzyme Drosha and its partnering component DGCR8, transforms these pri-miRNAs into 70-100 nt precursor RNAs (pre-miRNAs). Following this initial split, the pre-miRNAs are moved to the cytoplasm by Exportin-5/RanGTP, where they undergo further processing into a 19-25 nt duplex by the RNase III endonuclease Dicer and TRBP [182]. The ultimate step of Dicer processing likely leads to the incorporation of the two strands into the RNA-induced silencing complex (RISC), with an Argonaute protein serving as its key constituent [182].

Within RISC, miRNAs hinder the translation of target mRNAs by altering their stability, typically through binding to their 3' untranslated region (UTR), but sometimes also to the 5' UTR or the coding sequence [433]. Consequently, miRNAs can either lead to the degradation of perfectly complementary mRNA or incite translational repression through a variety of mechanisms [433].

MiRNAs are inherently dynamic and responsive entities. This characteristic is primarily attributed to their pivotal role in the following mechanism. MiRNAs primarily function at the post-transcriptional level to

regulate gene expression. This means that they act on mRNA molecules after transcription has occurred, either by inhibiting the translation of these mRNAs into proteins or by promoting their degradation [434]. Because of this post-transcriptional activity, miRNAs can rapidly modulate protein levels in response to cellular signals or environmental changes. A single miRNA can target multiple mRNAs, and a single mRNA can be targeted by multiple miRNAs. This network-like regulatory system allows miRNAs to quickly modulate a wide array of genes and pathways in response to cellular cues [435].

Due to the intricate nature of these regulatory mechanisms and the fact that one miRNA can influence multiple mRNAs, it’s unsurprising that miRNAs contribute to virtually all major cellular processes, including cell proliferation, differentiation, migration, apoptosis, and stemness maintenance [436]. Changes in the expression of miRNAs related to cancer may be triggered by chromosomal rearrangements, promoter methylation, or transcriptional deregulation. This fascinating aspect has led to an explosion in research, particularly in understanding the role of miRNAs as potential biomarkers for cancer diagnosis [437].

Different miRNAs and functional miRNA pathways have been reported in platelets in some non-cancer diseases [438-440]. For example, platelet

miRNAs have been shown to be released and be taken up by epithelial cells during myocardial infarction. For example, miR-22 and -423 were reported decreased in these patients [441]. A transfer of miRNA between platelets and vascular smooth muscle cells has also been shown in artery injury [442]. Plus, sequencing results showed that alterations in platelet miRNA expression during activation may lead to significant changes in the platelet proteome, revealing an association between microRNA profiles and platelet reactivity. This proposes a potential function for small regulatory RNA species in regulating mRNA translation within platelets [443]. There is no published proof of applying platelet miRNA for PCa detection currently. However, considering the platelet miRNA changes in other diseases and associated proteome alternation during activation, assessing the expression levels of specific miRNAs in platelet samples from both PCa and non-cancer patients may provide new insights into cancer diagnosis. Therefore, in this project, the further research of platelet miRNA expression was performed.

Overall, the dynamic nature and multifaceted role of platelets in health and disease make them an exciting area for continued research.

11. Hypothesis and Aims

11.1 Hypothesis

My hypothesis is that the RNA expression profile in the platelets of peripheral blood changes significantly when these platelets interact with PCa cells. We anticipate that these changes in RNA expression could serve as a basis for developing peripheral blood platelet RNA-based biomarkers for the early detection of PCa.

11.2 Aims

To identify platelet RNA changes in the blood samples of PCa patients evaluating their potential use in the early detection of PCa. To identify differentially expressed mRNA and/or miRNA in the platelets of PCa patients compared to a non-cancer control group, using RNA-sequencing (Next-Generation Sequencing).

To develop RNA panels based on these differential expressions and to validate these panels by comparing the PCa group with the non-cancer control group, using Reverse Transcription Quantitative PCR (RT-qPCR).

Additionally, investigate the potential of a platelet RNA panel as a tool for detecting unfavourable PCa. (Such a tool could be critical for the clinical management of PCa by allowing for earlier intervention in patients with clinically significant PCa.)

Chapter II: Material and Methods

1. Primary Patient Samples

Peripheral blood was obtained with informed consent from patients at St Bartholomew's Hospital (London, UK) and University College London Hospital (Project CPM: C-ProMeta-1). Patients were recruited in two cohorts: 1. patients with newly diagnosed PCa 2. Non-cancer patients. All blood samples were stored at room temperature and processed within 4 hours after the collection. Three ml of blood was used to extract platelets. 1ml of blood was used in the modification of platelet collection.

2. Platelet Isolation by Two-step Centrifugation

3ml whole blood was gently transferred from purple-cap EDTA-coated vacutainer tubes into an empty 3ml syringe shortly after its collection in the hospital. Platelets were isolated from whole blood by a two-step differential centrifugation (**Figure 1**).

The first centrifugation step (200 g at RT for 20 minutes) separated the platelet-rich plasma (PRP) from the erythrocytes and leukocytes. PRP was carefully pipetted into a 1.5ml Eppendorf tube. To minimize leukocyte contamination, only the upper 2/3 of the PRP was collected to avoid disturbing the leukocyte-containing buffy coat.

The second centrifugation step (400 g for 20 minutes) yielded the platelet pellet. The supernatant was removed by pipetting without disturbing the platelet pellet and was discarded. After isolation, platelet samples were stored in 700μl QIAzol Lysis Reagent (Qiagen, UK) at -80 ºC for future use.

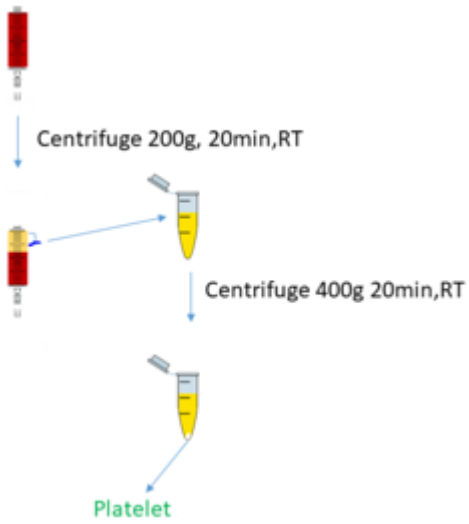

Figure 1. Two-step differential isolation of platelets.

Two steps were performed to acquire platelet pellets. Three ml of whole blood was centrifuged at 200g for 20 minutes under room temperature. Then the upper two third of the PRP was then transferred to an Eppendorf for another centrifugation of 400g for 20 minutes under room temperature to collect platelet pallet.

3. Total RNA Extraction from Platelets Using miRNeasy Micro Kit (Qiagen, UK)

Total RNA was extracted from platelets using the miRNeasy micro kit (Qiagen, UK). The extraction procedure was adhered to the manufacturer's protocol as follows: The platelet samples were first thawed at RT for five minutes after removal from -80 °C. In a fume hood, 140 µl of chloroform was added to each sample, which was then shaken vigorously by hand for 15 seconds after securely capping the tube. The samples were incubated for two minutes at RT before being centrifuged for 15 min at 12,000 g at 4°C. The upper aqueous phase was carefully transferred to a new 1.5 ml Eppendorf tube by angling the tube at 45° and pipetting the

solution out. Then 1.5 volumes (about 525 µl) of 100% ethanol were added to this mixture and mixed thoroughly by pipetting. The mixture was pipetted into a RNeasy MinElute spin column in a 2ml collection tube and centrifuged at 8500 g for 15 seconds. The flow-through was discarded. Seven hundred µl of RWT from the kit was added to the RNeasy MinElute spin column. Then the column was centrifuged for 15 seconds at 8500 g and the flow-through was discarded. 500µl Buffer RPE was added to the same column following centrifugation under the same conditions/parameters. Then 500µl of 80% ethanol was added to the spin column and the same procedure was repeated once. The spin column was placed in a new 2 ml collection tube (supplied by the kit) and centrifuged at 10000 g for 5 minutes with the column lid opened to dry the membrane. The spin column was then placed in a new 2ml collection tube (supplied by the kit). RNase-free water (14 µl) was added at the centre of the spin column membrane. Then the tube was centrifuged at 10000g for one minute to elute the RNA. RNA was stored at -80 °C.

4. Quantification and quality Control of RNA extraction

The quality and quantity of total RNA isolated were determined using NanoDrop 2000 spectrophotometer (ThermoFisher, USA) with a 1µl sample and an Agilent 2100 Bioanalyzer (RNA 6000 Picochip) (Agilent,

USA) with a 2ul sample.

5. Small RNA sequencing of a Chinese cohort

In the project (F18FTSECWLJ0101_HUMmuyS), total platelet RNA from 20 treatment-naïve PCa and 20 non-cancer Chinese samples were sent for small RNA-sequencing to the Beijing Genomics Institute in 2018.

By polyacrylamide gel electrophoresis (PAGE) gel, the separation of RNA segment was performed. The library was built following cDNA synthesis and PCR amplification. Small RNA (sRNA) sequencing was performed using BGISEQ-500 technology. Bowtie is used to map reads to the reference genome. MiRDeep2 was used to predict novel miRNA by exploring the characteristic hairpin structure of miRNA precursor. Small RNA expression level was calculated by using Transcripts PerKilobase Million. DEGseq was used to analyze differentially expressed RNAs. Both p-value (<0.05) and FDR were used to help determine which miRNAs were differentially expressed between the groups.

6. Fluidigm Multiple Reverse Transcription Quantitative Real-Time Polymerase Chain Reaction (RT-qPCR)

Samples for Fluidigm multiple RT-qPCR were prepared using the miRCURY LNA RT Kit (Qiagen)/ miRCURY LNA miRNA PCR assay

(Qiagen)/ TaqMan® PreAmp Master Mix/ and TaqMan Gene Expression Assays (Thermo Fisher ScientificTM).

cDNA synthesis

cDNA prepared in a reverse-transcription reaction using the miRCURY LNA RT Kit (Qiagen) serves as the template. RNA was thawed on ice. 5x miRCURY RT SYBR® Green Reaction Buffer and nuclease-free water, and 10x miRCURY RT Enzyme were thawed at room temperature. The reverse-transcription reaction mix was prepared on ice (**Table 5**). The reactions were incubated for 60 min at 42°C following another incubation at 95 °C for 5 min. The reactions were then placed on ice to cool down. The cDNA was then stored at -20°C for later use. The cDNA was diluted 1:10 in nuclease-free water.

Table 5. Reverse-transcription reaction components for cDNA preparation for Fluidigm system.

Components	Volume (µL)
5x miRCURY RT SYBR® Green Reaction Buffer	2
nuclease-free water	5.5
10x miRCURY RT Enzyme	1
Template RNA	1.5
Total volume	10

Pre-amplification

The pre-amplification was performed using miRCURY LNA miRNA PCR assay (Qiagen), TaqMan® PreAmp Master Mix and TaqMan Gene Expression Assays (Thermo Fisher ScientificTM).

The technology of locked nucleic acids (LNA) was used in the procedure. LNA are a class of high-affinity RNA analogues which have thermal stability during the PCR process. LNA enhanced primers improve the sensitivity and specificity of PCR.

To perform the preamplification reaction, TaqMan® PreAmp Master Mix (2.5 µL), pooled LNA primer mix (1.25 µL) and diluted cDNA (1.25 µL) were mixed to make a reaction mixture of a total of 5 µL. The list of used primer assays is shown in **Table 6**. The pre-amplification was then performed using the following PCR program: denaturation at 95 °C for 10 minutes, followed by 15 cycles at 95 °C for 15 seconds and 60 °C for 4

minutes for amplification. Finally, the amplified product was diluted 1:10 in nuclease-free water.

Table 6. List of primer assays used in Fluidigm multiple RT-qPCR

YP00206084-Hsa-miR-let7a-3p LNA primer
YP00205651-Hsa-miR-1250-5p LNA primer
YP02106758-Hsa-miR-1304-3p LNA primer
YP02105660-Hsa-miR-1306 LNA primer
YP00204763-Hsa-miR-190a-5p LNA primer
YP00204196-Hsa-miR-191-3p LNA primer
YP00205869-Hsa-miR-195-5p LNA primer
YP00204255-Hsa-miR-22-5p LNA primer
YP00204772-Hsa-miR-23a-3p LNA primer
YP00204676-Hsa-miR-26a-2-3p LNA primer
YP00204119-Hsa-miR-28-3p LNA primer
YP00204796-Hsa-miR-323b-5p LNA primer
YP00204516-Hsa-miR-342-5p LNA primer
YP02100646-Hsa-miR-3613-3p LNA primer
YP00204011-Hsa-miR-370-3p LNA primer
YP00204586-Hsa-miR-380-3p LNA primer
YP00204169-Hsa-miR-382-5p LNA primer
YP00204221-Hsa-miR-532-5p LNA primer
YP00205656-Hsa-miR-539-5p LNA primer
YP00205907-Hsa-miR-548d-5p LNA primer
YP02117351-Hsa-miR-5581-3p LNA primer
YP02111017-Hsa-miR-5582-3p LNA primer
YP00205979-Hsa-miR-627-5p LNA primer
YP02102689-Hsa-miR-652-5p LNA primer
YP00204725-Hsa-miR-664a-3p LNA primer
YP02112777-Hsa-miR-6805-5p LNA primer
YP00206082-Hsa-miR-744-3p LNA primer
YCP0039481-Hsa-novel miR-1174 LNA primer (acaaggggggccugucggcugugg)
YCP0039484-Hsa- novel miR-159 LNA primer (ggcggggagcagacagggg)
YCP0039487-Hsa- novel miR-948 LNA primer (gggcagcuaugggguggcgg)

LNA: locked nucleic acids

7. Analysis of qRT-PCR Data and Panel Development

For analysis of qRT-PCR results, ΔCt value for each target miRNA was calculated using the formula ΔCt = sample CtmiRNA – average Endogenous control Ct. Endogenous controls include U6, UniSP6, miR23, miR532, and miR548.

2^-ΔCt was used to compare the expression levels of each miRNA in different groups of patients. Expression levels were compared by Mann-Whitney U tests. Receiver operating characteristic (ROC) curve analysis was used to test the performance of predictors in identifying PCa patients.

The area under the curve (AUC) was used to evaluate the predictive value of parameters. PSA levels and CTC numbers were recorded for panel development. Simple logistic regression was used to produce the index of each RNA candidate and other biomarkers for panel development, as combined risk score (CRS) = a* X + b*Y…, where ‘a’ and ‘b’ are the estimated log odds ratios, and X and Y are the candidate variables, such as miRNA expression or other biomarkers. Statistical analyses were performed in Graph Prism 8.3.0.

Based on Youden index formula (sensitivity+ specificity-1), best cut-off points were determined [444].

8. Prediction of miR190’s Target Gene

For the prediction of miR190's target genes, we adopted miRWalk, a tool incorporating both TargetScan and miRDB databases (http://mirwalk.umm.uni-heidelberg.de/, Heidelberg University, Germany). We zeroed in on the genes commonly predicted by both TargetScan and miRDB.

To discern the potential roles of these genes in cancer development, we undertook a comprehensive literature review. Genes identified as oncogenes in prior studies were selected for further investigation in 'The Human Protein Atlas' (https://www.proteinatlas.org/), examining their expression in both normal prostate tissue and cancer tissue [445-447].

9. Preamplification by SMARTer-seq V4

After the Bioanalyzer results showed the low input RNA quantity, the SMARTer-seq V4 (Takara, Japan) (SSV4) PLUS kit was used to preamplify the total RNA in the Barts and the London Genome Centre core facility. The SSV4 PLUS included SSv4 ultra low kit (SSV4 kit) and a library preparation kit for further sequencing.

10. Platelet mRNA-sequencing and Analysis of mRNA Next-generation Sequencing Data

The RNA sequencing process (GC-EB-9183) was then executed on the Illumina NextSeq 500 platform. To exclusively concentrate on the mRNA population, an mRNA enrichment procedure was performed. This process involved the use of poly (A) tail-specific oligonucleotides for capturing mRNA molecules via their poly (A) tails, hence allowing for a more precise gene expression analysis. The enriched mRNA was reverse-transcribed into complementary DNA (cDNA). The cDNA was subsequently processed to create a sequencing library, which was then subjected to high-throughput sequencing on the Illumina NextSeq 500 platform. During this sequencing process, the cDNA fragments were read and converted into sequence reads that reflected the original mRNA molecules. Hisat2 was used to align these generated reads to an annotated reference genome (CRCh38/hg 38 classification) employing RUM and BLAT algorithms. This alignment enabled the quantification of gene expression levels by counting the number of reads mapped to each gene or transcript. Following the mapping and quantification of gene expression, HTSeq was used for counting, and DESeq2 was applied for identifying differentially expressed genes (DEGs) between the two groups.

DESeq2 is a commonly used statistical tool for RNA-seq data analysis, designed to identify DEGs between varying sample groups. It accounts for factors such as library size, composition biases, and biological variability to produce accurate results. DESeq2 also incorporates normalization techniques to adjust for differences in sequencing depth and gene length, facilitating more reliable comparisons across samples.

Data analysis was performed by Dr Faraz Khan from Dr Jun Wang's bioinformatics service team at the Barts Cancer Institute.

11. Evaluation of Platelet Recovery and Quantity in the Two-step Centrifugation Method

Each blood sample was gently transferred from the vacutainer into an Eppendorf and centrifuge at 200 g at RT for 20 minutes without brake. Two-thirds of the upper layer of PRP were collected individually with the volume recorded, and then were gently mixed. PRP (10μl) from each collection was used for platelet counting which was diluted accordingly and then was added in a manual haemocytometer. The result was calculated by using a microscope with 10x or 20x objective lens. By multiplying the platelet count in 10μl PRP and total volume of PRP, the initial total numbers of platelets in collection of PRP were performed.

Then the PRP collected in the first step was centrifuged at 400g for 20 min at RT to collect the platelet pellet. Then the pallet was resolved by 50μl PBS. After the mixture of suspension, 10μl suspension was collected, diluted and added in a manual haemocytometer for platelet counting like the above way. Platelet recovery was roughly estimated as the following (using the average value of platelet number in 0.5ml whole blood as 150 million):

Platelet recovery (%) = $\frac{\text{PLT count in collection}}{\text{150 million}}$ X 100%

The total number of platelets collected=platelet number in 10μl suspension X 5.

Additionally, the efficiency of platelet collection was calculated by the ratio between platelet count in PRP after the first centrifugation and final platelet count in collection after the secondary centrifugation.

12. 4', 6-Diamidino-2-phenylindole (DAPI) Staining for WBC Contamination in Platelets Collected from Two-step centrifugation

The platelet pellet collected from the two-step centrifugation was resuspended in 50μl PBS. The suspension (10 μl) was then loaded on a

glass slide. Mounting medium containing 4', 6-diamidino-2-phenylindole (DAPI) was added to count nucleated cells- contaminating leukocytes using the Axioplan fluorescence microscope with 10x objective lens.

WBC count under microscope can be classified into five groups as the following: 0, 1-10, 11-20, 21-50, 51-100 WBC/ slide.

WBC contamination rate was roughly estimated as the following (using the average value of platelet number in 1-ml whole blood as 300 million):

WBC contamination rate= $\frac{5 * \text{WBC count under a microscope}}{9}$ (per million platelets)

13. Accurate Evaluation of WBC Contamination Rate in Platelets Collected by Two-step Centrifugation

Two-step centrifugation for collecting platelets was performed as the same as the previously established protocol. The platelet pellet from the second step was also resuspended in 50μl PBS. Then 10μl resuspension was stained by DAPI and nucleated cells (WBCs) were counted by using the Axioplan fluorescence microscope with 10x objective lens at the same way, while another 10μl resuspension was used for platelet counting by manual haemocytometer under microscope (**Figure 2**). Finally, WBC contamination rate for each sample was calculated and expressed as

WBCs/ 1 million platelets.

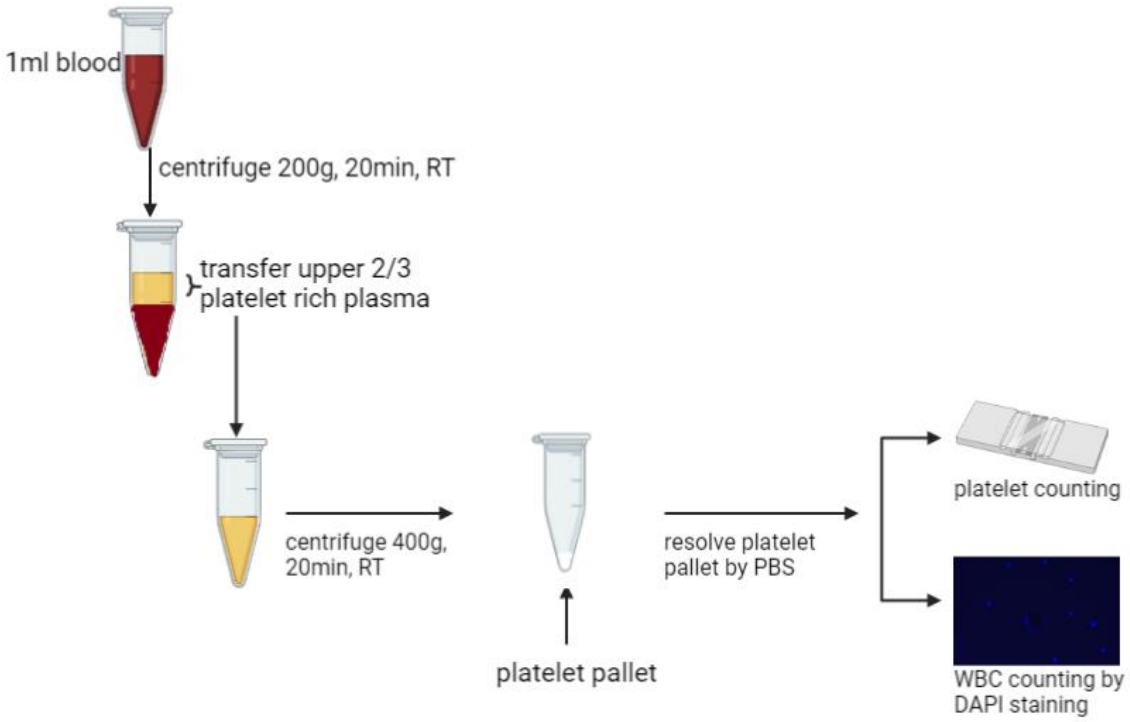

Figure 2. The workflow of evaluation of the two-step centrifugation.

After the pallet was collected and resolved in 50 μl PBS by the two-step method. 10μl resuspension was used for platelet counting, while another 10 μl received DAPI staining for WBC check. DAPI: 4',6-diamidino-2-phenylindole.

14. Method modifications for Platelet Collection

15.1 Taking the Upper ½ PRP for Platelet Collection

Each 1ml of whole blood was split into two 0.5ml samples, both of which were gently transferred from the vacutainer into an Eppendorf and centrifuged at 200g at RT for 20 minutes without brake (the same as previous two-step method).

Two-thirds and one-half of the upper layer of PRP were collected individually. After the first-step centrifugation, both collections were

centrifuged at 400g for 20 min at RT to collect the platelet pellet.

The pellet was resolved by 50μl PBS. After the mixture of suspension, 10μl suspension was collected for platelet counting, while another 10μl suspension was used for WBC contamination check by the same method mentioned previously. The platelet collection and the WBC contamination outcomes were compared by paired T-test in excel (Microsoft Office Professional Plus 2016).

15.2 Application of Magnetic Beads in Platelet Collection

Each sample of whole blood was gently transferred from the vacutainer into an Eppendorf and centrifuged at 200g at RT for 20 minutes without brake. Two-thirds of the upper layer of PRP was collected and then gently mixed. The PRP was split into two. One received additional centrifugation at 400g for 20 min at RT to collect the platelet pellet.

The other half was transferred to a 5ml polystyrene round-bottom tube and purified by magnetic beads. EasySep Human CD45 depletion cocktail II (50μl/ml) was added (Stemcell Technologies, Canada) to the sample, mixed, and incubated at RT for 5 mins. Vortex EasySep Dextran RapidSpheres (Stemcell Technologies, Canada) were vortexed for 30 seconds. RapidSpheres (75μl/ml) were added to the sample. Previously prepared buffer (PBS containing 2%FBS and 1mM EDTA) was then added

to top up the sample to 2.5ml, then mixed by gently pipetting up and down three times. The tube was placed without a lid into an EasySep™ Magnet (Stemcell Technologies, Canada) and incubated for five minutes at RT. The magnet was picked up and in one continuous motion, the magnet and tube were inverted. Then the suspension was poured into a new tube. The tube was then removed from the magnet. A new tube was placed without a lid into the magnet and the previous manipulation was repeated. The suspension was finally collected and centrifuged at 400g for 20 minutes for collecting the platelet pallet.

Finally, 50µl PBS was used to resolve the two pallets individually. Among them, 10µl resuspension each was used for platelet counting, while another 10µl resuspension each was used for DAPI check. WBC and platelet counting were performed and compared as the same method mentioned before (**Figure 3**).

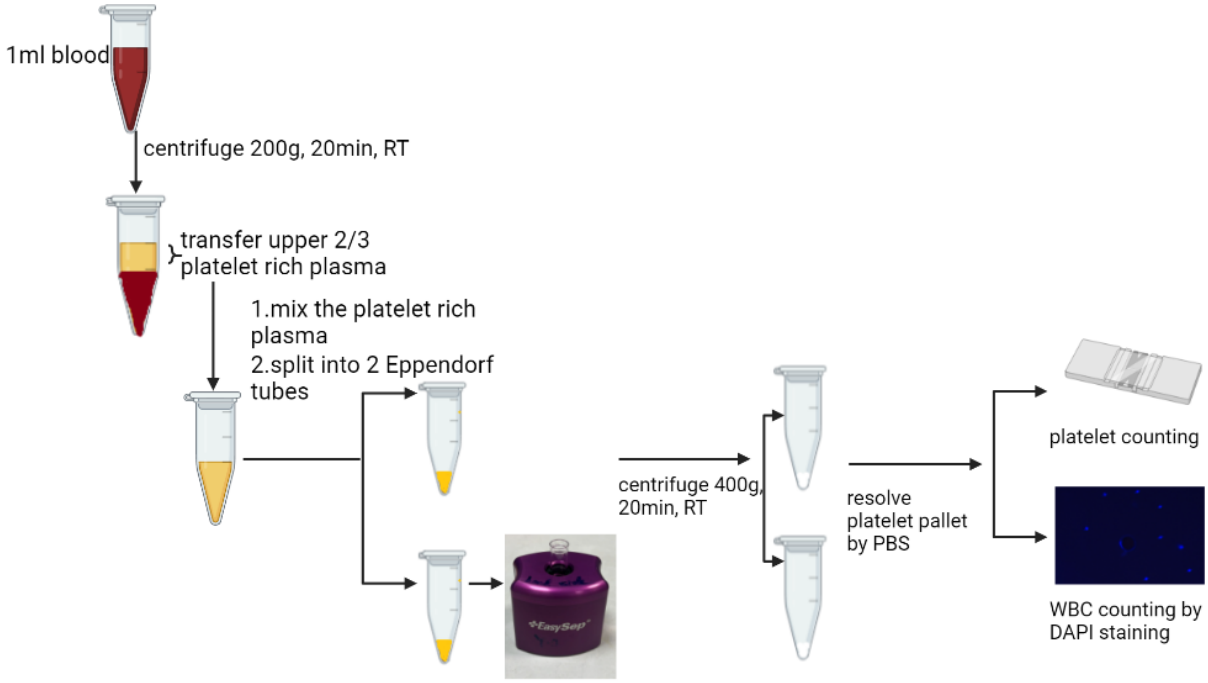

Figure 3. The workflow of the comparison of WBC contamination between magnetic beads and two-step collection methods.

Magnetic beads were added after the collection of the upper 2/3 PRP. Then further centrifugation of 400g at 20 min, platelet counting and DAPI staining were also performed. PRP: platelet rich plasma, DAPI: 4',6-diamidino-2-phenylindole.

15.3 Application of Additional Centrifugation in Platelet Collection

The total of 1.5ml whole blood of each sample was centrifuged at 200g for 20 min without brake. The upper 2/3 plasma was collected and was aliquot to three Eppendorfs evenly.

The first Eppendorf was not centrifuged (the 2-step centrifugation), while the 2nd and 3rd ones were centrifuged at an additional 100g and 200g respectively. Then the upper 2/3 plasma in three Eppendorf was further collected and centrifuged at 400g 20 min for collecting platelet pellet. The pellet was then resolved in 50μl PBS. After the mixture of suspension, 10μl

of the suspension was for WBC counting via DAPI, while another 10μl was for platelet counting via the same method mentioned before.

The lower 1/3 plasma in the three Eppendorf was also collected for WBC counting via a Countess II Automated Cell Counter (ThermoFisher Scientific, USA) (**Figure 4**).

Finally, WBC clean rates, the efficiency of platelet collection, and WBC contamination rates of different methods were calculated and compared separately.

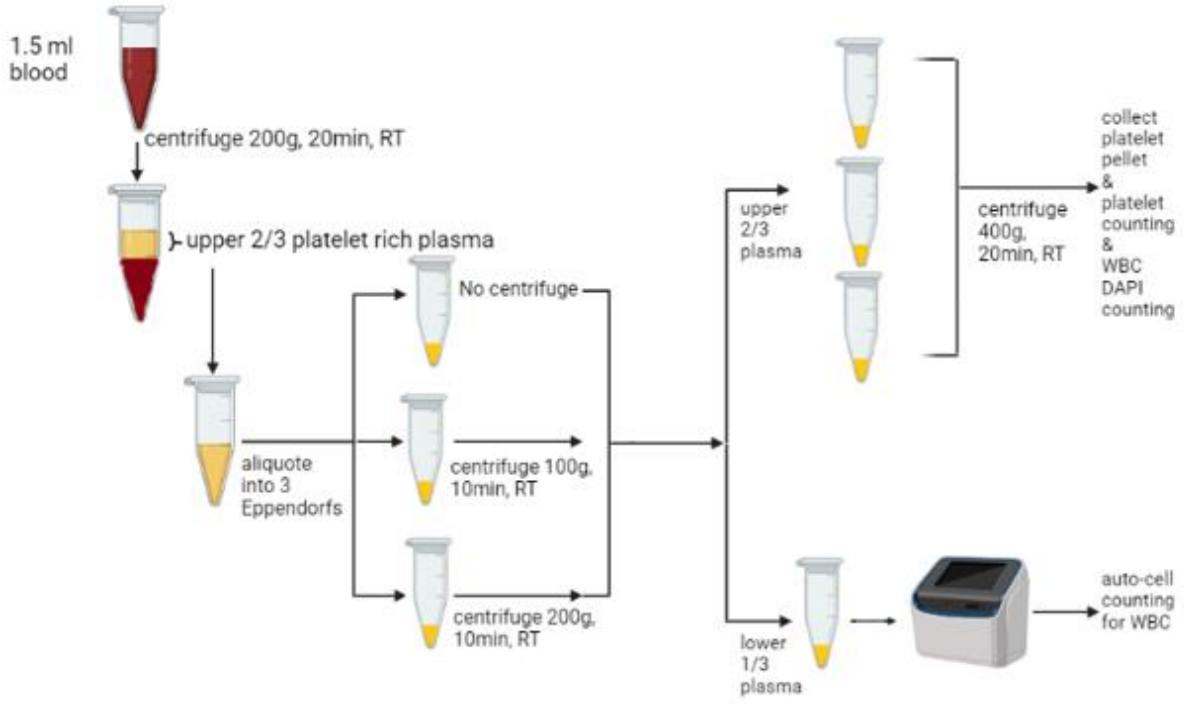

Figure 4. The workflow of the comparison between 3-step and 2-step purification methods.

An additional centrifuge (100g and 200g 10 min at RT) was added between the step of collecting the upper 2/3 PRP and the further centrifugation of 400g at 20 min, while the lower 1/3 PRP was directly used for WBC counting. RT: room temperature, PRP: platelet rich plasma, WBC: white blood cell.

15.4 Application of 3μm Filter in Platelet Collection

Each sample of whole blood was gently transferred from the vacutainer into an Eppendorf and centrifuge at 200 g at RT for 20 minutes without brake. Two-thirds of the upper layer of PRP were collected and then were gently mixed. The PRP was split into two. One received additional centrifugation at 400g for 20 min at RT to collect the platelet pellet. WBC and platelet counting was performed as the same method mentioned before.

The other half of upper 2/3 PRP was transferred to an Eppendorf, which included a 3μm membrane filter (3 μm, Ultiporn, Pall Corporation, USA) which was pre-wetted with 50μl water (**Figure 5**). The Eppendorf was centrifuged at 100g at RT for 1 minute to collect a purified PRP. The PRP was centrifuged at 400g for 20 min at RT to collect the platelet pellet. WBC (DAPI) and platelet manual counting were performed and compared as the same method mentioned before.

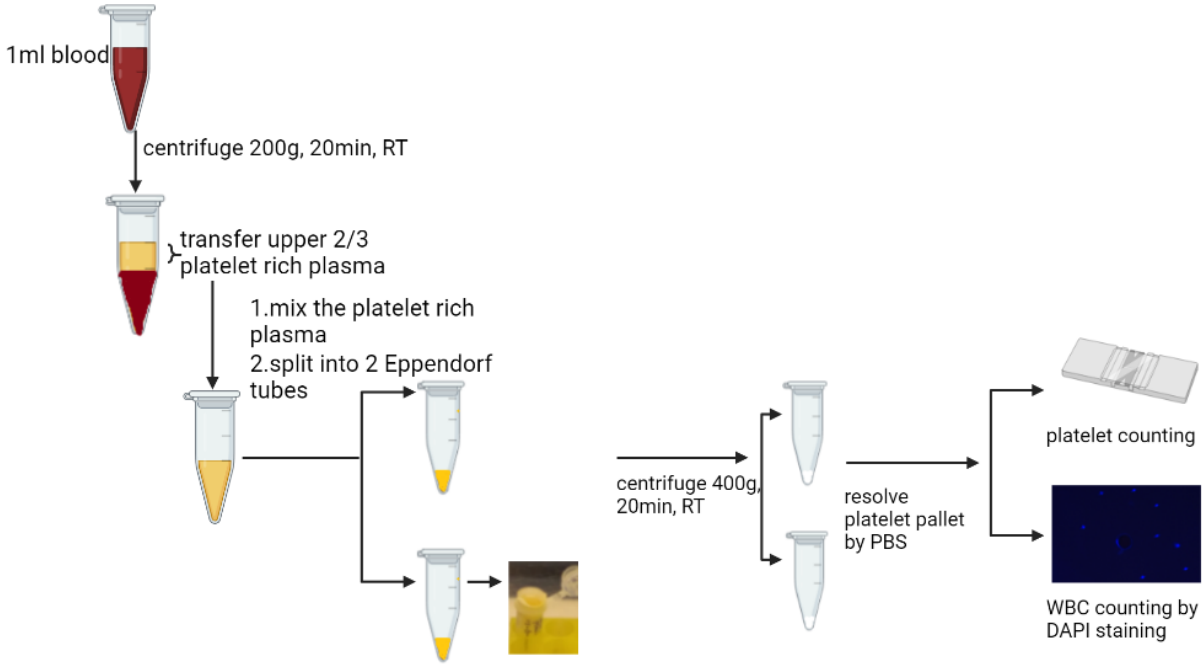

Figure 5. The workflow of new purification method with 3μm membrane filter.

After same first-step centrifugation, half of the upper 2/3 PRP was transferred to an Eppendorf with a 3μm membrane and was then centrifuged at 100g at RT for one minute to collect a purified PRP for the same second-step centrifugation. PRP: platelet rich plasma, RT: room temperature.

15.5 Application of 1μm Filter in Platelet Collection

Each sample of whole blood was gently transferred from the vacutainer into an Eppendorf and centrifuge at 200 g at RT for 20 minutes without brake. Two-thirds of the upper layer of PRP were collected and then were gently mixed. The PRP was split into two.

One received additional centrifugation at 400g for 20 min at RT to collect the platelet pellet. WBC and platelet counting was performed as the same method mentioned before (the same as the two-step centrifugation).

The other was transferred to a 1ml syringe, which was connected to a

1μm filter (Nylon Syringe Filters, 1 μm, SF18106, TISCH scientific, USA). The filter and syringe were then put in an AL-1000 syringe pump (Aladdin SyringeONE Programmable Syringe Pump, WPI, UK) in order to acquire a stable and slow speed. At the speed of 80μl per minute in the pump, the PRP passed through a filter and was collected by an Eppendorf. Then the PRP received a centrifugation at 400g for 20 min at RT to collect the platelet pellet. WBC and platelet counting were performed as the same (**Figure 6**).

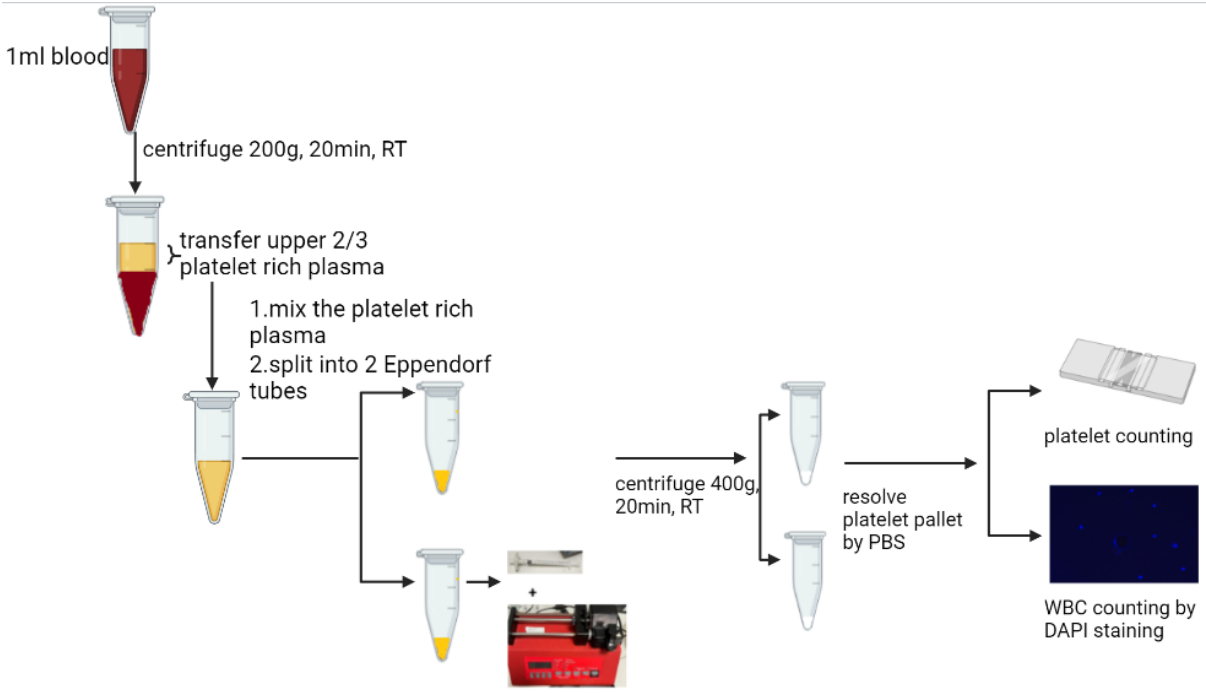

Figure 6. The workflow of new purification method with 1μm filter.

After the same first-step centrifugation, half of the upper 2/3 PRP was transferred to a 1μm filter with an AL-1000 syringe pump. Then the PRP passed through the filter and was collected. After that, the collection received the same second-step centrifugation and was analysed for platelet counting and WBC contamination. PRP: platelet rich plasma.

CHAPTER III: Platelet miRNA Sequencing and Validation for PCa Diagnostic Biomarker Development

1. Introduction

Previous research has suggested a correlation between miRNA expression changes and tumorigenesis [437], as well as demonstrated the presence of functional microRNA pathways and diverse microRNAs in platelets in relation to various non-cancer diseases or at different activities [438-440, 443]. Platelet mRNA has been reported to be changed in different cancers [352]. Based on miRNA's regulatory mechanisms to influence multiple mRNAs, we hypothesized that when interacting with PCa cells, the miRNA expression profile in peripheral blood platelets might exhibit notable changes, which could serve as an early detection marker for PCa.

A collaborative team previously conducted an experiment in China (Beijing Genomics Institute in 2018), wherein they collected platelets from 20 PCa patients and 20 non-cancer patients for RNA sequencing (RNA-seq) analysis (F18FTSECWLJ0101_HUMmuyS). Their primary objective was

to identify differentially expressed miRNAs. These findings will be summarised at the beginning of this chapter and I aim to further validate (Fluidigm multiple RT-qPCR) the differentially expressed miRNA in the UK to explore the potential in developing PCa diagnostic biomarkers.

2. Results

2.1 Small RNA-seq in China

In collaboration with a research team in China (Dr. Jiayu Gu and Prof. Ninghan Feng, Jiangnan University affiliated Central Hospital), small miRNA-seq of platelet samples from 20 Chinese PCa patients and 20 patients with benign prostate hyperplasia have been performed and differentially expressed microRNA (miRNA) between PCa and non-cancer patients have been identified. Twenty-one of most differentially expressed platelet miRNAs (p <0.001 and false discovery rate <0.1) were shown in **Table 7**.

Table 7. Differentially expressed platelet miRNAs between Chinese PCa and non-cancer patients with $p < 0.001$.

miRNA name	Log2FC	P value (Cancer vs. non-Cancer)	FDR (Cancer vs. non-Cancer)
Novel_mir1174	7.88	2.56E-16	4.41E-13
Hsa-let-7f-1-3p	3.44	9.42E-09	8.12E-0.6
Hsa-miR-5581-3p	3.81	2.55E-08	1.47E-05
Novel_mir159	5.87	4.23E-07	0.0002
Hsa-miR-378i	-6.08	6.28E-07	0.0002
Novel_mir948	2.66	2.47E-06	0.0007
Hsa-miR-1306-5p	2.49	2.79E-06	0.0007
Hsa-miR-370-3p	-1.67	9.17E-06	0.0020
Hsa-miR-378g	3.62	1.76E-05	0.0034
Hsa-miR-4685-3p	2.22	3.09E-05	0.0053
Hsa-miR-122-3p	-2.82	5.58E-05	0.0087
Novel_mir628	-2.61	6.16E-05	0.0089
Hsa-let-7e-3p	2.02	0.00011	0.0140
Hsa-miR-28-3p	1.46	0.0017	0.0206
Novel_mir1034	-2.53	0.00030	0.0400
Hsa-miR-664-3p	1.49	0.00040	0.0432
Has-miR-517-5p	2.72	0.00048	0.0470
Novel_mir323	0.95	0.00049	0.0470
Has-miR-1284	1.13	0.00054	0.0488
Has-miR-328-3p	1.29	0.00077	0.0661
Has-miR-6813-3p	-1.56	0.00090	0.0738

FC: fold change; FDR: false discovery rate; Log_2FC over 0 indicates a higher level in non-cancer group, PCa: prostate cancer.

2.2 Results of validation via Fluidigm in a larger British cohort of 206 PCa and 77 non-Ca patients

From November 2020 to July 2021, I extracted total RNA from a total of 233 platelet samples (comprising 192 from PCa and 41 from non-cancer patients) according to the aforementioned procedure. In total, 328 platelet RNA samples were extracted for future use, which includes 95 samples extracted by another team member, Jiaying Lu.

After obtaining the differentially expressed miRNAs from the Chinese RNA-seq, a British validation was performed, encompassing a cohort of 206 PCa and 77 non-Ca cases for analysis (details were included in appendix). All participants had undergone a tissue biopsy for diagnosis.

Initially, we compared the average ages of the PCa (64.8 years) and non-Cancer (63.7 years) groups, yielding a p-value of 0.38. This outcome suggests no significant difference in ages between the groups. The patient distribution includes 48 cases of clinically significant PCa (Gleason score > 3+4), 158 cases of indolent PCa, and 77 non-cancer cases. Out of all the patients, PSA levels were recorded for 258 patients, while CTC numbers were available for 198 PCa cases and 53 non-Cancer cases.

I compared the expression of five internal control genes: miR23, miR532, miR548, U6, and UniSp6, between PCa and non-cancer cases. Among

these, miR532's expression showed most stable (p=0.27) and was primarily calculated during comparison (**Table 8**).

Table 8. Expression of internal control genes (U6, UniSp6, miR32a, miR532, and miR548) in the cohort of 206 PCa and 77 non-cancer controls.

Expression of internal control genes	The cohort of 206 PCa and 77 non-cancer controls		
	PCa	Non-Cancer	p value
U6	21.06±3.83	20.14±3.95	0.07
UniSp6	16.75±10.36	12.46±9.74	0.07
miR23a	5.90±3.76	10.98±9.43	<0.0001
miR532	12.59±2.15	12.61±1.61	0.27
miR548	17.96±2.49	19.90±3.34	<0.0001

Among the five internal reference genes, miR532 exhibited the most stable expression (p= 0.27) with an acceptable standard deviation. (Expression values are represented as average ± standard deviation.) PCa: prostate cancer.

2.2.1 Analysis of miRNA Expression in PCa and Non-Cancer Patients

Five of the candidate miRNAs (miR195, 22, 28, 627 and 664) were expressed at a higher level in the non-Cancer group compared to the PCa group (all p values< 0.05). Among these five miRNAs, miR627 and miR22 showed their lowest p values< 0.0001.

Subsequently, we performed a three-step analysis in order to identify the best candidate miRNA(s) as a biomarker to distinguish PCa from non-PCa.

Firstly, AUC analysis of each miRNA was performed, which identified

miR627 as having the highest AUC of 0.6965 with *p* value less than 0.0001 (**Figure 7**). Secondly, CRSs was then calculated using different combinations of miRNAs. The combination of miR22 and miR627 resulted in highest AUC value of 0.7136, $p<0.0001$ (**Figure 8**). Finally, we compared the AUCs of CRSs consisting of miRNA combinations and other biomarkers, such as CTC number as well as PSA (**Figure 9**). The combination of miR22 and miR627 largely improved CTC's AUC value from 0.6541 to 0.7817, which was also significantly higher than the AUC of PSA alone (0.5315) in detecting PCa from non-Cancer cases in the study.

In summary, for detecting PCa from non-cancer control, the combinations of miR22, miR627 with and without CTC were chosen to make the panel as the following:

CRS without CTC number=-0.5163* (2^-ΔCTmiR22)-11.91* (2^-ΔCTmiR627)

CRS with CTC number=-0.5163*(2^-ΔCTmiR22)-11.91*(2^-ΔCTmiR627) +0.4818* (CTC number)

Compared with PSA's low specificity (16% at the cutoff of 4.0 ng/ml as well as sensitivity of 92%), using the cutoff point of -2.341 in the panel of miR22 and miR627 provided the best outcome of a sensitivity of 88.89%

with the specificity of 50.51%. Furthermore, using the cutoff point of -2.003 in the above panel with CTC number provided a close sensitivity of 88.24% and a better specificity of 62.58%.

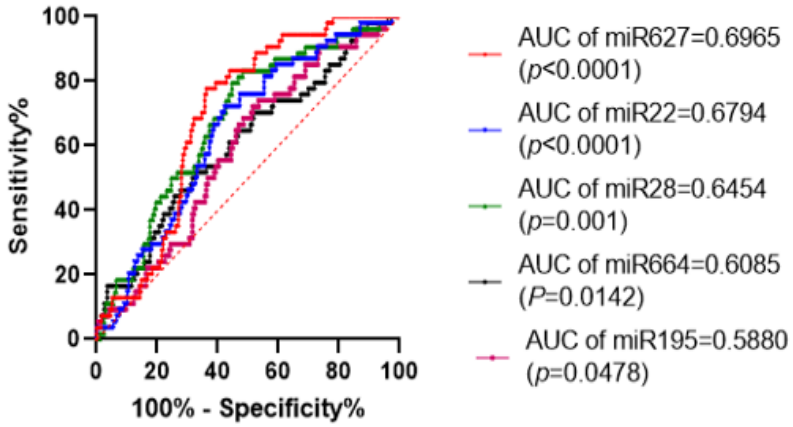

Figure 7. Comparison of miRNA expressions between PCa and non-Cancer.

The highest AUC value was found as 0.6965 in miR627 (fresh red) (p<0.0001), followed by miR22 (green) with 0.6794 (p<0.0001). PCa: prostate cancer, AUC: area under the curve.

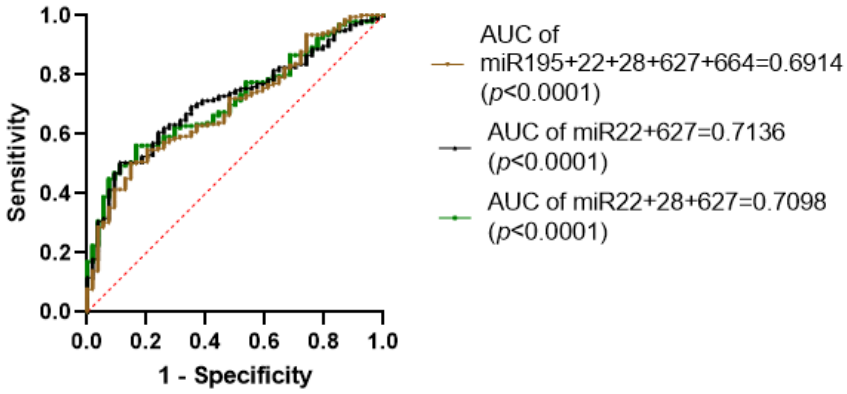

Figure 8. Comparison of different miRNA combinations between PCa and non-Cancer.

The combination (black) of miR22 and miR627 provided the highest AUC value of 0.7136 (p<0.0001). PCa: prostate cancer, AUC: area under the curve.

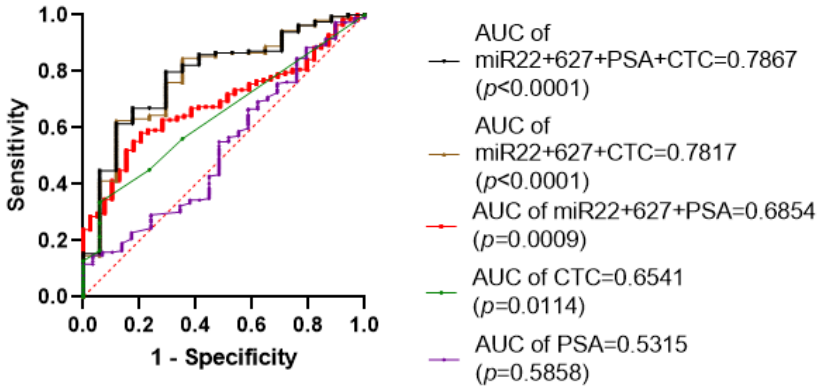

Figure 9. **Comparison of AUCs in miR22 and miR627 with other biomarkers.**

The combination (brown) of miR22 and miR627 with CTC number provided the most suitable AUC value of 0.7817. CTC: circulating tumour cell, PSA: prostate specific antigen, AUC: area under the curve.

2.2.2 Analysis of miRNA Expression in Distinguishing Aggressive PCa from Latent PCa and Non-cancer

The inability of PSA to distinguish between aggressive and latent PCa contributes to overdiagnosis and overtreatment [73]. Clinically, it is critical to identify and focus on aggressive PCa cases for effective management. In this study, candidate miRNA expression in aggressive and the rest (latent PCa and non-cancer patients) was analysed to evaluate the potential of platelet miRNA(s) as biomarkers to differentiate aggressive cancers from non-cancer and indolent patients.

I compared the expression of five internal control genes: miR23, miR532, miR548, U6, and UniSp6, between aggressive and latent PCa cases. MiR532's expression remained stable and was applied during the

following calculation. MiRNA 190 was the only significantly differentially expressed miRNAs which was highly expressed in the rest group between the two groups (p=0.0056) with AUC of 0.6299 (**Figure 10**).

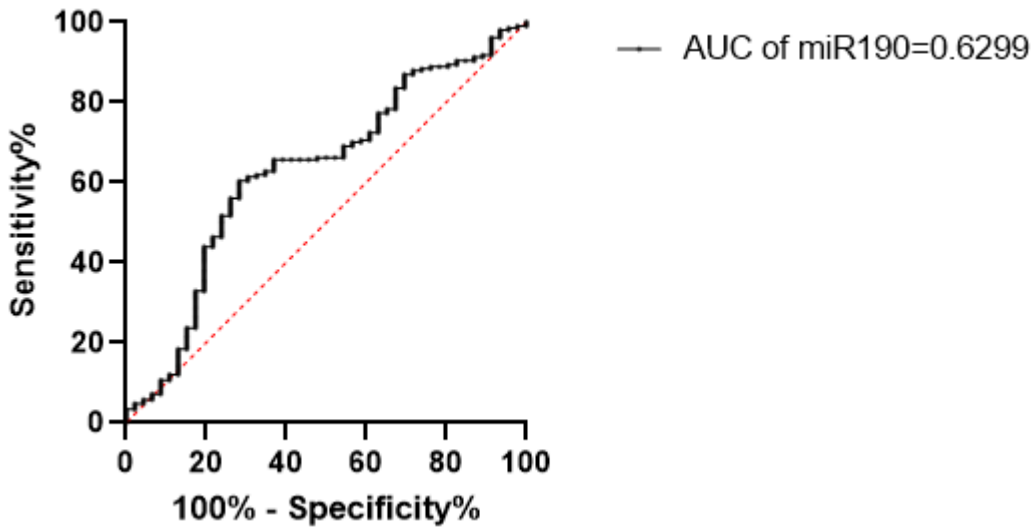

Figure 10. ROC of miR190 expression between aggressive PCa and the remaining.

AUC: area under the curve, ROC: receiver operating characteristic curve.

2.2.3 Analysis of miRNA expression in aggressive PCa and latent PCa patients

The comparison of miRNA expression between aggressive and latent PCa was also performed and significantly differentially expressed miRNAs (miR190, miR548, miR195 and miR28) between the two groups were shown in **Table 9**.

Table 9. Mann-Whitney T test of miRNAs expression in platelets between aggressive and latent PCa patients by internal control gene miR532.

control probes	Highly expressed in latent PCa	P value	Highly expressed in aggressive PCa	P value
miR532	miR190	0.0033	miR195	0.0452
	miR548	0.0266	miR28	0.0336

PCa: prostate cancer.

To determine the optimal candidate miRNA(s) for aggressive PCa detection, I performed a ROC analysis on each candidate miRNA. The miRNA with the highest area under the curve (AUC) was miR190 (AUC=0.6412, *p*=0.0033) (**Figure 11**), which showed higher expression in the latent PCa group.

Interestingly, combinations of miRNA candidates did not enhance detection over miR190 alone. However, a combination of miR190, CTC count, and PSA offered an improved AUC value of 0.77 ($p<0.0001$), outperforming PSA alone (AUC=0.7534) (**Figure 12**).

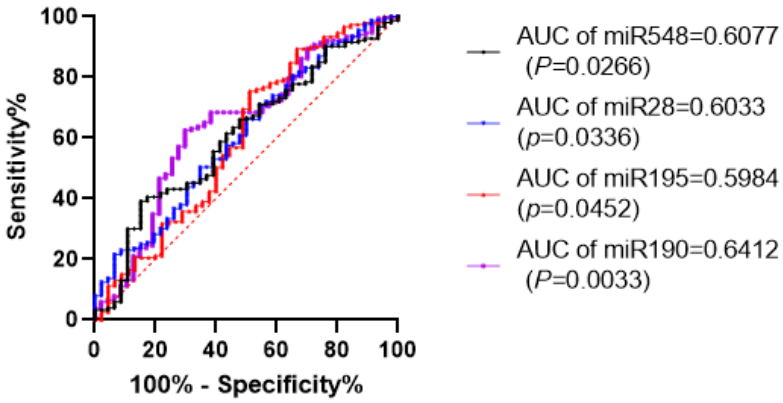

Figure 11. Comparison of miRNA expressions between aggressive and latent PCa.

MiR190 (purple) had the highest AUC value of 0.6412 (p=0.0033) in the four miRNA candidates. PCa: prostate cancer, AUC: area under the curve.

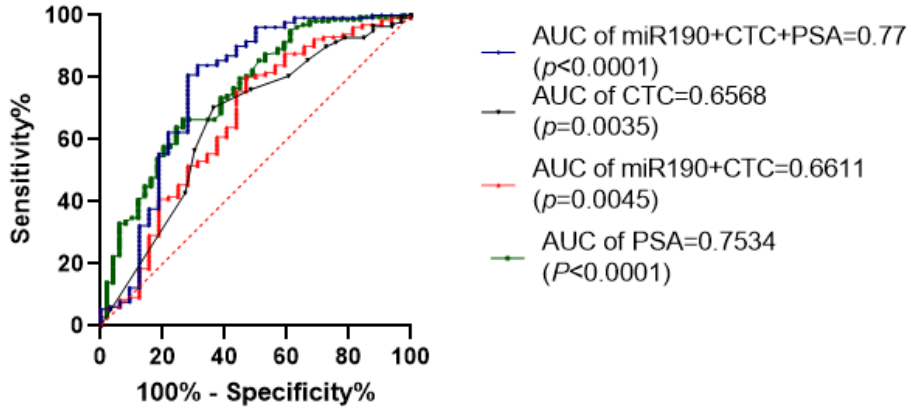

Figure 12. Comparison of AUCs in miR190 with other biomarkers.

The combination of miR190 with CTC and PSA (blue) showed the highest AUC of 0.77, while PSA (green) provided the AUC of 0.7534. PCa: prostate cancer, AUC: area under the curve, PSA: prostate specific antigen.

In summary, while miR190 alone (AUC=0.6412) underperformed against PSA (AUC=0.7534) in detecting aggressive from latent PCa, the combination of miR190, CTC count, and PSA further enhanced PSA's detection accuracy (AUC=0.77). This led to the following panel development:

CRS-2 = -0.7199*(2^-ΔCTmiR190) +0.07105*CTC number+0.0399*PSA

A cutoff point of -0.07563 provided a balanced sensitivity (80.77%) and specificity (71.88%) for aggressive PCa detection.

2.2.4 Results of the target genes of miR190

MiRNAs play crucial roles in various biological processes, including the regulation of gene expression. To gain insights into the potential impact of miR190a-5p, we sought to predict its downstream target genes. For this purpose, we used a well-established suite of bioinformatics tools, miRWalk, which includes two primary databases: TargetScan and miRDB. These databases utilize different algorithms to predict miRNA targets, thus, we consolidated the results to ensure predictions, focusing specifically on genes that were jointly identified by both.

Understanding the roles these target genes play in cancer development is critical to interpreting the potential impact of miR190. Given the reduced expression of miRNA190a-5p in the aggressive PCa group in this study, we posited an oncogenic role for the predicted genes. A comprehensive review of the existing literature for the predicted genes was conducted. Genes reported as oncogenes in published studies were highlighted for further investigation. Then 'The Human Protein Atlas' (https://www.proteinatlas.org/), an open-access resource was utilized to

provide information on the normal and cancer tissue-specific expression of proteins. This allowed us to examine the selected oncogenes' expression profiles in both normal and cancer tissue, adding another layer of complexity to our understanding of miR190's potential role in cancer.

Eleven genes were consistently predicted by both TargetScan and miRDB: *TRPS1*, *PAX6*, *MYO5A*, *PARP8*, *SMAD2*, *NUCKS1*, *PLD1*, *ZNF207*, *HMGA2*, *YARS1*, *and KIF2A*. Given that miRNA190a-5p showed lower expression in aggressive PCa in this study, we hypothesized that its target genes would exhibit oncogenic properties. A literature review revealed *SMAD2* [448-451], *PLD1* [452-457], *HMGA2* [458-464], and *KIF2A* [465] as documented oncogenes. These genes were then analyzed for their expression in both normal prostate tissues and PCa tissues using 'The Human Protein Atlas'. Moreover, I conducted a comparison of survival curves between high and low expression of these genes from the same database ('The Human Protein Atlas') (**Table 10**).

After analyzing gene expression in prostate tissue and the correlation with prognosis in survival curves, the high-mobility group AT-hook 2 gene (HMGA2) emerged as the most promising target gene for miR190. Generally, *HMGA2* demonstrated medium staining (indicating higher

expression) in prostate cancer tissue compared to the low staining in normal prostate tissue (**Figure 13**). Additionally, *HMGA2* expression correlated with poor prognosis (p=0.033) (**Figure 14**). The higher expression in PCa and its association with poor prognosis make HMGA2 a compelling candidate gene for miRNA190a-5p.

Table 10. List of the expression of four targeted genes of miR190a-5p in normal prostate tissue and prostate cancer tissue and the correlation between gene expression level and patient survival.

	Expression in normal prostate tissue	Expression in prostate cancer tissue	Poor prognosis in survival curve (*p* value)
SMAD2	high	medium	0.049
PLD1	low	high	NA
HMGA2	low	medium	0.033
KIF2A	Not detected	low	NA

HMGA2 showed higher expression in prostate cancer tissue with the poor prognosis (*p*=0.033). (data from https://www.proteinatlas.org)

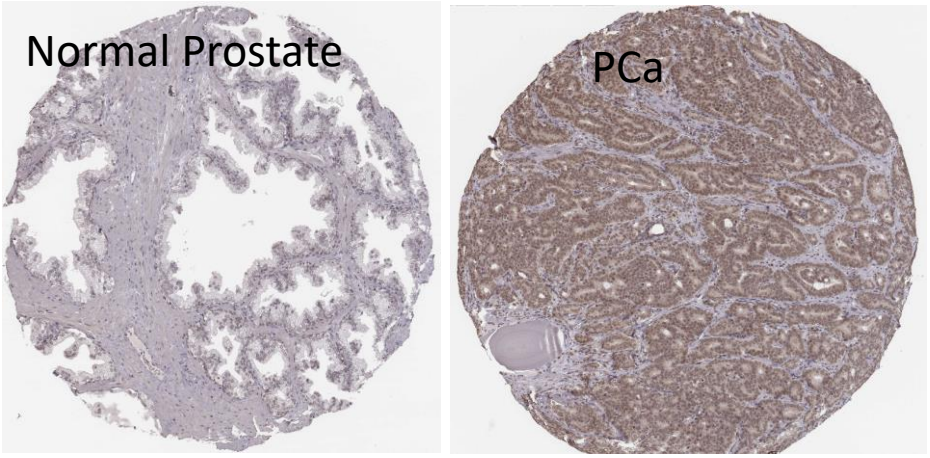

Figure 13. Expression of HMGA2 in normal prostate tissue and PCa tissue.

The expression in normal prostate tissue (left) is low, while it is high in prostate cancer tissue (right). (data from https:// https://www.proteinatlas.org/, image credit: Human Protein Atlas, image available from v 23.0. proteinatlas.org) PCa: prostate cancer.

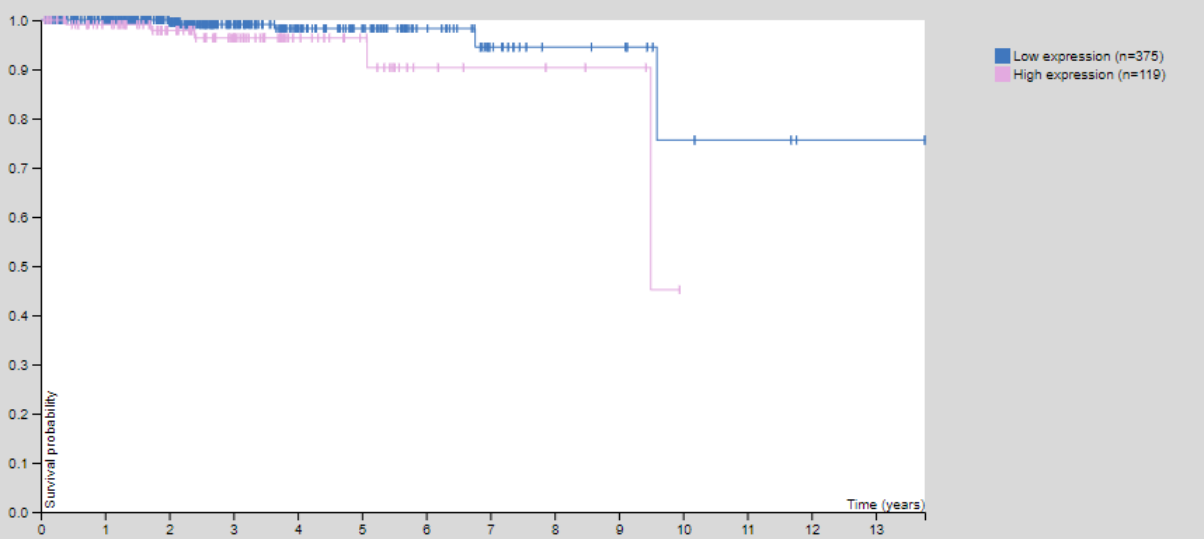

Figure 14. The survival curve of PCa patients with low and high expressions of HMGA2.

PCa patients with high expression of HMGA2 showed a poorer prognosis (p=0.033). (data from https://www.proteinatlas.org, data available from v 23.0. proteinatlas.org) PCa: prostate cancer.

3. Discussion

3.1 Small RNA sequencing

Both *p* value and FDR were used to help determine which miRNAs are differentially expressed between PCa and non-cancer groups in the RNA-seq.

The p-value describes the probability that in the data of the miRNA-seq, the null hypothesis is typically that there is no difference in the expression of a particular miRNA between the two groups. Here *p* value less than 0.05 indicates that the likelihood of the data arising by chance (assuming the null hypothesis is true) is low, therefore providing evidence against the null hypothesis.

The FDR is a method used to correct for multiple comparisons. In a miRNA-seq experiment, when the expression of thousands of miRNAs was compared, some statistically significant results just were achieved by chance (false positive) [466]. The FDR is a way of controlling for these false positives. A commonly used method to control the FDR is the Benjamini-Hochberg procedure [467]. A smaller FDR means that it is less likely to be making false discoveries.

In summary, *p* values provide an initial measure of statistical significance,

while FDR is used to correct for multiple testing and control the rate of false positives. Therefore, with the joint help of these two parameters, differentially expressed miRNAs were selected from the RNA-seq.

3.2 Validation in the British cohort of 206 PCa and 77 non-Ca patients

3.2.1 Patient Selection in the Cohort of 206 PCa and 77 Non-cancer Patients

Age difference has been reported as a significant confounding factor that could potentially contribute to disparities observed between cancer and non-cancer patients [120]. If, for instance, the majority of the non-cancer control group comprises younger donors, this age discrepancy may directly influence the outcome of the results. In this study, however, we've controlled for this factor. The average age of the prostate cancer (PCa) patients was 64.8 years, closely mirroring the non-cancer group's average age of 63.7 years (p=0.38). Thus, we've minimized age-related bias in our results, eliminating the need for further age adjustment prior to analysis.

Our primary clinical question revolves around distinguishing patients with PCa from those with benign diseases such as benign prostate hyperplasia and prostatitis. This question is crucial for the early detection of cancer [468]. Accordingly, our study's design has been tailored to address this clinical concern, incorporating patients who were suspected of having

PCa and had undergone age-matched prostate biopsy.

In my validation study of different miRNAs, the ratio between PCa and non-cancer is about 2.68:1 (206 PCa patients vs. 77 non-Cancer patients). The ratio between different groups is crucial for minimizing bias and ensuring statistical validity. An acceptable ratio often ranges between 1:1 and 2:1 for either group, as this helps to reduce potential biases and maintain sufficient statistical power. Ratios deviating from this range may introduce biases, such as increased false positives or negatives, which can compromise the study's integrity.

Therefore, in my study, the ratio of 2.68:1 might have led to an overestimation or underestimation of the association between specific miRNAs and cancer, potentially resulting in false positives or negatives, respectively. Although the sequencing phase maintained a balanced ratio of 1:1, this balance does not automatically mitigate potential biases arising in the subsequent validation phase. However, the balanced initial phase does add a degree of credibility to the findings, suggesting that the identified miRNAs are of genuine interest and not merely products of an imbalanced group effect.

To enhance the reliability, validity, and applicability of the study's findings, addressing the sample imbalance is essential. Future adjustment may

include:

Balancing the Ratios: Aim to increase the number of non-cancer samples or reduce the number of cancer samples in future studies to achieve a closer approximation to the desired ratio. This adjustment will help align the study more closely with standard practice and reduce bias.

Applying Statistical Adjustments: Implement techniques such as weighted analysis in the validation phase, where individuals from the underrepresented (non-cancer) group could be assigned more weight to counterbalance the analysis. This approach can help mitigate the impact of the imbalance and make the study's conclusions more robust.

Conducting Sensitivity Analysis: Perform statistical comparisons under different ratios of cancer to non-cancer patients to assess the sensitivity of the results to sample imbalance. Consistency in findings across various scenarios would indicate that the results are robust against the imbalance, lending greater confidence in the study's conclusions.

These strategies aim to correct the noted imbalance and should be considered critical components of future research design and analysis to ensure the production of reliable and generalizable results.

Furthermore, in my validation study, the observed proportion of clinically significant prostate cancer (PCa) was 23% (48/206). This figure is an

estimate of the true proportion in the broader population; hence, it is subject to sampling error, which refers to the discrepancy that arises from analysing a sample instead of the entire population. Due to this, there is inherent uncertainty around this estimate.

To address this uncertainty and assess the reliability of our sample proportion, confidence intervals (CIs) was added. The 95% confidence interval for the proportion of clinically significant PCa in my study was calculated to be approximately 17.25% to 28.75%. This range is consistent with proportions reported in other studies, supporting the conclusion that the proportion of clinically significant PCa samples in the cancer group of our validation study is statistically reasonable. This agreement with existing research reinforces the validity of our findings and suggests that our sample provides an accurate reflection of the true distribution of clinically significant PCa [469].

3.2.2 The Choice of Fluidigm Multiple RT-qPCR

Potential bias in RNA-seq experiments can be induced by factors such as selective amplification and variations in library preparations, not to mention the influence exerted by subsequent data interpretation. RT-qPCRs, employing TaqMan and SYBR Green methods, deliver highly accurate and specific evaluations of predetermined targets [302].

Therefore, to validate those miRNAs found in Chinese patients, these methods were used to confirm profiling data derived from the RNA-seq experiment in British platelet samples.

Fluidigm® BioMark microfluidic system was used in our study, which is an automated, high-performance qPCR system. It applies microfluidics technology to process samples at nanoliter-scale volumes for multiple qRT-PCR [470]. Its microfluidic technology is based on dynamic arrays of integrated fluidic circuits (IFCs). There are thousands of controlled valves and interconnected channels in IFCs. By the patterns in IFCs, molecules of samples and reagents can be mixed accordingly. A typical chip format from Fluidigm is capable of building 9,216 PCR reactions (96.96 chip format; 96 samples × 96 assays) in one qPCR run[471]. Besides, Fluidigm system reduces the requirement of the reaction volume from 10 μL–20 μL down to 10nL scale, making it more cost-effective and less time-consuming[470]. In the study, regarding multiple targeted miRNAs, this method largely saved materials and time.

Compared to traditional PCR technology, Fluidigm system uses microfluidic chips with a pre-determined layout for samples and assays, causing limited flexibility. However, these multiple tests could still cause potential bias. Once a chip is loaded and running, it cannot be paused,

modified, or added to. Furthermore, due to Fluidigm's chip-specific layout, the number of reactions is fixed by the type of chip used (for example, in the study, 96.96 chip was used for 96 samples against 96 assays), meaning that for smaller experiments, there can be a significant number of unused reaction chambers.

3.2.3 The Choice of the miRNA Targets for Fluidigm Multiple RT-qPCR

To a fixed 96.96 chip, there could be 96 RT-qPCRs performed at maximum. Considering three biological replicates, 32 targets could be chosen for the maximum utility in one 96.96 chip. Due to the accessibility of miRNA primers in the preparation for the Fluidigm multiple RT-qPCR, totally, 30 miRNAs were selected from the previous Chinese RNA-seq for further validation by Fluidigm, including the first three novel miRNAs. U6 and Unisp6 were also included in the Fluidigm as the internal control genes. In this way, the final 32 targets were confirmed.

3.2.4 The Choice of Endogenous Control Genes in the Data Analysis

In this study, five endogenous control genes—U6, UniSp6, miR548, miR532, and miR23a—were utilized. Reference genes are essential to normalize qPCR data and account for variability introduced during the experimental process [472]. U6 and UniSP6 are frequently employed in miRNA studies due to their typically stable expression across diverse

conditions and samples. However, their expression can vary depending on the specific experimental setup, tissue types, and disease states [473]. Thus, the stability of these commonly used controls was evaluated before their use as reference genes in this study.

Since the selection of reference genes does not have a "one-size-fits-all" solution [474], all the five candidates of reference genes were compared in the study. On one hand, both U6 and UniSp6which are commonly used in miRNA analysis exhibited a marginal variability in the Fluidigm results (both p=0.07). Moreover, UniSp6 has a high standard deviation. On the other hand, miR532 from the three (miR548, miR532, and miR23a) miRNAs which demonstrated relatively consistent expression across all samples based on the miRNA sequencing data showed its stability (p=0.27) with low standard deviation. Consequently, miR532 was treated more reliable as the internal control gene than others. And the stability was further confirmed via different grouping, such as the comparison between aggressive and the rest groups or between aggressive and latent groups. To enhance the reliability of results and prevent misinterpretation, miR532 was prioritized to normalize Fluidigm (RT-qPCR) data. Subsequent calculations, including AUC, combination, and comparison, were based on miR532 accordingly. Additionally, in the following analysis

between aggressive and the rest (p=0.52) or latent PCa (p=0.73), the stable expression of miR532 was also confirmed.

In summary, in the context of analyzing platelet miRNAs in PCa in this study, U6 and UniSP6, despite being commonly used, were not the best controls compared to miR532 due to the stability of expression. This finding may help to identify a new set of internal control genes for further analysis of platelet miRNAs in qPCR studies.

3.2.5 Potential Reasons for Low Rate of Differentially Expressed miRNAs Validated by Fluidigm qRT-PCR

Both of the results from the Chinese sequencing and the British validation showed differentially expressed miRNAs in platelets between PCa and non-Cancer groups, supporting the project's hypothesis of RNA change during the interaction between platelets and PCa. The positive result is also instrumental in designing a larger validation to build better statistical outcome due to the case limitation of the Fluidigm test.

However, compared to multiple differentially expressed miRNAs in the Chinese sequencing data, only five out of 30 miRNA candidates have been shown lower expression in the PCa group of validation.

Several causes could potentially explain the difference.

First, it could be the result of ethnic variation. In contrast to the high incidence of PCa in the UK (173/100,000 rank first with 26% in new male malignancy in 2017 from CRUK), China has a low incident rate of PCa [26, 475] (7.1/100,000 rank 7th in new male malignancy in 2015 [476]). Although there is a rapid increase of PCa in China in recent years, the disparity between China and Western countries remains [477] and the basis for this is unknown. Additionally, distinct genomic alterations [478] and environmental factors [30, 32] may contribute to the difference. 10% of PCa risk single-nucleotide polymorphism previously identified in European data could be successfully confirmed in Asian group. The racial difference was also confirmed by the other publication which found different risk loci of PCa in Chinese men [479]. Different risk loci might imply that the different pathways of tumour development could exist, providing a window to deeply understand racial differences in PCa [480]. The difference might also imply genetic and molecular alterations which play important roles in disparity between different racial groups of PCa [481].

Second, bias could be easier formed due to a small-size study. There are only 20 PCa and 20 non-cancer cases in the Chinese miRNA-sequencing, reaching the minimum request of sequencing. This small size could

decrease the statistical power by increasing the margin of error.

Finally, different detection technology has different detection sensitivity and limitation. For example, the primer set used for qRT-PCR are custom designed and may not be perfect, resulting in unreliability in those RNAs with low expression level (low reads). Hence, there could be different results upon the same sample group from Fluidigm multiple RT-qPCR and RNA-seq.

3.2.6 Analysis of differentially expressed miRNAs between PCa and non-Cancer control in the cohort of 206 PCa and 77 non-cancer patients

3.2.6.1 Analysis of Single miRNA in the Cohort

My analysis of AUC for each miRNA candidate revealed that miR627 had the highest AUC value of 0.6965, closely followed by miR22 at 0.6794 and miR28, miR664 and miR195 (0.6454, 0.6085 and 0.5880). When it comes to biomarker development, AUC values can be interpreted as follows: an AUC between 0.8 and 0.9 signifies good performance, while an AUC between 0.7 and 0.8 denotes fair performance, and an AUC ranging from 0.6 to 0.7 indicates poor performance [482]. In this study, the AUC values of the individual miRNAs suggest that a single platelet miRNA biomarker may only be able to distinguish between prostate cancer (PCa) and non-cancerous states to a limited extent, resulting in less-than-optimal AUC

values.

3.2.6.2 Panel Development

Cancer represents a multifaceted ailment, making it improbable for a solitary genetic abnormality to adequately encompass the complexities within a tumour, thus providing sufficient diagnostic information for clinical decisions. However, combining these miRNA biomarkers, each potentially illuminating a special facet of the disease, could pave the way for more accurate diagnoses.

The study experimented with various combinations among these five miRNA candidates, finding that a panel combining miR22 and miR627 offered the highest AUC value of 0.7136, elevating the performance from poor to fair. The enhanced AUC value from this combination suggests that each miRNA provides unique insights into the disease's state, and collectively, they give a more comprehensive view of the disease, which is a commonly observed concept in multi-marker diagnostic assays [483]. The five miRNAs' low expressions in the PCa group implied the potential role as suppressor genes. The findings of miRNAs could inspire new research questions. For example, why do these specific miRNAs have such a significant impact on prostate cancer detection? Understanding the underlying mechanisms might lead to further improvements in diagnostic

tests, or even suggest new targets for treatment. Finally, the combination of miR627 and miR22 could provide a sensitivity of 88.89% and a specificity of 50.51%. The improvement of the specificity (PSA's specificity: 16%) for PCa detection could be helpful to avoid more unnecessary prostate biopsy.

Our research then focused on refining the miRNA panel. Available data provided us with Circulating Tumour Cell (CTC) counts for 198 out of 206 PCa cases and 53 out of 77 non-cancer cases as well as PSA in blood samples. The decision to incorporate the CTC number into the panel is informed by findings across various cancers. It's been observed that CTCs can be detected during the early stages of diseases such as breast cancer [206-208], lung cancer [209, 210], and colorectal cancer [211-213]. Specifically regarding PCa, studies have shown that asymptomatic PCa patients, particularly those with a family history of cancer or of advanced age, reported positive CTC counts in approximately half of the participants [222]. Furthermore, prior research by our team identified the presence of at least one CTC in roughly 30% of latent and over 50% of aggressive PCa patients in the early stage [223]. Given these attributes of CTCs, their inclusion in the panel was anticipated to boost its specificity, prompting us to incorporate CTC numbers into the panel's development. Finally, a panel

comprising miRNA22, miRNA627, and the CTC count was developed, which yielded the highest AUC value of 0.7817, nearing the criterion for a good AUC performance at 0.8. The panel with CTC number then provided a slightly decreased sensitivity of 88.24% as well as a better specificity of 62.58% compared to the miRNA combination alone. With the help of CTC's tumour specificity, the addition to miRNA combo further enhances the panel's specificity of more than 10% at the expense of a slight decrease in sensitivity due to the low detection rate in the PCa [223]. Thus, including CTC count in our panel gives more potential of the panel for early cancer detection. This panel could potentially lead to an increase in early detection rates of PCa, which in turn could result in less unnecessary biopsy.

While this study has its limitations—such as the limited AUC value of the platelet miRNA combinations solely or with CTC—the discoveries offer a fresh perspective for future cancer detection methodologies. Even though the results may not be immediately ready for clinical application, they do underline the potential utility of platelet miRNA as a component in the development of a comprehensive cancer detection panel.

In cancer diagnostics, there are precedents for the beneficial use of combined markers that individually might not yield substantial information.

For instance, in evaluating indeterminate lung masses identified by computed tomography-positron emission tomography (CT-PET), a combination of previously known but individually uninformative biomarkers has proven beneficial [484]. In the context of prostate cancer, an interesting parallel can be drawn with prostate cancer gene 3 (PCA3). While PCA3 had limited individual value in detecting prostate cancer (with a sensitivity of 64% and specificity of 76% at a cut-off of 35), it was found to enhance the specificity of PSA screenings [485]. This reinforces the potential role of platelet miRNA in the development of a multi-faceted approach to prostate cancer detection. Further trial may be focused on searching other markers to boost the panel's prediction.

3.2.6.3 Comparison to PSA

In comparison to the low AUC value of PSA (0.5315) in the study, both miRNA panel (miR22 and miR627) and the panel incorporating CTC count demonstrated substantially higher AUC values (0.7136 and 0.7817 respectively), emphasizing the potential of miRNAs for prostate cancer detection. These findings could be particularly significant for early prostate cancer diagnosis. Considering our samples were predominantly obtained from clinical visitors, who might already be symptomatic or have other benign prostate diseases such as BPH or prostatitis, their PSA levels

could be potentially higher than asymptomatic individuals screened in the general population. This could explain the relatively lower AUC value of PSA in distinguishing between prostate cancer and non-cancer cases in this study.

Compared to the reported PSA' sensitivity of 92% and a specificity of 16%, the miRNA panels, with and without CTC count, delivered a close sensitivity (over 88%), whilst a relatively high specificity (approximately 50% and 62% respectively). The miRNA panel could be used because of its improved specificity, avoiding more unnecessary tissue biopsy. Striking a balance between higher sensitivity and potential costs of lower specificity is key to achieving an acceptable positive predictive value of >10% [111]. Future attempt could look for a better balance following a new combination.

Generally, the results showed that platelet miRNA could make up for current PSA's low specificity and to build a panel with other markers for PCa detection.

3.2.7 Analysis of MiR190 for the Detection of Aggressive PCa groups

The final goal of cancer biomarker is to enhance patient care and health outcomes. Regarding the prognosis of PCa, patients of aggressive PCa (Gleason score > 3+4) have a clear worse prognosis. Further analysis of the study was performed in the evaluation of platelet miRNA's detection

of aggressive PCa.

In the findings, miR190 was lowly expressed in the aggressive PCa group (AUC=0.6412, p=0.0033). Additionally, the combination of miRNA190, CTC number and PSA provided an AUC of 0.77. While the study brings to light promising correlations, it also underscores some challenges in using miRNAs as diagnostic biomarkers for aggressive PCa.

The analysis revealed that the use of miR190 alone as a biomarker for aggressive PCa provided no significant improvement over traditional PSA testing (AUC: 0.65 and 0.75 respectively). This highlights the inherent difficulty of identifying biomarkers that outperform PSA, which despite its limitations, remains a robust indicator for aggressive PCa.

The combination of miR190, CTC count, and PSA offered an AUC of 0.77. It indicates that the integration of these factors does not translate to significant gains in sensitivity and specificity in the detection of aggressive PCa.

Interestingly, the combination of different miRNA candidates did not enhance the detection of aggressive PCa beyond what was achievable with miR190 alone. This could suggest a lack of synergistic interaction between the miRNAs in influencing the disease phenotype or could be due to the complex regulatory networks of miRNAs, where different

miRNAs can target the same genes and vice versa. This complexity might have diluted the potential cumulative effect of combined miRNAs. Understanding the underlying mechanisms of miRNA regulation in PCa could also shed light on why some combinations of miRNAs fail to improve detection accuracy.

HMGA2 is frequently amplified in human cancers, and in PCa, *HMGA2* messenger RNA was significantly elevated ($p<0.05$). Moreover, it was more prevalent in the high Gleason grade group ($p<0.05$) [458]. *HMGA2* was found to stimulate the expression of human telomerase reverse transcriptase, which in turn enhanced telomerase activities and increased telomere length. The upregulation of *HMGA2* may be linked with telomere maintenance for tumorigenesis [459]. In pancreatic cancer, knockdown of HMGA2 inhibited cell proliferation [486]. In LNCaP, DU145 or PC3 cell lines, downregulation of HMGA2 could inhibit cellular proliferation, invasion, and metastasis, and improve cellular apoptosis [458, 460-464].

In summary, after a comprehensive analysis of miR190's downstream gene, HMGA2 emerges as a promising candidate.

CHAPTER IV: mRNA Sequencing of Platelet from PCa and Non-Cancer Patients

1. Introduction

Following the success of miRNA analysis, the next step of my study turned to the platelet mRNA. Prior research indicated that platelet may interact with cancer with RNA alternation [352, 421, 422]. Platelet mRNAs exhibited differential expression between other cancer patients and controls, suggesting their potential as diagnostic markers [351, 352]. Therefore, in this project, mRNA expression profile in the platelets of peripheral blood was hypothesized changed significantly when interacting with PCa cells and was valuable for early detection of PCa. Therefore, platelets from 20 PCa patients and 20 non-Ca patients were collected and extracted for further mRNA-seq analysis to identify differentially expressed mRNA.

Regarding total RNA extraction from platelets, miRNeasy Micro Kit (Qiagen, UK) was applied. The SMARTer-seq V4 (Takara, Japan) (SSV4) PLUS kit was used to preamplify the total RNA in the Barts and the London Genome Centre core facility. The RNA sequencing process was then executed on the Illumina NextSeq 500 platform. The results and analysis

will be introduced in the following paragraphs.

2. Results

2.1 Results of Platelet RNA Sample Preparation

The 20 RNA samples from PCa and 20 samples from non-cancer patients were selected (**Table 11**).

Table 11. Details of RNA quality and quantity measured by Bioanalyzer and Nanodrop in the final 40 cases for RNA-seq.

Sample ID	Nanodrop conc (ng/ µL)	260/280	260/230	RIN Score	Bioanalyser conc (ng/µL)	Total RNA yield (ng)
PPPP017	72.38	1.96	1.14	7	18.5	148
PPPP047	36.1	2.17	0.71	7.2	4	32
PPPP049	42.11	1.91	0.58	8.2	16	128
PPPP053	32.58	1.74	0.82	7.1	5	40
PPPP056	35.43	1.72	0.59	7.2	6	48
PPPP063	36.46	1.81	0.47	7.9	8	64
PPPP067	26.12	1.87	0.19	6.7	6.8	54.4
PPPP074	37.07	1.82	0.88	8.9	7	56
PPPP122	40.52	1.71	0.68	8.4	6	48
PPPP123	58.4	1.81	0.39	8.5	2.193	17.544
PPPP127	54.27	1.9	0.88	8.9	13	104
PPPP139	22.74	1.83	0.83	6.3	4.4	35.2
PPPP141	18.58	1.73	0.39	7.9	4	32
PPPP153	31.92	1.79	0.96	8.3	0.66	5.28
PPPP156	65.29	1.86	0.15	8	2.4	12
PPPP164	79.67	2	0.67	6.9	23.9	191.2
PPPP170	56.75	1.82	0.3	7.2	1.9	9.5
PPPP178	49.17	1.82	0.21	8.5	2.138	17.104
PPPP216	35.7	1.75	0.29	7.7	0.7	3.5
PPPP257	41.91	1.75	0.49	7.8	13	104
PPPP267	49.23	1.89	0.71	7.7	17.4	139.2
PPPP272	41.44	1.97	0.35	8.4	14.6	116.8
PPPP278	38.38	1.95	0.41	7.4	11.9	95.2

PPPP279	32.54	1.77	0.28	7.3	8.9	71.2
PPPP294	39.8	1.88	0.97	6.9	15.3	122.4
PPPP308	35.36	1.84	0.22	7.4	0.5	2.5
PPPP310	63.78	1.9	0.39	8.2	1.7	8.5
PPPP316	73.72	1.87	0.36	7	2.1	10.5
PPPP329	64.35	1.9	0.95	7.8	3.8	19
PPPP338	42.83	1.82	0.67	8.1	1.5	7.5
PPPP341	49.54	1.89	0.24	7.6	2.5	12.5
PPPP342	49.59	1.93	0.11	8.8	12	60
PPPP343	43.98	1.77	0.12	7.5	0.9	4.5
PPPP344	33.92	1.63	0.26	6.7	0.6	3
PPPP347	32.05	1.89	0.33	7.3	1.3	6.5
PPPP348	54.19	1.8	0.47	8.2	1.8	9
PPPP350	58.17	1.74	0.37	7.8	1.9	9.5
PPPP355	42.2	1.79	0.1	8.1	1	5
PPPP356	39.54	1.78	0.27	7.5	0.9	4.5
PPPP361	74.95	1.9	0.68	8.2	2.1	10.5

RIN: RNA Integrity Number.

2.2 Results of Quality and Quantity Control for RNA Extraction from Platelets

2.2.1 Evaluation and Improvement of Platelet RNA Extraction Quality: A Comparative Analysis of Two Extraction Rounds

To assess the quality of platelet RNA extraction, all six samples extracted in the first round were sent for analysis. Four out of six RNA samples (PPPP307, PPPP321, PPPP352, and PPPP359) were initially analyzed

by the Bioanalyzer at Barts Cancer Institute, yielding low RIN scores (**Table 12**). Two additional samples, PPPP104 and PPPP108, were included in a secondary analysis for reference. After the first-round quality check, all reagents used for RNA extraction and downstream analysis were replaced to rule out potential contamination. Due to budget constraints, the quality of eight samples from the secondary extraction, as well as two from the initial extraction (PPPP104 and PPPP108), were assessed using the Bioanalyzer at the Barts and the London Genome Centre core facility. The enhanced RNA quality in subsequent batches was evident in the second round of Bioanalyzer results (**Table 13**, **Figure 15**).

Table 12. The first-round Bioanalyzer quality results.

Sample Info

Well	RINe	28S/18S (Area)	Conc. [pg/µl]	Sample Description	Alert	Observations
A1	-	-	5010	Ladder	⚠	Caution! Expired ScreenTape device; Ladder
B1	3.1	-	710	pppp359	⚠	Caution! Expired ScreenTape device; RNA concentration outside recommended range for RINe; The upper ribosomal fragment has degraded
C1	-	-	353	pppp352	▲	Caution! Expired ScreenTape device; Sample concentration outside functional range for RINe and the assay
D1	-	-	338	pppp321	▲	Caution! Expired ScreenTape device; Sample concentration outside functional range for RINe and the assay
E1	-	-	323	pppp307	▲	Caution! Expired ScreenTape device; Sample concentration outside functional range for RINe and the assay

In the primary analysis of four RNA samples, only one sample (PPPP359) registered a RIN score of 3.1, with the quality of the remaining samples being too low to quantify. RIN: RNA Integrity Number. (The table's formatting and color are fixed as per the original report.)

Table 13.The second-round RNA quality check by Bioanalyzer.

Sample Name	Sample Comment	Statu s	Result Label
Agilent Human Ref RNA 5ng/uL		✔	RIN: 8.20
PPPP153	PPPP153	✔	RIN: 8.30
PPPP129 27-09-18	PPPP129 27-09-18	✔	RIN: 6.90
PPPP129 01-03-18	PPPP129 01-03-18	✔	RIN: 7.20
PPPP123	PPPP123	✔	RIN: 8.50
PPPP168	PPPP168	✔	RIN: 7.50
PPPP108	PPPP108	✔	RIN: 3.40
PPPP104	PPPP104	✔	RIN: 2.10
PPPP210	PPPP210	✔	RIN: 5.80
PPPP206	PPPP206	✔	RIN:6
PPPP178	PPPP178	✔	RIN: 8.50
Ladder		✔	All Other Samples

A total of ten samples (including two blood samples from PPPP129 taken at different times and the initial samples PPPP104 and PPPP108) were evaluated in the Barts and the London Genome Centre core facility. The highest RIN score (8.5) was found in PPPP178, while the lowest RIN score (2.1) was associated with PPPP104 from the initial extraction. (The table's formatting and color are fixed as per the original report.)

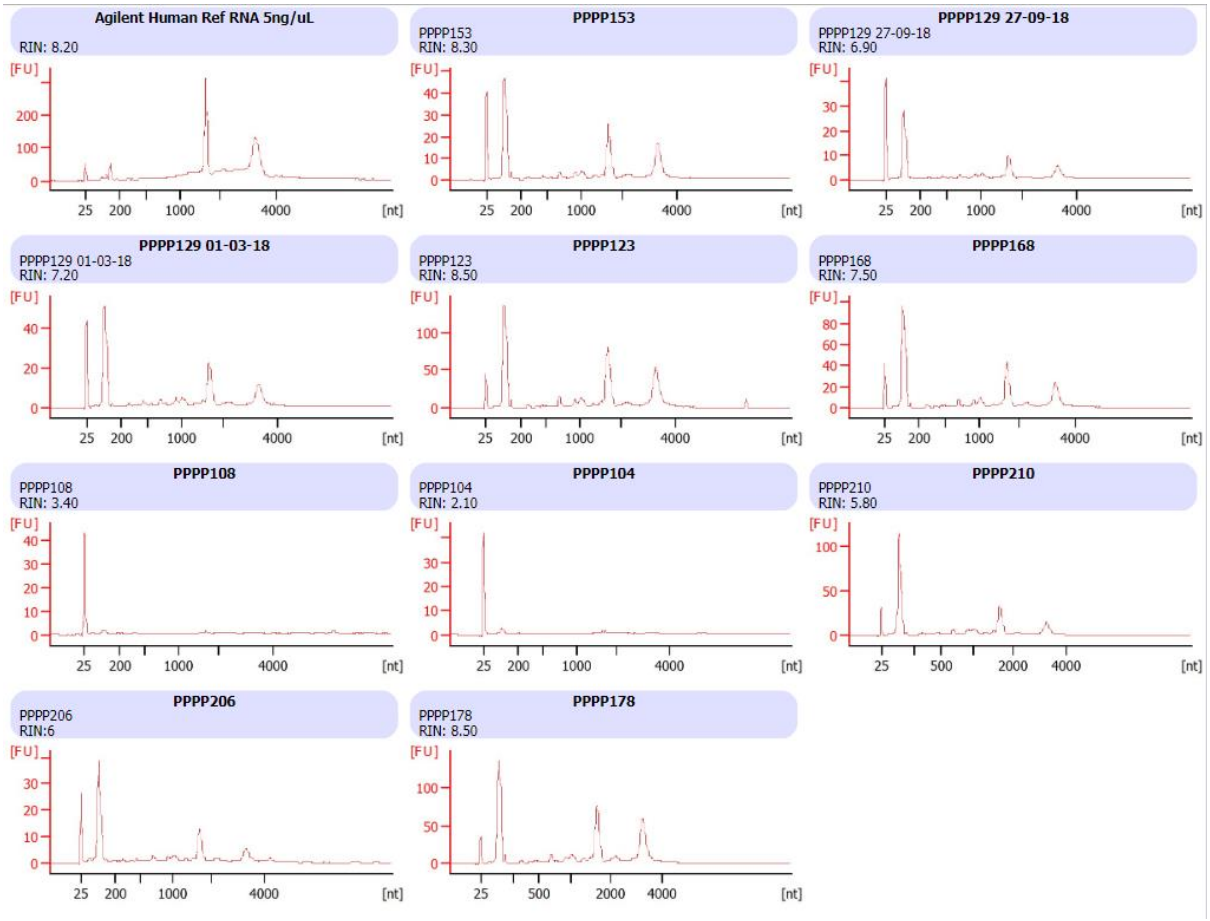

Figure 15. The second-round RNA quality check by Bioanalyzer.

Using the Agilent Bioanalyzer RNA pico chip, traces of total platelet RNA were isolated from ten samples taken from nine individuals. The quality evaluation of platelet RNA was demonstrated by the presence of 5S, 18S, and 28S ribosomal RNA near the 100-, 2,000-, and 4,000-nt product sizes. The quality checks of the second-round were stable except the first-round extraction samples PPPP104 and PPPP108 which lacked obvious peaks of ribosomal RNAs. (The figure's formatting and color are fixed as per the original report.)

2.2.2 Assessing and Overcoming RNA Quality and Quantity Challenges for mRNA Sequencing in Platelet Samples.

After the stability of my RNA extraction technique was confirmed by the secondary bioanalyzer check, 20 platelet samples from PCa and 20 samples from non-cancer patients were first selected, then extracted and sent to the Genomic Centre (Blizard Institute, the Faculty of Medicine and Dentistry, Queen Mary University of London) for mRNA sequencing. The RNA quality and quantity were checked both by Nanodrop and Bioanalyzer by the Genome Centre (**Table 14**).

Table 14. Details of all RNA quality and quantity measured by Bioanalyzer and Nanodrop of the first 40 platelet RNA samples selected for RNA-seq in Blizard Institute.

Sample ID	Nanodrop concentration (ng/μL)	260/280	260/230	RIN Score	Bioanalyser concentration (ng/μL)	volume remaining (μL)	Total ng
PPPP047	36.1	2.17	0.71	7.2	4	8	32
PPPP053	32.58	1.74	0.82	7.1	5	8	40
PPPP056	35.43	1.72	0.59	7.2	6	8	48
PPPP061	26.43	1.77	0.57	5.7	3	8	24
PPPP062	30.07	1.8	0.5	5.7	5	8	40
PPPP063	36.46	1.81	0.47	7.9	8	8	64
PPPP074	37.07	1.82	0.88	8.9	7	8	56
PPPP080	39.77	1.78	0.73	6.1	7	8	56
PPPP122	40.52	1.71	0.68	8.4	6	8	48
PPPP127	54.27	1.9	0.88	8.9	13	8	104
PPPP141	18.58	1.73	0.39	7.9	4	8	32
PPPP239	33.16	1.75	0.25	4.6	6.9	8	55.2
PPPP278	38.38	1.95	0.41	7.4	11.9	8	95.2
PPPP054	36.14	1.91	0.64	4.7	9.9	8	79.2
PPPP067	26.12	1.87	0.19	6.7	6.8	8	54.4
PPPP164	79.67	2	0.67	6.9	23.9	8	191.2
PPPP260	79.39	1.55	0.82	6.6	15.4	8	123.2
PPPP314	37.51	1.88	0.65	5.4	6.1	8	48.8
PPPP348	38.61	1.82	0.23	6.6	8.4	8	67.2
PPPP353	35.81	1.67	0.15	5.2	2.4	8	19.2
PPPP017	72.38	1.96	1.14	7	18.5	8	148
PPPP049	42.11	1.91	0.58	8.2	16	8	128

PPPP211	36.19	1.74	0.44	5.8	8.2	8	65.6
PPPP257	41.91	1.75	0.49	7.8	13	8	104
PPPP267	49.23	1.89	0.71	7.7	17.4	8	139.2
PPPP272	41.44	1.97	0.35	8.4	14.6	8	116.8
PPPP275	38.06	1.87	1.03	5	16.7	8	133.6
PPPP279	32.54	1.77	0.28	7.3	8.9	8	71.2
PPPP284	34.3	1.81	0.86	5.8	9.5	8	76
PPPP288	19.27	1.8	0.46	2.4	2.7	8	21.6
PPPP294	39.8	1.88	0.97	6.9	15.3	8	122.4
PPPP308	21.04	1.68	0.56	4.4	4.6	8	36.8
PPPP329	36.96	1.9	0.34	6.3	9.5	8	76
PPPP343	21.01	1.89	0.68	4.2	4.8	8	38.4
PPPP342	46.36	1.95	0.83	6.1	18.4	8	147.2
PPPP346	45.36	1.64	0.57	N/A	0.159	8	1.272
PPPP118	38.98	1.89	0.71	4.6	5.6	8	44.8
PPPP139	22.74	1.83	0.83	6.3	4.4	8	35.2
PPPP145	29.55	1.86	0.58	5.4	5.5	8	44
PPPP172	37.62	1.65	0.35	7.9	0.194	8	1.552

Since not of all the first 40 cases were able to meet the minimum requirements of RNA-seq (at least 100ng total RNA per case with RIN score equal or over 7), more cases were provided. Totally, 50 PCa and 41 non-cancer samples were selected and sent to the Genomic Centre for quality and quantity measurement. The RNA quality and quantity results are shown in appendix. Regarding RNA quantity, 11 samples from these

91 cases met the requirement of over 100ng for standard RNA sequencing, while 38 samples' RIN scores equaled or were more than 7. Due to the inadequate quantity of total RNA in the majority of the samples, amplification of RNA was applied in all the RNA samples with the help of SMARTer-seq V4 (Takara, Japan) ahead of the mRNA-seq. Then the 20 RNA samples from PCa and 20 from non-cancer patients were finally chosen for RNA-seq.

2.3 Results of mRNA-seq

2.3.1 Analysis of mRNA Expression in PCa and Non-cancerous Groups Using Hisat2 and HTSeq

Gene counts of each sample were shown in **Table 15**. Hisat2 was used to align these generated reads to an annotated reference genome. Following the mapping and quantification of gene expression, HTSeq was used for counting. The analysis revealed no significant difference in mRNA expression between the PCa and non-cancerous groups.

Table 15. Gene counts of the 40 samples for mRNA sequence.

Sample Name	gene_counts (>5 reads)	Sample Name	gene_counts
PPPP049	14193	PPPP067	10841
PPPP272	13836	PPPP053	10736
PPPP278	13639	PPPP047	10533
PPPP257	13335	PPPP056	10506
PPPP348	13040	PPPP216	10465
PPPP164	13031	PPPP338	10358
PPPP127	13017	PPPP063	10269
PPPP153	12857	PPPP170	10218
PPPP017	12708	PPPP139	10187
PPPP267	12470	PPPP356	10186
PPPP123	12356	PPPP074	10122
PPPP347	12215	PPPP350	10112
PPPP344	12103	PPPP342	10086
PPPP294	11954	PPPP355	9925
PPPP279	11854	PPPP329	9694
PPPP122	11637	PPPP316	9625
PPPP310	11628	PPPP341	9513
PPPP308	11566	PPPP141	9489
PPPP343	11458	PPPP156	9119
PPPP361	10984	PPPP178	6576

One gene which was counted for more than 5 times was included.

2.3.2 Principal Component Analysis

In this RNA-seq study, a principal component analysis (PCA) was

performed to investigate the variation in gene expression between PCa and control patients (**Figure 16**). The PCA plot demonstrated that the samples did not form distinct clusters. In this plot, the principal components are not linear combinations of gene expression data that encapsulate the maximum variation within the dataset. The first principal component (PC1) accounted for 61% of the variance, while PC2 represented 6% (**Figure 16**).

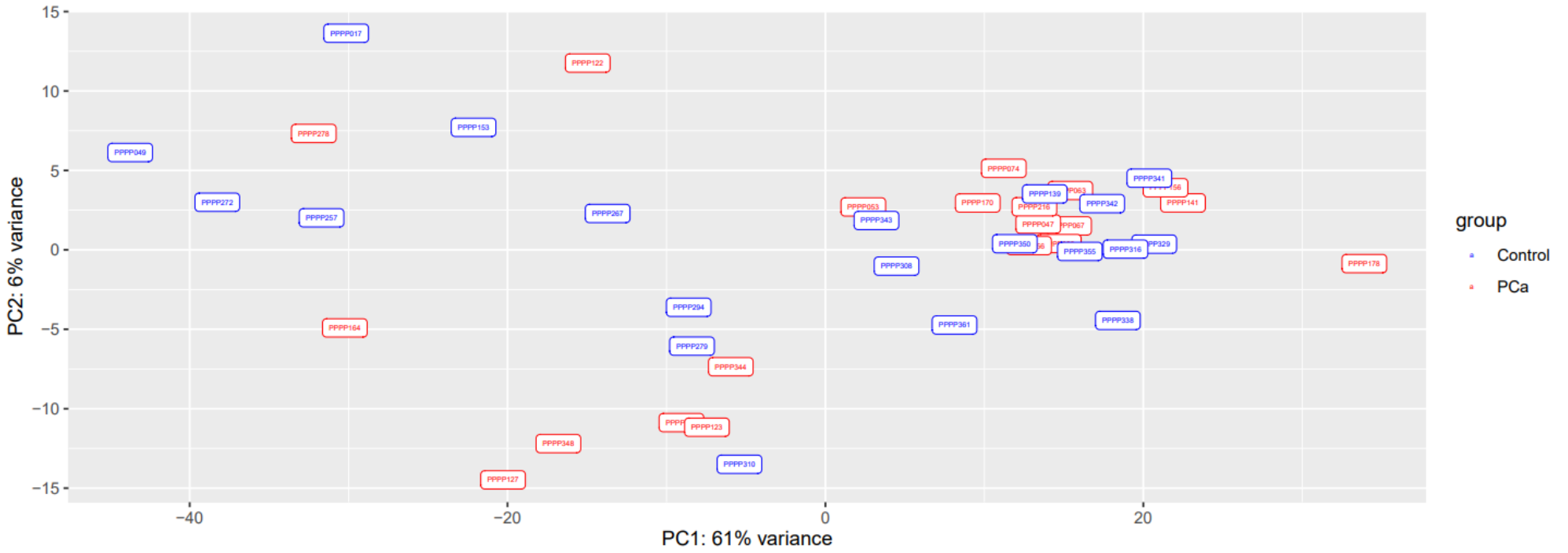

Figure 16. Principal component analysis (PCA) plot of the RNA-seq data.

Each point on the plot represents an individual sample, and its position is determined by its scores on PC1 and PC2. There was no clear separation between the subgroups with PC1 at 61% and PC2 at 6%. PC: principal component.

2.3.3 DESeq2 analysis for DEGs

432 differentially expressed genes between PCa and control with p-values less than 0.05 were identified after the DESeq2 analysis. However, their adjusted p-values were far from reaching 0.05. The results of the differentially expressed genes as evaluated by DESeq2 are depicted in (appendix).

2.3.4 Existence of WBC in platelet samples

The presence of WBC-associated genes in platelet samples were shown both in my sequencing data and previously published data from Best's study on platelet RNA for cancer detection [314].

We identified genes such as P2RY12, PTPRC, ITGAL, CD4, CD8A, ITGAM, FUT4, HLA-DRA, and CD68 as WBC markers which were not shown in platelets based on literature reports with the reads of each gene founded in both our and previous published data.

To validate these markers further and address potential WBC contamination in our platelet samples, I turned to the Human Protein Atlas (HPA). Based on this validation, P2RY12, CD68, and FUT4 from the list of WBC markers were excluded due to their unavailability in blood or lack of relevance to WBC contamination. This process provided a solid alternative confirmation, ensuring our final marker candidates are

accurate and reliable.

Finally, the table of WBC gene markers, reflecting this validation, has been incorporated into the thesis (**Table 16**):

Table 16. Comparison of WBC marker's reads in our and Best *et al.* sequencing data.

Gene.ID in our seq	Gene.Symbol	function	average of all case reads (our)	average of all case reads (Best's)
ENSG00000081237	PTPRC	Pan-WBC	1529.2	696.2
ENSG00000005844	ITGAL	lymphocyte	161.4	45.4
ENSG00000010610	CD4	CD4	121.5	24.1
ENSG00000153563	CD8A	CD8	84.2	2.8
ENSG00000169896	ITGAM	macrophage	141.6	104.5
ENSG00000204287	HLA-DRA	APC	1262.4	373.1

The reads of markers in WBC (PTPRC), lymphocyte markers (ITGAL, CD4 and CD8) and other subtype cells were confirmed existence both in our and Best's results [352]. WBC: white blood cell.

3. Discussion

3.1 Biological Reasons for the Absence of Differential mRNA Expression in RNA-seq

The DESeq2 analysis did not reveal any differentially expressed genes between the platelet mRNA of PCa and non-cancer patients. The result could be attributed to either a true and biological absence of differences at the mRNA expression level between PCa and non-cancer, and/or potential technical issues. Regarding the former, there are several factors at mRNA level.

While the initial study introducing the use of platelet mRNA for cancer detection was published in 2015 [352], the same group indicated ongoing research in this area specifically for PCa detection in 2018 [487]. To date, there hasn't been any published paper on the use of platelet mRNA for PCa detection. This lack of publications may suggest a potential absence of differential mRNA expression between PCa and non-cancer cases.

As we know, the majority of platelet RNA originates from megakaryocytes. If the mRNA profile remains largely consistent when interacting with cancer cells, this might suggest that the mRNA within platelets is inherently stable and resistant to alterations from external cancerous factors. Combining the different result at miRNA level in the study, it seems

that differential expression at the miRNA level might not necessarily translate to noticeable changes at the mRNA level in platelet if the miRNAs target multiple mRNAs or if their effect on mRNA stability is subtle. Since miRNAs often work by downregulating their target mRNAs, either by repressing translation or promoting mRNA degradation, a ‘silenced’ mRNA without degradation might also explain the ‘stability’ which is insignificant corresponding change in mRNA levels after the interaction with miRNA.

Even if RNA transfer occurs between PCa cells and platelets, it might not necessarily lead to significant differential expression in platelet mRNA. It's possible that the amount of RNA transferred isn't substantial enough to impact the overall profile or that the transferred RNA doesn't remain stable or functional within the platelets for a time interval.

It might be possible if there is no noticeable difference in the expression profile of mRNA, it does not necessarily mean that there is no functional impact. Some mRNA molecules, even if not differentially expressed, might still play crucial roles in mediating interactions between PCa cells and platelets. This could involve changes in translation, modifications, or other non-expression-based interactions.

Overall, the above analysis could imply a robust mechanism ensuring

platelet mRNA stability, which would be interesting to delve into even at a protein level. It could be also interesting to explore if megakaryocytes themselves show any differential mRNA expression in the presence of PCa. In the following part, I will analyze other reasons for the absence of difference.

3.2 Other Reasons for the Absence of Differential mRNA Expression Between PCa and Non-cancer Groups

3.2.1 Small Effect Size between Groups

Using 20 samples from each of the PCa and non-cancer groups is a moderate sample size for RNA-seq experiments. The adequacy of this size depends on the anticipated effect sizes (differences in gene expression) and the variability within each group. While a larger sample pool enhances the statistical power of the analysis, the decision to include 20 samples from each group in this study was primarily due to budget constraints. Given previous studies that reported clear differential mRNA expressions between cancerous and non-cancerous controls [351, 352, 429], there was an optimistic anticipation of detecting large effect sizes in PCa in the study.

The observed lack of differences might suggest a small effect size in the data. Such nuances in gene expression could get obscured by

background variability, especially in smaller sample sizes. Hence, to assert that this subtle effect is genuine and not a product of random variation, an increased sample size for future RNA-seq experiments may be essential.

3.2.2 Potential High variability in the Cancer Group

The heterogeneity in the PCa group might have introduced high variability. For instance, based on the Gleason score, the PCa cases in this study encompassed both clinically significant (GS>3+4) and favourable PCa (GS<3+4) cases. Given the varied prognosis between these subgroups [82, 83], combining them might have augmented the intra-group variability of gene expression. If the overarching aim is biomarker development that discriminates between PCa and non-cancer cases, then the broad spectrum of PCa cases should be acknowledged. To mitigate the potential variability introduced by such heterogeneity, a larger sample size might be warranted.

Alternatively, because the detection of clinically significant PCa is one clinical emphasis, a focused analysis comparing clinically significant PCa with non-cancer controls could provide clearer insights with relatively low variability.

3.2.3 Limited Depth of Sequencing

The inability to detect differences might also stem from inadequate sequencing depth, which is especially crucial for lowly expressed genes. If the budget permits, deeper sequencing in future analyses might elucidate any differential expressions.

3.2.4 Quality Consideration

The Quality issues could also be attributed to the absence of difference in results. For example, sequencing itself and sample quality (suboptimal RNA quality, phenol contamination, and contamination of WBCs) will be discussed in the following part.

The quality of RNA-seq data is paramount for accurate differential expression analysis. If sequencing data is of poor quality or if there's a low mapping rate, it becomes challenging to accurately quantify gene expression levels, leading to false negatives in the case.

Quality of sequencing reads: Low-quality reads can introduce noise and make it difficult to discern genuine expression differences from artifacts. Alternatively, in the initial RNA extraction, low RNA quantity was revealed and pre-amplification (SMARTer V4) was applied. This additional step could introduce potential sources of error and bias, causing uneven amplification, increased noises, and the reduction in complexity.

Mapped sequencing reads: After sequencing, the next step is to map the

sequencing reads to a reference genome or transcriptome. If a significant proportion of the reads cannot be mapped to the reference, it suggests potential issues with the data quality.

In summary, the quality of the sequencing data, which can influence the outcomes of the RNA-seq analysis.

Lower-than-optimal RIN scores and RNA quality might introduce high levels of noise into the sequencing data, obscuring potential differences [488]. The requirement for optimal RIN scores varies between kits. For instance, mRNA sequencing necessitates a RIN score of at least 7.0, whereas the SMARTer V4 kit requires a higher RIN score of 8.0. The average RIN score for my samples was 7.7, part of which was less than the recommended value. To minimize contamination, we procured new reagents for individual use and enforced the use of filter-tipped pipette tips. We also changed gloves frequently and regularly cleaned lab equipment and areas with purifying agents.

3.2.5 Potential Phenol Contamination

Phenol can inhibit PCR reactions and reverse transcription, negatively affecting the SMARTer preamplification and library construction for sequencing, thereby leading to inaccuracies in downstream analysis. The inhibitory effect of phenol has been observed when the levels were as low

as 0.02% [489, 490].

In our dataset, disparities in RNA quantities measured by the Nanodrop and Bioanalyzer hinted at potential phenol contamination. Specifically, while a 260/280 ratio between 1.8 to 2.2 in Nanodrop results is generally viewed as indicative of acceptable quality, ratios below 1.8 often suggest contamination by phenol or guanidine salt in nucleic acid samples [524, 528].

Of our mRNA-seq samples, 13 out of 40 displayed ratios under 1.8. These samples also exhibited a rightward shift in the 260 nm peak, which aligns with the absorbance peak of phenol around 270 nm, indicating possible contamination [507]. Upon a direct comparison of RNA quality and quantity between these 13 samples and the remaining 27, no significant difference was observed in RIN scores ($p=0.62$) or RNA quantities ($p=0.12$). These findings suggest that while phenol contamination might be present, it doesn't appear to markedly affect the RNA's quality and quantity in the study.

For future endeavors, it would be prudent to accurately measure the percentage of phenol in samples to quantify the extent of contamination. Furthermore, investigation of any differences in RNA-seq data between potentially contaminated (13 cases) and uncontaminated platelet samples

(27 cases) could be considered in order to discern any broader impacts on data quality.

3.2.6 Confirmed White Blood Cell Contamination

The dilution of RNA signatures due to contaminated WBCs could have biased the results [491]. Moreover, one WBC has been found to contain 12,500 times more mRNA than a single platelet [492], possibly causing a larger bias in the mRNA-seq results.

The suspect was supported both by the WBC contamination check in those samples by DAPI during platelet collection (See **Chapter V** in the part of evaluating the WBC contamination rate in the two-step differential centrifugation) and by the existence of reads of WBC markers which were reported mainly expressed in leucocytes rather than platelets in the sequencing data [493, 494]. Furthermore, this presumption of WBC contamination in platelets was corroborated by examining WBC markers' reads in other published datasets, even when those studies employed different methods of platelet isolation, sequencing, and data analysis [352].

In conclusion, addressing these above technical issues could potentially reveal obscured differences and could potentially identify differences in platelet RNA between PCa and non-cancer patients. Given the potential influence of WBC contaminants on platelet isolation and subsequent

RNA-seq results, we've conducted further evaluations. Details of these assessments are available in Chapter V. For future research endeavors, cross-verifying findings using independent datasets, preferably in collaboration with other teams, could be invaluable in ensuring the robustness of our results.

3.3 Analysis of PCA plot

In the PCA plot, the absence of clear separation between the groups indicates that the underlying biological or experimental factors might not significantly contribute to the observed gene expression patterns.

The combined contribution of PC1 and PC2 to the total variance in the data is less than 80%. This threshold is often considered to determine how many principal components are required to adequately represent the data [495, 496]. These results suggest that PC1 and PC2 do not capture a significant enough portion of the overall variation to account for the majority (80% or more) of the dataset's variability. Therefore, they might not be closely associated with the differences between groups.

There are several possible explanations for this observation. Firstly, the most significant sources of variation captured by PCA might not reflect all group-specific differences. There might be other minor sources of variation that drive the differences between the groups. Secondly, PCA

assumes linear relationships between variables, but gene expression patterns can exhibit non-linear behavior. Therefore, if the differences between the groups are non-linear, PCA might not effectively capture them with only the top principal components. Finally, technical noise, batch effects, or confounding factors unrelated to the groups of interest can introduce additional variation that might dilute the group-specific differences, making them harder to detect.

In such cases, other methods designed for group comparisons, such as DESeq2, was considered for identifying differentially expressed genes.

3.4 The preparation for RNA-seq

3.4.1 Total RNA vs. Poly-A RNA: the Choice of RNA Isolation

Both total RNA isolation and polyadenylated (poly-A) RNA isolation techniques are viable options for mRNA sequencing preparation. Total RNA isolation involves the extraction and purification of all RNA molecules present in a sample, including ribosomal RNA (rRNA), transfer RNA (tRNA), messenger RNA (mRNA), and other non-coding RNAs, while Poly-A RNA isolation specifically targets and enriches for mRNA molecules that contain a polyadenylated tail at their 3' end, which is a characteristic feature of most eukaryotic mRNAs and plays a crucial role in mRNA stability, translation, and regulation [497].

In this project, the reason that the method of total RNA isolation was applied due to the following points. Firstly, total RNA isolation methods capture all RNA species present in the sample, providing a more comprehensive representation of the transcriptome while Poly-A RNA isolation methods, such as oligo(dT)-based capture, typically have high enrichment efficiency for mRNA molecules where can be some bias towards abundant transcripts. Secondly, regardless to sample compatibility: Poly-A RNA isolation is more commonly used in eukaryotic systems, where the majority of mRNA molecules have a poly-A tail [498]. However, for platelets with atypical mRNA characteristic, total RNA extraction may be suitable. Finally, based on the current accessible technique support in the Institute, such as isolation protocol, the quality and quantity evaluation of total RNA and sequencing, total RNA extraction is more practical.

3.4.2 Quality Improvement of RNA extraction

The Bioanalyzer detected subpar RNA quality in the initial RNA extraction experiment. The Bioanalyzer is a chip-based capillary electrophoresis device that employs fluorescence dyes to bind to RNA [499]. This process separates sample components based on electrophoretic mobility, with smaller fragments migrating faster than larger ones. The fluorescent dye

molecules bind to DNA or RNA strands, allowing for their detection. By examining the distribution and integrity of RNA samples, particularly rRNA (5s, 18s, and 28s), the Bioanalyzer evaluates the quality of the RNA samples [500, 501]. These rRNAs are more stable compared to other RNA species, making them a valuable benchmark. When these stable RNAs show signs of degradation, it often suggests that the less stable RNA species are likely also degraded. A common metric used to evaluate RNA integrity is the 28/18S rRNA peak ratio. A ratio close to 2:1 is typically considered an indicator of high-quality RNA, as it represents a natural abundance of the 28S rRNA relative to the 18S rRNA. This ratio can vary based on the sample and tissue type, and a deviation from this ratio can suggest potential RNA degradation [498, 500, 501]. However, a report that rRNA underwent complete degradation, while the mRNA remained intact was also published [502]. Regarding mRNA integrity, some publications [498, 503] preferred 28S as an indicator rather than 18S, while others disagreed [504].

Bioanalyzer assigns a numerical score, known as the RNA Integrity Number (RIN), ranging from 1 to 10 [505]. To assess the quality of RNA samples, a higher RIN value indicates superior RNA integrity [506]. In the initial Bioanalyzer assessment for the four samples from the first RNA

extraction, only PPPP359 achieved a RIN score of 3.1. The other samples had scores too low to register, indicating that the first extraction provided a poor RNA quality.

Several factors may have led to the low RNA yields. Firstly, RNA quality and quantity can vary due to pre-extraction procedures [507]. However, as all initial samples displayed poor quality, this explanation seems unlikely. Secondly, RNA degradation may occur if samples are stored at room temperature for extended periods post-isolation, activating RNases [508]. To prevent this, we used cold QIAzol as the guanidine lysis buffer and stored samples in a -80℃ freezer within 10 minutes of isolation to prevent RNase activation. Thirdly, RNase contamination during the RNA extraction process may have led to RNA degradation. RNases are pervasive in laboratory environments [509] and can degrade RNA samples [510, 511]. To prevent potential contamination, new reagents were acquired for individual use. Other precautions included the strict use of filter-tipped pipette tips, frequent glove changes, and regular cleaning of laboratory instruments and work areas using purifying agents such as RNaseZap (Thermo USA). Additionally, there were concerns about potential errors in the preparation of the wash buffers. Two washing buffers (RWT and RPE) require the addition of ethanol when a new bottle

is opened. Ethanol-containing solutions are capable of washing salts but not extracting RNA [512]. The previously used buffers lacked clear labelling regarding the addition of ethanol, as they had been used by other team members. Therefore, I obtained new buffers with detailed labels indicating the date of ethanol addition.

As a result of these adjustments, the average RIN score improved from 2.9, as determined by the first-round Bioanalyzer assessment, to a mean of 7.7 in the subsequent Bioanalyzer examination. This marked improvement in RIN in the secondary bioanalyzer evaluation confirms the enhanced stability and quality of RNA extraction, validating the procedures we undertook.

3.4.3 Analysis of the difference in RNA quantity between Nanodrop and Bioanalyzer

Out of the 91 samples with sufficient RNA concentration (> 100 ng) for sequencing based on Nanodrop results, only 11 samples were found to be higher than 100 ng according to the Bioanalyzer measurements. The substantial disparity observed between Nanodrop and Bioanalyzer prompts a need for further comprehension of their mechanisms and comprehensive comparison. The difference in the mechanisms of RNA quantity detection should be considered. On the other hand, Nanodrop,

functioning as a spectrophotometer, quantifies RNA concentration by measuring the absorbance of nucleic acids at a wavelength of 260 nm [513]. When a 260 nm light source is shone on the sample, the amount of light passing through and the amount of light absorbed by the sample can be determined [514]. The RNA quantity observed by Nanodrop, however, could be mistakenly higher due to phenol or salt contamination.

In the platelet isolation protocol used in the project, QIAzol, a phenol/guanidine-based reagent, was routinely employed to lyse platelets and release RNA. After phenol serves to lyse platelets to free RNA and remove nucleases [499], its complete removal through following chloroform extraction is crucial. Otherwise residual phenol may cause contamination in the RNA samples. Due to the obvious higher RNA concentration from the Nanodrop check, this kind of contamination was suspected. Further studies have demonstrated that QIAzol contamination, particularly by phenol, can lead to more pronounced increases in Nanodrop readings compared to those obtained with the bioanalyzer [499, 515, 516]. In the Nanodrop results, a 260/280 ratio ranging from 1.8 to 2.2 is generally considered indicative of pure RNA, while ratios below 1.8 suggest the presence of phenol or guanidine salt contamination in nucleic acid samples [513, 517]. In my findings in the later 91 RNA samples, 40

out of 91 cases had ratios less than 1.8, implying that contamination could exist in more than 40% of cases. Additionally, A rightward shift was detected in the 260 peak in my samples (The picture was not shown due to the incapability of download in Nanodrop.), which was consistent with previous reports that the addition of QIAzol could cause such a shift in the 260 peak [518].

Thus, it was suspected that the so-called ‘high’ RNA concentration observed in the samples could be due to contamination, such as residual QIAzol. Although the protocol applied in the study was consistent with the ratio of 5:1 recommended by the Qiagen QIAzol handbook, it may be still challenging to avoid such contamination during RNA extraction from limited-volume sample materials, leaving phenol in the upper phase after centrifugation with chloroform.

The Bioanalyzer, as a representative of microfluidics-based "lab-on-a-chip" technology, utilizes chip-based capillary electrophoresis, employing traditional gel electrophoresis principles and fluorescence dyes that specifically bind to RNA [499]. By separating the sample components through microchannels based on their size and detecting the fluorescent dye molecules that intercalate into the RNA strands, the Bioanalyzer provides automated sizing and quantitation information in a digital format.

The quantification of RNA is performed through the comparison of the RNA sample to a set of RNA standards of known concentration that are run alongside the testing sample. The Bioanalyzer's software interprets the electropherogram generated by the device, and it uses the fluorescent signal intensities of testing samples compared to the signals of the standards to calculate the concentration of RNA in a sample. Specifically, for each fragment of RNA in the sample, the Bioanalyzer measures the area under the curve in the electropherogram, which correlates with the quantity of that RNA fragment. By adding together the areas for all the RNA fragments, the Bioanalyzer can estimate the total concentration of RNA in the sample [519]. The Bioanalyzer quantifies RNA based on the fluorescence signal, and the RIN score is used to indicate the integrity of the RNA. While the fluorescence-based quantification gives an estimate of RNA quantity, the actual state of the RNA (whether intact or degraded) is better reflected by the RIN value. A lower RIN score indicates more degraded RNA, whereas a higher RIN score suggests the RNA is largely intact. Thus, while the quantity measured by the Bioanalyzer is consistent, the RIN score serves as a measure of RNA quality. It is crucial to consider both quantity and quality (RIN score) when selecting samples for RNA-seq, with a preference for samples with higher RIN scores to ensure the

integrity of the RNA being sequenced. Finally, by using the criteria from Bioanalyzer, I selected samples for the RNA-seq.

In the first 40 RNA samples sent to the Genomic Centre, 12 out of 17 cases whose RIN were equal or over 7 had less than 100ng RNA. Based on the mechanism of Bioanalyzer, the 12 cases' quantities may be close to the real value, implying inadequate RNA production in the samples.

3.4.4 Addressing Contamination Concerns in RNA Extraction

Regarding the improvement of the contamination, several potential measures can be implemented to address the persistent concern of residual phenol in the RNA extraction protocol. One such measure is the careful transfer of the upper aqueous phase, which contains the RNA, to a fresh tube. It is crucial to exercise caution to avoid disturbing the interphase or the organic phase and prevent the transfer of any lower organic phase that may contain residual phenol. Additionally, the duration of the previous 15 minutes in the centrifugation for RNA separation could be lengthened.

Another possible approach is to perform an additional isopropanol precipitation step. Following the separation of the RNA-containing aqueous phase, isopropanol can be gently added, and the mixture can be incubated at -20°C for an adequate duration. Subsequently, the mixture

can be centrifuged to pelletize the RNA, and the supernatant, which contains residual isopropanol and any contaminants, can be discarded. However, it is important to consider the cost of RNA consumption associated with this supplementary step.

The Takara SSV4 kit was initially used as a popular choice for single-cell RNA sequencing applications by generating full-length cDNA from low-input RNA samples with as little as 10pg of total RNA, making it suitable for capturing the entire transcriptome of individual cells [520]. The SMART technique involves the use of a modified reverse transcription reaction, where a chimeric oligonucleotide called SMARTer oligo is used, enabling the synthesis of full-length cDNA by utilizing a template-switching mechanism. During reverse transcription, the SMARTer II A portion of the oligo anneals to the RNA template and primes the synthesis of the first strand cDNA. At the end of the first strand synthesis, the reverse transcriptase enzyme undergoes a template-switching event, allowing the reverse transcriptase to continue the synthesis of the second strand of cDNA, resulting in a full-length cDNA molecule [521]. The SSV4 kit is optimized for amplification from low-input RNA samples, requiring only the number of platelets in a single drop of blood with high sensitivity [428], which is crucial for my project of low RNA input, only 11/91 cases had RNA

more than 100ng after RNA extraction. Additionally, the SSV4 kit is known for its reproducibility and reliability in generating high-quality RNA-seq data and can be used for a wide range of downstream applications, including library preparation for Illumina sequencing platforms in the project [522].

This technology requires RNA of high quality, preferring RIN score of 8 according to the manufacturer's instructions. It is sensitive to the quality of the input RNA. Since it aims to amplify full-length cDNA, it requires intact RNA molecules with minimal degradation. If the RNA samples are degraded or of poor quality, it can lead to biased or unreliable results. The 40 cases for the amplification in the project had high RIN scores of an average of 7.7, close to the instruction. Therefore, it was applied as the pre-amplification method ahead of mRNA sequencing.

Regardless of the efficiency of library preparation for mRNA sequencing, TaKaRa SSV4 was reported to produce a relatively lower amount of coding mRNA [523] and/or higher output of ribosomal [522, 524] as well as non-coding RNAs [523]. However, the difference in expression profiles between the SSV4 kit and Illumina TruSeq stranded mRNA Sample Preparation kit was indicated as unnoticeable [522].

Like any amplification-based method, the SSV4 kit can also introduce

amplification bias, leading to the uneven representation of transcripts in the resulting cDNA. This bias can affect the accuracy and quantification of gene expression measurements, particularly for low-abundance transcripts.

CHAPTER V: Evaluation and Modifications of the Method of Platelet Collection

1. Introduction

The double-spin centrifugation method has garnered popularity in laboratory settings for platelet isolation, primarily due to its favorable platelet yield, cost-effectiveness, and simplicity of operation compared to other methods [525, 526]. However, despite its widespread use, there remains a lack of standardization in platelet preparation [525, 527]. In our study, we adhered to previously reported protocols, employing a first spin at 200g for 20 minutes to segregate platelets and a subsequent spin at 400g for 20 minutes to concentrate them [428, 528-532].

Platelet isolation aims to separate platelets from other components present in whole blood. Due to their small size and low density, platelets can be effectively separated through centrifugation [533]. During the first centrifugation step, the whole blood sample is subjected to a relatively low centrifugal force, resulting in the formation of two distinct layers: the upper PRP layer, which appears yellow and contains a higher concentration of platelets compared to whole blood, a buffy coat in the middle, and the bottom layer consisting of RBCs which are heavier [428, 525].

Interestingly, larger and heavier platelets were reported to be mixed with RBCs in the upper part of the lower RBC layer [534].

A pivotal concern in platelet collection is the potential contamination with WBCs. Given the significantly higher RNA content in WBCs, their presence could dilute the distinctive RNA signature of platelets, thereby skewing results [491, 492, 535]. Alarmingly, upon detecting WBC markers in our mRNA-seq data, our subsequent assessment unveiled an average contamination rate of 40.4 WBCs per million platelets, higher than the reported range between 0 to 5 WBCs per million platelets [7, 9, 13]. Such a discrepancy underscores the need to re-evaluate and possibly refine our current double-spin technique, prompting the exploration of modifications to enhance its efficacy.

2. Results

2.1 Evaluation of the Current Two-step Centrifugation for Platelet Collection

The evaluation of the current method initiated with the calculation of the platelet count collected as well as the platelet recovery rate, then was moved to the check of WBC contamination.

To assess platelet recovery, whole blood samples from a total of 47 PCa patients with platelets isolated using the 2-step centrifugation method between December 2021 and November 2022 were included. The number of platelet collection was 12,476,738 averagely by the 2-step centrifugation, ranging from 325,000 to 47,333,333 per sample (0.5ml whole blood). Furthermore, on average, across the 47 cases, the platelet recovery was found to be approximately 8.32% (details in appendix).

Additionally, it was observed that approximately one-third (0.37) of the platelets collected after the first-step centrifugation (details in appendix).

2.1.1 Results of the Accurate Evaluation of WBC Contamination in the Two-step Centrifugation

Due to the existence of WBC markers' reads in my sequencing data, as well as the situation that the previous WBC check was unable to accurately estimate the WBC contamination, further accurate evaluation of WBC contamination was performed. Between December 2021 and November 2022, a total of 47 samples from PCa patients were analysed to assess WBC contamination rate.

Briefly, the difference between the current and the previous evaluation method is that an additional platelet counting was performed each time following PRP transfer. The observed WBC contamination rates varied, ranging from 0 to 309.9 WBCs per 1 million platelets. The average WBC contamination rate was determined to be 40.4 WBCs per 1 million platelets, with a standard deviation (SD) of 72.9 WBCs per 1 million platelets (**Table 17**).

Based on the results of the 47 cases, about 25% of the samples collected by the 2-step centrifugation provided equal or less than 5 WBCs per 1 million platelets the WBC contamination rate (**Figure 17**).

Table 17. The accurate evaluation of WBC contamination rates in 47 platelet samples with the method of two-step centrifugation.

ID	Platelet count	WBC count	WBC contamination rate (WBC/1million platelets)
PPPP415	1575000	75	47.6
PPPP416	6362500	25	3.9
PPPP417	2505000	70	27.9
PPPP418	2325000	0	0
PPPP419	325000	0	0
CPM1 008	3377500	70	20.7
CPM1 009	2480000	75	30.2
CPM1 010	1890000	10	5.3
CPM1 011	2175000	0	0
CPM1 012	16950000	10	0.6
PPPP420	3725000	15	4.0
CPM1 014	7675000	15	2
CPM1 015	5525000	50	9.1
CPM1 016	8275000	55	6.7
PPPP440	5566667	500	89.8
PPPP441	7400000	127	17.2
PPPP442	3200000	200	62.5
PPPP443	9366667	200	21.4
PPPP444	9600000	500	52.1
PPPP445	15700000	184	11.7
PPPP446	1596667	64	40.1
PPPP447	556667	25	44.9
PPPP448	1480000	49	33.1

CPM1 065	1263333	382	302.4
CPM1 066	2233333	8	3.6
CPM1 067	1090000	18	16.5
CPM1 071	2665000	31	11.6
CPM1 073	1420000	23	16.2
CPM1 028	1190000	5	4.2
CPM1 076	1330000	26	19.6
CPM1 077	2213333	43	19.4
CPM1 019	1613333	500	309.9
CPM1 011	4100000	13	3.2
PPPP433	6833333	52	30.2
CPM1 055	430000	129	300
CPM1 059	1220000	89	73
CPM1 060	3333333	115	34.5
CPM1 050	2936667	54	18.4
CPM1 049	3920000	22	5.6
CPM1 048	833333.3	19	22.8
CPM1 047	6033333	131	21.7
CPM1 046	750000	57	76
PPPP437	31333333	154	49.1
PPPP438	1.89E+08	173	9.1
PPPP439	1.17E+08	36	3.1
CPM1 062	68333333	69	10.1
CPM1 065	15700000	9	5.7
average	12490922	95.3	40.4

WBC: white blood cell.

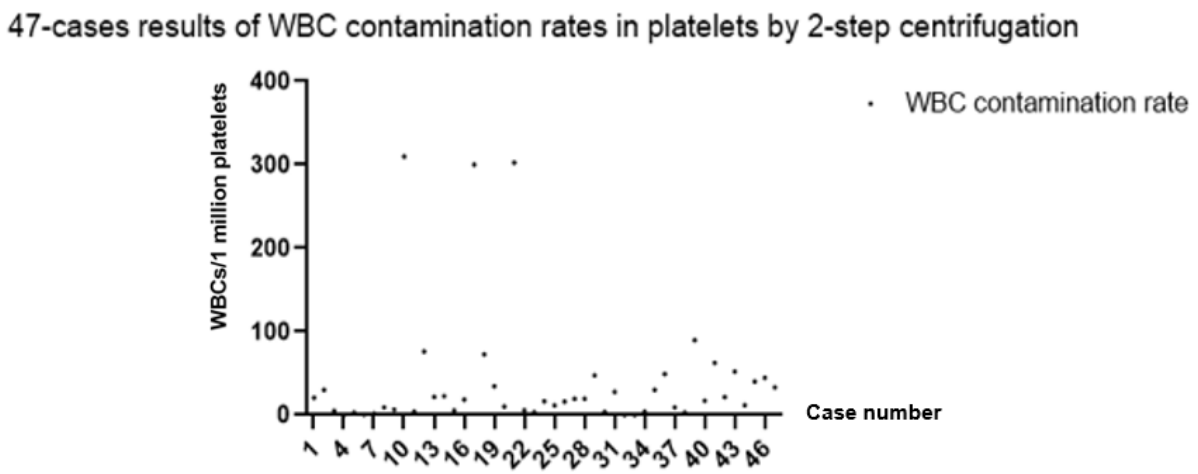

Figure 17. Descriptive Statistics of WBC Contamination Rates in 47 Platelet Samples Isolated by a Two-step Centrifugation.

The X axial represented the case numbers, while the Y axial illustrated the WBC contamination rates (WBCs/ 1 million platelets).

2.2 The modification of the current method of 2-step centrifugation

2.2.1 Taking ½ Upper PRP in Platelet Collection

From December 2021 to March 2022, a total of 14 patient samples with prostate cancer (PCa) were included in the study. There was no statistically significant difference in the WBC contamination rate between the upper half and 2/3 PRP, with contamination rates of about 20 and 11 WBCs per 1 million platelets, respectively (*P*=0.18) (**Figure 18**). On average, when comparing the two methods using the same amount of starting blood sample of 0.5ml, taking 2/3 of platelet-rich plasma (PRP) yielded an average of 4,654,643 platelets. However, when taking only half of the PRP, the average number of platelets largely decreased to 3,195,714 (*P*=0.004) (**Table 18**). And 4/14 cases provided the WBC

contamination rate less than 5 WBCs per 1 million platelets.

Table 18. The results of platelet count, WBC count and WBC contamination rate in 14 cases via upper ½ and 2/3 PRP.

	Upper ½ PRP transfer			Upper 2/3 PRP transfer		
ID	Platelet count	WBC count	WBC contamination rate (WBC/1million platelets)	Platelet count	WBC count	WBC contamination rate (WBC/1million platelets)
PPPP415	962500	60	62.3	1575000	75	47.6
PPPP416	2287500	25	10.9	6362500	25	3.9
PPPP417	1452500	40	27.5	2505000	70	27.9
PPPP418	425000	10	23.5	2325000	0	0
PPPP419	125000	10	80	325000	0	0
CPM1008	1412500	15	10.6	3377500	70	20.7
CPM1009	1517500	20	13.2	2480000	75	30.2
CPM1010	1232500	15	12.2	1890000	10	5.3
CPM1011	1747500	0	0	2175000	0	0
CPM1012	18425000	5	0.3	16950000	10	0.6
PPPP420	2667500	5	1.9	3725000	15	4.0
CPM1014	4550000	5	1.1	7675000	15	2
CPM1015	1110000	40	36.0	5525000	50	9.1
CPM1016	6825000	20	2.9	8275000	55	6.7
average	3195714	19.3	20.2	4654643	33.6	11.3

Less platelets were collected (*P*=0.004) when taking the upper 1/2 PRP, while there was no difference in WBC contamination rates (*P*=0.18). WBC: white blood cell, PRP: platelet rich plasma.

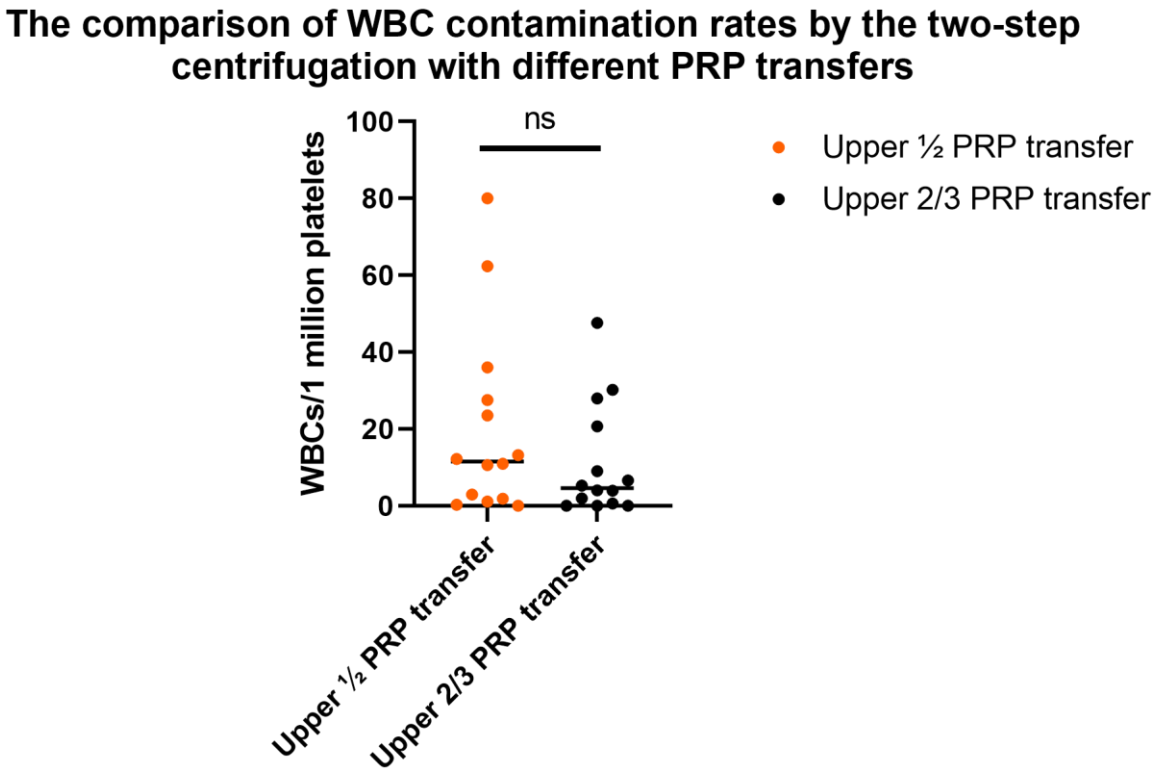

Figure 18. The comparison of WBC contamination rates by the two-step centrifugation with different PRP transfer (between taking upper ½ PRP and taking upper 2/3 PRP groups) (*p*=0.18).

WBC: white blood cell, PRP: platelet rich plasma.

2.2.2 Using CD45-Labeled Micro-bead Negative Selection for Platelet Purification

Between September 2022 and November 2022, a total of nine samples of PCa were included in the study. The average WBC contamination rates calculated for 2-step centrifugation and the modified method were 41.4

and 40.8 WBCs per 1 million platelets respectively (p=0.96) (**Figure 19**). Within these nine cases, averagely, 6,051,852 platelets were collected using the traditional two-step centrifugation method, while the lower average number of 875,630 platelets were collected using the two-step centrifugation plus magnetic beads method (**Table 19**).

Table 19. The results of platelet count, WBC count and WBC contamination rate (WBCs/ 1 million platelets) in nine cases via the two-step centrifugation method and further magnetic bead purification after the two-step centrifugation.

ID	two-step centrifugation			two-step centrifugation + magnetic beads		
	Platelet count	WBC count	WBC contamination rate	Platelet count	WBC count	WBC contamination rate
PPPP440	5566667	500	89.8	1666667	3	1.8
PPPP441	7400000	127	17.2	1470000	14	9.5
PPPP442	3200000	200	62.5	276667	26	94
PPPP443	9366667	200	21.6	750000	51	68
PPPP444	9600000	500	52.1	1963333	99	50.4
PPPP445	15700000	184	11.7	1393333	47	33.7
PPPP446	1596667	64	40.1	59000	4	67.8
PPPP447	556667	25	44.9	160000	1	6.3
PPPP448	1480000	49	33.1	141667	5	35.3
average	6051852	205	41.4	875630	27.8	40.8

On average, less platelets were collected (875,630) in the method of using magnetic beads with similar WBC contamination rate of 40.8 WBCs per one million platelets. In case PPPP440 and PPPP444, by DAPI staining, there were full of WBCs under microscope which were then recorded as 500. WBC: white blood cell, DAPI: 4’,6-diamidino-2-phenylindole.

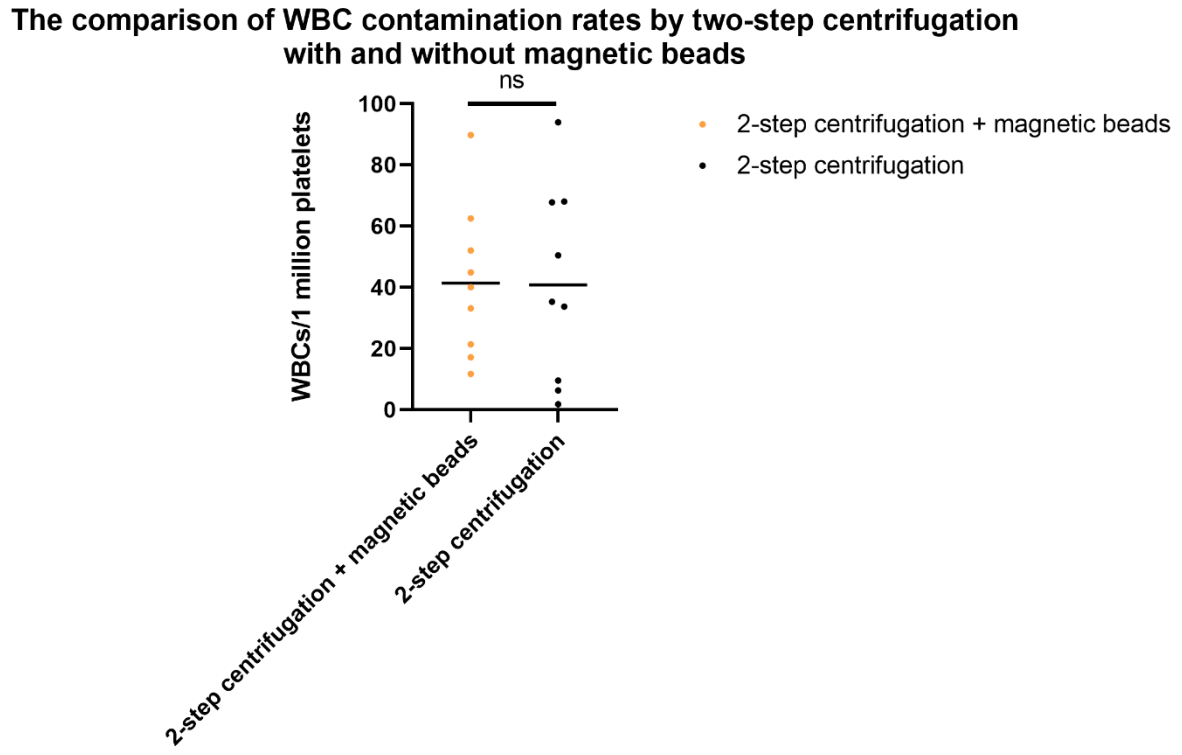

Figure 19. The comparison of WBC contamination rates by the two-step centrifugation with and without magnetic beads (*p*=0.96).

WBC: white blood cell.

2.2.3 Application of Three-step Centrifugation in Platelet Collection

2.2.3.1 Comparison of the WBC Contamination Rates Between the Three-step (100g and 200g in the additional step) and The two-step Centrifugation

From August 2022 to September 2022, a total of nine PCa patient samples were included. An additional centrifugation of 100g and 200g was individually added between the two steps of traditional collection. Comparing the WBC contamination rates to the traditional two-step

method (78.2 WBCs/1 million platelets), the 3-step centrifugation methods showed lower contamination rates: 24 in the 100g group and 28.6 WBCs/1 million platelets in the 200g group. Five out of the nine cases had a WBC contamination rate of less than 5 WBCs/1 million platelets in the three-step (200g) group, and 3/9 met the same criteria in the three-step (100g) group, while only 2/9 cases in the two-step group had acceptable WBC contamination rate (**Table 20**). However, there was no significant difference between these methods and the two-step method (p=0.26 and 0.32 in methods of 100g and 200g, respectively) (**Figure 20**).

2.2.3.2 Platelet Collection Efficiency Between 100g and 200g Methods in the Three-step Centrifugation

With regards to platelet collection in the two groups including an additional centrifugation, averagely, 194,593 platelets were collected by the method of 100g per 1ml whole blood, while 139,370 platelets were collected by the method of 200g per 1ml whole blood (p= 0.09), as well as platelet collection efficiency of 11.89% and 8.17% respectively (p= 0.08). (The method of 2-step centrifugation provided the average platelet collection of 1,668,704 per 1ml whole blood.)

The main purpose of the additional centrifugation is to purify WBC in the transferred plasma. After the additional step of centrifugation was added,

most residual WBCs in the upper 2/3 PRP transferred were purified in the different speeds (100g and 200g). The effectiveness was confirmed by both DAPI staining and automated cytometer. Using DAPI staining, the 96.24% and 97.36% of the WBCs in the transferred plasma were cleaned by the methods of additional centrifugation (100g and 200g). Similar results were acquired by an automated cytometer, showing that 99.78% and 99.92% of WBCs in the transferred plasma were cleaned (**Table 21**).

Table 20. The results of WBC contamination rates in nine cases via the three-step (100g and 200g) and two-step centrifugations.

ID	WBC count			Platelet count			WBC contamination rate/ 1 million platelets		
	2-step	100g	200g	2-step	100g	200g	2-step	100g	200g
CPM1-065	382	4	0	1263333	157000	84000	302	25	0
CPM1-066	8	0	2	2233333	316667	410000	4	0	5
CPM1-067	18	2	4	1090000	25000	45333	17	80	88
CPM1-071	31	4	0	2665000	156500	79500	12	26	0
CPM1-073	23	1	0	1420000	208000	82000	16	5	0
CPM1-028	5	0	0	1190000	128500	54500	4	0	0
CPM1-076	26	5	2	1330000	215333	59333	20	23	34
CPM1-077	43	9	4	2213333	187666.7	43000	19.4	48	93
CPM1-019	500	3	15	1613333	356666.7	396666.7	309.9	8.4	37.8
average	115.1	3.1	3	1668704	194592.6	139370.4	78.2	24	28.6

WBC: white blood cell.

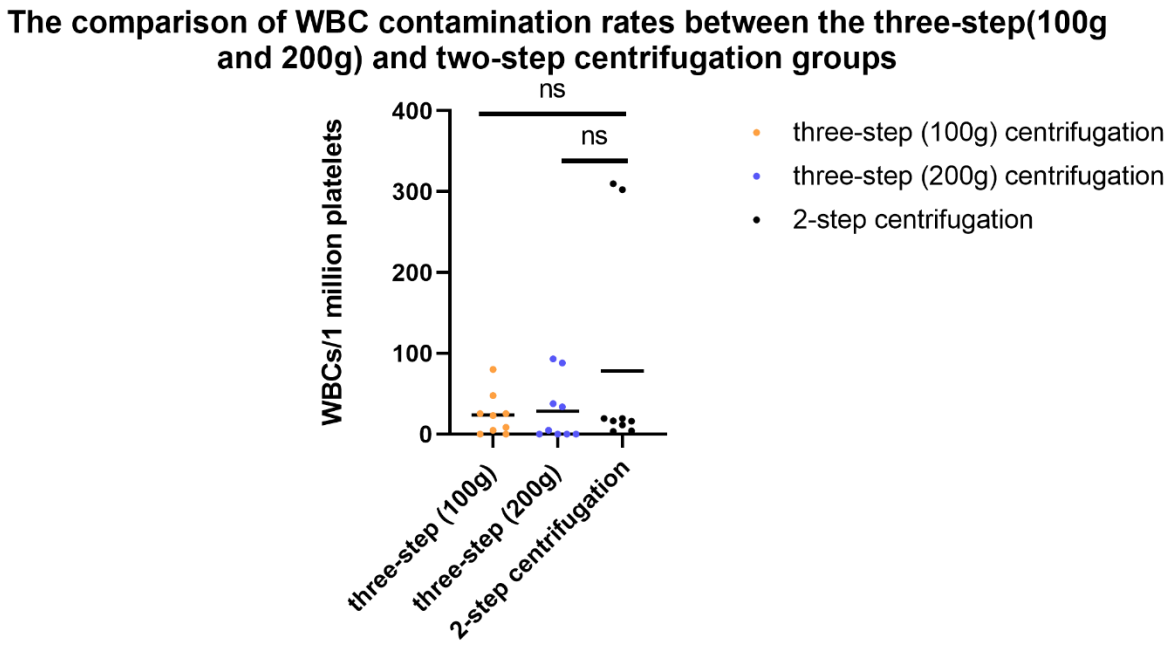

Figure 20. The comparison of WBC contamination rates in 9 platelet samples isolated by a 2-step, 3-step (100g) (*p*=0.26), and 3-step (200g) (*p*=0.32) centrifugations.

The X axial represented the different groups, while the Y axial illustrated the WBC contamination rates (WBCs/ 1 million platelets). Better WBC contamination rates were acquired in the groups of 3-step methods. WBC: white blood cell.

Table 21. The results of WBC clean rate during the additional step of centrifugation in nine cases via the three-step (100g and 200g) and two-step centrifugations.

ID	WBC clean rate (%) (DAPI)			WBC clean rate (%) (auto cytometer)		
	2-step	100g	200g	2-step	100g	200g
CPM1 065	17.49	98.88	100	50	99.97	99.97
CPM1 066	91.75	100	97.5	64.52	100.00	100
CPM1 067	61.70	87.5	87.10	62.63	99.97	100
CPM1 071	68.69	95.18	100	42.28	98.93	99.98
CPM1 073	45.24	98.33	100	8.56	99.93	99.99

CPM1 028	73.68	100	100	49.055	99.50	99.72
CPM1 076	57.38	93.90	96.72	30.55	99.95	99.87
CPM1 077	42.67	92.68	96.36	2.33	99.99	99.87
CPM1 019	50	99.7	98.52	41.24	99.74	99.92
average	56.51	96.24	97.36	39.02	99.78	99.92

WBC clean rates were calculated by both DAPI and auto cytometer. WBC: white blood cell, DAPI: 4',6-diamidino-2-phenylindole.

2.2.4 Using 3μm membrane filter for platelet collection

From July 2022 to August 2022, 10 PCa patient samples were collected. On average, The WBC contamination rates were 90.3 and 58.5 WBCs per 1 million platelets, calculated between the 3-μm membrane filter and the upper 2/3 PRP, respectively (p=0.013) (**Table 22**)(**Figure 21**). Additionally, there were 142,433 platelets and 3,039,000 platelets from each 0.5 ml of whole blood (P=0.001) by 3-μm membrane filter and the 2-step centrifugation. The new method only provided approximately 5% of the platelets obtained using the traditional method.

Table 22. The comparison of platelet count, WBC count and WBC contamination rate in 10 cases via 3μm membrane filter and upper 2/3 PRP.

	3μm membrane filter+ 2-step centrifugation			2-step centrifugation		
ID	Platelet count	WBC count	WBC contamination rate (WBC/1million platelets)	Platelet count	WBC count	WBC contamination rate (WBC/1million platelets)
CPM1 011	170000	5	29.4	4100000	13	3.2
PPPP433	19333.3	2	51.7	6833333	52	30.2
CPM1 055	16000	6	375	430000	129	300
CPM1 059	64333.3	7	108.8	1220000	89	73
CPM1 060	135666.7	13	95.8	3333333	115	34.5
CPM1 050	370000	8	21.6	2936667	54	18.4
CPM1 049	200333.3	9	44.9	3920000	22	5.6
CPM1 048	132666.7	2	15.1	833333.3	19	22.8
CPM1 047	283333.3	2	7.1	6033333	131	21.7
CPM1 046	32666.7	5	153.1	750000	57	76
average	142433.3	5.9	90.3	3039000	68.1	58.5

There was a higher average of WBC contamination rate (90.3 WBCs per one million platelets) in the filter group (*P*=0.013). WBC: white blood cell, PRP: platelet rich plasma.

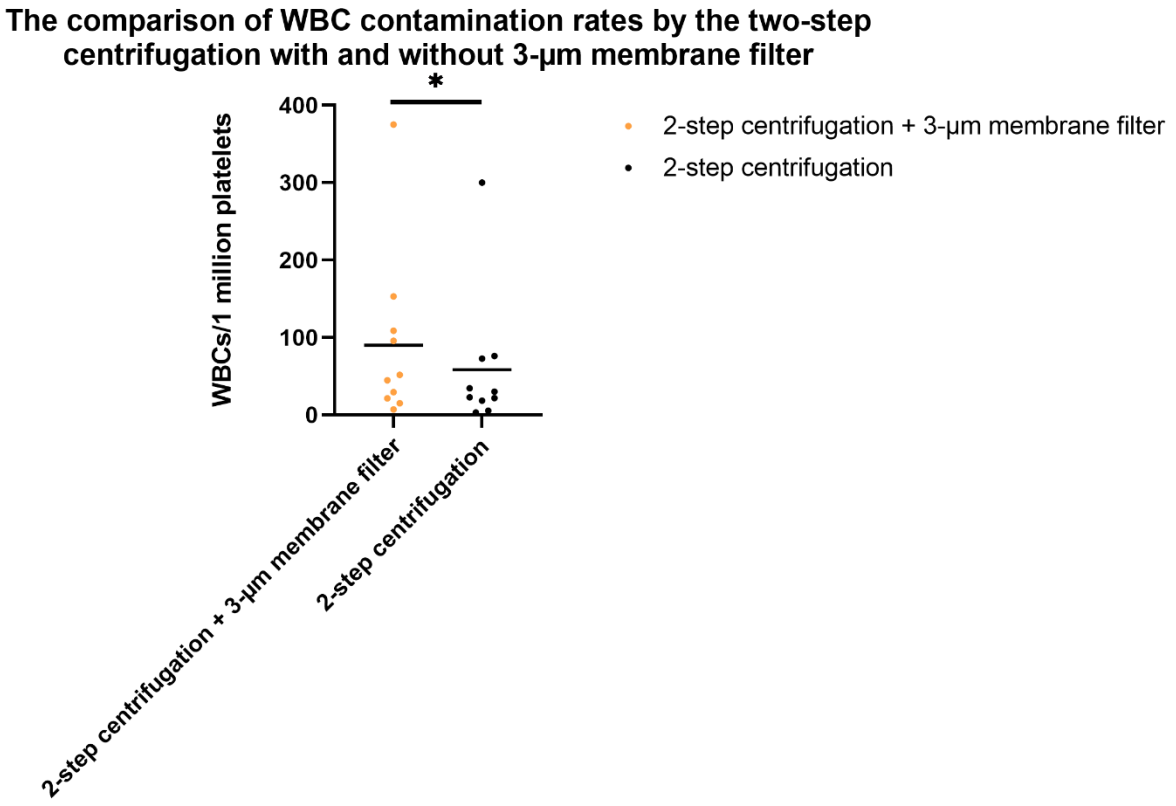

Figure 21. The comparison of WBC contamination rates in 10 platelet samples isolated by 3μm membrane filter and two-step centrifugation (*p*=0.013).

WBC: white blood cell.

2.5 Using 1μm Membrane Filter in Platelet Collection

From August 2, 2022, to August 25, 2022, a total of 0.5ml of whole blood was collected from five PCa patient samples. A comparison was made between the 2-step centrifugation method and the use of a 1μm filter in this group. The results showed that the 1μm filter yielded a WBC contamination rate of 1.2 leucocytes per one million platelets, compared to 15.4 leucocytes per one million platelets in the 2-step collection (*p*=0.18)

(**Figure 22**). Additionaly, the application of the 1-μm filter significantly decreased the platelet collection, with only approximately 2.6% of the platelets collected compared to the 2-step method (650,167 platelets vs. 25,303,333 platelets, *p*=0.03) (**Table 23**)

Finally, the summary of all the methods of modification has been listed in **Table 24**.

Table 23. The comparison of platelet count, WBC count and WBC contamination rate in five cases between the usage of 1um filter and two-step centrifugation.

	1-um filter+ 2-step centrifugation			2-step centrifugation		
ID	Platelet count	WBC count	WBC contamination rate (WBC/1million platelets)	Platelet count	WBC count	WBC contamination rate (WBC/1million platelets)
PPPP437	180000	0	0	31333333	154	49.1
PPPP438	1716667	0	0	189333333	173	9.1
PPPP439	483333	0	0	117333333	36	3.1
CPM1-062	866667	1	5.8	68333333	69	10.1
CPM1-065	4167	0	0	15700000	9	5.7
average	650167	0.2	1.2	84406667	88.2	15.4

Using 1μm filter provided 1.2 leucocytes per one million platelets, compared to 15.4 leucocytes per one million platelets in 2-step collection. WBC: white blood cell.

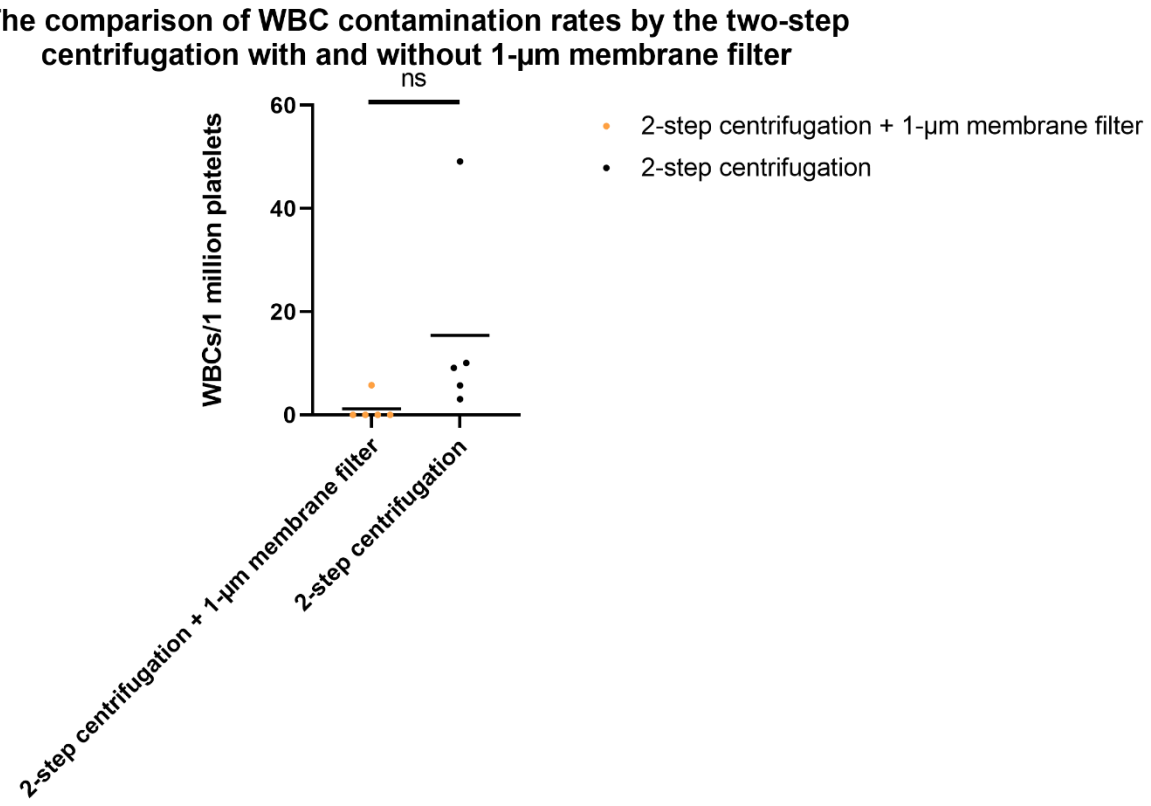

Figure 22. The comparison of WBC contamination rates in 5 platelet samples isolated by 1μm membrane filter and two-step centrifugation (*p*=0.18).

WBC: white blood cell.

Table 24. The comparison of taking upper ½ PRP, 1, 3μm filters, three-step centrifugation and magnetic beads in the modification of platelet collection.

	platelet loss	WBC contamination rate	Expense for additional instrument	duration
1/2 upper PRP	97.9%	20	N/A	minutes
3μm filter	99.9%	90	Less than one pounds/ each	minutes
1μm filter	99.6%	1	Less than one pounds/ each	minutes
3-step centrifugation(100g)	99.9%	24	N/A	minutes

3-step centrifugation(200g)	99.9%	29	N/A	minutes
magnetic beads	99.4%	45	More than hundred pounds	0.8-1hour

At the cost of highest loss of platelets, 1μm filter provided best WBC contamination rate of 1 WBCs per one million platelets, while 3-step centrifugation demonstrated a cheap and simple manipulation. PRP: platelet rich plasma, WBC: white blood cell, N/A: not available.

3. Discussion

3.1 Evaluation of the current two-step differential centrifugation for platelet collection

In our study, a first spin at 200g for 20 minutes was applied to segregate platelets, while a subsequent spin at 400g for 20 minutes was used to concentrate them. My research suggests that the observed low platelet recovery rate (7.37%) from the upper 2/3 of the PRP might indicate significant platelet loss during the first centrifugation step. The result implied that many platelets remain in other parts of the sample after centrifugation. Besides, it is critical to know that along the increase of centrifugation speed, the activation of platelets may also begin spontaneously [491, 536, 537], potentially changing the RNA profiling [270].

3.1.1 Determining Optimal Centrifugation Speeds

Currently, there is no standardization of PRP preparation [525, 527]. Technically, it is understandable that the low speed of the first centrifugation may potentially cause more residual leukocytes in the transferred PRP [428]. Regarding the first step, the velocities have been set mildly, ranging from 50g to 300g within 20 minutes [428, 528-532] to collect PRP where platelets suspended [538]. There was a report showed

that 100-250 g in the first-step had a lower platelet activation by P-selectin expression for about 11-15% increase [536] (**Table 25**). In the current study, 200 g as the speed of the first spin was in the reported range.

The second centrifugation step is performed on the PRP obtained from the first step to collect platelet [536]. This step involves a higher centrifugation speed to further separate the platelets from residual contaminants, resulting in the formation of a platelet pellet at the bottom of the tube. Technically, a spin of a higher speed may yield more platelets. However, it is important to consider that higher speeds may also pose a risk of platelet activation, which can potentially affect RNA profiling. Among the various reported choices for the second centrifugation speed ranging from 360g to 1000g [428, 528-532, 537], one study demonstrated the safety of using 360g for 20 minutes, as evaluated by flow cytometry analysis of CD63 and P-selectin, which are markers of platelet activation [351]. Another report recommended 400 g for the second spin for platelets yield with the proof that a spin of over 800g for 10 min caused platelet activation [537]. Therefore, considering the balance of risk of platelet activation and production, 400g was accepted for the second centrifugation in the project.

Table 25. The parameters of the two-step differential centrifugations in previous publications.

	first–step (centrifugation)	second -step (centrifugation)
Hamburger S.A. et al. [528]	300 g 15 min	500 g 15 min
Weyrich A.S. et al. [529]	200 g 20 min	500 g 20 min
Rowley J.W. et al. [530]	115 g 10 min	500 g 10 min
Best M.G. et al. [428] [351]	120 g 20 min	360 g 20 min
Zellner M. et al. [531]	50 g 20 min	N/A
Rolf N. et al. [532]	100 g 20 min	N/A
Finamore F. et al. [539]	150 g 15 min	1000 g
O' Neill E.E. et al. [540]	200 g 20 min	N/A
Perez A.G. et al. [537]	100 g 10 min	400 g 10 min

N/A: not available.

3.1.2 Platelet Isolation Challenge

Platelet isolation seeks to effectively separate platelets from other components of whole blood. The pivotal phase in this process occurs during the transfer of the PRP for the second centrifugation step. Typically, the upper portion of the PRP, which houses a concentrated amount of platelets, is selected, ensuring the buffy coat and the red blood cell layer remain undisturbed [525].

However, the fraction of PRP to be transferred presents a conundrum. On one hand, extracting a larger amount of PRP can optimize platelet yield

but might compromise its purity. Conversely, methods geared towards achieving pure platelets might fall short in terms of platelet volume [541]. The question then becomes: Should the procedure prioritize maximizing platelet yield or minimizing contamination from other blood components [538]?

Different studies propose various fractions of PRP to be transferred, ranging from 30% [428, 532] to as much as 90% [428, 532]. While collecting 90% of the upper PRP theoretically maximizes yield, it presents practical challenges. For instance, how to remain the buffy coat undisturbed as it's a major reservoir of WBC is a significant concern. A study which attempted to collect 90% of the PRP noted that the remaining PRP displayed a turbid appearance with a yellow and red hue, suggesting contamination from the buffy coat and the red blood cell layer [428]. Moreover, the lack of a calibrated scale on the tubes further complicates the precise collection of the proposed 90%.

In light of these challenges and with the intent to strike a balance between platelet yield and contamination, this study opted for a more conservative approach. Instead of the 90% PRP transfer as in some studies, we transferred the upper 2/3 of the PRP, aiming to ensure reduced WBC contamination and a reasonable platelet yield. Additionally, further

discussion about evaluation of platelet recovery and purity will be introduced later.

3.1.3 Platelet Recovery and Yield in the Two-Step Centrifugation Method

It is known to all that there is no process of 100% efficiency. When choosing a process as the key method of isolation and collection, calculation of the platelet production should be understood. In this project, before platelet RNA sequencing, a challenge of obtaining a sufficient quantity of RNA from a subset of platelet samples was encountered. The quantity of platelet RNA did not meet the minimum sequencing requirement at the beginning. This underscored the importance of evaluating platelet recovery from platelet isolation, especially in those blood samples with volume less than 3–5 ml.

3.1.3.1 Evaluating Platelet Recovery with the Two-Step Centrifugation

Based on the results obtained using the 2-step centrifugation method in the project, the platelet recovery was approximately 7.37% from 0.5ml blood samples collected from 47 participants. Furthermore, it was found that the upper two-thirds of the platelet-rich plasma (PRP) contained approximately 22% of the total platelets present in the blood sample.

As we are aware, there is an average range of 150 million to 450 million platelets per ml of peripheral blood [313]. Despite the widespread use of

the 2-step centrifugation method in laboratories, the efficiency of platelet collection has been rarely reported. Our results showed that the two-step centrifugation method provided a limited platelet recovery.

3.1.3.2 Potential for Enhanced Platelet Recovery

To enhance platelet recovery, there are two potential approaches for collecting more platelets in the future. On one hand, after 2-step centrifugation, roughly 10% of the total platelets were present in the upper two-thirds of PRP, while the remaining 90% of platelets were in the rest part of sample. Therefore, one direction for maximizing platelet collection would be to increase the volume of PRP collected. Previous studies have explored this by collecting the upper 90% of PRP [428, 532], with a focus on capturing more platelets, albeit at the cost of including more leukocytes.

On the other hand, it is worth noting the remaining platelets in the upper two-thirds of PRP, which did not form a pellet during the centrifugation process. Technically, by increasing the speed of the secondary centrifugation, it may be possible to acquire more platelets. However, it is important to consider that higher centrifugation speeds can potentially induce platelet activation, which could alter the RNA composition of the platelets.

3.1.3.3 Limitations and Considerations in Calculating Platelet Recovery

Ideally, obtaining the actual platelet counts for each patient would provide more accurate and reliable data for calculating the platelet recovery. Due to the unavailability of individual patient's platelet count data from the National Health Service (NHS), the calculation of the platelet recovery had to be based on the average platelet count (300 million/1ml). As platelet counts can vary significantly among individuals, this calculation may introduce bias. Furthermore, the estimation of platelet recovery was based on a small sample size of 47 cases, which may be considered statistically weak. A larger sample size would provide more robust and reliable data for calculating platelet recovery and drawing accurate conclusions.

Although the 2-step centrifugation method alone was unable to provide sufficient platelets for RNA sequencing, the challenge was fortunately overcome by implementing platelet RNA amplification technology (details of which were introduced in the corresponding section). By utilizing the switch mechanism at the 5' end of RNA templates (SMART), platelet RNA profiling became feasible for the study [532, 542]. Following the pre-amplification step, the RNA quantity ultimately met the criteria required for sequencing. Thus, requirement for a higher quantity of platelets in RNA-sequencing has been reduced.

In summary, the analysis of our current results necessitates further study to elucidate optimal individual platelet collection.

3.1.4 WBC contamination evaluation in the two-step centrifugation

The observed WBC contamination rates ranged from 0 to 309.9 WBCs per 1 million platelets, with an average value of 40.4 WBCs per 1 million platelets. This variability may be due to multiple reasons, one of which could be the inherent instability of the technology itself.

Based on the results obtained from the analysis of the 47 cases, the method of the two-step centrifugation provided about 25% cases whose WBC contamination rates were less than 5 WBCs per 1 million platelets, which aligns closely with the recommended values for platelet RNA profiling suggested by other publications [428, 532, 543].

Thus, by employing an individually accurate evaluation and selection of samples with low WBC contamination, the current 2-step centrifugation method can provide qualified platelet samples, albeit at the expense of approximately three times the required initial sample size. For instance, if an RNA sequencing experiment necessitates platelet samples from 20 PCa patients and 20 non-cancer controls, an initial pool of 80 PCa and 80 non-cancer candidates would be required to ultimately obtain a sufficient quantity of purified platelets.

3.1.4.1 Inherent Instability of Manual Isolation

In the data, due to the 2ml volume of initial blood collection, the CPM1-011 and CPM1-065 were split and used twice as two independent cases for the method evaluation. However, the WBC contamination rates of CPM1-065 showed a large difference (302.37 *vs.* 5.73 WBCs per one million platelets) while the results were close in CPM1-011 (0 *vs*. 3.17 WBCs per one million platelets). The distinction in CPM1-065 at least partly showed the instability of this collection method. The most unstable part of the manual isolation process is the transfer of the upper 2/3 of PRP. During this process of the slight and gradual dipping of the pipette tip from the surface of the sample to the plane of the upper 2/3 PRP, any uneven advancing of pipette or aspiration of plasma could lead to disturbances in the lower buffy coat, facilitating contamination. To overcome this, further trial could be performed by comparison between current manual pipette and electric one which may provide a more stable and slower speed to reduce the variation in each suction movement. Additionally, the instability can be amplified when working with small volumes of samples in the laboratory. The smaller the volume of whole blood provided, the greater the chance of significant bias occurring. Finally, it should be noted that all isolations were performed by one person (XK. Wang), and individual

preferences can also impact technical outcomes.

3.1.4.2 Recommendations and Improvements

Considering the unstable nature of the two-step centrifugation isolation method, the estimation of WBC contamination rate in each case is needed. Therefore, the additional 10μl suspension of platelets following the second centrifugation for checking the individual platelet count may be crucial in selecting suitable cases for platelet RNA profiling, despite the additional cost of 25% of the final platelet collection. This manual and simple modification appears to be beneficial and can be implemented in laboratory platelet collection protocols of 2-step centrifugation involving small volumes using the 2-step centrifugation method.

In conclusion, the 2-step centrifugation platelet isolation method yielded a subset of samples (approximately 1/4) with WBC contamination rates below 5 WBCs per one million platelets in 0.5 ml of whole blood. Further efforts should be directed towards enhancing the stability of this method or how to decrease the variation of this manipulation to produce more purified platelets.

3.2 The Analysis of the Different Modifications of the Current Two-step Differential Centrifugation

3.2.1 Evaluation of Taking the Upper ½ PRP and the Three-step Centrifugation in Platelet Collection

The initial centrifugation step at 200g for 20 minutes was expected to separate most of the leukocytes to the lower part of PRP and buffy coat. Therefore, it was logical to assume that taking a smaller volume from the upper part of PRP would reduce the chances of including WBCs. However, based on our data, taking the upper half of PRP for platelet collection did not result in a significant improvement in WBC contamination (P=0.18).

From the data, the absolute number of WBC detected was lower in the group of ½ upper PRP (average 19.3 WBC vs. 33.6 WBC separately, P=0.028) which consisted with the assumption. The insignificance could be explained that the more pronounced decrease in platelets led to a higher absolute value of WBC contamination rate in the 1/2 upper PRP group. The absolute number of platelets collected was lower in the group that took 1/2 upper PRP compared to the control group (average of 3195714 vs. 4654643, P=0.004).

Therefore, it may not be practical to improve WBC contamination by reducing the amount of PRP taken. It is important to note that this study

had a small sample size of only 14 cases, which may be considered statistically weak. Further data collection with a larger sample size would be necessary to provide a more accurate estimation.

3.2.2 Challenges and Limitations of CD45-Labeled Micro-bead Negative Selection for Platelet Purification

This method, known as CD45-labeled micro-beads negative selection, separates leukocytes from samples based on the specific surface marker CD45. Leukocytes attach to magnetic nanoparticles coated with antibodies against CD45. Leukocyte-depleted platelets can then be collected using magnetic separation columns [544].

This method of magnetic beads has been widely reported for its efficiency [493, 544, 545]. However, in my study, the application of magnetic beads did not lead to an improvement in WBC contamination. The WBC contamination rate was 40.76 WBCs per 1 million platelets, compared to 41.42 WBCs per 1 million platelets with the 2-step centrifugation method (P=0.96). Although the absolute number of WBCs detected was lower in the magnetic bead group (average of 27.78 WBCs), the more loss of approximately 99% of collected platelets during this step resulted in a similar WBC contamination after the mathematic calculation. There are several possible causes for the platelet loss during this step. Firstly, the

repeated inversion of the tube containing the platelet suspension may lead to platelet attachment to the tube's walls. This effect could be more pronounced when a limited number of platelets are included, as was the case with the 0.5ml samples in this study. Another possible cause is the non-specific binding of platelets when leukocytes attach to magnetic nanoparticles. Given the challenges with small volume samples and the associated costs, this method seems unsuitable for platelet purification in such contexts.

3.2.3 Discussion of the Three-step Centrifugation in Platelet Collection

In a previous evaluation of 47 platelet samples collected using the 2-step centrifugation method, only 25% of the samples had a WBC contamination rate lower than 5 leucocytes per 1 million platelets, which could be a consensus for RNA sequencing requirements. However, the additional 200g centrifugation step increased the number of purified platelet samples with a WBC contamination rate below 5 from 25% to more than 50% (5 out of 9 cases), which shows promise in providing more qualified platelet samples.

The choice of 100g and 200g centrifugation speeds in the additional centrifugation steps was based on the effectiveness of 200g in the initial centrifugation step for separating components in whole blood. It was

logical to assume that lower speeds would be effective for simpler components in PRP, with a higher concentration of platelets and a limited number of WBCs and red blood cells. The results confirmed the effectiveness of the chosen speeds. Furthermore, the set of the speeds in the study was based on previous experience that speeds below 250g were considered relatively safe to protect platelets from activation based on previous experience [536].

Between the two additional centrifugation groups, the data showed that in a 0.5ml blood sample, the 100g centrifugation collected more platelets (972,963 platelets per sample) with a lower average WBC contamination rate (23.94 WBCs/1 million platelets). In the 200g centrifugation group, 5 out of 9 cases had WBC contamination rates below 5 WBCs (4 cases had 0 WBCs, and 1 case had around 4 WBCs) per 1 million platelets. Further research can explore more suitable speed sets between 100 and 200g for this additional centrifugation.

One benefit of the additional centrifugation step is that it might add the stability to the 2-step platelet isolation method by cleaning majority of WBC in the transferred plasma after the first-step centrifugation. It was showed that compared to the highest WBC contamination rate of about 300 leucocytes per million platelets in the 2-step method, the highest

values of WBC contamination in the two additional centrifugation groups were both less than 100, resulting in a narrower contamination range. Although a single example cannot be used to explain the value of a method, the case of CPM1-019 at least showed the potential of this modification could be meaningful. There was heavy WBC contamination after the first centrifugation. However, after undergoing the additional 100g centrifugation, the WBC contamination rate was 8.4 WBCs per one million platelets, compared to 309.92 WBCs per one million platelets in the 2-step method. This implied that the additional centrifugation step has the potential to compensate for the possible high contamination from the first step, potentially reducing effect of contamination. Therefore, this added step shows promise in modifying the stability of the 2-step centrifugation method to obtain a purified sample.

Furthermore, compared to other modifications, the 3-step centrifugation method is simple to manipulate, making it practical. However, due to the approximately over 99% platelet loss (approximately 99.9% in both the 100g and 200g centrifugation groups) in the additional centrifugation step, the final WBC contamination rates were found to be statistically insignificant (p=0.26 and p=0.32, respectively).

In summary, the 3-step method of centrifugation shows potential in producing more stable and purified platelets. Further studies can be conducted to determine the optimal speed set between 100-200g for the additional centrifugation step, striking a balance between platelet collection and WBC exclusion.

3.2.4 Analysis of Using 3μm Membrane Filter in Platelet Collection

The purpose of using the 3μm filter was to improve leucocyte depletion by blocking larger-sized leukocytes [540]. The filter was expected to allow only particles within a certain size range to pass through, effectively obstructing most leukocytes whose sizes are more over 7μm. However, from the data, it appears that the use of a 3μm filter in the platelet isolation process did not improve WBC contamination. On the contrary, it actually increased the contamination, likely due to the loss of platelets during the additional filtration step.

In this method, we purified the PRP by putting membrane filter in an Eppendorf with a centrifugation of low speed (100g 1min). This set was for the passage of PRP without influencing platelets' activity [536]. The data showed that some leukocytes were still able to pass through the filter, indicating that they might have changed their shape or form to do so. Additionally, using the filter resulted in a finally higher WBC contamination

rate of 90 WBCs per one million platelets (P=0.013), at the cost of losing 99% of the platelets, compared to the 2-step centrifugation method. The significant loss of platelets during the filtration step suggests the inefficiency of this method, particularly when working with small volumes of whole blood (0.5ml). Similar findings have been reported in other studies [546], which recommend using filters specifically designed for larger volumes of whole blood [546].

In summary, the experiment of using 3μm filter in platelet isolation provided a poor platelet collection and WBC contamination in the study.

3.2.5 Using 1μm Membrane Filter in Platelet Collection: a Promising Direction?

Comparing the results to the 2-step centrifugation method, the use of a 1-μm filter which is smaller than the diameter of a platelet (about 1.5-3 μm) [271] resulted in an average contamination of 1.15 leucocytes per one million platelets (p=0.18) with the collection of 2.6% of the platelets from the five samples. Interestingly, in four out of the five samples, no stained white blood cells (WBCs) were observed under a microscope after using the filters. This suggests that although the filters primarily blocked platelets, they inadvertently provided a potentially pure collection of limited platelet numbers.

Furthermore, in the case of CPM1-062, some leucocytes were still observed, despite their average diameter being approximately 7-15 μm [547]. This might be explained that WBCs could have undergone a transformation to pass through the smaller filter. The 1μm filter appeared to be more effective in blocking most of the leucocytes based on the comparison to 3μm filter. Additionally, a syringe pump was used during the filtration process to ensure a stable and consistent speed as the platelets passed through the filter, enabling a fair comparison among the five cases.

Apart from the finding that the 1μm filter might provide relatively high-purity platelets, another question arises regarding the suitability of these collected small-sized platelets for RNA profiling. Several factors should be considered in this regard. Firstly, the composition of the collected small-sized platelets needs to be analyzed. This includes platelets that were originally within the normal size range (1.5-3μm) but may have undergone transformation during the filtration process due to pumping-induced stress. Previous reports suggest that platelets can be activated by physical stress [536] potentially leading to alterations in RNA profiling [548], which could significantly impact sequencing results. To address this issue and prepare this group of platelets for future use, additional methods to fix platelet activation and maintain stabilization prior to filtration, such as

paraformaldehyde [549] and Formaldehyde [550], could be considered.

In the study of 1-μm filter, it is possible that small-sized platelets obtained after filtration are those with diameters less than 1 μm prior to filtration. This raises the question of whether these small platelets can represent the overall characteristics of the entire platelet population and serve as suitable candidates for further RNA research. The concept of platelet size as a functional distinction has been debated for the past 70 years. Initially, larger platelets were considered a younger and more reactive subpopulation [534]. Larger platelets were reported to contain more mRNA associated with hemostatic processes [311], suggesting that small-size platelets may not be ideal for RNA studies. However, other published studies have questioned this concept [551-554]. For example, decreased platelet size has been linked to poorer outcomes in patients with cancer-associated thrombosis in the Vienna Cancer and Thrombosis Study [13], suggesting that small-size platelets may be more relevant to cancer development. Therefore, the role and value of small platelets in cancer research have not been definitively established [555].

In summary, the use of a 1-μm filter for platelet isolation appears to yield a more purified result, although further cases are required to clarify its value and determine its suitability for RNA profiling.

The calculation of sample sizes for each modification was not initially performed, reflecting a deviation from the ideal study design process. The initial sample sizes in the pilot study were constrained by available resources and funding.

Despite observing insignificant results with the employed sample sizes, suggesting inadequate statistical power, I now recognize the necessity of a more systematic approach. After retrospectively analyzing my data to estimate the power and effect sizes, I have outlined the required sample sizes for each method alongside the sample sizes originally used. These calculations aim for a study power of 80% at a significance level of 0.05, assuming a two-sided test (**Table 26**):

Table 26. The parameters of the two-step differential centrifugations in previous publications.

	Current sample size	Effect size (Cohen's d)	Required sample size per group
1/2 upper PRP	14	0.441	82
3-step centrifugation(100g)	9	-0.581	48
3-step centrifugation(200g)	9	-0.519	60
magnetic beads	9	-0.025	26,042
3μm filter	10	0.317	158
1μm filter	5	-1.051	16

These findings underscore the need for larger sample sizes in future studies to ensure robust and statistically sound results, particularly for methods where the required sample size far exceeds what was initially used. In future research, priority could be to secure sufficient samples to properly evaluate the methods of platelet collection by using 1-μm filter, 3-step centrifugation, and ½ upper PRP, as these require fewer than 100 cases each.

4. Conclusion

The current two-step centrifugation provided a one-in-four successful rate of qualified platelets (WBC contamination rate is less than 5 WBCs/ 1 million platelets) for RNA profiling.

No modification brings better results compared with the current two-step centrifugation in my pilot study.

However, three-step centrifugation brought a chance (5/9) of purified platelets with simple manipulation and low expense. The future plan could be focused on how to explore a more suitable speed set between 100 and 200 g in the method of 3-step centrifugation. The application of 1um filter provided a good purification as well as the potential platelet activation. More cases are needed to reach the ideal sample size for each method to clarify the efficiency of platelet collection.

CHAPTER VI: Final Discussion and Future Research

1. Final Discussion

Platelets offer an abundant pool of molecules in circulation, and they have been reported to receive molecules from cancer cells, enabling communication during early cancer stages [273]. Platelets' ability to undergo activation [334], RNA changes during their interaction with non-cancer [438-440, 443] and cancer cells [352] and the close relationship between mRNA and miRNA [434] helped us build up the hypothesis that microRNAs could change in PCa and hold potential as early cancer detection biomarkers.

In this study, we identified differential expressions of miRNA627, 22, 195, 28, and 664 in the PCa group, supporting the hypothesis of platelet miRNA involvement in PCa detection. Importantly, these findings were confirmed in independent Chinese discovery and British validation groups, indicating their potential value as cancer detection biomarkers across different racial and geographical backgrounds. While individual miRNAs showed limited predictive power with AUC values all below 0.7, combining miRNA627, miRNA22, and CTC number in a panel significantly improved the AUC

value to 0.7817 in the detection of PCa. Additionally, miR190 exhibited lower expression in clinically significant PCa, suggesting its potential as a specific biomarker for aggressive disease.

Regarding PCa detection, the widely used PSA test has been long-termly questioned for its low specificity (16%) at the cutoff point of 4 ng/mL, leading to unnecessary tissue biopsy [116]. Furthermore, PSA's limited ability to detect aggressive PCa from indolent tumour also result to overdiagnosis and overtreatment.

1.1 Platelet miRNA Might Contribute to Improve PSA's Specificity in PCa Detection

To make up for PSA's low specificity in PCa detection, the panel of miR627 and miR22 provided a specificity of 50.51% with sensitivity of 88.89% (the cutoff point of -2.341) Furthermore, based on keeping the similar sensitivity (88.24%), the panel of miR627 and miR22 with CTC number provided a better specificity of 62.58% (the cutoff point of -2.003). Platelet miRNA with or without CTC number could improve PSA's low specificity and avoid more unnecessary biopsy.

The reason to include the CTC data is mainly due to the previous finding in our team that at least one CTC was detected in about 30% latent and over 50% aggressive PCa patients [223]. Due to the feature of CTCs,

enhancement of the panel's specificity was expected. With the help of CTC's tumour specificity, the addition to miRNA further enhances the panel's specificity of more than 10% at the expense of a slight decrease in sensitivity due to the low detection rate in the PCa [223]. Thus, including CTC count in our panel gives more potential of the panel for early cancer detection. Because the role of CTCs in PCa early detection remains investigation, this combination might still face the following challenge which needs further validation (For example, a biomarker detects disease relatively well among patients with late-stage disease but detects disease poorly among patients with early-stage disease [111]). Therefore, the sensitivity and specificity of panel with and without CTC number were both provided.

1.2 Investigating Tumour Specificity of the panel

For a biomarker of PCa detection to be effective, it should ideally be highly tumour specific compared to the low specificity of PSA, or at least tumour associated, minimising interference from other sources and non-cancer diseases. A negative example is that the elevation of PSA in benign prostate diseases raises long-term concerns about its low specificity for PCa detection. This results in patients with BPH or prostatitis undergoing unnecessary biopsies. Similarly, after my study

demonstrated that platelet miRNA190 was expressed differently between aggressive and the latent PCa groups, the AUC value in the comparison between aggressive and latent PCa was then calculated higher than that between aggressive PCa and the remaining (0.64 *vs.* 0.63), implying miR190 might also be expressed in some benign prostate diseases.

1.3 Limitations in my study of biomarker development

Generally, problems of biomarker can develop at many stages of biomarker discovery and validation. These problems can be divided into analytical (Test itself and the immediate results, e.g. sensitivity and specificity) and preanalytical (Conditions and methods leading up to the test, such as sample collection.) types during cancer biomarker discovery and validation [556]. The list of the possible limitations in my study was arranged based on this classification.

1.3.1 Analytical limitation of the study

In this study, the individual miRNAs and the panel of miRNAs combined with CTC numbers fell short of achieving an ideal AUC value exceeding 0.8 for detecting prostate cancer (PCa). Similarly, even in the detection of clinically significant PCa, miRNA 190 only yielded an AUC value of about 0.64. The modest AUC values observed for platelet miRNA in isolation

suggest that platelet RNA may not be sufficient as a standalone biomarker for PCa detection due to its limited predictive value.

Despite the limitations of individual platelet miRNA as biomarkers (AUCs<0.7), their combination with other biomarkers, such as CTC numbers, improved PCa detection, resulting in an AUC value (0.78) close to the desired threshold of 0.8. This finding suggests that although platelet miRNA alone might not be good enough to be developed as an independent marker, it could play a role in enhancing the predictive value of a panel with other biomarkers. Similar experiences in previous studies have demonstrated that combining biomarkers, even when individually suboptimal, can synergistically enhance panel prediction value [485, 557]. Thus, one of the future focuses could be on the selection of other biomarkers to build a better panel for PCa detection.

1.3.2 The Bias Caused by the Sequencing Methods

Potential biases from the sequencing methods, including disparities in read length, error rates, and sequencing depth, may have affected our RNA-seq results.

Our mRNA-seq, conducted on the Illumina platform, may exhibit GC bias, causing over- or under-representation of regions with high or low GC content. Although normalization attempted to mitigate this, residual GC

effects could influence gene quantification [558, 559]. Due to the inadequate RNA, additional preamplification was also performed, which can also potentially skew expression estimates. If not properly trimmed, residual adapter sequences can interfere with mapping and quantification.

Our microRNA-seq was performed on the BGISEQ-500 platform, known for its sensitivity in small RNA detection. Its use of Rolling Circle Amplification may introduce bias in amplifying certain sequences, potentially affecting miRNA quantification. Issues like droplet formation inefficiencies could lead to representation bias, and the platform's unique sensitivity may skew detection of some low-abundant miRNAs.

Thus, the potential influence of these biases on our results should be acknowledged as a limitation of the study.

1.3.3 The Limitation of Group Size

Regarding the incorporation of power analysis prior to the validation, I now recognize the importance of this statistical method in determining the appropriate sample size for my validation cohort.

I have conducted a preliminary power analysis aimed at achieving a power of at least 80%, with an alpha level of 0.05, using a medium effect size (d = 0.5). This analysis indicates that at least 64 participants per group in the validation cohort may be necessary to detect clinically meaningful

differences in miRNA expression between PCa and non-cancer patients. Given the existing data, we have 77 non-cancer patients, which meets the minimum requirement; thus, the number of PCa patients could be between 77 to 154 to maintain a balanced design while maximizing statistical validity.

1.3.4 WBC Contamination in Platelet Samples is One Potential Technical Issue

There was no observable difference in mRNA expression profiles between PCa and non-cancer groups. This indifference could stem from two sources: a genuine lack of variance at the mRNA expression level or potential technical challenges. It is conceivable that mRNA expression patterns between PCa and non-cancer groups are truly similar. This may indicate that differences in these groups might not be readily apparent at the mRNA level (detailed explanation has been shown), warranting a deeper exploration of other biomarkers or molecular indicators.

One of the technical concerns relates to the contamination from WBCs. Addressing this contamination is pivotal not just for enhancing platelet collection but also for refining platelet-specific analysis in the future, including platelet sequencing and *in vitro* co-culture investigations. To mitigate this contamination, a suite of experiments was designed to

enhance platelet collection techniques: using smaller RPR volumes, introducing filters, adding an extra centrifugation step, and employing magnetic beads. Comprehensive testing in larger cohorts for fine-tuning centrifugation and filtration methods is imperative.

Given that WBC contamination could affect both mRNA and miRNA data, it's essential to understand that the results of miRNA sequencing might also be influenced by this preanalytical phase limitation. Consequently, it's vital that validations of the miRNAs identified in this study are performed in an independent cohort, using a reliable and accepted platelet collection method.

1.3.5 Potential Change of Platelet Activity during the Collection

The secondary thinking is the potential change of platelet activity during the collection which might subsequently influence the RNA profile in platelets [428, 536]. In the current study, 200g was applied as the speed of the first step in centrifugation, which lies in the reported safe range between 100 to 250g with small and acceptable change of platelet activity [428, 536]. Furthermore, the speed of the secondary centrifugation in the study is also close to the reported safe value [428].

Although it is well known that the two-step centrifugation has been widely applied for platelet collection, further accurate evaluation of platelet

activity during the collection could be considered based on the purpose of using platelet analysis. Additionally, whether the application of platelet activation stabilizer, such as formalin or paraformaldehyde during the collection is needed to clarify.

1.3.6 Uncertainty of Individual Characteristics

Finally, the uncertainty of various individual characteristics in the study cohort could be another limitation. In the study, although the ages between cancer and non-cancer patients were compared with no difference (p=0.38), more details of patients (such as diet, ethnicity, lifestyle, drugs other than the treatment of PCa or exercise) were not clear. All the above factors could independently affect biomarker levels.

2. Future Research

2.1 Refining Platelet Isolation Techniques: A Look into Centrifugation and Filtration Methods

In our experimental setup, the application of a three-step centrifugation process demonstrated a higher likelihood (5 out of 9 trials) of obtaining purified platelets compared to the conventional two-step method. Moving forward, it would be beneficial to conduct tests on more samples, aiming to determine the optimal centrifugation speed within the range of 100 to 200 g for this additional step.

Concurrently, the use of a 1µm filter exhibited remarkable purification capabilities in our trials, yielding approximately 1 WBC for every million platelets in five instances. To solidify these findings, more experiments are necessary. They should focus not only on the efficiency of platelet collection using this filtration method but also on evaluating potential platelet activation throughout the process.

2.2 Strengthening miRNA Signatures: in vitro Strategies for Tumour Association Confirmation

The prevalent issue of PSA's low specificity in prostate cancer screening stems, in part, from its weak tumour association [560]. This limitation,

which often leads to unnecessary biopsies, prompted the direction of my project.

Part of my hypothesis was derived from studies suggesting alterations in platelet miRNAs in non-cancerous conditions, such as cardiovascular injuries [441]. While my study identified several miRNAs with differential expression between PCa and non-cancer groups, as well as between aggressive and latent PCa categories, implying their genuine tumour association. The validation in independent large cohorts comparing the microRNA expression in platelets from PCa patients versus non-cancer control is another key to acquire strong scientific evidence. Regarding the choice of control cases, the inclusion of age-matched patients with benign prostate disease could be primarily considered.

This is especially so given the potential influences from non-cancer related biological factors. Hence, the true tumour-related nature of these miRNAs warrants further investigation, potentially through *in vitro* studies and additional independent validations.

By performing *in vitro* co-culture experiments between different PCa cell lines (both aggressive e.g., PC3 and latent types e.g., LNCap) and normal platelets, I plan to create a controlled environment to study the interaction between the two and observe any changes in platelet activity and

microRNA expression. It is essential to include appropriate control groups in the experiments. These control groups can include platelets cultured alone, and non-cancerous cells (e.g., prostate epithelial cells) as a non-tumour-specific control.

The aim of this step is to determine if platelets become activated or undergoing any significant changes due to the interaction with PCa cells, as has been reported in some previous studies [322, 334]. Platelet activity can be assessed by measuring changes in surface markers like P-selectin after co-culturing platelets with PCa cells. This experiment could further compare platelet activity between co-cultures with aggressive (e.g., PC3) and latent (e.g., LNCaP) PCa cell lines to see if there is difference. Measuring P-selectin and other activation markers would clarify whether PCa cells trigger platelet activation and if the response varies between cancer cell lines.

After confirming the status of platelet activity, extraction of RNA from the co-cultured platelets and control platelets can be performed. The expression of the previously identified microRNAs can be checked by RT-qPCR. This analysis will help determine if the microRNA expression changes exist and are induced by the presence of cancer.

Transfection of human platelets with small interfering RNA has been

reported [561]. By using transfection of human platelets with target microRNA mimics and inhibitors, investigation is to focus on the functional role of those differentially expressed microRNAs in the study.

After successful transfection, the platelets can be co-cultured with PCa cell lines. Functional assays such as proliferation, migration, or invasion assays can be conducted in PCa cells to understand the biological implications of the platelet microRNAs to cancer cells.

2.3 Prediction of miRNA190's target genes and Potential pathways

In this study, miR190 demonstrated differential expression between aggressive PCa and both non-cancer controls and latent PCa as well as between aggressive PCa and latent PCa. To elucidate the potential functional impact of miR190, the bioinformatics tool, miRWalk, was employed to predict its targets. Through a combined effort of this prediction and subsequent literature review, 11 genes emerged as potential targets for miRNA190. With the help of 'The Human Protein Atlas' (https://www.proteinatlas.org/), HMGA2 was identified as the most promising target gene for miR190 from the 11 candidates. (Notably, HMGA2 exhibited elevated expression in PCa cases associated with a predicted poor prognosis (details are elaborated in the miRNA-seq results discussion CHAPTER III 2.2 Page 127)).

With ethical considerations in mind for both animal and patient sample use, future validation efforts will span in vitro and in vivo studies, as well as analyses utilizing patient samples:

In Vitro Validation

Luciferase Reporter Assays: Cloning the 3'UTR of predicted mRNAs (e.g., HMGA2) downstream of a luciferase reporter will serve to test for direct targeting by miRNA190. A decrease in luciferase activity upon miRNA co-transfection would signify a targeting interaction.

miRNA Modulation Experiments: Utilizing miRNA190 mimics and inhibitors to alter miRNA levels will be followed by the analysis of impacts on mRNA and protein expression in co-cultured platelets and prostate cancer cells. These experiments aim to elucidate the functional impact of miRNA190 modulation.

The primary objectives of in vitro validation are to confirm the direct interaction between miRNA190 and its target mRNA. Once this relationship is established, we will perform additional assays to assess its implications on tumor characteristics such as proliferation (e.g., MTT assays), and invasion and migration (e.g., wound healing or transwell assays).

In Vivo Validation

We will select an appropriate mouse model, such as the TRAMP genetically engineered model or cell line-derived xenografts, that closely mirrors human prostate cancer biology.

We plan to develop methods to modify miRNA/mRNA expression levels within these models, ensuring that the chosen delivery method is effective for the target tissue.

This phase will further involve evaluating the impact of miRNA190-targeted mRNA modulation on tumor growth, progression, and metastasis in mouse models.

Patient Samples

Whenever feasible, we will corroborate the in vitro and in vivo findings with analyses of miRNA and mRNA expression in platelets and prostate cancer tissues from patients. This phase is crucial for validating the clinical relevance of our findings, confirming the expression patterns observed in vitro and in vivo, or further correlating miRNA190 levels with disease stages or prognosis.

While HMGA2 stands out as a particularly promising target, it's worth noting that miRNAs often have pleiotropic effects, targeting multiple genes

that can influence various cellular pathways. From the initial 11 predicted genes, the other candidates should not be overlooked. Similar procedures as detailed above for HMGA2 can be applied to validate the interactions between miRNA190 and these other genes. This comprehensive approach ensures that we capture the full spectrum of miRNA190's influence and can lead to a more holistic understanding of its role in PCa progression.

2.4 Enhancing Prostate Cancer Detection: Potential Synergy of Platelet miRNAs and Other Biomarkers

In our study, while the individual combination of platelet miRNAs displayed limited clinical utility (with an AUC of approximately 0.71 for miR627 and miR22), the combined evaluation of platelet miRNAs and CTC numbers yielded a significantly improved AUC value approaching 0.8. This enhancement aligns with prior research demonstrating the augmented diagnostic power achieved by combining biomarkers that may individually exhibit modest accuracy [484, 557, 562]. Our findings underscore the potential to further optimize diagnostic performance through the synergistic integration of platelet miRNAs with other biomarkers. An avenue worth exploring could be the systematic pairing of these miRNAs with clinical patient’s examination result, such as imaging

(ultrasonography or MRI) which is accessible. By rigorously assessing diverse biomarker combinations, we aim to bolster diagnostic precision, thus elevating early detection capabilities and potentially revolutionizing prostate cancer screening and patient prognosis.

In conclusion, this study on developing potential biomarker from platelet RNA for PCa Detection lays a foundation for further investigations. By addressing the identified limitations and exploring the suggested future directions, we aim to refine and validate the biomarker panel's clinical utility. Ultimately, our efforts strive to advance early detection and improve the management of prostate cancer, leading to better patient outcomes and reduced healthcare burden. Collaborative endeavours among researchers, clinicians, and industry partners will be key to translating these findings into tangible benefits for patients worldwide.

Reference

1. Lee, C.H., O. Akin-Olugbade, and A. Kirschenbaum, *Overview of prostate anatomy, histology, and pathology.* Endocrinol Metab Clin North Am, 2011. **40**(3): p. 565-75, viii-ix.
2. Sathianathen, N.J., et al., *Landmarks in prostate cancer.* Nat Rev Urol, 2018. **15**(10): p. 627-642.
3. McNeal, J.E., et al., *Zonal distribution of prostatic adenocarcinoma. Correlation with histologic pattern and direction of spread.* Am J Surg Pathol, 1988. **12**(12): p. 897-906.
4. Marker, P.C., et al., *Hormonal, cellular, and molecular control of prostatic development.* Dev Biol, 2003. **253**(2): p. 165-74.
5. Kellokumpu-Lehtinen, P., R. Santti, and L.J. Pelliniemi, *Correlation of early cytodifferentiation of the human fetal prostate and Leydig cells.* Anat Rec, 1980. **196**(3): p. 263-73.
6. Aaron, L., O.E. Franco, and S.W. Hayward, *Review of Prostate Anatomy and Embryology and the Etiology of Benign Prostatic Hyperplasia.* Urol Clin North Am, 2016. **43**(3): p. 279-88.
7. Wang, G., et al., *Genetics and biology of prostate cancer.* Genes Dev, 2018. **32**(17-18): p. 1105-1140.
8. van Leenders, G.J. and J.A. Schalken, *Epithelial cell differentiation in the human prostate epithelium: implications for the pathogenesis and therapy of prostate cancer.* Crit Rev Oncol Hematol, 2003. **46 Suppl**: p. S3-10.
9. Shen, M.M. and C. Abate-Shen, *Molecular genetics of prostate cancer: new prospects for old challenges.* Genes Dev, 2010. **24**(18): p. 1967-2000.
10. Kwon, O.J. and L. Xin, *Prostate epithelial stem and progenitor cells.* Am J Clin Exp Urol, 2014. **2**(3): p. 209-18.
11. Nicholson, T.M. and W.A. Ricke, *Androgens and estrogens in benign prostatic hyperplasia: past, present and future.* Differentiation, 2011. **82**(4-5): p. 184-99.
12. Cunha, G.R., et al., *Hormonal, cellular, and molecular regulation of normal and neoplastic prostatic development.* J Steroid Biochem Mol Biol, 2004. **92**(4): p. 221-36.
13. Lee, S.H. and M.M. Shen, *Cell types of origin for prostate cancer.* Curr Opin Cell Biol, 2015. **37**: p. 35-41.
14. Wang, X., et al., *A luminal epithelial stem cell that is a cell of origin for prostate cancer.* Nature, 2009. **461**(7263): p. 495-500.
15. Yoo, Y.A., et al., *Bmi1 marks distinct castration-resistant luminal progenitor cells competent for prostate regeneration and tumour initiation.* Nat Commun, 2016. **7**: p. 12943.
16. Goldstein, A.S., et al., *Identification of a cell of origin for human prostate cancer.* Science, 2010. **329**(5991): p. 568-71.
17. Wang, Z.A., et al., *Lineage analysis of basal epithelial cells reveals their unexpected plasticity and supports a cell-of-origin model for prostate cancer heterogeneity.* Nat Cell Biol, 2013. **15**(3): p. 274-83.
18. van Leenders, G.J., et al., *Intermediate cells in human prostate epithelium are enriched in proliferative inflammatory atrophy.* Am J Pathol, 2003. **162**(5): p. 1529-37.
19. Leão, R., et al., *Cancer Stem Cells in Prostate Cancer: Implications for Targeted Therapy.* Urol Int, 2017. **99**(2): p. 125-136.
20. Partin, A.W., *High-grade prostatic intraepithelial neoplasia on a prostate biopsy-what does it mean?* Rev Urol, 2002. **4**(3): p. 157-8.
21. Culp, M.B., et al., *Recent Global Patterns in Prostate Cancer Incidence and Mortality Rates.* Eur Urol, 2020. **77**(1): p. 38-52.
22. Bell, K.J., et al., *Prevalence of incidental prostate cancer: A systematic review of autopsy studies.* Int J Cancer, 2015. **137**(7): p. 1749-57.
23. Kimura, T., et al., *Global Trends of Latent Prostate Cancer in Autopsy Studies.* Cancers (Basel), 2021. **13**(2).
24. Haas, G.P., et al., *The worldwide epidemiology of prostate cancer: perspectives from autopsy studies.* Can J Urol, 2008. **15**(1): p. 3866-71.
25. Sánchez-Chapado, M., et al., *Prevalence of prostate cancer and prostatic intraepithelial neoplasia in Caucasian Mediterranean males: an autopsy study.* Prostate, 2003. **54**(3): p. 238-47.
26. Litwin, M.S. and H.J. Tan, *The Diagnosis and Treatment of Prostate Cancer: A Review.* Jama, 2017. **317**(24): p. 2532-2542.

27. Zeigler-Johnson, C.M., et al., *Genetic susceptibility to prostate cancer in men of African descent: implications for global disparities in incidence and outcomes.* Can J Urol, 2008. **15**(1): p. 3872-82.
28. Carter, B.S., et al., *Mendelian inheritance of familial prostate cancer.* Proc Natl Acad Sci U S A, 1992. **89**(8): p. 3367-71.
29. Ross, R.K., et al., *5-alpha-reductase activity and risk of prostate cancer among Japanese and US white and black males.* Lancet, 1992. **339**(8798): p. 887-9.
30. Rennert, H., et al., *Association of susceptibility alleles in ELAC2/HPC2, RNASEL/HPC1, and MSR1 with prostate cancer severity in European American and African American men.* Cancer Epidemiol Biomarkers Prev, 2005. **14**(4): p. 949-57.
31. Breslow, N., et al., *Latent carcinoma of prostate at autopsy in seven areas. The International Agency for Research on Cancer, Lyons, France.* Int J Cancer, 1977. **20**(5): p. 680-8.
32. Ellison, G.L., et al., *Psychosocial stress and prostate cancer: a theoretical model.* Ethn Dis, 2001. **11**(3): p. 484-95.
33. Klabunde, C.N., et al., *Trends and black/white differences in treatment for nonmetastatic prostate cancer.* Med Care, 1998. **36**(9): p. 1337-48.
34. Amin Al Olama, A., et al., *Multiple novel prostate cancer susceptibility signals identified by fine-mapping of known risk loci among Europeans.* Hum Mol Genet, 2015. **24**(19): p. 5589-602.
35. Eeles, R.A., et al., *Identification of 23 new prostate cancer susceptibility loci using the iCOGS custom genotyping array.* Nat Genet, 2013. **45**(4): p. 385-91, 391e1-2.
36. Schumacher, F.R., et al., *Association analyses of more than 140,000 men identify 63 new prostate cancer susceptibility loci.* Nat Genet, 2018. **50**(7): p. 928-936.
37. Conti, D.V., et al., *Trans-ancestry genome-wide association meta-analysis of prostate cancer identifies new susceptibility loci and informs genetic risk prediction.* Nat Genet, 2021. **53**(1): p. 65-75.
38. Giri, V.N., et al., *Germline genetic testing for inherited prostate cancer in practice: Implications for genetic testing, precision therapy, and cascade testing.* Prostate, 2019. **79**(4): p. 333-339.
39. Nicolosi, P., et al., *Prevalence of Germline Variants in Prostate Cancer and Implications for Current Genetic Testing Guidelines.* JAMA Oncol, 2019. **5**(4): p. 523-528.
40. Castro, E., et al., *Germline BRCA mutations are associated with higher risk of nodal involvement, distant metastasis, and poor survival outcomes in prostate cancer.* J Clin Oncol, 2013. **31**(14): p. 1748-57.
41. Mano, R., et al., *Malignant Abnormalities in Male BRCA Mutation Carriers: Results From a Prospectively Screened Cohort.* JAMA Oncol, 2018. **4**(6): p. 872-874.
42. Na, R., et al., *Germline Mutations in ATM and BRCA1/2 Distinguish Risk for Lethal and Indolent Prostate Cancer and are Associated with Early Age at Death.* Eur Urol, 2017. **71**(5): p. 740-747.
43. Nyberg, T., et al., *Prostate Cancer Risks for Male BRCA1 and BRCA2 Mutation Carriers: A Prospective Cohort Study.* Eur Urol, 2020. **77**(1): p. 24-35.
44. Page, E.C., et al., *Interim Results from the IMPACT Study: Evidence for Prostate-specific Antigen Screening in BRCA2 Mutation Carriers.* Eur Urol, 2019. **76**(6): p. 831-842.
45. Wang, Q., et al., *Androgen receptor regulates a distinct transcription program in androgen-independent prostate cancer.* Cell, 2009. **138**(2): p. 245-56.
46. Desai, K., J.M. McManus, and N. Sharifi, *Hormonal Therapy for Prostate Cancer.* Endocr Rev, 2021. **42**(3): p. 354-373.
47. Gottlieb, B., et al., *The androgen receptor gene mutations database: 2012 update.* Hum Mutat, 2012. **33**(5): p. 887-94.
48. Taylor, B.S., et al., *Integrative genomic profiling of human prostate cancer.* Cancer Cell, 2010. **18**(1): p. 11-22.
49. Montgomery, R.B., et al., *Maintenance of intratumoral androgens in metastatic prostate cancer: a mechanism for castration-resistant tumor growth.* Cancer Res, 2008. **68**(11): p. 4447-54.
50. Esposito, K., et al., *Effect of metabolic syndrome and its components on prostate cancer risk: meta-analysis.* J Endocrinol Invest, 2013. **36**(2): p. 132-9.
51. Blanc-Lapierre, A., et al., *Metabolic syndrome and prostate cancer risk in a population-based case-control study in Montreal, Canada.* BMC Public Health, 2015. **15**: p. 913.
52. Vidal, A.C., et al., *Obesity increases the risk for high-grade prostate cancer: results from the REDUCE study.* Cancer Epidemiol Biomarkers Prev, 2014. **23**(12): p. 2936-42.

53. Davies, N.M., et al., *The effects of height and BMI on prostate cancer incidence and mortality: a Mendelian randomization study in 20,848 cases and 20,214 controls from the PRACTICAL consortium.* Cancer Causes Control, 2015. **26**(11): p. 1603-16.
54. Zhao, J., et al., *Is alcohol consumption a risk factor for prostate cancer? A systematic review and meta-analysis.* BMC Cancer, 2016. **16**(1): p. 845.
55. Chen, X., et al., *Coffee consumption and risk of prostate cancer: a systematic review and meta-analysis.* BMJ Open, 2021. **11**(2): p. e038902.
56. Zhang, M., et al., *Is phytoestrogen intake associated with decreased risk of prostate cancer? A systematic review of epidemiological studies based on 17,546 cases.* Andrology, 2016. **4**(4): p. 745-56.
57. Schiffman, J.D., P.G. Fisher, and P. Gibbs, *Early detection of cancer: past, present, and future.* Am Soc Clin Oncol Educ Book, 2015: p. 57-65.
58. Crosby, D., et al., *Early detection of cancer.* Science, 2022. **375**(6586): p. eaay9040.
59. Loeb, S., et al., *Pathological characteristics of prostate cancer detected through prostate specific antigen based screening.* J Urol, 2006. **175**(3 Pt 1): p. 902-6.
60. Hodge, K.K., et al., *Random systematic versus directed ultrasound guided transrectal core biopsies of the prostate.* J Urol, 1989. **142**(1): p. 71-4; discussion 74-5.
61. Smeenge, M., et al., *Role of transrectal ultrasonography (TRUS) in focal therapy of prostate cancer: report from a Consensus Panel.* BJU Int, 2012. **110**(7): p. 942-8.
62. Rouvière, O., et al., *Use of prostate systematic and targeted biopsy on the basis of multiparametric MRI in biopsy-naive patients (MRI-FIRST): a prospective, multicentre, paired diagnostic study.* Lancet Oncol, 2019. **20**(1): p. 100-109.
63. Eklund, M., et al., *MRI-Targeted or Standard Biopsy in Prostate Cancer Screening.* N Engl J Med, 2021. **385**(10): p. 908-920.
64. Eldred-Evans, D., et al., *Population-Based Prostate Cancer Screening With Magnetic Resonance Imaging or Ultrasonography: The IP1-PROSTAGRAM Study.* JAMA Oncol, 2021. **7**(3): p. 395-402.
65. Bratan, F., et al., *Influence of imaging and histological factors on prostate cancer detection and localisation on multiparametric MRI: a prospective study.* Eur Radiol, 2013. **23**(7): p. 2019-29.
66. Borofsky, S., et al., *What Are We Missing? False-Negative Cancers at Multiparametric MR Imaging of the Prostate.* Radiology, 2018. **286**(1): p. 186-195.
67. Epstein, J.I., *An update of the Gleason grading system.* J Urol, 2010. **183**(2): p. 433-40.
68. Epstein, J.I., et al., *The 2005 International Society of Urological Pathology (ISUP) Consensus Conference on Gleason Grading of Prostatic Carcinoma.* Am J Surg Pathol, 2005. **29**(9): p. 1228-42.
69. Epstein, J.I., et al., *The 2014 International Society of Urological Pathology (ISUP) Consensus Conference on Gleason Grading of Prostatic Carcinoma: Definition of Grading Patterns and Proposal for a New Grading System.* Am J Surg Pathol, 2016. **40**(2): p. 244-52.
70. Epstein, J.I., et al., *Contemporary Gleason Grading of Prostatic Carcinoma: An Update With Discussion on Practical Issues to Implement the 2014 International Society of Urological Pathology (ISUP) Consensus Conference on Gleason Grading of Prostatic Carcinoma.* Am J Surg Pathol, 2017. **41**(4): p. e1-e7.
71. Buyyounouski, M.K., et al., *Prostate cancer - major changes in the American Joint Committee on Cancer eighth edition cancer staging manual.* CA Cancer J Clin, 2017. **67**(3): p. 245-253.
72. Mottet, N., et al., *EAU-ESTRO-SIOG Guidelines on Prostate Cancer. Part 1: Screening, Diagnosis, and Local Treatment with Curative Intent.* Eur Urol, 2017. **71**(4): p. 618-629.
73. Moyer, V.A., *Screening for prostate cancer: U.S. Preventive Services Task Force recommendation statement.* Ann Intern Med, 2012. **157**(2): p. 120-34.
74. Fütterer, J.J., et al., *Can Clinically Significant Prostate Cancer Be Detected with Multiparametric Magnetic Resonance Imaging? A Systematic Review of the Literature.* Eur Urol, 2015. **68**(6): p. 1045-53.
75. Anderson, B.B., et al., *Extraprostatic Extension Is Extremely Rare for Contemporary Gleason Score 6 Prostate Cancer.* Eur Urol, 2017. **72**(3): p. 455-460.
76. Ross, H.M., et al., *Do adenocarcinomas of the prostate with Gleason score (GS) $\leqslant$6 have the potential to metastasize to lymph nodes?* Am J Surg Pathol, 2012. **36**(9): p. 1346-52.
77. Kasivisvanathan, V., et al., *MRI-Targeted or Standard Biopsy for Prostate-Cancer Diagnosis.* N Engl J Med, 2018. **378**(19): p. 1767-1777.

78. van der Leest, M., et al., *Head-to-head Comparison of Transrectal Ultrasound-guided Prostate Biopsy Versus Multiparametric Prostate Resonance Imaging with Subsequent Magnetic Resonance-guided Biopsy in Biopsy-naïve Men with Elevated Prostate-specific Antigen: A Large Prospective Multicenter Clinical Study.* Eur Urol, 2019. **75**(4): p. 570-578.
79. Emmett, L., et al., *The Additive Diagnostic Value of Prostate-specific Membrane Antigen Positron Emission Tomography Computed Tomography to Multiparametric Magnetic Resonance Imaging Triage in the Diagnosis of Prostate Cancer (PRIMARY): A Prospective Multicentre Study.* Eur Urol, 2021. **80**(6): p. 682-689.
80. Van der Kwast, T.H. and M.J. Roobol, *Defining the threshold for significant versus insignificant prostate cancer.* Nat Rev Urol, 2013. **10**(8): p. 473-82.
81. Schreiber, D., et al., *Prostate biopsy concordance in a large population-based sample: a Surveillance, Epidemiology and End Results study.* J Clin Pathol, 2015. **68**(6): p. 453-7.
82. Klotz, L., et al., *Long-term follow-up of a large active surveillance cohort of patients with prostate cancer.* J Clin Oncol, 2015. **33**(3): p. 272-7.
83. Ruiz-Cerdá, J.L., et al., *3+4 = 6? Implications of the stratification of localised Gleason 7 prostate cancer by number and percentage of positive biopsy cores in selecting patients for active surveillance.* Actas Urol Esp (Engl Ed), 2018. **42**(2): p. 103-113.
84. Dieffenbacher, S., et al., *Standardized Magnetic Resonance Imaging Reporting Using the Prostate Cancer Radiological Estimation of Change in Sequential Evaluation Criteria and Magnetic Resonance Imaging/Transrectal Ultrasound Fusion with Transperineal Saturation Biopsy to Select Men on Active Surveillance.* Eur Urol Focus, 2021. **7**(1): p. 102-110.
85. Gallagher, K.M., et al., *Four-year outcomes from a multiparametric magnetic resonance imaging (MRI)-based active surveillance programme: PSA dynamics and serial MRI scans allow omission of protocol biopsies.* BJU Int, 2019. **123**(3): p. 429-438.
86. Lam, T.B.L., et al., *EAU-EANM-ESTRO-ESUR-SIOG Prostate Cancer Guideline Panel Consensus Statements for Deferred Treatment with Curative Intent for Localised Prostate Cancer from an International Collaborative Study (DETECTIVE Study).* Eur Urol, 2019. **76**(6): p. 790-813.
87. Luo, X., et al., *Prostatectomy Versus Observation for Localized Prostate Cancer: A Meta-Analysis.* Scand J Surg, 2021. **110**(1): p. 78-85.
88. Studer, U.E., et al., *Using PSA to guide timing of androgen deprivation in patients with T0-4 N0-2 M0 prostate cancer not suitable for local curative treatment (EORTC 30891).* Eur Urol, 2008. **53**(5): p. 941-9.
89. Donohue, J.F., et al., *Poorly differentiated prostate cancer treated with radical prostatectomy: long-term outcome and incidence of pathological downgrading.* J Urol, 2006. **176**(3): p. 991-5.
90. Yossepowitch, O., et al., *Radical prostatectomy for clinically localized, high risk prostate cancer: critical analysis of risk assessment methods.* J Urol, 2007. **178**(2): p. 493-9; discussion 499.
91. Bastian, P.J., et al., *Clinical and pathologic outcome after radical prostatectomy for prostate cancer patients with a preoperative Gleason sum of 8 to 10.* Cancer, 2006. **107**(6): p. 1265-72.
92. Briganti, A., et al., *Updated nomogram predicting lymph node invasion in patients with prostate cancer undergoing extended pelvic lymph node dissection: the essential importance of percentage of positive cores.* Eur Urol, 2012. **61**(3): p. 480-7.
93. Gandaglia, G., et al., *Development and Internal Validation of a Novel Model to Identify the Candidates for Extended Pelvic Lymph Node Dissection in Prostate Cancer.* Eur Urol, 2017. **72**(4): p. 632-640.
94. Bill-Axelson, A., et al., *Radical prostatectomy or watchful waiting in early prostate cancer.* N Engl J Med, 2014. **370**(10): p. 932-42.
95. Coughlin, G.D., et al., *Robot-assisted laparoscopic prostatectomy versus open radical retropubic prostatectomy: 24-month outcomes from a randomised controlled study.* Lancet Oncol, 2018. **19**(8): p. 1051-1060.
96. Bianco, F.J., Jr., P.T. Scardino, and J.A. Eastham, *Radical prostatectomy: long-term cancer control and recovery of sexual and urinary function ("trifecta").* Urology, 2005. **66**(5 Suppl): p. 83-94.
97. Roach, M., 3rd, et al., *Short-term neoadjuvant androgen deprivation therapy and external-beam radiotherapy for locally advanced prostate cancer: long-term results of RTOG 8610.* J Clin Oncol, 2008. **26**(4): p. 585-91.

98. D'Amico, A.V., et al., *Androgen suppression and radiation vs radiation alone for prostate cancer: a randomized trial.* Jama, 2008. **299**(3): p. 289-95.
99. Lawton, C.A., et al., *An update of the phase III trial comparing whole pelvic to prostate only radiotherapy and neoadjuvant to adjuvant total androgen suppression: updated analysis of RTOG 94-13, with emphasis on unexpected hormone/radiation interactions.* Int J Radiat Oncol Biol Phys, 2007. **69**(3): p. 646-55.
100. Tward, J.D., K.E. Kokeny, and D.C. Shrieve, *Radiation therapy for clinically node-positive prostate adenocarcinoma is correlated with improved overall and prostate cancer-specific survival.* Pract Radiat Oncol, 2013. **3**(3): p. 234-240.
101. Lin, C.C., et al., *Androgen deprivation with or without radiation therapy for clinically node-positive prostate cancer.* J Natl Cancer Inst, 2015. **107**(7).
102. Huggins, C. and C.V. Hodges, *Studies on prostatic cancer. I. The effect of castration, of estrogen and androgen injection on serum phosphatases in metastatic carcinoma of the prostate.* CA Cancer J Clin, 1972. **22**(4): p. 232-40.
103. *Maximum androgen blockade in advanced prostate cancer: an overview of the randomised trials. Prostate Cancer Trialists' Collaborative Group.* Lancet, 2000. **355**(9214): p. 1491-8.
104. Schmitt, B., et al., *Maximal androgen blockade for advanced prostate cancer.* Cochrane Database Syst Rev, 2000(2): p. Cd001526.
105. Scott, E., *Chemohormonal therapy in metastatic hormone-sensitive prostate cancer. Sweeney CJ, Chen YH, Carducci M, Liu G, Jarrard DF, Eisenberger M, Wong YN, Hahn N, Kohli M, Cooney MM, Dreicer R, Vogelzang NJ, Picus J, Shevrin D, Hussain M, Garcia JA, DiPaola RS. Department of Medicine; Department of Biostatistics and Computational Biology; Dana-Farber Cancer Institute, Boston; Harvard Medical School, Boston; Johns Hopkins University, Baltimore; University of Wisconsin Carbone Cancer Center; School of Medicine and Public Health; Madison; Fox Chase Cancer Center, Temple University Health System, Philadelphia; Indiana University Melvin and Bren Simon Cancer Center, Indianapolis; Mayo Clinic, Rochester, MN; University Hospitals Case Medical Center, Seidman Cancer Center; Cleveland Clinic Taussig Cancer Institute; Both in Cleveland; University of Virginia Cancer Center, Charlottesville; Comprehensive Cancer Centers of Nevada, Las Vegas; Siteman Cancer Center, Washington University School of Medicine, St. Louis; NorthShore University Health System, Evanston, IL; University of Michigan Comprehensive Cancer Center, Ann Arbor; Rutgers Cancer Institute of New Jersey, New Brunswick.N Engl J Med. 2015 Aug 20;373(8):737-46. [Epub 2015 Aug 5]. doi: 10.1056/NEJMoa1503747.* Urol Oncol, 2017. **35**(3): p. 123.
106. Kyriakopoulos, C.E., et al., *Chemohormonal Therapy in Metastatic Hormone-Sensitive Prostate Cancer: Long-Term Survival Analysis of the Randomized Phase III E3805 CHAARTED Trial.* J Clin Oncol, 2018. **36**(11): p. 1080-1087.
107. Gravis, G., et al., *Burden of Metastatic Castrate Naive Prostate Cancer Patients, to Identify Men More Likely to Benefit from Early Docetaxel: Further Analyses of CHAARTED and GETUG-AFU15 Studies.* Eur Urol, 2018. **73**(6): p. 847-855.
108. Parker, C.C., et al., *Radiotherapy to the primary tumour for newly diagnosed, metastatic prostate cancer (STAMPEDE): a randomised controlled phase 3 trial.* Lancet, 2018. **392**(10162): p. 2353-2366.
109. Henry, N.L. and D.F. Hayes, *Cancer biomarkers.* Mol Oncol, 2012. **6**(2): p. 140-6.
110. Karanfil, Ö. and J. Sterman, *"Saving lives or harming the healthy?" Overuse and fluctuations in routine medical screening.* System Dynamics Review, 2020. **36**(3): p. 294-329.
111. Diamandis, E.P., *The failure of protein cancer biomarkers to reach the clinic: why, and what can be done to address the problem?* BMC Med, 2012. **10**: p. 87.
112. Meiser, B., *Psychological impact of genetic testing for cancer susceptibility: an update of the literature.* Psychooncology, 2005. **14**(12): p. 1060-74.
113. Lilja, H., D. Ulmert, and A.J. Vickers, *Prostate-specific antigen and prostate cancer: prediction, detection and monitoring.* Nat Rev Cancer, 2008. **8**(4): p. 268-78.
114. Li, H.F., et al., *Prostate specific antigen as a biomarker for breast cancer: a meta-analysis study.* Eur Rev Med Pharmacol Sci, 2018. **22**(13): p. 4188-4195.
115. Thorlacius, S., et al., *A single BRCA2 mutation in male and female breast cancer families from Iceland with varied cancer phenotypes.* Nat Genet, 1996. **13**(1): p. 117-9.

116. Jin, Y., et al., *Diagnostic accuracy of prostate-specific antigen below 4 ng/mL as a cutoff for diagnosing prostate cancer in a hospital setting: A systematic review and meta-analysis.* Investig Clin Urol, 2022. **63**(3): p. 251-261.
117. Dhanasekaran, S.M., et al., *Delineation of prognostic biomarkers in prostate cancer.* Nature, 2001. **412**(6849): p. 822-6.
118. Stamey, T.A., et al., *Prostate-specific antigen as a serum marker for adenocarcinoma of the prostate.* N Engl J Med, 1987. **317**(15): p. 909-16.
119. Ahmed, H.U., et al., *Diagnostic accuracy of multi-parametric MRI and TRUS biopsy in prostate cancer (PROMIS): a paired validating confirmatory study.* Lancet, 2017. **389**(10071): p. 815-822.
120. Diamandis, E.P., *A Word of Caution on New and Revolutionary Diagnostic Tests.* Cancer Cell, 2016. **29**(2): p. 141-2.
121. Mettlin, C., et al., *Defining and updating the American Cancer Society guidelines for the cancer-related checkup: prostate and endometrial cancers.* CA Cancer J Clin, 1993. **43**(1): p. 42-6.
122. Loeb, S., *Guideline of guidelines: prostate cancer screening.* BJU Int, 2014. **114**(3): p. 323-5.
123. Schröder, F.H., et al., *Screening and prostate-cancer mortality in a randomized European study.* N Engl J Med, 2009. **360**(13): p. 1320-8.
124. Etzioni, R., et al., *Limitations of basing screening policies on screening trials: The US Preventive Services Task Force and Prostate Cancer Screening.* Med Care, 2013. **51**(4): p. 295-300.
125. Andriole, G.L., et al., *Mortality results from a randomized prostate-cancer screening trial.* N Engl J Med, 2009. **360**(13): p. 1310-9.
126. Young, G.J., et al., *Prostate-specific antigen (PSA) testing of men in UK general practice: a 10-year longitudinal cohort study.* BMJ Open, 2017. **7**(10): p. e017729.
127. Carter, H.B., et al., *Early detection of prostate cancer: AUA Guideline.* J Urol, 2013. **190**(2): p. 419-26.
128. Hu, J.C., et al., *Increase in Prostate Cancer Distant Metastases at Diagnosis in the United States.* JAMA Oncol, 2017. **3**(5): p. 705-707.
129. Jemal, A., et al., *Prostate Cancer Incidence and PSA Testing Patterns in Relation to USPSTF Screening Recommendations.* Jama, 2015. **314**(19): p. 2054-61.
130. Gaylis, F.D., et al., *Change in prostate cancer presentation coinciding with USPSTF screening recommendations at a community-based urology practice.* Urol Oncol, 2017. **35**(11): p. 663.e1-663.e7.
131. Walsh, P.C., *Re: Screening for prostate cancer: U.S. Preventive Services Task Force recommendation statement.* J Urol, 2012. **188**(4): p. 1181.
132. Kelly, S.P., et al., *Past, Current, and Future Incidence Rates and Burden of Metastatic Prostate Cancer in the United States.* Eur Urol Focus, 2018. **4**(1): p. 121-127.
133. Hugosson, J., et al., *A 16-yr Follow-up of the European Randomized study of Screening for Prostate Cancer.* Eur Urol, 2019. **76**(1): p. 43-51.
134. Bibbins-Domingo, K., D.C. Grossman, and S.J. Curry, *The US Preventive Services Task Force 2017 Draft Recommendation Statement on Screening for Prostate Cancer: An Invitation to Review and Comment.* Jama, 2017. **317**(19): p. 1949-1950.
135. Cooperberg, M.R., *The New US Preventive Services Task Force "C" Draft Recommendation for Prostate Cancer Screening.* Eur Urol, 2017. **72**(3): p. 326-328.
136. Grossman, D.C., et al., *Screening for Prostate Cancer: US Preventive Services Task Force Recommendation Statement.* Jama, 2018. **319**(18): p. 1901-1913.
137. Bryant, R.J., et al., *Predicting high-grade cancer at ten-core prostate biopsy using four kallikrein markers measured in blood in the ProtecT study.* J Natl Cancer Inst, 2015. **107**(7).
138. de la Calle, C., et al., *Multicenter Evaluation of the Prostate Health Index to Detect Aggressive Prostate Cancer in Biopsy Naïve Men.* J Urol, 2015. **194**(1): p. 65-72.
139. Nordström, T., et al., *Comparison Between the Four-kallikrein Panel and Prostate Health Index for Predicting Prostate Cancer.* Eur Urol, 2015. **68**(1): p. 139-46.
140. Deras, I.L., et al., *PCA3: a molecular urine assay for predicting prostate biopsy outcome.* J Urol, 2008. **179**(4): p. 1587-92.
141. Hessels, D., et al., *DD3(PCA3)-based molecular urine analysis for the diagnosis of prostate cancer.* Eur Urol, 2003. **44**(1): p. 8-15; discussion 15-6.
142. Auprich, M., et al., *Contemporary role of prostate cancer antigen 3 in the management of prostate*

cancer. Eur Urol, 2011. **60**(5): p. 1045-54.
143. Hessels, D., et al., *Detection of TMPRSS2-ERG fusion transcripts and prostate cancer antigen 3 in urinary sediments may improve diagnosis of prostate cancer.* Clin Cancer Res, 2007. **13**(17): p. 5103-8.
144. Tomlins, S.A., et al., *Urine TMPRSS2:ERG Plus PCA3 for Individualized Prostate Cancer Risk Assessment.* Eur Urol, 2016. **70**(1): p. 45-53.
145. Van Neste, L., et al., *Detection of High-grade Prostate Cancer Using a Urinary Molecular Biomarker-Based Risk Score.* Eur Urol, 2016. **70**(5): p. 740-748.
146. Maggi, M., et al., *SelectMDx and Multiparametric Magnetic Resonance Imaging of the Prostate for Men Undergoing Primary Prostate Biopsy: A Prospective Assessment in a Multi-Institutional Study.* Cancers (Basel), 2021. **13**(9).
147. Margolis, E., et al., *Predicting high-grade prostate cancer at initial biopsy: clinical performance of the ExoDx (EPI) Prostate Intelliscore test in three independent prospective studies.* Prostate Cancer Prostatic Dis, 2022. **25**(2): p. 296-301.
148. Kretschmer, A. and D. Tilki, *Biomarkers in prostate cancer - Current clinical utility and future perspectives.* Crit Rev Oncol Hematol, 2017. **120**: p. 180-193.
149. Gaur, K. and M.M. Jagtap, *Role of Artificial Intelligence and Machine Learning in Prediction, Diagnosis, and Prognosis of Cancer.* Cureus, 2022. **14**(11): p. e31008.
150. Tătaru, O.S., et al., *Artificial Intelligence and Machine Learning in Prostate Cancer Patient Management-Current Trends and Future Perspectives.* Diagnostics (Basel), 2021. **11**(2).
151. Goldenberg, S.L., G. Nir, and S.E. Salcudean, *A new era: artificial intelligence and machine learning in prostate cancer.* Nat Rev Urol, 2019. **16**(7): p. 391-403.
152. Fenton, J.J., et al., *Prostate-Specific Antigen-Based Screening for Prostate Cancer: Evidence Report and Systematic Review for the US Preventive Services Task Force.* Jama, 2018. **319**(18): p. 1914-1931.
153. Allott, E.H., et al., *Intratumoral heterogeneity as a source of discordance in breast cancer biomarker classification.* Breast Cancer Res, 2016. **18**(1): p. 68.
154. Remon, J. and M. Majem, *EGFR mutation heterogeneity and mixed response to EGFR tyrosine kinase inhibitors of non small cell lung cancer: a clue to overcoming resistance.* Transl Lung Cancer Res, 2013. **2**(6): p. 445-8.
155. Barranha, R., et al., *Genetic Heterogeneity in Colorectal Cancer and its Clinical Implications.* Acta Med Port, 2015. **28**(3): p. 370-5.
156. Wang, Y., et al., *The implications of cell-free DNAs derived from tumor viruses as biomarkers of associated cancers.* J Med Virol, 2022. **94**(10): p. 4677-4688.
157. Tivey, A., et al., *Circulating tumour DNA - looking beyond the blood.* Nat Rev Clin Oncol, 2022. **19**(9): p. 600-612.
158. Lo, K.W., et al., *Analysis of cell-free Epstein-Barr virus associated RNA in the plasma of patients with nasopharyngeal carcinoma.* Clin Chem, 1999. **45**(8 Pt 1): p. 1292-4.
159. Kopreski, M.S., et al., *Detection of tumor messenger RNA in the serum of patients with malignant melanoma.* Clin Cancer Res, 1999. **5**(8): p. 1961-5.
160. Ignatiadis, M., G.W. Sledge, and S.S. Jeffrey, *Liquid biopsy enters the clinic - implementation issues and future challenges.* Nat Rev Clin Oncol, 2021. **18**(5): p. 297-312.
161. Stroun, M., et al., *Isolation and characterization of DNA from the plasma of cancer patients.* Eur J Cancer Clin Oncol, 1987. **23**(6): p. 707-12.
162. Schwarzenbach, H., D.S. Hoon, and K. Pantel, *Cell-free nucleic acids as biomarkers in cancer patients.* Nat Rev Cancer, 2011. **11**(6): p. 426-37.
163. Leon, S.A., et al., *Free DNA in the serum of cancer patients and the effect of therapy.* Cancer Res, 1977. **37**(3): p. 646-50.
164. Cheng, F., L. Su, and C. Qian, *Circulating tumor DNA: a promising biomarker in the liquid biopsy of cancer.* Oncotarget, 2016. **7**(30): p. 48832-48841.
165. Hironaka-Mitsuhashi, A., et al., *Towards Circulating-Tumor DNA-Based Precision Medicine.* J Clin Med, 2019. **8**(9).
166. Postel, M., et al., *Droplet-based digital PCR and next generation sequencing for monitoring circulating tumor DNA: a cancer diagnostic perspective.* Expert Rev Mol Diagn, 2018. **18**(1): p. 7-17.
167. Bardelli, A. and K. Pantel, *Liquid Biopsies, What We Do Not Know (Yet).* Cancer Cell, 2017. **31**(2): p. 172-

179.
168. Merker, J.D., et al., *Circulating Tumor DNA Analysis in Patients With Cancer: American Society of Clinical Oncology and College of American Pathologists Joint Review.* J Clin Oncol, 2018. **36**(16): p. 1631-1641.
169. Beaver, J.A., et al., *Detection of cancer DNA in plasma of patients with early-stage breast cancer.* Clin Cancer Res, 2014. **20**(10): p. 2643-2650.
170. Gormally, E., et al., *TP53 and KRAS2 mutations in plasma DNA of healthy subjects and subsequent cancer occurrence: a prospective study.* Cancer Res, 2006. **66**(13): p. 6871-6.
171. Aravanis, A.M., M. Lee, and R.D. Klausner, *Next-Generation Sequencing of Circulating Tumor DNA for Early Cancer Detection.* Cell, 2017. **168**(4): p. 571-574.
172. Haldrup, C., et al., *Biomarker potential of ST6GALNAC3 and ZNF660 promoter hypermethylation in prostate cancer tissue and liquid biopsies.* Mol Oncol, 2018. **12**(4): p. 545-560.
173. Constâncio, V., et al., *DNA Methylation-Based Testing in Liquid Biopsies as Detection and Prognostic Biomarkers for the Four Major Cancer Types.* Cells, 2020. **9**(3).
174. Tong, Y.K. and Y.M. Lo, *Diagnostic developments involving cell-free (circulating) nucleic acids.* Clin Chim Acta, 2006. **363**(1-2): p. 187-96.
175. Fleischhacker, M. and B. Schmidt, *Circulating nucleic acids (CNAs) and cancer--a survey.* Biochim Biophys Acta, 2007. **1775**(1): p. 181-232.
176. Chan, K.C. and Y.M. Lo, *Circulating tumour-derived nucleic acids in cancer patients: potential applications as tumour markers.* Br J Cancer, 2007. **96**(5): p. 681-5.
177. Chen, X., et al., *Characterization of microRNAs in serum: a novel class of biomarkers for diagnosis of cancer and other diseases.* Cell Res, 2008. **18**(10): p. 997-1006.
178. Valadi, H., et al., *Exosome-mediated transfer of mRNAs and microRNAs is a novel mechanism of genetic exchange between cells.* Nat Cell Biol, 2007. **9**(6): p. 654-9.
179. Hunter, M.P., et al., *Detection of microRNA expression in human peripheral blood microvesicles.* PLoS One, 2008. **3**(11): p. e3694.
180. Lawrie, C.H., et al., *Detection of elevated levels of tumour-associated microRNAs in serum of patients with diffuse large B-cell lymphoma.* Br J Haematol, 2008. **141**(5): p. 672-5.
181. Mitchell, P.S., et al., *Circulating microRNAs as stable blood-based markers for cancer detection.* Proc Natl Acad Sci U S A, 2008. **105**(30): p. 10513-8.
182. Fabris, L., et al., *The Potential of MicroRNAs as Prostate Cancer Biomarkers.* Eur Urol, 2016. **70**(2): p. 312-22.
183. Filella, X. and L. Foj, *miRNAs as novel biomarkers in the management of prostate cancer.* Clin Chem Lab Med, 2017. **55**(5): p. 715-736.
184. Rolfo, C., et al., *Challenges and opportunities of cfDNA analysis implementation in clinical practice: Perspective of the International Society of Liquid Biopsy (ISLB).* Crit Rev Oncol Hematol, 2020. **151**: p. 102978.
185. Endzeliņš, E., et al., *Detection of circulating miRNAs: comparative analysis of extracellular vesicle-incorporated miRNAs and cell-free miRNAs in whole plasma of prostate cancer patients.* BMC Cancer, 2017. **17**(1): p. 730.
186. Pessoa, L.S., M. Heringer, and V.P. Ferrer, *ctDNA as a cancer biomarker: A broad overview.* Crit Rev Oncol Hematol, 2020. **155**: p. 103109.
187. Heitzer, E., et al., *Current and future perspectives of liquid biopsies in genomics-driven oncology.* Nat Rev Genet, 2019. **20**(2): p. 71-88.
188. Volckmar, A.L., et al., *A field guide for cancer diagnostics using cell-free DNA: From principles to practice and clinical applications.* Genes Chromosomes Cancer, 2018. **57**(3): p. 123-139.
189. de Wit, S., G. van Dalum, and L.W. Terstappen, *Detection of circulating tumor cells.* Scientifica (Cairo), 2014. **2014**: p. 819362.
190. Parkinson, D.R., et al., *Considerations in the development of circulating tumor cell technology for clinical use.* J Transl Med, 2012. **10**: p. 138.
191. Mego, M., *Emerging role of circulating tumor cells in cancer management.* Indian J Med Paediatr Oncol, 2014. **35**(4): p. 237-8.
192. Kleiner, D.E. and W.G. Stetler-Stevenson, *Matrix metalloproteinases and metastasis.* Cancer Chemother Pharmacol, 1999. **43 Suppl**: p. S42-51.

193. Khoja, L., et al., *A pilot study to explore circulating tumour cells in pancreatic cancer as a novel biomarker.* Br J Cancer, 2012. **106**(3): p. 508-16.
194. Ahn, J.C., et al., *Detection of Circulating Tumor Cells and Their Implications as a Biomarker for Diagnosis, Prognostication, and Therapeutic Monitoring in Hepatocellular Carcinoma.* Hepatology, 2021. **73**(1): p. 422-436.
195. Godinho, S.A., et al., *Oncogene-like induction of cellular invasion from centrosome amplification.* Nature, 2014. **510**(7503): p. 167-71.
196. Yu, M., et al., *Circulating breast tumor cells exhibit dynamic changes in epithelial and mesenchymal composition.* Science, 2013. **339**(6119): p. 580-4.
197. Aceto, N., et al., *Circulating tumor cell clusters are oligoclonal precursors of breast cancer metastasis.* Cell, 2014. **158**(5): p. 1110-1122.
198. Micalizzi, D.S., S. Maheswaran, and D.A. Haber, *A conduit to metastasis: circulating tumor cell biology.* Genes Dev, 2017. **31**(18): p. 1827-1840.
199. Cristofanilli, M., et al., *Circulating tumor cells, disease progression, and survival in metastatic breast cancer.* N Engl J Med, 2004. **351**(8): p. 781-91.
200. Templeman, A., et al., *Analytical performance of the FDA-cleared Parsortix(®) PC1 system.* J Circ Biomark, 2023. **12**: p. 26-33.
201. Guo, T., et al., *The Isolation and Analysis of Circulating Tumor Cells.* Methods Mol Biol, 2019. **2054**: p. 115-128.
202. Cristofanilli, M., et al., *Circulating tumor cells in metastatic breast cancer: biologic staging beyond tumor burden.* Clin Breast Cancer, 2007. **7**(6): p. 471-9.
203. Groen, L., et al., *Transcriptome Profiling of Circulating Tumor Cells to Predict Clinical Outcomes in Metastatic Castration-Resistant Prostate Cancer.* Int J Mol Sci, 2023. **24**(10).
204. Lorente, D., et al., *Decline in Circulating Tumor Cell Count and Treatment Outcome in Advanced Prostate Cancer.* Eur Urol, 2016. **70**(6): p. 985-992.
205. Climent, M., et al., *Weekly cabazitaxel plus prednisone is effective and less toxic for 'unfit' metastatic castration-resistant prostate cancer: Phase II Spanish Oncology Genitourinary Group (SOGUG) trial.* Eur J Cancer, 2017. **87**: p. 30-37.
206. Hüsemann, Y., et al., *Systemic spread is an early step in breast cancer.* Cancer Cell, 2008. **13**(1): p. 58-68.
207. Weng, D., et al., *Metastasis is an early event in mouse mammary carcinomas and is associated with cells bearing stem cell markers.* Breast Cancer Res, 2012. **14**(1): p. R18.
208. Jin, L., et al., *Evaluation of the diagnostic value of circulating tumor cells with CytoSorter(®) CTC capture system in patients with breast cancer.* Cancer Med, 2020. **9**(5): p. 1638-1647.
209. Ilie, M., et al., *"Sentinel" circulating tumor cells allow early diagnosis of lung cancer in patients with chronic obstructive pulmonary disease.* PLoS One, 2014. **9**(10): p. e111597.
210. Hofman, V., et al., *Morphological analysis of circulating tumour cells in patients undergoing surgery for non-small cell lung carcinoma using the isolation by size of epithelial tumour cell (ISET) method.* Cytopathology, 2012. **23**(1): p. 30-8.
211. Tsai, W.-S., et al., *Prospective clinical study of circulating tumor cells for colorectal cancer screening.* Journal of Clinical Oncology, 2018. **36**(4_suppl): p. 556-556.
212. Tsai, W.S., et al., *Novel Circulating Tumor Cell Assay for Detection of Colorectal Adenomas and Cancer.* Clin Transl Gastroenterol, 2019. **10**(10): p. e00088.
213. Baek, D.H., et al., *Clinical Potential of Circulating Tumor Cells in Colorectal Cancer: A Prospective Study.* Clin Transl Gastroenterol, 2019. **10**(7): p. e00055.
214. Cheng, Y., et al., *Diagnostic Value of Different Phenotype Circulating Tumor Cells in Hepatocellular Carcinoma.* J Gastrointest Surg, 2019. **23**(12): p. 2354-2361.
215. Rhim, A.D., et al., *EMT and dissemination precede pancreatic tumor formation.* Cell, 2012. **148**(1-2): p. 349-61.
216. Wei, T., et al., *Vimentin-positive circulating tumor cells as a biomarker for diagnosis and treatment monitoring in patients with pancreatic cancer.* Cancer Lett, 2019. **452**: p. 237-243.
217. Alix-Panabières, C. and K. Pantel, *Challenges in circulating tumour cell research.* Nat Rev Cancer, 2014. **14**(9): p. 623-31.
218. Coumans, F.A., S. Siesling, and L.W. Terstappen, *Detection of cancer before distant metastasis.* BMC

Cancer, 2013. **13**: p. 283.
219. Zhou, L., et al., *Circulating tumor cells: silent predictors of metastasis.* F1000Res, 2017. **6**.
220. Kuske, A., et al., *Improved detection of circulating tumor cells in non-metastatic high-risk prostate cancer patients.* Sci Rep, 2016. **6**: p. 39736.
221. Lawrence, R., et al., *Circulating tumour cells for early detection of clinically relevant cancer.* Nat Rev Clin Oncol, 2023. **20**(7): p. 487-500.
222. Ried, K., P. Eng, and A. Sali, *Screening for Circulating Tumour Cells Allows Early Detection of Cancer and Monitoring of Treatment Effectiveness: An Observational Study.* Asian Pac J Cancer Prev, 2017. **18**(8): p. 2275-2285.
223. Xu, L., et al., *Noninvasive Detection of Clinically Significant Prostate Cancer Using Circulating Tumor Cells.* J Urol, 2020. **203**(1): p. 73-82.
224. Enikeev, D., et al., *A Systematic Review of Circulating Tumor Cells Clinical Application in Prostate Cancer Diagnosis.* Cancers (Basel), 2022. **14**(15).
225. Choi, S.Y., et al., *Circulating Tumor Cell Counts in Patients With Localized Prostate Cancer Including Those Under Active Surveillance.* In Vivo, 2019. **33**(5): p. 1615-1620.
226. Todenhöfer, T., et al., *Microfluidic enrichment of circulating tumor cells in patients with clinically localized prostate cancer.* Urol Oncol, 2016. **34**(11): p. 483.e9-483.e16.
227. Alvarez Cubero, M.J., et al., *Circulating Tumor Cells: Markers and Methodologies for Enrichment and Detection.* Methods Mol Biol, 2017. **1634**: p. 283-303.
228. Okajima, W., et al., *Liquid biopsy in patients with hepatocellular carcinoma: Circulating tumor cells and cell-free nucleic acids.* World J Gastroenterol, 2017. **23**(31): p. 5650-5668.
229. Kang, B.J., et al., *Circulating Tumor Cell Number Is Associated with Primary Tumor Volume in Patients with Lung Adenocarcinoma.* Tuberc Respir Dis (Seoul), 2020. **83**(1): p. 61-70.
230. Ali, A., et al., *Assessment of circulating tumor cells (CTCs) in prostate cancer patients with low-volume tumors.* Pathol Int, 2010. **60**(10): p. 667-72.
231. Meyer, C.P., et al., *Limited prognostic value of preoperative circulating tumor cells for early biochemical recurrence in patients with localized prostate cancer.* Urol Oncol, 2016. **34**(5): p. 235.e11-6.
232. Helo, P., et al., *Circulating prostate tumor cells detected by reverse transcription-PCR in men with localized or castration-refractory prostate cancer: concordance with CellSearch assay and association with bone metastases and with survival.* Clin Chem, 2009. **55**(4): p. 765-73.
233. Davis, J.W., et al., *Circulating tumor cells in peripheral blood samples from patients with increased serum prostate specific antigen: initial results in early prostate cancer.* J Urol, 2008. **179**(6): p. 2187-91; discussion 2191.
234. Loh, J., et al., *Circulating tumor cell detection in high-risk non-metastatic prostate cancer.* J Cancer Res Clin Oncol, 2014. **140**(12): p. 2157-62.
235. Cieślikowski, W.A., et al., *Circulating Tumor Cells as a Marker of Disseminated Disease in Patients with Newly Diagnosed High-Risk Prostate Cancer.* Cancers (Basel), 2020. **12**(1).
236. Fizazi, K., et al., *High detection rate of circulating tumor cells in blood of patients with prostate cancer using telomerase activity.* Ann Oncol, 2007. **18**(3): p. 518-21.
237. Puche-Sanz, I., et al., *A comprehensive study of circulating tumour cells at the moment of prostate cancer diagnosis: biological and clinical implications of EGFR, AR and SNPs.* Oncotarget, 2017. **8**(41): p. 70472-70480.
238. Bankó, P., et al., *Technologies for circulating tumor cell separation from whole blood.* J Hematol Oncol, 2019. **12**(1): p. 48.
239. Edgar, J.R., *Q&A: What are exosomes, exactly?* BMC Biol, 2016. **14**: p. 46.
240. Thakur, B.K., et al., *Double-stranded DNA in exosomes: a novel biomarker in cancer detection.* Cell Res, 2014. **24**(6): p. 766-9.
241. Zhang, C., et al., *Exosome: Function and Role in Cancer Metastasis and Drug Resistance.* Technol Cancer Res Treat, 2018. **17**: p. 1533033818763450.
242. Tai, Y.L., et al., *Exosomes in cancer development and clinical applications.* Cancer Sci, 2018. **109**(8): p. 2364-2374.
243. Raimondo, S., et al., *Chronic myeloid leukemia-derived exosomes promote tumor growth through an autocrine mechanism.* Cell Commun Signal, 2015. **13**: p. 8.

244. Luga, V., et al., *Exosomes mediate stromal mobilization of autocrine Wnt-PCP signaling in breast cancer cell migration.* Cell, 2012. **151**(7): p. 1542-56.
245. Chen, W.X., et al., *Exosomes from drug-resistant breast cancer cells transmit chemoresistance by a horizontal transfer of microRNAs.* PLoS One, 2014. **9**(4): p. e95240.
246. Semina, S.E., et al., *Exosome-Mediated Transfer of Cancer Cell Resistance to Antiestrogen Drugs.* Molecules, 2018. **23**(4).
247. Santos, J.C., et al., *Exosome-mediated breast cancer chemoresistance via miR-155 transfer.* Sci Rep, 2018. **8**(1): p. 829.
248. Yu, W., et al., *Exosome-based liquid biopsies in cancer: opportunities and challenges.* Ann Oncol, 2021. **32**(4): p. 466-477.
249. Cappello, F., et al., *Exosome levels in human body fluids: A tumor marker by themselves?* Eur J Pharm Sci, 2017. **96**: p. 93-98.
250. Huang, X., et al., *Exosomal miR-1290 and miR-375 as prognostic markers in castration-resistant prostate cancer.* Eur Urol, 2015. **67**(1): p. 33-41.
251. Liu, T., D.E. Mendes, and C.E. Berkman, *Functional prostate-specific membrane antigen is enriched in exosomes from prostate cancer cells.* Int J Oncol, 2014. **44**(3): p. 918-22.
252. Yan, Y., G. Fu, and L. Ming, *Role of exosomes in pancreatic cancer.* Oncol Lett, 2018. **15**(5): p. 7479-7488.
253. Stevic, I., et al., *Specific microRNA signatures in exosomes of triple-negative and HER2-positive breast cancer patients undergoing neoadjuvant therapy within the GeparSixto trial.* BMC Med, 2018. **16**(1): p. 179.
254. Soekmadji, C., P.J. Russell, and C.C. Nelson, *Exosomes in prostate cancer: putting together the pieces of a puzzle.* Cancers (Basel), 2013. **5**(4): p. 1522-44.
255. Yang, B., et al., *Exosomal miRNAs as Biomarkers of Cancer: a Meta-Analysis.* Clin Lab, 2019. **65**(5).
256. Hessvik, N.P., K. Sandvig, and A. Llorente, *Exosomal miRNAs as Biomarkers for Prostate Cancer.* Front Genet, 2013. **4**: p. 36.
257. Li, P., et al., *Progress in Exosome Isolation Techniques.* Theranostics, 2017. **7**(3): p. 789-804.
258. Théry, C., et al., *Isolation and characterization of exosomes from cell culture supernatants and biological fluids.* Curr Protoc Cell Biol, 2006. **Chapter 3**: p. Unit 3.22.
259. Gardiner, C., et al., *Techniques used for the isolation and characterization of extracellular vesicles: results of a worldwide survey.* J Extracell Vesicles, 2016. **5**: p. 32945.
260. Yuana, Y., et al., *Co-isolation of extracellular vesicles and high-density lipoproteins using density gradient ultracentrifugation.* J Extracell Vesicles, 2014. **3**.
261. Webber, J. and A. Clayton, *How pure are your vesicles?* J Extracell Vesicles, 2013. **2**.
262. Mitchell, P.J., et al., *Can urinary exosomes act as treatment response markers in prostate cancer?* J Transl Med, 2009. **7**: p. 4.
263. Caradec, J., et al., *Reproducibility and efficiency of serum-derived exosome extraction methods.* Clin Biochem, 2014. **47**(13-14): p. 1286-92.
264. Kanwar, S.S., et al., *Microfluidic device (ExoChip) for on-chip isolation, quantification and characterization of circulating exosomes.* Lab Chip, 2014. **14**(11): p. 1891-900.
265. Chen, C., et al., *Microfluidic isolation and transcriptome analysis of serum microvesicles.* Lab Chip, 2010. **10**(4): p. 505-11.
266. Nahavandi, S., et al., *Microfluidic platforms for biomarker analysis.* Lab Chip, 2014. **14**(9): p. 1496-514.
267. Rho, J., et al., *Magnetic nanosensor for detection and profiling of erythrocyte-derived microvesicles.* ACS Nano, 2013. **7**(12): p. 11227-33.
268. Brewer, D.B., *Max Schultze (1865), G. Bizzozero (1882) and the discovery of the platelet.* Br J Haematol, 2006. **133**(3): p. 251-8.
269. Sharda, A. and R. Flaumenhaft, *The life cycle of platelet granules.* F1000Res, 2018. **7**: p. 236.
270. van der Meijden, P.E.J. and J.W.M. Heemskerk, *Platelet biology and functions: new concepts and clinical perspectives.* Nat Rev Cardiol, 2019. **16**(3): p. 166-179.
271. Lefrançais, E., et al., *The lung is a site of platelet biogenesis and a reservoir for haematopoietic progenitors.* Nature, 2017. **544**(7648): p. 105-109.
272. Bender, M. and R. Palankar, *Platelet Shape Changes during Thrombus Formation: Role of Actin-Based Protrusions.* Hamostaseologie, 2021. **41**(1): p. 14-21.

273. D'Ambrosi, S., R.J. Nilsson, and T. Wurdinger, *Platelets and tumor-associated RNA transfer.* Blood, 2021. **137**(23): p. 3181-3191.
274. Lindemann, S., et al., *Platelets, inflammation and atherosclerosis.* J Thromb Haemost, 2007. **5 Suppl 1**: p. 203-11.
275. Colling, M.E., B.E. Tourdot, and Y. Kanthi, *Inflammation, Infection and Venous Thromboembolism.* Circ Res, 2021. **128**(12): p. 2017-2036.
276. Langer, H.F., et al., *Interaction of platelets and inflammatory endothelium in the development and progression of coronary artery disease.* Semin Thromb Hemost, 2010. **36**(2): p. 131-8.
277. Lindemann, S., et al., *Molecular pathways used by platelets to initiate and accelerate atherogenesis.* Curr Opin Lipidol, 2007. **18**(5): p. 566-73.
278. Haemmerle, M., et al., *The Platelet Lifeline to Cancer: Challenges and Opportunities.* Cancer Cell, 2018. **33**(6): p. 965-983.
279. Xu, X.R., G.M. Yousef, and H. Ni, *Cancer and platelet crosstalk: opportunities and challenges for aspirin and other antiplatelet agents.* Blood, 2018. **131**(16): p. 1777-1789.
280. Levin, J. and C.L. Conley, *THROMBOCYTOSIS ASSOCIATED WITH MALIGNANT DISEASE.* Arch Intern Med, 1964. **114**: p. 497-500.
281. Rendu, F. and B. Brohard-Bohn, *The platelet release reaction: granules' constituents, secretion and functions.* Platelets, 2001. **12**(5): p. 261-73.
282. McNicol, A. and S.J. Israels, *Platelet dense granules: structure, function and implications for haemostasis.* Thromb Res, 1999. **95**(1): p. 1-18.
283. Blair, P. and R. Flaumenhaft, *Platelet alpha-granules: basic biology and clinical correlates.* Blood Rev, 2009. **23**(4): p. 177-89.
284. Fuentes, E., R. Araya-Maturana, and F.A. Urra, *Regulation of mitochondrial function as a promising target in platelet activation-related diseases.* Free Radic Biol Med, 2019. **136**: p. 172-182.
285. White, J.G. and C.C. Clawson, *The surface-connected canalicular system of blood platelets--a fenestrated membrane system.* Am J Pathol, 1980. **101**(2): p. 353-64.
286. White, J.G., *The transfer of thorium particles from plasma to platelets and platelet granules.* Am J Pathol, 1968. **53**(4): p. 567-75.
287. White, J.G., *Fine structural alterations induced in platelets by adenosine diphosphate.* Blood, 1968. **31**(5): p. 604-22.
288. Chen, C.H., et al., *α-granule biogenesis: from disease to discovery.* Platelets, 2017. **28**(2): p. 147-154.
289. Smith, C.W., *Release of α-granule contents during platelet activation.* Platelets, 2022. **33**(4): p. 491-502.
290. Risitano, A., et al., *Platelets and platelet-like particles mediate intercellular RNA transfer.* Blood, 2012. **119**(26): p. 6288-95.
291. Kirschbaum, M., et al., *Horizontal RNA transfer mediates platelet-induced hepatocyte proliferation.* Blood, 2015. **126**(6): p. 798-806.
292. Clancy, L. and J.E. Freedman, *The role of circulating platelet transcripts.* J Thromb Haemost, 2015. **13 Suppl 1**: p. S33-9.
293. Booyse, F. and M.E. Rafelson, Jr., *In vitro incorporation of amino-acids into the contractile protein of human blood platelets.* Nature, 1967. **215**(5098): p. 283-4.
294. Warshaw, A.L., L. Laster, and N.R. Shulman, *Protein synthesis by human platelets.* J Biol Chem, 1967. **242**(9): p. 2094-7.
295. Plow, E.F., *Extracellular factors influencing the in vitro protein synthesis of platelets.* Thromb Haemost, 1979. **42**(2): p. 666-78.
296. Booyse, F.M. and M.E. Rafelson, Jr., *Studies on human platelets. I. synthesis of platelet protein in a cell-free system.* Biochim Biophys Acta, 1968. **166**(3): p. 689-97.
297. Steiner, M., *Platelet protein synthesis studied in a cell-free system.* Experientia, 1970. **26**(7): p. 786-9.
298. Tjon-Kon-Fat, L.A., et al., *Platelets harbor prostate cancer biomarkers and the ability to predict therapeutic response to abiraterone in castration resistant patients.* Prostate, 2018. **78**(1): p. 48-53.
299. Asghar, S., et al., *Tumor educated platelets, a promising source for early detection of hepatocellular carcinoma: Liquid biopsy an alternative approach to tissue biopsy.* Clin Res Hepatol Gastroenterol, 2020. **44**(6): p. 836-844.
300. Gnatenko, D.V., et al., *Transcript profiling of human platelets using microarray and serial analysis of gene*

expression. Blood, 2003. **101**(6): p. 2285-93.
301. Davizon-Castillo, P., J.W. Rowley, and M.T. Rondina, *Megakaryocyte and Platelet Transcriptomics for Discoveries in Human Health and Disease.* Arterioscler Thromb Vasc Biol, 2020. **40**(6): p. 1432-1440.
302. Gutmann, C., et al., *The Landscape of Coding and Noncoding RNAs in Platelets.* Antioxid Redox Signal, 2021. **34**(15): p. 1200-1216.
303. Londin, E.R., et al., *The human platelet: strong transcriptome correlations among individuals associate weakly with the platelet proteome.* Biol Direct, 2014. **9**: p. 3.
304. McRedmond, J.P., et al., *Integration of proteomics and genomics in platelets: a profile of platelet proteins and platelet-specific genes.* Mol Cell Proteomics, 2004. **3**(2): p. 133-44.
305. Calverley, D.C., et al., *Significant downregulation of platelet gene expression in metastatic lung cancer.* Clin Transl Sci, 2010. **3**(5): p. 227-32.
306. Cecchetti, L., et al., *Megakaryocytes differentially sort mRNAs for matrix metalloproteinases and their inhibitors into platelets: a mechanism for regulating synthetic events.* Blood, 2011. **118**(7): p. 1903-11.
307. Davizon-Castillo, P., et al., *TNF-α-driven inflammation and mitochondrial dysfunction define the platelet hyperreactivity of aging.* Blood, 2019. **134**(9): p. 727-740.
308. Bray, P.F., et al., *The complex transcriptional landscape of the anucleate human platelet.* BMC Genomics, 2013. **14**: p. 1.
309. Denis, M.M., et al., *Escaping the nuclear confines: signal-dependent pre-mRNA splicing in anucleate platelets.* Cell, 2005. **122**(3): p. 379-91.
310. Shashkin, P.N., et al., *Lipopolysaccharide is a direct agonist for platelet RNA splicing.* J Immunol, 2008. **181**(5): p. 3495-502.
311. Clancy, L., et al., *The role of RNA uptake in platelet heterogeneity.* Thromb Haemost, 2017. **117**(5): p. 948-961.
312. Nilsson, R.J., et al., *Blood platelets contain tumor-derived RNA biomarkers.* Blood, 2011. **118**(13): p. 3680-3.
313. van der Meijden, P.E.J. and J.W.M. Heemskerk, *Platelet biology and functions: new concepts and clinical perspectives.* Nature Reviews Cardiology, 2019. **16**(3): p. 166-179.
314. Riess, L., *Zur pathologischen Anatomie des Blutes.* Arch. Anat. Physiol. Wissensch Medical, 1872. **39**: p. 237-240.
315. Varki, A., *Trousseau's syndrome: multiple definitions and multiple mechanisms.* Blood, 2007. **110**(6): p. 1723-9.
316. Hamilton, W., et al., *What are the clinical features of lung cancer before the diagnosis is made? A population based case-control study.* Thorax, 2005. **60**(12): p. 1059-65.
317. Shephard, E., et al., *Clinical features of kidney cancer in primary care: a case-control study using primary care records.* Br J Gen Pract, 2013. **63**(609): p. e250-5.
318. Stapley, S., et al., *The risk of oesophago-gastric cancer in symptomatic patients in primary care: a large case-control study using electronic records.* Br J Cancer, 2013. **108**(1): p. 25-31.
319. Walker, S., C. Hyde, and W. Hamilton, *Risk of uterine cancer in symptomatic women in primary care: case-control study using electronic records.* Br J Gen Pract, 2013. **63**(614): p. e643-8.
320. Stone, R.L., et al., *Paraneoplastic thrombocytosis in ovarian cancer.* N Engl J Med, 2012. **366**(7): p. 610-8.
321. Zhang, Q., et al., *Patterns and functional implications of platelets upon tumor "education".* Int J Biochem Cell Biol, 2017. **90**: p. 68-80.
322. Falanga, A. and F.R. Rickles, *Pathophysiology of the thrombophilic state in the cancer patient.* Semin Thromb Hemost, 1999. **25**(2): p. 173-82.
323. Qi, C., et al., *P-Selectin-Mediated Adhesion between Platelets and Tumor Cells Promotes Intestinal Tumorigenesis in Apc(Min/+) Mice.* Int J Biol Sci, 2015. **11**(6): p. 679-87.
324. Ay, C. and I. Pabinger, *Predictive potential of haemostatic biomarkers for venous thromboembolism in cancer patients.* Thromb Res, 2012. **129 Suppl 1**: p. S6-9.
325. Mammadova-Bach, E., et al., *Platelet integrin α6β1 controls lung metastasis through direct binding to cancer cell-derived ADAM9.* JCI Insight, 2016. **1**(14): p. e88245.
326. Kim, Y.J., et al., *P-selectin deficiency attenuates tumor growth and metastasis.* Proc Natl Acad Sci U S A, 1998. **95**(16): p. 9325-30.

327. Yang, H., et al., *Fibrinogen is required for maintenance of platelet intracellular and cell-surface P-selectin expression.* Blood, 2009. **114**(2): p. 425-36.
328. Amirkhosravi, A., et al., *Inhibition of tumor cell-induced platelet aggregation and lung metastasis by the oral GpIIb/IIIa antagonist XV454.* Thromb Haemost, 2003. **90**(3): p. 549-54.
329. Lonsdorf, A.S., et al., *Engagement of αIIbβ3 (GPIIb/IIIa) with αvβ3 integrin mediates interaction of melanoma cells with platelets: a connection to hematogenous metastasis.* J Biol Chem, 2012. **287**(3): p. 2168-78.
330. Du, X.P., et al., *Ligands "activate" integrin alpha IIb beta 3 (platelet GPIIb-IIIa).* Cell, 1991. **65**(3): p. 409-16.
331. Estevez, B., et al., *Signaling-mediated cooperativity between glycoprotein Ib-IX and protease-activated receptors in thrombin-induced platelet activation.* Blood, 2016. **127**(5): p. 626-36.
332. Mammadova-Bach, E., et al., *Platelet glycoprotein VI binds to polymerized fibrin and promotes thrombin generation.* Blood, 2015. **126**(5): p. 683-91.
333. Jain, S., et al., *Platelet glycoprotein Ib alpha supports experimental lung metastasis.* Proc Natl Acad Sci U S A, 2007. **104**(21): p. 9024-8.
334. Cooke, N.M., et al., *Increased platelet reactivity in patients with late-stage metastatic cancer.* Cancer Med, 2013. **2**(4): p. 564-70.
335. Zhang, Y., et al., *Prohibitins are involved in protease-activated receptor 1-mediated platelet aggregation.* J Thromb Haemost, 2012. **10**(3): p. 411-8.
336. Bastida, E., et al., *Morphometric evaluation of thrombogenesis by microvesicles from human tumor cell lines with thrombin-dependent (U87MG) and adenosine diphosphate-dependent (SKNMC) platelet-activating mechanisms.* J Lab Clin Med, 1986. **108**(6): p. 622-7.
337. Chung, A.W., et al., *Mechanisms of action of proteinase-activated receptor agonists on human platelets.* Br J Pharmacol, 2002. **135**(5): p. 1123-32.
338. van den Berg, Y.W., et al., *The relationship between tissue factor and cancer progression: insights from bench and bedside.* Blood, 2012. **119**(4): p. 924-32.
339. Geddings, J.E. and N. Mackman, *Tumor-derived tissue factor-positive microparticles and venous thrombosis in cancer patients.* Blood, 2013. **122**(11): p. 1873-80.
340. Heinmöller, E., et al., *Studies on tumor-cell-induced platelet aggregation in human lung cancer cell lines.* J Cancer Res Clin Oncol, 1996. **122**(12): p. 735-44.
341. Boukerche, H., et al., *Human melanoma cell lines differ in their capacity to release ADP and aggregate platelets.* Br J Haematol, 1994. **87**(4): p. 763-72.
342. Jurasz, P., et al., *Matrix metalloproteinase 2 in tumor cell-induced platelet aggregation: regulation by nitric oxide.* Cancer Res, 2001. **61**(1): p. 376-82.
343. Alonso-Escolano, D., et al., *Membrane type-1 matrix metalloproteinase stimulates tumour cell-induced platelet aggregation: role of receptor glycoproteins.* Br J Pharmacol, 2004. **141**(2): p. 241-52.
344. de Leval, X., et al., *Pharmacological evaluation of the novel thromboxane modulator BM-567 (II/II). Effects of BM-567 on osteogenic sarcoma-cell-induced platelet aggregation.* Prostaglandins Leukot Essent Fatty Acids, 2003. **68**(1): p. 55-9.
345. Tzanakakis, G.N., et al., *The preventive effect of ketoconazole on experimental metastasis from a human pancreatic carcinoma may be related to its effect on prostaglandin synthesis.* Int J Gastrointest Cancer, 2002. **32**(1): p. 23-30.
346. Pacchiarini, L., et al., *Thromboxane production by platelets during tumor cell-induced platelet activation.* Invasion Metastasis, 1991. **11**(2): p. 102-9.
347. Tesselaar, M.E., et al., *Microparticle-associated tissue factor activity: a link between cancer and thrombosis?* J Thromb Haemost, 2007. **5**(3): p. 520-7.
348. Khorana, A.A., et al., *Plasma tissue factor may be predictive of venous thromboembolism in pancreatic cancer.* J Thromb Haemost, 2008. **6**(11): p. 1983-5.
349. Sartori, M.T., et al., *Circulating microparticles of glial origin and tissue factor bearing in high-grade glioma: a potential prothrombotic role.* Thromb Haemost, 2013. **110**(2): p. 378-85.
350. Meikle, C.K., et al., *Cancer and Thrombosis: The Platelet Perspective.* Front Cell Dev Biol, 2016. **4**: p. 147.
351. Best, M.G., et al., *Swarm Intelligence-Enhanced Detection of Non-Small-Cell Lung Cancer Using Tumor-Educated Platelets.* Cancer Cell, 2017. **32**(2): p. 238-252.e9.

352. Best, M.G., et al., *RNA-Seq of Tumor-Educated Platelets Enables Blood-Based Pan-Cancer, Multiclass, and Molecular Pathway Cancer Diagnostics.* Cancer Cell, 2015. **28**(5): p. 666-676.
353. López, J.A., *Introduction to a review series on platelets and cancer.* Blood, 2021. **137**(23): p. 3151-3152.
354. Battinelli, E.M., B.A. Markens, and J.E. Italiano, Jr., *Release of angiogenesis regulatory proteins from platelet alpha granules: modulation of physiologic and pathologic angiogenesis.* Blood, 2011. **118**(5): p. 1359-69.
355. Honn, K.V., D.G. Tang, and J.D. Crissman, *Platelets and cancer metastasis: a causal relationship?* Cancer Metastasis Rev, 1992. **11**(3-4): p. 325-51.
356. Gay, L.J. and B. Felding-Habermann, *Contribution of platelets to tumour metastasis.* Nat Rev Cancer, 2011. **11**(2): p. 123-34.
357. Kos, M. and A. Dabrowski, *Tumour's angiogenesis--the function of VEGF and bFGF in colorectal cancer.* Ann Univ Mariae Curie Sklodowska Med, 2002. **57**(2): p. 556-61.
358. Heldin, C.H. and B. Westermark, *Mechanism of action and in vivo role of platelet-derived growth factor.* Physiol Rev, 1999. **79**(4): p. 1283-316.
359. Heldin, C.H., B. Westermark, and A. Wasteson, *Platelet-derived growth factor. Isolation by a large-scale procedure and analysis of subunit composition.* Biochem J, 1981. **193**(3): p. 907-13.
360. Bos, R., et al., *Hypoxia-inducible factor-1alpha is associated with angiogenesis, and expression of bFGF, PDGF-BB, and EGFR in invasive breast cancer.* Histopathology, 2005. **46**(1): p. 31-6.
361. Quintero-Fabián, S., et al., *Role of Matrix Metalloproteinases in Angiogenesis and Cancer.* Front Oncol, 2019. **9**: p. 1370.
362. Foda, H.D. and S. Zucker, *Matrix metalloproteinases in cancer invasion, metastasis and angiogenesis.* Drug Discov Today, 2001. **6**(9): p. 478-482.
363. Verheul, H.M., et al., *Platelet and coagulation activation with vascular endothelial growth factor generation in soft tissue sarcomas.* Clin Cancer Res, 2000. **6**(1): p. 166-71.
364. Bao, M.H. and C.C. Wong, *Hypoxia, Metabolic Reprogramming, and Drug Resistance in Liver Cancer.* Cells, 2021. **10**(7).
365. Zheng, S., et al., *Identification and validation of a combined hypoxia and immune index for triple-negative breast cancer.* Mol Oncol, 2020. **14**(11): p. 2814-2833.
366. Sabrkhany, S., A.W. Griffioen, and M.G. Oude Egbrink, *The role of blood platelets in tumor angiogenesis.* Biochim Biophys Acta, 2011. **1815**(2): p. 189-96.
367. Ho-Tin-Noé, B., et al., *Platelet granule secretion continuously prevents intratumor hemorrhage.* Cancer Res, 2008. **68**(16): p. 6851-8.
368. Nishida, N., et al., *Angiogenesis in cancer.* Vasc Health Risk Manag, 2006. **2**(3): p. 213-9.
369. Cho, M.S., et al., *Platelets increase the proliferation of ovarian cancer cells.* Blood, 2012. **120**(24): p. 4869-72.
370. Janowska-Wieczorek, A., et al., *Microvesicles derived from activated platelets induce metastasis and angiogenesis in lung cancer.* Int J Cancer, 2005. **113**(5): p. 752-60.
371. Wang, J., et al., *The platelet isoform of phosphofructokinase contributes to metabolic reprogramming and maintains cell proliferation in clear cell renal cell carcinoma.* Oncotarget, 2016. **7**(19): p. 27142-57.
372. Razavi, A.S., et al., *TGF-β signaling and the interaction between platelets and T-cells in tumor microenvironment: Foes or friends?* Cytokine, 2022. **150**: p. 155772.
373. Oft, M., et al., *TGF-beta1 and Ha-Ras collaborate in modulating the phenotypic plasticity and invasiveness of epithelial tumor cells.* Genes Dev, 1996. **10**(19): p. 2462-77.
374. Oft, M., K.H. Heider, and H. Beug, *TGFbeta signaling is necessary for carcinoma cell invasiveness and metastasis.* Curr Biol, 1998. **8**(23): p. 1243-52.
375. Guan, P.P., et al., *By activating matrix metalloproteinase-7, shear stress promotes chondrosarcoma cell motility, invasion and lung colonization.* Oncotarget, 2015. **6**(11): p. 9140-59.
376. Alonso-Escolano, D., et al., *Protein kinase C delta mediates platelet-induced breast cancer cell invasion.* J Pharmacol Exp Ther, 2006. **318**(1): p. 373-80.
377. Chen, Y.Q., et al., *Fatty acid modulation of tumor cell-platelet-vessel wall interaction.* Cancer Metastasis Rev, 1992. **11**(3-4): p. 389-409.
378. Schumacher, D., et al., *Platelet-derived nucleotides promote tumor-cell transendothelial migration and metastasis via P2Y2 receptor.* Cancer Cell, 2013. **24**(1): p. 130-7.

379. Stanger, B.Z. and M.L. Kahn, *Platelets and tumor cells: a new form of border control.* Cancer Cell, 2013. **24**(1): p. 9-11.
380. Scheel, C., et al., *Adaptation versus selection: the origins of metastatic behavior.* Cancer Res, 2007. **67**(24): p. 11476-9; discussion 11479-80.
381. Labelle, M., S. Begum, and R.O. Hynes, *Direct signaling between platelets and cancer cells induces an epithelial-mesenchymal-like transition and promotes metastasis.* Cancer Cell, 2011. **20**(5): p. 576-90.
382. Kakavandi, E., et al., *Anoikis resistance and oncoviruses.* J Cell Biochem, 2018. **119**(3): p. 2484-2491.
383. Gkolfinopoulos, S., R.L. Jones, and A. Constantinidou, *The Emerging Role of Platelets in the Formation of the Micrometastatic Niche: Current Evidence and Future Perspectives.* Front Oncol, 2020. **10**: p. 374.
384. Leblanc, R., et al., *Interaction of platelet-derived autotaxin with tumor integrin αVβ3 controls metastasis of breast cancer cells to bone.* Blood, 2014. **124**(20): p. 3141-50.
385. Ibar, C. and K.D. Irvine, *Integration of Hippo-YAP Signaling with Metabolism.* Dev Cell, 2020. **54**(2): p. 256-267.
386. Haemmerle, M., et al., *Platelets reduce anoikis and promote metastasis by activating YAP1 signaling.* Nat Commun, 2017. **8**(1): p. 310.
387. Li, T., et al., *Platelet-derived growth factor-BB mediates pancreatic cancer malignancy via regulation of the Hippo/Yes-associated protein signaling pathway.* Oncol Rep, 2021. **45**(1): p. 83-94.
388. Nash, G.F., et al., *Platelets and cancer.* Lancet Oncol, 2002. **3**(7): p. 425-30.
389. Philippe, C., et al., *Protection from tumor necrosis factor-mediated cytolysis by platelets.* Am J Pathol, 1993. **143**(6): p. 1713-23.
390. Nieswandt, B., et al., *Lysis of tumor cells by natural killer cells in mice is impeded by platelets.* Cancer Res, 1999. **59**(6): p. 1295-300.
391. Placke, T., et al., *Platelet-derived MHC class I confers a pseudonormal phenotype to cancer cells that subverts the antitumor reactivity of natural killer immune cells.* Cancer Res, 2012. **72**(2): p. 440-8.
392. Kopp, H.G., T. Placke, and H.R. Salih, *Platelet-derived transforming growth factor-beta down-regulates NKG2D thereby inhibiting natural killer cell antitumor reactivity.* Cancer Res, 2009. **69**(19): p. 7775-83.
393. Zhang, N., et al., *Platelet adhesion and fusion to endothelial cell facilitate the metastasis of tumor cell in hypoxia-reoxygenation condition.* Clin Exp Metastasis, 2011. **28**(1): p. 1-12.
394. Wang, Y. and H. Zhang, *Platelet-induced inhibition of tumor cell growth.* Thromb Res, 2008. **123**(2): p. 324-30.
395. Ibele, G.M., et al., *Human platelets exert cytotoxic effects on tumor cells.* Blood, 1985. **65**(5): p. 1252-5.
396. Sagawa, T., et al., *Cytotoxicity of unstimulated and thrombin-activated platelets to human tumour cells.* Immunology, 1993. **78**(4): p. 650-6.
397. Yaftian, M., et al., *Induction of Apoptosis in Cancer Cells of pre-B ALL Patients after Exposure to Platelets, Platelet-Derived Microparticles and Soluble CD40 Ligand.* Cell J, 2018. **20**(1): p. 120-126.
398. Mehta, N., S. Muthusamy, and A. Bhatia, *Do Platelets Inhibit the Effect of Aspirin on Cancer Cells?* Cancer Microenviron, 2015. **8**(2): p. 119-22.
399. Golubeva, T.S., et al., *Cytotoxic protein from human platelets.* FEBS Lett, 1997. **405**(3): p. 312-4.
400. Reyes-Reyes, M.E., et al., *P-selectin activates integrin-mediated colon carcinoma cell adhesion to fibronectin.* Exp Cell Res, 2006. **312**(20): p. 4056-69.
401. Mantur, M., et al., *Does renal carcinoma affect the expression of P-selectin on platelets?* Neoplasma, 2002. **49**(4): p. 243-5.
402. Feng, S., et al., *Platelets are not hyperreactive in patients with ovarian cancer.* Platelets, 2016. **27**(7): p. 716-718.
403. Riedl, J., et al., *Decreased platelet reactivity in patients with cancer is associated with high risk of venous thromboembolism and poor prognosis.* Thromb Haemost, 2017. **117**(1): p. 90-98.
404. Huveneers, S. and E.H. Danen, *The interaction of SRC kinase with beta3 integrin tails: a potential therapeutic target in thrombosis and cancer.* ScientificWorldJournal, 2010. **10**: p. 1100-5.
405. Shimada, H., et al., *Thrombocytosis associated with poor prognosis in patients with esophageal carcinoma.* J Am Coll Surg, 2004. **198**(5): p. 737-41.
406. Sano, M., et al., *Blocking VCAM-1 inhibits pancreatic tumour progression and cancer-associated thrombosis/thromboembolism.* Gut, 2021. **70**(9): p. 1713-1723.
407. Zhou, L., et al., *Risk factors of poor prognosis and portal vein tumor thrombosis after curative resection*

of solitary hepatocellular carcinoma. Hepatobiliary Pancreat Dis Int, 2013. **12**(1): p. 68-73.
408. Mounce, L.T., W. Hamilton, and S.E. Bailey, *Cancer incidence following a high-normal platelet count: cohort study using electronic healthcare records from English primary care.* Br J Gen Pract, 2020. **70**(698): p. e622-e628.
409. Watts, E.L., et al., *Hematologic Markers and Prostate Cancer Risk: A Prospective Analysis in UK Biobank.* Cancer Epidemiol Biomarkers Prev, 2020. **29**(8): p. 1615-1626.
410. Bailey, S.E., et al., *How useful is thrombocytosis in predicting an underlying cancer in primary care? a systematic review.* Fam Pract, 2017. **34**(1): p. 4-10.
411. Bailey, S.E., et al., *Clinical relevance of thrombocytosis in primary care: a prospective cohort study of cancer incidence using English electronic medical records and cancer registry data.* Br J Gen Pract, 2017. **67**(659): p. e405-e413.
412. Giannakeas, V., et al., *Analysis of Platelet Count and New Cancer Diagnosis Over a 10-Year Period.* JAMA Netw Open, 2022. **5**(1): p. e2141633.
413. Sabrkhany, S., et al., *A combination of platelet features allows detection of early-stage cancer.* Eur J Cancer, 2017. **80**: p. 5-13.
414. Adhyatma, K.P. and S.M. Warli, *Diagnostic Value of Platelet-To-Lymphocyte Ratio in Prostate Cancer.* Open Access Maced J Med Sci, 2019. **7**(7): p. 1093-1096.
415. Yuksel, O.H., et al., *Predictive Value of the Platelet-To-Lymphocyte Ratio in Diagnosis of Prostate Cancer.* Asian Pac J Cancer Prev, 2015. **16**(15): p. 6407-12.
416. Sabrkhany, S., et al., *Platelets: the holy grail in cancer blood biomarker research?* Angiogenesis, 2019. **22**(1): p. 1-2.
417. Gasparyan, A.Y., et al., *Mean platelet volume: a link between thrombosis and inflammation?* Curr Pharm Des, 2011. **17**(1): p. 47-58.
418. Kaynar, M., et al., *Benign prostatic hyperplasia and prostate cancer differentiation via platelet to lymphocyte ratio.* Cancer Biomark, 2015. **15**(3): p. 317-23.
419. Weyrich, A.S., et al., *Signal-dependent translation of a regulatory protein, Bcl-3, in activated human platelets.* Proc Natl Acad Sci U S A, 1998. **95**(10): p. 5556-61.
420. Power, C.A., et al., *Chemokine and chemokine receptor mRNA expression in human platelets.* Cytokine, 1995. **7**(6): p. 479-82.
421. Wurdinger, T., S. In 't Veld, and M.G. Best, *Platelet RNA as Pan-Tumor Biomarker for Cancer Detection.* Cancer Res, 2020. **80**(7): p. 1371-1373.
422. Kuznetsov, H.S., et al., *Identification of luminal breast cancers that establish a tumor-supportive macroenvironment defined by proangiogenic platelets and bone marrow-derived cells.* Cancer Discov, 2012. **2**(12): p. 1150-65.
423. Asselta, R., et al., *Molecular characterization of in-frame and out-of-frame alternative splicings in coagulation factor XI pre-mRNA.* Blood, 2010. **115**(10): p. 2065-72.
424. Rondina, M.T., et al., *The septic milieu triggers expression of spliced tissue factor mRNA in human platelets.* J Thromb Haemost, 2011. **9**(4): p. 748-58.
425. Bugert, P., et al., *Messenger RNA profiling of human platelets by microarray hybridization.* Thromb Haemost, 2003. **90**(4): p. 738-48.
426. Ts'ao, C.H., *Rough endoplasmic reticulum and ribosomes in blood platelets.* Scand J Haematol, 1971. **8**(2): p. 134-40.
427. Kieffer, N., et al., *Biosynthesis of major platelet proteins in human blood platelets.* Eur J Biochem, 1987. **164**(1): p. 189-95.
428. Best, M.G., et al., *RNA sequencing and swarm intelligence-enhanced classification algorithm development for blood-based disease diagnostics using spliced blood platelet RNA.* Nat Protoc, 2019. **14**(4): p. 1206-1234.
429. Sol, N., et al., *Tumor-Educated Platelet RNA for the Detection and (Pseudo)progression Monitoring of Glioblastoma.* Cell Rep Med, 2020. **1**(7): p. 100101.
430. Heinhuis, K.M., et al., *RNA-Sequencing of Tumor-Educated Platelets, a Novel Biomarker for Blood-Based Sarcoma Diagnostics.* Cancers (Basel), 2020. **12**(6).
431. Ge, X., et al., *Identification of seven tumor-educated platelets RNAs for cancer diagnosis.* J Clin Lab Anal, 2021. **35**(6): p. e23791.

432. Ambros, V., *The functions of animal microRNAs.* Nature, 2004. **431**(7006): p. 350-5.
433. Valinezhad Orang, A., R. Safaralizadeh, and M. Kazemzadeh-Bavili, *Mechanisms of miRNA-Mediated Gene Regulation from Common Downregulation to mRNA-Specific Upregulation.* Int J Genomics, 2014. **2014**: p. 970607.
434. Baek, D., et al., *The impact of microRNAs on protein output.* Nature, 2008. **455**(7209): p. 64-71.
435. Ghanbarian, H., M.T. Yıldız, and Y. Tutar, *MicroRNA Targeting.* Methods Mol Biol, 2022. **2257**: p. 105-130.
436. Jansson, M.D. and A.H. Lund, *MicroRNA and cancer.* Mol Oncol, 2012. **6**(6): p. 590-610.
437. Cho, W.C., *MicroRNAs: potential biomarkers for cancer diagnosis, prognosis and targets for therapy.* Int J Biochem Cell Biol, 2010. **42**(8): p. 1273-81.
438. Landry, P., et al., *Existence of a microRNA pathway in anucleate platelets.* Nat Struct Mol Biol, 2009. **16**(9): p. 961-6.
439. Nagalla, S., et al., *Platelet microRNA-mRNA coexpression profiles correlate with platelet reactivity.* Blood, 2011. **117**(19): p. 5189-97.
440. Osman, A. and K. Fälker, *Characterization of human platelet microRNA by quantitative PCR coupled with an annotation network for predicted target genes.* Platelets, 2011. **22**(6): p. 433-41.
441. Gidlof, O., et al., *Platelets activated during myocardial infarction release functional miRNA, which can be taken up by endothelial cells and regulate ICAM1 expression.* Blood, 2013. **121**(19): p. 3908-17, s1-26.
442. Zeng, Z., et al., *Platelet-derived miR-223 promotes a phenotypic switch in arterial injury repair.* J Clin Invest, 2019. **129**(3): p. 1372-1386.
443. Cimmino, G., et al., *Activating stimuli induce platelet microRNA modulation and proteome reorganisation.* Thromb Haemost, 2015. **114**(1): p. 96-108.
444. Ruopp, M.D., et al., *Youden Index and optimal cut-point estimated from observations affected by a lower limit of detection.* Biom J, 2008. **50**(3): p. 419-30.
445. Thul, P.J., et al., *A subcellular map of the human proteome.* Science, 2017. **356**(6340).
446. Uhlén, M., et al., *Proteomics. Tissue-based map of the human proteome.* Science, 2015. **347**(6220): p. 1260419.
447. Uhlen, M., et al., *A pathology atlas of the human cancer transcriptome.* Science, 2017. **357**(6352).
448. Zhao, B., et al., *Overexpression of lncRNA ANRIL promoted the proliferation and migration of prostate cancer cells via regulating let-7a/TGF-β1/ Smad signaling pathway.* Cancer Biomark, 2018. **21**(3): p. 613-620.
449. Huang, S., et al., *miR-582-3p and miR-582-5p Suppress Prostate Cancer Metastasis to Bone by Repressing TGF-β Signaling.* Mol Ther Nucleic Acids, 2019. **16**: p. 91-104.
450. Latil, A., et al., *Expression and mutational analysis of the MADR2/Smad2 gene in human prostate cancer.* Prostate, 1999. **40**(4): p. 225-31.
451. Wen, J., et al., *Dysregulation of cell cycle related genes and microRNAs distinguish the low- from high-risk of prostate cancer.* Diagn Pathol, 2014. **9**: p. 156.
452. Borel, M., et al., *Increased phospholipase D activity contributes to tumorigenesis in prostate cancer cell models.* Mol Cell Biochem, 2020. **473**(1-2): p. 263-279.
453. Zhou, W., et al., *Inhibition of Phospholipase D1 mRNA Expression Slows Down the Proliferation Rate of Prostate Cancer Cells That Have Transited to Androgen Independence.* J Cancer, 2018. **9**(19): p. 3620-3625.
454. Noble, A.R., et al., *Phospholipase D inhibitors reduce human prostate cancer cell proliferation and colony formation.* Br J Cancer, 2018. **118**(2): p. 189-199.
455. Kook, S. and J.H. Exton, *Identification of interaction sites of protein kinase Calpha on phospholipase D1.* Cell Signal, 2005. **17**(11): p. 1423-32.
456. Schmitt, J., et al., *Phorbol ester stimulates ethanolamine release from the metastatic basal prostate cancer cell line PC3 but not from prostate epithelial cell lines LNCaP and P4E6.* Br J Cancer, 2014. **111**(8): p. 1646-56.
457. Dükel, M., et al., *Protein kinase C Inhibitors selectively modulate dynamics of cell adhesion molecules and cell death in human colon cancer cells.* Cell Adh Migr, 2019. **13**(1): p. 83-97.
458. Cai, J., et al., *Downregulation of HMGA2 inhibits cellular proliferation and invasion, improves cellular apoptosis in prostate cancer.* Tumour Biol, 2016. **37**(1): p. 699-707.

459. Li, A.Y., et al., *High-mobility group A2 protein modulates hTERT transcription to promote tumorigenesis.* Mol Cell Biol, 2011. **31**(13): p. 2605-17.
460. Khajouee, S., et al., *Downregulation of HMGA2 by Small Interfering RNA Affects the Survival, Migration, and Apoptosis of Prostate Cancer Cell Line.* Adv Pharm Bull, 2022. **12**(2): p. 398-403.
461. Wang, P., et al., *hsa_circ_0062019 promotes the proliferation, migration, and invasion of prostate cancer cells via the miR-195-5p/HMGA2 axis.* Acta Biochim Biophys Sin (Shanghai), 2021. **53**(7): p. 815-822.
462. Guo, Z., et al., *Long non-coding RNA-NEAT1, a sponge for miR-98-5p, promotes expression of oncogene HMGA2 in prostate cancer.* Biosci Rep, 2019. **39**(9).
463. Shi, Z., et al., *Silencing of HMGA2 promotes apoptosis and inhibits migration and invasion of prostate cancer cells.* J Biosci, 2016. **41**(2): p. 229-36.
464. Huang, W.T., et al., *MiR-219-5p inhibits prostate cancer cell growth and metastasis by targeting HMGA2.* Eur Rev Med Pharmacol Sci, 2020. **24**(9): p. 4710-4718.
465. Tao, T., et al., *Involvement of EZH2 in aerobic glycolysis of prostate cancer through miR-181b/HK2 axis.* Oncol Rep, 2017. **37**(3): p. 1430-1436.
466. Korthauer, K., et al., *A practical guide to methods controlling false discoveries in computational biology.* Genome Biol, 2019. **20**(1): p. 118.
467. Benjamini, Y. and Y. Hochberg, *Controlling the False Discovery Rate - a Practical and Powerful Approach to Multiple Testing.* Journal of the Royal Statistical Society Series B-Statistical Methodology, 1995. **57**(1): p. 289-300.
468. Diamandis, E.P. and M. Li, *The side effects of translational omics: overtesting, overdiagnosis, overtreatment.* Clin Chem Lab Med, 2016. **54**(3): p. 389-96.
469. Rebello, R.J., et al., *Prostate cancer.* Nat Rev Dis Primers, 2021. **7**(1): p. 9.
470. Jang, J.S., et al., *Quantitative miRNA expression analysis using fluidigm microfluidics dynamic arrays.* BMC Genomics, 2011. **12**: p. 144.
471. Thorsen, T., S.J. Maerkl, and S.R. Quake, *Microfluidic large-scale integration.* Science, 2002. **298**(5593): p. 580-4.
472. Kaur, J., et al., *Identification of a suitable endogenous control miRNA in bone aging and senescence.* Gene, 2022. **835**: p. 146642.
473. Benz, F., et al., *U6 is unsuitable for normalization of serum miRNA levels in patients with sepsis or liver fibrosis.* Exp Mol Med, 2013. **45**(9): p. e42.
474. Zhang, Q., et al., *Selection and Evaluation of Reference Genes for miRNA Expression Analysis in Bemisia tabaci Under Insecticide Tolerance.* Front Genet, 2022. **13**: p. 899756.
475. Peng, P., et al., *[Estimates and prediction of prostate cancer incidence, mortality and prevalence in China, 2008].* Zhonghua Liu Xing Bing Xue Za Zhi, 2012. **33**(10): p. 1056-9.
476. Pang, C., et al., *Urologic cancer in China.* Jpn J Clin Oncol, 2016. **46**(6): p. 497-501.
477. Marzec, J., et al., *A genetic study and meta-analysis of the genetic predisposition of prostate cancer in a Chinese population.* Oncotarget, 2016. **7**(16): p. 21393-403.
478. Mao, X., et al., *Distinct genomic alterations in prostate cancers in Chinese and Western populations suggest alternative pathways of prostate carcinogenesis.* Cancer Res, 2010. **70**(13): p. 5207-12.
479. Xu, J., et al., *Genome-wide association study in Chinese men identifies two new prostate cancer risk loci at 9q31.2 and 19q13.4.* Nat Genet, 2012. **44**(11): p. 1231-5.
480. Bandera, E.V., et al., *Racial and ethnic disparities in the impact of obesity on breast cancer risk and survival: a global perspective.* Adv Nutr, 2015. **6**(6): p. 803-19.
481. Karakas, C., et al., *Molecular mechanisms involving prostate cancer racial disparity.* Am J Clin Exp Urol, 2017. **5**(3): p. 34-48.
482. Xia, J., et al., *Translational biomarker discovery in clinical metabolomics: an introductory tutorial.* Metabolomics, 2013. **9**(2): p. 280-299.
483. Boström, P.J., et al., *Genomic Predictors of Outcome in Prostate Cancer.* Eur Urol, 2015. **68**(6): p. 1033-44.
484. Molina, R., et al., *Diagnostic relevance of circulating biomarkers in patients with lung cancer.* Cancer Biomark, 2010. **6**(3-4): p. 163-78.
485. de la Taille, A., et al., *Clinical evaluation of the PCA3 assay in guiding initial biopsy decisions.* J Urol, 2011.

185(6): p. 2119-25.
486. Watanabe, S., et al., *HMGA2 maintains oncogenic RAS-induced epithelial-mesenchymal transition in human pancreatic cancer cells.* Am J Pathol, 2009. **174**(3): p. 854-68.
487. Best, M.G., P. Wesseling, and T. Wurdinger, *Tumor-Educated Platelets as a Noninvasive Biomarker Source for Cancer Detection and Progression Monitoring.* Cancer Res, 2018. **78**(13): p. 3407-3412.
488. Johnson, M.T., et al., *Evaluating methods for isolating total RNA and predicting the success of sequencing phylogenetically diverse plant transcriptomes.* PLoS One, 2012. **7**(11): p. e50226.
489. Rossen, L., et al., *Inhibition of PCR by components of food samples, microbial diagnostic assays and DNA-extraction solutions.* Int J Food Microbiol, 1992. **17**(1): p. 37-45.
490. Katcher, H.L. and I. Schwartz, *A distinctive property of Tth DNA polymerase: enzymatic amplification in the presence of phenol.* Biotechniques, 1994. **16**(1): p. 84-92.
491. Trichler, S.A., et al., *Ultra-pure platelet isolation from canine whole blood.* BMC Vet Res, 2013. **9**: p. 144.
492. Fink, L., et al., *Characterization of platelet-specific mRNA by real-time PCR after laser-assisted microdissection.* Thromb Haemost, 2003. **90**(4): p. 749-56.
493. Amisten, S., *A rapid and efficient platelet purification protocol for platelet gene expression studies.* Methods Mol Biol, 2012. **788**: p. 155-72.
494. Pohler, P., et al., *Pathogen reduction by ultraviolet C light effectively inactivates human white blood cells in platelet products.* Transfusion, 2015. **55**(2): p. 337-47.
495. Pan, Y., et al., *Computational genomics insights into cold acclimation in wheat.* Front Genet, 2022. **13**: p. 1015673.
496. Laudencia-Chingcuanco, D., et al., *Genome-wide gene expression analysis supports a developmental model of low temperature tolerance gene regulation in wheat (Triticum aestivum L.).* BMC Genomics, 2011. **12**: p. 299.
497. Bustin, S.A., et al., *Quantitative real-time RT-PCR--a perspective.* J Mol Endocrinol, 2005. **34**(3): p. 597-601.
498. Fleige, S. and M.W. Pfaffl, *RNA integrity and the effect on the real-time qRT-PCR performance.* Mol Aspects Med, 2006. **27**(2-3): p. 126-39.
499. Unger, C., et al., *Detection of phenol contamination in RNA samples and its impact on qRT-PCR results.* Anal Biochem, 2019. **571**: p. 49-52.
500. Davies, J., T. Denyer, and J. Hadfield, *Bioanalyzer chips can be used interchangeably for many analyses of DNA or RNA.* Biotechniques, 2016. **60**(4): p. 197-9.
501. Schroeder, A., et al., *The RIN: an RNA integrity number for assigning integrity values to RNA measurements.* BMC Mol Biol, 2006. **7**: p. 3.
502. Mayne, M., P.N. Shepel, and J.D. Geiger, *Recovery of high-integrity mRNA from brains of rats killed by high-energy focused microwave irradiation.* Brain Res Brain Res Protoc, 1999. **4**(3): p. 295-302.
503. Santiago, T.C., et al., *The relationship between mRNA stability and length in Saccharomyces cerevisiae.* Nucleic Acids Res, 1986. **14**(21): p. 8347-60.
504. Miller, C.L., et al., *Evaluating RNA status for RT-PCR in extracts of postmortem human brain tissue.* Biotechniques, 2004. **36**(4): p. 628-33.
505. Sheng, Q., et al., *Multi-perspective quality control of Illumina RNA sequencing data analysis.* Brief Funct Genomics, 2017. **16**(4): p. 194-204.
506. Puchta, M., M. Boczkowska, and J. Groszyk, *Low RIN Value for RNA-Seq Library Construction from Long-Term Stored Seeds: A Case Study of Barley Seeds.* Genes (Basel), 2020. **11**(10).
507. Max, K.E.A., et al., *Human plasma and serum extracellular small RNA reference profiles and their clinical utility.* Proc Natl Acad Sci U S A, 2018. **115**(23): p. E5334-e5343.
508. Grinstein, M., et al., *A robust method for RNA extraction and purification from a single adult mouse tendon.* PeerJ, 2018. **6**: p. e4664.
509. Cortés-Maldonado, L., et al., *A method for the extraction of high quality fungal RNA suitable for RNA-seq.* J Microbiol Methods, 2020. **170**: p. 105855.
510. Voigt, F., et al., *Detection and quantification of RNA decay intermediates using XRN1-resistant reporter transcripts.* Nat Protoc, 2019. **14**(5): p. 1603-1633.
511. Wu, Y., et al., *Advances in the study of exosomal lncRNAs in tumors and the selection of research methods.* Biomed Pharmacother, 2020. **123**: p. 109716.

512. Niu, Q., et al., *Effective and economical column-based method for RNA isolation from animal cells.* Biotechnol Lett, 2019. **41**(8-9): p. 915-920.
513. Desjardins, P. and D. Conklin, *NanoDrop microvolume quantitation of nucleic acids.* J Vis Exp, 2010(45).
514. Landolt, L., et al., *RNA extraction for RNA sequencing of archival renal tissues.* Scand J Clin Lab Invest, 2016. **76**(5): p. 426-34.
515. Nakayama, Y., et al., *Pitfalls of DNA Quantification Using DNA-Binding Fluorescent Dyes and Suggested Solutions.* PLoS One, 2016. **11**(3): p. e0150528.
516. Kapp, J.R., et al., *Variation in pre-PCR processing of FFPE samples leads to discrepancies in BRAF and EGFR mutation detection: a diagnostic RING trial.* J Clin Pathol, 2015. **68**(2): p. 111-8.
517. Manchester, K.L., *Use of UV methods for measurement of protein and nucleic acid concentrations.* Biotechniques, 1996. **20**(6): p. 968-70.
518. Toni, L.S., et al., *Optimization of phenol-chloroform RNA extraction.* MethodsX, 2018. **5**: p. 599-608.
519. Tang, Y.T., et al., *Comparison of isolation methods of exosomes and exosomal RNA from cell culture medium and serum.* Int J Mol Med, 2017. **40**(3): p. 834-844.
520. Ntostis, P., et al., *The impact of maternal age on gene expression during the GV to MII transition in euploid human oocytes.* Hum Reprod, 2021. **37**(1): p. 80-92.
521. Siriwach, R., et al., *An optimized protocol to identify keratinocyte subpopulations in vitro by single-cell RNA sequencing analysis.* STAR Protoc, 2022. **3**(4): p. 101906.
522. Sarantopoulou, D., et al., *Comparative evaluation of RNA-Seq library preparation methods for strand-specificity and low input.* Sci Rep, 2019. **9**(1): p. 13477.
523. Song, Y., et al., *A comparative analysis of library prep approaches for sequencing low input translatome samples.* BMC Genomics, 2018. **19**(1): p. 696.
524. Herbert, Z.T., et al., *Cross-site comparison of ribosomal depletion kits for Illumina RNAseq library construction.* BMC Genomics, 2018. **19**(1): p. 199.
525. Dashore, S., et al., *Preparation of Platelet-Rich Plasma: National IADVL PRP Taskforce Recommendations.* Indian Dermatol Online J, 2021. **12**(Suppl 1): p. S12-s23.
526. Tamimi, F.M., et al., *A comparative study of 2 methods for obtaining platelet-rich plasma.* J Oral Maxillofac Surg, 2007. **65**(6): p. 1084-93.
527. Kramer, M.E. and T.C. Keaney, *Systematic review of platelet-rich plasma (PRP) preparation and composition for the treatment of androgenetic alopecia.* J Cosmet Dermatol, 2018. **17**(5): p. 666-671.
528. Hamburger, S.A. and R.P. McEver, *GMP-140 mediates adhesion of stimulated platelets to neutrophils.* Blood, 1990. **75**(3): p. 550-4.
529. Weyrich, A.S., et al., *Activated platelets signal chemokine synthesis by human monocytes.* J Clin Invest, 1996. **97**(6): p. 1525-34.
530. Rowley, J.W., et al., *Genome-wide RNA-seq analysis of human and mouse platelet transcriptomes.* Blood, 2011. **118**(14): p. e101-11.
531. Zellner, M., et al., *Quantitative validation of different protein precipitation methods in proteome analysis of blood platelets.* Electrophoresis, 2005. **26**(12): p. 2481-9.
532. Rolf, N., et al., *Optimized procedure for platelet RNA profiling from blood samples with limited platelet numbers.* Clin Chem, 2005. **51**(6): p. 1078-80.
533. Vollmar, B., et al., *Comparative analysis of platelet isolation techniques for the in vivo study of the microcirculation.* Microcirculation, 2003. **10**(2): p. 143-52.
534. Karpatkin, S., *Heterogeneity of human platelets. I. Metabolic and kinetic evidence suggestive of young and old platelets.* J Clin Invest, 1969. **48**(6): p. 1073-82.
535. Teruel-Montoya, R., et al., *MicroRNA expression differences in human hematopoietic cell lineages enable regulated transgene expression.* PLoS One, 2014. **9**(7): p. e102259.
536. Söderström, A.C., et al., *The effect of centrifugation speed and time on pre-analytical platelet activation.* Clin Chem Lab Med, 2016. **54**(12): p. 1913-1920.
537. Perez, A.G., et al., *Relevant aspects of centrifugation step in the preparation of platelet-rich plasma.* ISRN Hematol, 2014. **2014**: p. 176060.
538. Wrzyszcz, A., et al., *An efficient method for isolation of representative and contamination-free population of blood platelets for proteomic studies.* Platelets, 2017. **28**(1): p. 43-53.
539. Finamore, F., et al., *Proteomics investigation of human platelets by shotgun nUPLC-MSE and 2DE*

experimental strategies: a comparative study. Blood Transfus, 2010. **8 Suppl 3**(Suppl 3): p. s140-8.
540. O'Neill, E.E., et al., *Towards complete analysis of the platelet proteome.* Proteomics, 2002. **2**(3): p. 288-305.
541. Magalon, J., et al., *DEPA classification: a proposal for standardising PRP use and a retrospective application of available devices.* BMJ Open Sport Exerc Med, 2016. **2**(1): p. e000060.
542. Rox, J.M., et al., *Gene expression analysis in platelets from a single donor: evaluation of a PCR-based amplification technique.* Clin Chem, 2004. **50**(12): p. 2271-8.
543. Graham, J.M., *Isolation of human platelets (thrombocytes).* ScientificWorldJournal, 2002. **2**: p. 1607-9.
544. Wang, X., et al., *Microfluidic chip combined with magnetic-activated cell sorting technology for tumor antigen-independent sorting of circulating hepatocellular carcinoma cells.* PeerJ, 2019. **7**: p. e6681.
545. Chebbo, M., et al., *Platelets Purification Is a Crucial Step for Transcriptomic Analysis.* Int J Mol Sci, 2022. **23**(6).
546. Parguina, A.F., I. Rosa, and A. Garcia, *Proteomics applied to the study of platelet-related diseases: aiding the discovery of novel platelet biomarkers and drug targets.* J Proteomics, 2012. **76 Spec No.**: p. 275-86.
547. Wheater, P.R., H.G. Burkitt, and V.G. Daniels, *Functional histology : a text and colour atlas*. 1979.
548. Gutmann, C. and M. Mayr, *Circulating microRNAs as biomarkers and mediators of platelet activation.* Platelets, 2022. **33**(4): p. 512-519.
549. Atar, O.D., et al., *Stability validation of paraformaldehyde-fixed samples for the assessment of the platelet PECAM-1, P-selectin, and PAR-1 thrombin receptor by flow cytometry.* J Thromb Thrombolysis, 2010. **30**(1): p. 79-83.
550. Rochat, S. and L. Alberio, *Formaldehyde-fixation of platelets for flow cytometric measurement of phosphatidylserine exposure is feasible.* Cytometry A, 2015. **87**(1): p. 32-6.
551. Riedl, J., et al., *Association of mean platelet volume with risk of venous thromboembolism and mortality in patients with cancer. Results from the Vienna Cancer and Thrombosis Study (CATS).* Thromb Haemost, 2014. **111**(4): p. 670-8.
552. Chesnutt, J.K. and H.C. Han, *Platelet size and density affect shear-induced thrombus formation in tortuous arterioles.* Phys Biol, 2013. **10**(5): p. 056003.
553. Mangalpally, K.K., et al., *Platelet activation patterns in platelet size sub-populations: differential responses to aspirin in vitro.* J Thromb Thrombolysis, 2010. **30**(3): p. 251-62.
554. Opper, C., et al., *Analysis of GTP-binding proteins, phosphoproteins, and cytosolic calcium in functional heterogeneous human blood platelet subpopulations.* Biochem Pharmacol, 1997. **54**(9): p. 1027-35.
555. Handtke, S. and T. Thiele, *Large and small platelets-(When) do they differ?* J Thromb Haemost, 2020. **18**(6): p. 1256-1267.
556. Diamandis, E.P., *Cancer biomarkers: can we turn recent failures into success?* J Natl Cancer Inst, 2010. **102**(19): p. 1462-7.
557. Høgdall, C., et al., *A novel proteomic biomarker panel as a diagnostic tool for patients with ovarian cancer.* Gynecol Oncol, 2011. **123**(2): p. 308-13.
558. Risso, D., et al., *GC-content normalization for RNA-Seq data.* BMC Bioinformatics, 2011. **12**: p. 480.
559. Hansen, K.D., S.E. Brenner, and S. Dudoit, *Biases in Illumina transcriptome sequencing caused by random hexamer priming.* Nucleic Acids Res, 2010. **38**(12): p. e131.
560. Sadi, M.V., *PSA screening for prostate cancer.* Rev Assoc Med Bras (1992), 2017. **63**(8): p. 722-725.
561. Hong, W., et al., *Transfection of human platelets with short interfering RNA.* Clin Transl Sci, 2011. **4**(3): p. 180-2.
562. Molina, R., et al., *HE4 a novel tumour marker for ovarian cancer: comparison with CA 125 and ROMA algorithm in patients with gynaecological diseases.* Tumour Biol, 2011. **32**(6): p. 1087-95.

Appendix

Table 27. Details of all RNA quality and quantity measured by Bioanalyzer and Nanodrop for RNA-seq candidates (91 cases).

Sample ID	Nanodrop conc (ng/μL)	260/280	260/230	RIN Score	Bioanalyser concentration (ng/μL)	Total RNA yield (ng)
GPB-260	25.57	1.87	0.37	5.7	0.6	3
GPB-260	23.08	1.86	0.45	4.7	1.0	7.98
PPPP017	72.38	1.96	1.14	7	18.5	148
PPPP047	36.1	2.17	0.71	7.2	4	32
PPPP049	42.11	1.91	0.58	8.2	16	128
PPPP053	32.58	1.74	0.82	7.1	5	40
PPPP054	36.14	1.91	0.64	4.7	9.9	79.2
PPPP056	35.43	1.72	0.59	7.2	6	48
PPPP061	26.43	1.77	0.57	5.7	3	24
PPPP062	30.07	1.8	0.5	5.7	5	40
PPPP063	36.46	1.81	0.47	7.9	8	64
PPPP065	34.16	1.54	0.17	5.8	0.4	2
PPPP067	26.12	1.87	0.19	6.7	6.8	54.4
PPPP068	33.6	1.78	0.5	N/A	3	15
PPPP074	37.07	1.82	0.88	8.9	7	56
PPPP080	39.77	1.78	0.73	6.1	7	56
PPPP087	45.68	1.88	0.27	6.7	1.3	6.5
PPPP104	10.27	1.73	0.32	2.1	0.13	1.05
PPPP108	15.72	1.65	0.09	3.4	0.1	0.8
PPPP118	38.98	1.89	0.71	4.6	5.6	44.8

PPPP122	40.52	1.71	0.68	8.4	6	48
PPPP123	58.4	1.81	0.39	8.5	2.19	17.54
PPPP127	54.27	1.9	0.88	8.9	13	104
PPPP129	30.29	1.74	0.13	2.9	0.2	1
PPPP129	27.18	1.81	0.39	7.2	0.74	5.93
PPPP129	23.68	1.81	0.21	6.9	0.36	2.90
PPPP139	22.74	1.83	0.83	6.3	4.4	35.2
PPPP141	18.58	1.73	0.39	7.9	4	32
PPPP145	29.55	1.86	0.58	5.4	5.5	44
PPPP153	31.92	1.79	0.96	8.3	0.66	5.28
PPPP156	65.29	1.86	0.15	8	2.4	12
PPPP164	79.67	2	0.67	6.9	23.9	191.2
PPPP165	33.85	1.75	0.14	5.3	0.3	1.5
PPPP168	37.68	1.75	0.87	7.5	1.34	10.70
PPPP170	56.75	1.82	0.3	7.2	1.9	9.5
PPPP172	37.62	1.65	0.35	7.9	0.19	1.55
PPPP178	49.17	1.82	0.21	8.5	2.14	17.10
PPPP206	33.86	1.89	0.09	6	0.516	4.128
PPPP210	39.56	1.71	0.3	5.8	1.281	10.248
PPPP211	36.19	1.74	0.44	5.8	8.2	65.6
PPPP216	35.7	1.75	0.29	7.7	0.7	3.5
PPPP217	32	1.81	0.55	5.7	0.5	2.5
PPPP239	33.16	1.75	0.25	4.6	6.9	55.2
PPPP257	41.91	1.75	0.49	7.8	13	104
PPPP260	79.39	1.55	0.82	6.6	15.4	123.2
PPPP267	49.23	1.89	0.71	7.7	17.4	139.2
PPPP269	52.17	1.87	0.11	4.2	1.2	6

PPPP272	41.44	1.97	0.35	8.4	14.6	116.8
PPPP275	38.06	1.87	1.03	5	16.7	133.6
PPPP278	38.38	1.95	0.41	7.4	11.9	95.2
PPPP279	32.54	1.77	0.28	7.3	8.9	71.2
PPPP284	34.3	1.81	0.86	5.8	9.5	76
PPPP288	19.27	1.8	0.46	2.4	2.7	21.6
PPPP294	39.8	1.88	0.97	6.9	15.3	122.4
PPPP307	37.17	1.74	0.41	3	5.6	28
PPPP308	35.36	1.84	0.22	7.4	0.5	2.5
PPPP308	21.04	1.68	0.56	4.4	4.6	36.8
PPPP310	63.78	1.9	0.39	8.2	1.7	8.5
PPPP312	54.25	1.8	0.26	2.1	0.5	2.5
PPPP314	36.7	1.79	0.43	6.6	1.3	6.5
PPPP314	37.51	1.88	0.65	5.4	6.1	48.8
PPPP316	73.72	1.87	0.36	7	2.1	10.5
PPPP320	39.06	1.71	0.1	5.8	0.3	1.5
PPPP323	37.69	1.75	0.15	6.7	0.5	2.5
PPPP324	30.16	1.8	0.1	3	0.2	1
PPPP325	40.28	1.72	0.14	5.8	0.3	1.5
PPPP326	43.13	1.84	0.35	6.1	1.2	6
PPPP328	53.49	1.74	0.2	4.6	0.4	2
PPPP329	64.35	1.9	0.95	7.8	3.8	19
PPPP329	36.96	1.9	0.34	6.3	9.5	76
PPPP330	79.27	1.91	0.63	5.8	1.9	9.5
PPPP332	33.28	1.72	0.21	4.6	0.6	3
PPPP338	42.83	1.82	0.67	8.1	1.5	7.5
PPPP340	38.7	1.49	0.51	3.3	0.6	3

PPPP341	49.54	1.89	0.24	7.6	2.5	12.5
PPPP342	49.59	1.93	0.11	8.8	12	60
PPPP342	46.36	1.95	0.83	6.1	18.4	147.2
PPPP343	43.98	1.77	0.12	7.5	0.9	4.5
PPPP343	21.01	1.89	0.68	4.2	4.8	38.4
PPPP344	33.92	1.63	0.26	6.7	0.6	3
PPPP346	45.36	1.64	0.57	N/A	0.159	1.272
PPPP346	36.61	1.75	0.53	1	10	50
PPPP347	32.05	1.89	0.33	7.3	1.3	6.5
PPPP348	54.19	1.8	0.47	8.2	1.8	9
PPPP348	38.61	1.82	0.23	6.6	8.4	67.2
PPPP350	58.17	1.74	0.37	7.8	1.9	9.5
PPPP353	36.79	1.68	0.24	6.5	0.2	1
PPPP353	35.81	1.67	0.15	5.2	2.4	19.2
PPPP355	42.2	1.79	0.1	8.1	1	5
PPPP356	39.54	1.78	0.27	7.5	0.9	4.5
PPPP361	74.95	1.9	0.68	8.2	2.1	10.5

Patients (GPB-260, PPPP129, PPPP308, PPPP314, PPPP329, PPPP342, PPPP343, PPPP346, PPPP348, and PPPP353) provided several samples at different visits. N/A: not available, RIN: RNA Integrity Number.

Table 28. Results of genes that passed the p-value of 0.05 by DESeq2 in mRNA-seq.

GeneID	baseMean	log2FoldChange	lfcSE	pvalue	padj
ENSG00000267243	7.138767	2.34739	0.579181	5.06E-05	0.157328
ENSG00000152760	33.20336	1.240571	0.307513	5.48E-05	0.157328
ENSG00000256618	36.07418	2.210061	0.565759	9.37E-05	0.230626
ENSG00000250548	6.806856	3.007858	0.868812	0.000536	0.999413
ENSG00000147647	6.9973	3.318948	0.973885	0.000655	0.999413
ENSG00000259347	5.080325	2.649459	0.77806	0.000661	0.999413
ENSG00000187950	5.217582	2.680596	0.842713	0.001468	0.999413
ENSG00000238178	2.159389	3.199887	1.028338	0.00186	0.999413
ENSG00000254186	11.41751	1.694026	0.56221	0.002585	0.999413
ENSG00000286241	1.338554	3.544826	1.189139	0.002873	0.999413
ENSG00000175395	93.67106	0.595633	0.200752	0.003007	0.999413
ENSG00000278791	23.40913	1.40578	0.475593	0.003118	0.999413
ENSG00000152689	54.7423	0.854305	0.289875	0.003207	0.999413
ENSG00000237973	244.5836	1.064108	0.361493	0.003244	0.999413
ENSG00000078596	764.5915	0.580182	0.197548	0.003315	0.999413

ENSG00000242193	68.23285	0.593488	0.206273	0.004012	0.999413
ENSG00000198088	10.13778	1.732157	0.60207	0.004015	0.999413
ENSG00000279504	9.815908	0.970652	0.340894	0.004408	0.999413
ENSG00000234156	15.22398	2.158067	0.763848	0.004724	0.999413
ENSG00000198744	77.17294	1.106136	0.392602	0.004841	0.999413
ENSG00000163734	122.4071	0.540516	0.193647	0.005251	0.999413
ENSG00000125869	125.6411	0.933467	0.336915	0.005595	0.999413
ENSG00000185742	1.007532	3.294506	1.197872	0.005954	0.999413
ENSG00000226252	459.1189	0.647726	0.237515	0.006389	0.999413
ENSG00000236438	19.05019	1.289473	0.479221	0.007129	0.999413
ENSG00000153363	32.68359	0.92843	0.346959	0.007453	0.999413
ENSG00000267026	14.77648	1.630621	0.610379	0.007552	0.999413
ENSG00000282968	14.27687	3.580871	1.344817	0.007751	0.999413
ENSG00000187715	12.93581	1.222424	0.465598	0.008652	0.999413
ENSG00000258791	25.78034	1.449954	0.559508	0.009556	0.999413
ENSG00000243069	16.3827	1.11281	0.429879	0.009635	0.999413
ENSG00000131477	1.62504	2.381857	0.921659	0.009757	0.999413

ENSG00000076770	660.2113	0.479947	0.187456	0.010458	0.999413
ENSG00000157927	2.306545	2.500796	0.979811	0.010701	0.999413
ENSG00000122778	5.446705	1.6344	0.6415	0.010841	0.999413
ENSG00000115896	130.1195	0.865479	0.341771	0.011331	0.999413
ENSG00000213185	15.87321	1.296116	0.516344	0.012067	0.999413
ENSG00000226415	21.67429	0.752502	0.301223	0.012484	0.999413
ENSG00000165288	77.147	0.463094	0.186521	0.013035	0.999413
ENSG00000188177	338.2955	0.430086	0.17346	0.013159	0.999413
ENSG00000245975	1.801443	3.04497	1.230312	0.013325	0.999413
ENSG00000154723	395.499	0.313222	0.126839	0.013532	0.999413
ENSG00000157680	40.71881	0.944815	0.38765	0.014798	0.999413
ENSG00000224861	4.145589	2.059143	0.845603	0.014887	0.999413
ENSG00000176593	27.01973	0.65881	0.272773	0.015725	0.999413
ENSG00000196118	6.674935	1.625418	0.673158	0.015752	0.999413
ENSG00000091651	2.488619	2.268948	0.940427	0.015836	0.999413
ENSG00000149531	24.50973	0.789525	0.328125	0.016121	0.999413
ENSG00000137267	109.76	1.981278	0.827627	0.016669	0.999413

ENSG00000213453	56.06759	0.604011	0.252736	0.016853	0.999413
ENSG00000233338	1.309787	2.961164	1.241031	0.01703	0.999413
ENSG00000240497	168.4315	0.486121	0.204244	0.017308	0.999413
ENSG00000165775	207.9069	0.298004	0.125327	0.017416	0.999413
ENSG00000271047	0.955247	2.80326	1.182345	0.017743	0.999413
ENSG00000113356	93.78837	0.594114	0.251364	0.0181	0.999413
ENSG00000177854	5.16747	1.514818	0.642715	0.018428	0.999413
ENSG00000256045	335.9865	0.861243	0.367784	0.019196	0.999413
ENSG00000160766	1.364032	2.994261	1.279287	0.019254	0.999413
ENSG00000278771	4.083455	1.614206	0.691561	0.019588	0.999413
ENSG00000283475	5.542114	1.182428	0.507015	0.019694	0.999413
ENSG00000172819	66.22183	0.544336	0.233766	0.019883	0.999413
ENSG00000237852	12.60811	0.957307	0.411297	0.019937	0.999413
ENSG00000115808	119.2861	0.284366	0.122279	0.020042	0.999413
ENSG00000075618	2.287035	2.157275	0.940736	0.021838	0.999413
ENSG00000111445	51.55254	0.463653	0.202557	0.02208	0.999413
ENSG00000250550	2.009908	2.705236	1.183381	0.022253	0.999413

ENSG00000135226	45.06538	1.024724	0.448609	0.022358	0.999413
ENSG00000213362	43.57406	0.782247	0.342939	0.022548	0.999413
ENSG00000247498	62.02137	1.203936	0.52959	0.023006	0.999413
ENSG00000275569	1.056582	2.84735	1.253277	0.023091	0.999413
ENSG00000267098	1.701578	3.350963	1.475785	0.023169	0.999413
ENSG00000164687	16.68327	0.801586	0.35431	0.023673	0.999413
ENSG00000112984	3.050623	1.818973	0.806799	0.024161	0.999413
ENSG00000163634	249.0919	0.292926	0.130495	0.024785	0.999413
ENSG00000182648	28.12463	0.879005	0.392478	0.025115	0.999413
ENSG00000215548	2.41762	2.281502	1.01994	0.025293	0.999413
ENSG00000184611	1.381255	2.915336	1.303673	0.025336	0.999413
ENSG00000102174	16.48262	1.124547	0.502994	0.025371	0.999413
ENSG00000270689	5.304962	1.680728	0.754702	0.025947	0.999413
ENSG00000213123	1.280194	2.615125	1.176123	0.026181	0.999413
ENSG00000122483	131.3088	0.443937	0.200142	0.026547	0.999413
ENSG00000217648	0.977671	2.900771	1.308172	0.026594	0.999413
ENSG00000137776	475.2965	0.205273	0.092985	0.027273	0.999413

ENSG00000126870	34.84157	0.629357	0.285357	0.027419	0.999413
ENSG00000136878	215.5276	0.46627	0.212107	0.027929	0.999413
ENSG00000282912	5.520126	1.319391	0.600448	0.027996	0.999413
ENSG00000104635	4.031878	2.114555	0.962906	0.028091	0.999413
ENSG00000259032	3.124055	1.422166	0.648246	0.028245	0.999413
ENSG00000276975	1.717621	2.930371	1.340631	0.028829	0.999413
ENSG00000285884	336.9712	0.661247	0.302645	0.028897	0.999413
ENSG00000233087	13.64035	0.933932	0.428229	0.029189	0.999413
ENSG00000210140	38.18868	0.581145	0.267835	0.030023	0.999413
ENSG00000267724	64.67428	0.40202	0.18546	0.030182	0.999413
ENSG00000081041	9.204932	1.214385	0.560725	0.030331	0.999413
ENSG00000273199	3.631355	1.544348	0.715001	0.030779	0.999413
ENSG00000276278	2.929755	1.457924	0.676816	0.031233	0.999413
ENSG00000101470	258.8602	0.388387	0.180563	0.031478	0.999413
ENSG00000160124	3.664675	1.759781	0.818921	0.031642	0.999413
ENSG00000271043	18.14139	0.741301	0.346357	0.032332	0.999413
ENSG00000244757	15.54657	1.282104	0.602373	0.033302	0.999413

ENSG00000113249	1.102139	3.094629	1.457265	0.033705	0.999413
ENSG00000168032	2.756836	1.733982	0.818203	0.034069	0.999413
ENSG00000186577	46.32043	0.480224	0.226839	0.034257	0.999413
ENSG00000172137	1.813039	2.53183	1.198386	0.034626	0.999413
ENSG00000273747	30.47154	0.520701	0.246545	0.034688	0.999413
ENSG00000235238	9.098738	0.979	0.46396	0.03485	0.999413
ENSG00000172572	132.1801	0.440864	0.209482	0.035331	0.999413
ENSG00000255028	71.45532	0.541693	0.257437	0.035363	0.999413
ENSG00000248494	3.328317	1.989074	0.946004	0.0355	0.999413
ENSG00000157554	7.123432	1.312539	0.624786	0.03566	0.999413
ENSG00000198816	5.586819	1.000743	0.477045	0.035923	0.999413
ENSG00000223969	39.73619	0.656637	0.313043	0.035941	0.999413
ENSG00000230562	4.988926	1.006595	0.482207	0.036845	0.999413
ENSG00000247708	2.572041	1.897398	0.913636	0.037824	0.999413
ENSG00000105355	226.1235	0.303145	0.145987	0.037846	0.999413
ENSG00000232727	18.79345	0.610237	0.295434	0.03887	0.999413
ENSG00000135951	21.89163	0.947543	0.459972	0.039398	0.999413

ENSG00000108387	322.2205	0.518111	0.253114	0.040663	0.999413
ENSG00000260625	3.004249	1.639059	0.802181	0.041027	0.999413
ENSG00000196693	121.7032	0.530744	0.260129	0.04132	0.999413
ENSG00000259577	132.4262	0.651718	0.319771	0.041542	0.999413
ENSG00000255733	3.308532	1.965819	0.965924	0.041834	0.999413
ENSG00000162407	4.666436	1.360803	0.669314	0.042039	0.999413
ENSG00000116678	1357.959	0.4266	0.210554	0.042756	0.999413
ENSG00000128617	1.909858	1.993947	0.987264	0.043418	0.999413
ENSG00000247400	15.19847	0.698963	0.346251	0.043523	0.999413
ENSG00000111674	523.4257	0.43804	0.217857	0.04436	0.999413
ENSG00000128708	306.1859	0.276099	0.137447	0.044562	0.999413
ENSG00000139168	64.22089	0.458327	0.228591	0.044962	0.999413
ENSG00000262728	3.434446	1.495115	0.747102	0.045369	0.999413
ENSG00000166444	1.90664	2.073052	1.036407	0.045475	0.999413
ENSG00000257511	26.60323	0.419729	0.210292	0.045941	0.999413
ENSG00000180209	2.673948	1.271844	0.637558	0.046057	0.999413
ENSG00000257167	20.59901	0.625423	0.313567	0.046093	0.999413

ENSG00000231725	34.70924	0.584694	0.293731	0.046528	0.999413
ENSG00000272636	2.490097	1.751293	0.880868	0.046796	0.999413
ENSG00000070718	60.03945	0.387668	0.195357	0.04721	0.999413
ENSG00000228649	11.67315	0.919375	0.46335	0.047234	0.999413
ENSG00000236078	5.665866	1.150816	0.580039	0.047253	0.999413
ENSG00000168610	1393.612	0.292592	0.14757	0.047398	0.999413
ENSG00000154240	2.251581	2.273115	1.147113	0.047524	0.999413
ENSG00000169519	15.51402	0.757625	0.382358	0.04754	0.999413
ENSG00000159450	4.422961	1.747089	0.882942	0.047848	0.999413
ENSG00000113924	985.7989	0.406736	0.205564	0.047857	0.999413
ENSG00000236279	255.3577	0.691499	0.34976	0.048034	0.999413
ENSG00000226833	2.050486	1.951247	0.98817	0.048313	0.999413
ENSG00000278931	1.125262	3.101905	1.571471	0.048395	0.999413
ENSG00000172893	76.03544	0.602214	0.305568	0.048747	0.999413
ENSG00000272799	11.13603	1.770025	0.899084	0.048988	0.999413
ENSG00000271198	3.215097	1.146164	0.58243	0.04908	0.999413
ENSG00000117519	5.717772	1.217531	0.619235	0.049277	0.999413

ENSG00000184661	1.791942	1.920656	0.977753	0.049489	0.999413
ENSG00000225422	10.08817	-1.84001	0.382861	1.54E-06	0.026536
ENSG00000090382	1668.534	-2.53662	0.549183	3.86E-06	0.033235
ENSG00000257764	1042.472	-2.4904	0.551624	6.34E-06	0.036422
ENSG00000276085	76.32318	-2.39887	0.55391	1.49E-05	0.063998
ENSG00000196236	11.64906	-1.18996	0.342418	0.000511	0.999413
ENSG00000274487	19.12457	-1.59871	0.472229	0.000711	0.999413
ENSG00000066926	113.9754	-1.02958	0.307237	0.000805	0.999413
ENSG00000198074	2.000471	-3.74296	1.139091	0.001016	0.999413
ENSG00000258086	2.323475	-2.79071	0.895185	0.001824	0.999413
ENSG00000273226	4.013183	-2.56347	0.826324	0.001921	0.999413
ENSG00000130147	2.851771	-2.15248	0.699943	0.002103	0.999413
ENSG00000106565	23.69021	-3.04499	0.997852	0.002277	0.999413
ENSG00000266969	2.652444	-2.13317	0.723539	0.003196	0.999413
ENSG00000204010	5.569584	-2.45096	0.839393	0.003501	0.999413
ENSG00000257252	2.524277	-2.63123	0.912276	0.003923	0.999413
ENSG00000214226	6.156519	-1.36355	0.472831	0.003929	0.999413

ENSG00000213020	17.97284	-1.02699	0.357975	0.004119	0.999413
ENSG00000182853	3.269101	-2.53705	0.886374	0.004206	0.999413
ENSG00000235724	1.320307	-3.28904	1.155194	0.004411	0.999413
ENSG00000196576	32.93914	-1.21372	0.428219	0.004592	0.999413
ENSG00000272430	4.663764	-1.3403	0.478335	0.005079	0.999413
ENSG00000004939	33.92093	-1.5153	0.541964	0.005175	0.999413
ENSG00000108239	3.954587	-1.90963	0.683737	0.005223	0.999413
ENSG00000184785	3.351242	-2.10301	0.758179	0.005541	0.999413
ENSG00000137959	35.67369	-1.65505	0.597857	0.005635	0.999413
ENSG00000137331	9.193802	-1.72364	0.624042	0.005744	0.999413
ENSG00000169402	2.284415	-3.24082	1.180927	0.006064	0.999413
ENSG00000119535	145.1903	-1.84965	0.6751	0.006147	0.999413
ENSG00000125740	2.525163	-2.49539	0.916886	0.006497	0.999413
ENSG00000134955	9.21738	-1.99984	0.734961	0.006508	0.999413
ENSG00000062282	7.354856	-2.60594	0.965042	0.006927	0.999413
ENSG00000169429	52.30275	-2.55705	0.948399	0.007014	0.999413
ENSG00000158578	133.8813	-1.50867	0.563302	0.0074	0.999413

ENSG00000202360	1.785936	-2.9936	1.128657	0.007993	0.999413
ENSG00000204103	67.3347	-1.0028	0.381489	0.008573	0.999413
ENSG00000128250	1.198755	-3.46893	1.324742	0.00883	0.999413
ENSG00000170396	3.344496	-1.85706	0.710284	0.008935	0.999413
ENSG00000188536	4758.277	-1.02147	0.391142	0.009015	0.999413
ENSG00000198010	2.88474	-2.10801	0.807265	0.00902	0.999413
ENSG00000258057	3.484099	-2.28671	0.879271	0.009304	0.999413
ENSG00000113070	4.122264	-2.16176	0.834963	0.009624	0.999413
ENSG00000196642	17.71252	-0.65461	0.253214	0.009732	0.999413
ENSG00000105229	18.27886	-0.63798	0.247082	0.009822	0.999413
ENSG00000180871	84.76018	-1.12371	0.435435	0.009862	0.999413
ENSG00000113369	233.1713	-0.58511	0.227077	0.009975	0.999413
ENSG00000230457	2.365844	-1.97955	0.768627	0.010011	0.999413
ENSG00000277632	25.19995	-1.93813	0.753174	0.010074	0.999413
ENSG00000177169	19.21521	-0.7748	0.301703	0.010226	0.999413
ENSG00000276070	16.75057	-1.75316	0.683026	0.010266	0.999413
ENSG00000175137	45.48307	-0.60198	0.235161	0.010471	0.999413

ENSG00000197601	171.9733	-0.49336	0.192885	0.010534	0.999413
ENSG00000074964	8.113135	-1.84255	0.724953	0.011034	0.999413
ENSG00000196943	24.41416	-0.98454	0.38744	0.011049	0.999413
ENSG00000235945	1.317285	-2.92008	1.155196	0.011479	0.999413
ENSG00000126461	4.556531	-1.26169	0.500356	0.011683	0.999413
ENSG00000167657	56.81047	-0.47078	0.186745	0.011703	0.999413
ENSG00000269176	5.012089	-1.48695	0.590546	0.011805	0.999413
ENSG00000268849	1.204238	-3.01365	1.197452	0.011845	0.999413
ENSG00000106066	155.7296	-1.65656	0.658399	0.011868	0.999413
ENSG00000204634	18.88983	-1.17766	0.468432	0.011936	0.999413
ENSG00000141505	7.043677	-1.52244	0.607258	0.012174	0.999413
ENSG00000160883	29.62982	-1.40043	0.558774	0.012202	0.999413
ENSG00000100106	76.57831	-0.47975	0.191493	0.012235	0.999413
ENSG00000162711	12.577	-1.81889	0.730086	0.012727	0.999413
ENSG00000129911	8.024881	-0.85681	0.344428	0.01286	0.999413
ENSG00000136867	44.61056	-1.30162	0.524761	0.013123	0.999413
ENSG00000285948	1.358126	-2.62813	1.059978	0.01316	0.999413

ENSG00000030582	172.1399	-0.85204	0.34482	0.013475	0.999413
ENSG00000183496	2.468068	-2.3113	0.937925	0.013729	0.999413
ENSG00000165731	17.08985	-0.82883	0.337144	0.013957	0.999413
ENSG00000228395	6.898486	-1.37643	0.561004	0.014147	0.999413
ENSG00000006534	21.90678	-1.04416	0.425793	0.014196	0.999413
ENSG00000260296	1.274644	-3.72588	1.522721	0.014411	0.999413
ENSG00000161664	5.773204	-1.27107	0.521303	0.014758	0.999413
ENSG00000168961	26.96674	-0.96232	0.395248	0.014904	0.999413
ENSG00000147454	174.636	-0.84726	0.348386	0.015017	0.999413
ENSG00000143416	12.48482	-1.59933	0.65814	0.015096	0.999413
ENSG00000186300	3.663555	-1.77966	0.732543	0.015123	0.999413
ENSG00000126003	29.34297	-0.9038	0.372738	0.015319	0.999413
ENSG00000167850	8.955505	-1.97238	0.815072	0.015525	0.999413
ENSG00000273723	1.478469	-2.95011	1.219263	0.015538	0.999413
ENSG00000258428	5.759043	-1.63106	0.67508	0.015688	0.999413
ENSG00000232024	9.298242	-0.91111	0.378169	0.015985	0.999413
ENSG00000180509	1.282052	-3.06542	1.277694	0.016432	0.999413

ENSG00000230555	2.270457	-2.08346	0.870314	0.01667	0.999413
ENSG00000176890	16.03134	-0.89229	0.372892	0.016716	0.999413
ENSG00000160345	1.797482	-1.66535	0.696837	0.016855	0.999413
ENSG00000185507	32.98826	-1.01766	0.426355	0.016991	0.999413
ENSG00000177302	10.56863	-1.30605	0.547234	0.017003	0.999413
ENSG00000112299	75.43382	-0.61975	0.260197	0.017225	0.999413
ENSG00000170345	139.7308	-1.7751	0.745726	0.017296	0.999413
ENSG00000283839	29.90158	-0.7515	0.315774	0.017319	0.999413
ENSG00000244734	25738.96	-1.04887	0.441228	0.017446	0.999413
ENSG00000051180	3.956966	-1.57786	0.665551	0.017752	0.999413
ENSG00000166928	5.024818	-1.89606	0.800391	0.01784	0.999413
ENSG00000286193	26.03847	-1.14266	0.482593	0.017896	0.999413
ENSG00000164258	80.56988	-0.4219	0.178267	0.01795	0.999413
ENSG00000113712	219.307	-0.25598	0.108211	0.018005	0.999413
ENSG00000100226	92.07553	-0.47801	0.202728	0.01838	0.999413
ENSG00000143344	5.706176	-1.5402	0.656593	0.018989	0.999413
ENSG00000133246	29.24502	-1.16291	0.495929	0.019031	0.999413

ENSG00000206172	933.4397	-1.06084	0.453108	0.019219	0.999413
ENSG00000171365	2.636334	-2.50502	1.072837	0.019546	0.999413
ENSG00000266751	14.93692	-0.75062	0.321654	0.019616	0.999413
ENSG00000175489	64.89377	-1.17543	0.504035	0.019698	0.999413
ENSG00000229043	12.60196	-1.01159	0.434448	0.019888	0.999413
ENSG00000013306	185.0889	-0.82196	0.353017	0.019892	0.999413
ENSG00000172493	121.189	-0.33484	0.144548	0.020533	0.999413
ENSG00000214688	2.964376	-2.23488	0.964925	0.020552	0.999413
ENSG00000038427	201.7414	-1.87981	0.811981	0.020608	0.999413
ENSG00000008394	21.2693	-0.99531	0.430149	0.020675	0.999413
ENSG00000159788	4.802759	-1.71634	0.742091	0.020731	0.999413
ENSG00000249992	944.9157	-0.56509	0.244428	0.020785	0.999413
ENSG00000239559	4.090029	-1.37124	0.595594	0.021318	0.999413
ENSG00000136521	80.83214	-0.54416	0.236468	0.021381	0.999413
ENSG00000025708	131.572	-0.7936	0.345721	0.021704	0.999413
ENSG00000183784	13.06948	-1.5573	0.678712	0.021762	0.999413
ENSG00000236682	3.698504	-1.45153	0.636103	0.022495	0.999413

ENSG00000119328	47.85939	-0.44443	0.195097	0.022726	0.999413
ENSG00000007237	31.29858	-1.03838	0.456594	0.022955	0.999413
ENSG00000182022	37.16339	-1.31282	0.577825	0.023087	0.999413
ENSG00000249502	1.211643	-2.97547	1.310845	0.023215	0.999413
ENSG00000257878	4.614976	-1.96034	0.863835	0.023247	0.999413
ENSG00000149591	4.989497	-1.52857	0.674708	0.02348	0.999413
ENSG00000110944	2.265549	-2.08719	0.921529	0.023518	0.999413
ENSG00000123213	18.94434	-0.9805	0.43327	0.023634	0.999413
ENSG00000186047	1.716118	-2.34712	1.038803	0.023856	0.999413
ENSG00000160753	18.69081	-0.84953	0.376739	0.024136	0.999413
ENSG00000197629	181.4113	-1.3839	0.614071	0.024218	0.999413
ENSG00000110721	8.167921	-1.14909	0.50988	0.024218	0.999413
ENSG00000163607	12.98263	-0.93149	0.413522	0.024285	0.999413
ENSG00000274021	50.63872	-0.68491	0.304761	0.024617	0.999413
ENSG00000185262	22.51558	-0.62697	0.279746	0.025012	0.999413
ENSG00000100092	5.31867	-1.42556	0.636452	0.0251	0.999413
ENSG00000272273	6.737579	-1.52997	0.684712	0.025452	0.999413

ENSG00000161381	3.539373	-2.10235	0.943552	0.025872	0.999413
ENSG00000112715	3.049748	-2.63759	1.184039	0.025906	0.999413
ENSG00000248429	3.806561	-2.11295	0.948715	0.025936	0.999413
ENSG00000165637	197.8067	-0.28135	0.126566	0.026222	0.999413
ENSG00000211959	2.610576	-1.81959	0.81927	0.026352	0.999413
ENSG00000102030	20.28699	-0.66097	0.297855	0.026479	0.999413
ENSG00000177380	4.447324	-1.4032	0.633733	0.026816	0.999413
ENSG00000274767	38.03798	-0.8728	0.394563	0.026962	0.999413
ENSG00000136928	3.288921	-1.26502	0.57218	0.027044	0.999413
ENSG00000203804	2.580107	-2.36141	1.070051	0.027326	0.999413
ENSG00000240498	1.29108	-2.31373	1.048652	0.027357	0.999413
ENSG00000231160	48.60975	-0.39683	0.179931	0.027424	0.999413
ENSG00000273382	3.890324	-1.35604	0.615064	0.027474	0.999413
ENSG00000271380	12.76997	-0.80726	0.366523	0.027631	0.999413
ENSG00000235008	8.651984	-0.8961	0.407273	0.02779	0.999413
ENSG00000130368	2.059256	-2.04466	0.929944	0.0279	0.999413
ENSG00000270734	9.485878	-1.1069	0.503964	0.028065	0.999413

ENSG00000143382	4.924819	-1.96205	0.894324	0.028243	0.999413
ENSG00000214787	1.76257	-2.74447	1.251819	0.028352	0.999413
ENSG00000120705	75.61504	-0.47854	0.218439	0.02847	0.999413
ENSG00000138613	65.00203	-0.53369	0.243621	0.028476	0.999413
ENSG00000259352	10.77272	-1.26453	0.5786	0.028852	0.999413
ENSG00000105967	20.19944	-1.22236	0.559985	0.029048	0.999413
ENSG00000196562	42.35119	-1.21804	0.558431	0.02917	0.999413
ENSG00000140044	11.92253	-1.2745	0.584333	0.029174	0.999413
ENSG00000238113	5.201933	-1.3743	0.630187	0.029199	0.999413
ENSG00000181322	3.513695	-1.13311	0.51978	0.029259	0.999413
ENSG00000198876	338.0879	-0.5181	0.238006	0.029493	0.999413
ENSG00000245532	456.2676	-0.4527	0.207973	0.029501	0.999413
ENSG00000187097	87.33357	-0.5125	0.235691	0.02967	0.999413
ENSG00000085265	280.3449	-1.51761	0.698506	0.029806	0.999413
ENSG00000146070	19.44089	-1.03032	0.474579	0.029929	0.999413
ENSG00000166170	78.41687	-0.4065	0.187426	0.030094	0.999413
ENSG00000005187	31.36097	-0.78464	0.363268	0.030776	0.999413

ENSG00000260908	5.523458	-1.3245	0.613338	0.030812	0.999413
ENSG00000152749	65.70116	-0.52269	0.242201	0.030923	0.999413
ENSG00000249437	6.454065	-1.99448	0.924471	0.030972	0.999413
ENSG00000250848	1.399915	-2.14001	0.992221	0.031022	0.999413
ENSG00000173548	1.850724	-2.12797	0.986783	0.031046	0.999413
ENSG00000030110	39.60832	-0.47918	0.222541	0.0313	0.999413
ENSG00000205269	51.49809	-0.87963	0.408779	0.031409	0.999413
ENSG00000234036	1.232023	-1.77613	0.827302	0.031802	0.999413
ENSG00000119321	89.58582	-0.83073	0.387255	0.03194	0.999413
ENSG00000104918	1.176385	-2.5453	1.186567	0.031945	0.999413
ENSG00000120833	55.47333	-0.5572	0.259765	0.031952	0.999413
ENSG00000121316	81.54378	-1.67499	0.781997	0.032199	0.999413
ENSG00000214654	7.518945	-0.96203	0.449307	0.032263	0.999413
ENSG00000167637	3.532681	-1.78175	0.833072	0.032454	0.999413
ENSG00000163464	26.89689	-1.40231	0.656568	0.032694	0.999413
ENSG00000276384	3.370656	-1.42219	0.666086	0.03275	0.999413
ENSG00000247699	1.284674	-2.00319	0.939022	0.032902	0.999413

ENSG00000179094	10.75692	-1.12365	0.528298	0.033426	0.999413
ENSG00000131042	62.78901	-1.3215	0.622076	0.033642	0.999413
ENSG00000023191	171.0636	-0.29225	0.137619	0.033702	0.999413
ENSG00000027697	301.4314	-0.46934	0.221254	0.033899	0.999413
ENSG00000268996	7.438141	-0.95576	0.451402	0.034234	0.999413
ENSG00000249263	1.332288	-2.38104	1.126041	0.034471	0.999413
ENSG00000197766	21.4822	-1.71037	0.809703	0.034657	0.999413
ENSG00000240563	3.311794	-2.03832	0.965012	0.034668	0.999413
ENSG00000010295	23.06113	-1.18931	0.563443	0.034791	0.999413
ENSG00000114268	10.37194	-1.3513	0.640451	0.034865	0.999413
ENSG00000249087	3.434328	-1.24237	0.589607	0.035107	0.999413
ENSG00000139531	4.910126	-1.3203	0.626599	0.03511	0.999413
ENSG00000272277	3.827664	-1.49159	0.707894	0.035111	0.999413
ENSG00000112761	1.757982	-2.01572	0.956942	0.035168	0.999413
ENSG00000204054	50.71251	-0.42893	0.2041	0.035589	0.999413
ENSG00000100292	73.77004	-0.75398	0.35884	0.035626	0.999413
ENSG00000006756	3.545258	-1.9142	0.911101	0.035643	0.999413

ENSG00000255987	2.077711	-2.1766	1.036164	0.035673	0.999413
ENSG00000144339	1.469252	-2.11344	1.006808	0.035804	0.999413
ENSG00000133142	48.44975	-0.43328	0.206643	0.036015	0.999413
ENSG00000135740	4.542518	-1.06807	0.510408	0.036386	0.999413
ENSG00000129480	6.223013	-1.41108	0.675507	0.036715	0.999413
ENSG00000264578	16.69475	-0.64818	0.311645	0.037538	0.999413
ENSG00000179820	74.67067	-1.02828	0.494404	0.037541	0.999413
ENSG00000004799	41.92639	-0.99379	0.479148	0.038073	0.999413
ENSG00000166947	8.232301	-1.46064	0.704447	0.03813	0.999413
ENSG00000182197	10.86902	-1.02	0.49199	0.038153	0.999413
ENSG00000256263	32.65023	-0.78296	0.379936	0.039325	0.999413
ENSG00000114859	1.536298	-1.89188	0.918653	0.039455	0.999413
ENSG00000139318	197.8579	-0.74634	0.362516	0.039515	0.999413
ENSG00000169951	4.00902	-1.30313	0.633203	0.039591	0.999413
ENSG00000164054	295.4023	-0.38379	0.186493	0.039598	0.999413
ENSG00000116221	78.73015	-0.61471	0.29892	0.03974	0.999413
ENSG00000130821	3.567353	-1.93731	0.942463	0.039823	0.999413

ENSG00000049249	2.159653	-1.94963	0.948989	0.039935	0.999413
ENSG00000254236	4.308729	-1.36533	0.665075	0.040082	0.999413
ENSG00000243335	35.34929	-0.7304	0.35618	0.040301	0.999413
ENSG00000151116	43.42442	-0.62394	0.304446	0.040421	0.999413
ENSG00000122218	474.0196	-0.19257	0.094041	0.040588	0.999413
ENSG00000131759	25.23727	-0.75401	0.369111	0.041076	0.999413
ENSG00000254415	12.76896	-1.66247	0.814643	0.041278	0.999413
ENSG00000136098	5.522857	-1.35661	0.66533	0.041449	0.999413
ENSG00000162599	14.00446	-0.98882	0.485013	0.041474	0.999413
ENSG00000272434	1.881357	-2.06023	1.012237	0.041818	0.999413
ENSG00000261423	4.227816	-1.14985	0.565869	0.042152	0.999413
ENSG00000084234	196.9798	-0.85185	0.419664	0.042373	0.999413
ENSG00000278396	1.37763	-2.10637	1.038118	0.042455	0.999413
ENSG00000141279	224.2569	-0.2299	0.113739	0.043247	0.999413
ENSG00000248668	1.190678	-2.35657	1.167117	0.043473	0.999413
ENSG00000134072	33.11042	-0.59731	0.296036	0.043623	0.999413
ENSG00000123684	123.422	-0.55811	0.276663	0.043665	0.999413

ENSG00000134531	1.282515	-3.57273	1.771481	0.043716	0.999413
ENSG00000204482	181.8401	-0.58504	0.290186	0.04379	0.999413
ENSG00000255108	20.20953	-0.63144	0.313392	0.043921	0.999413
ENSG00000028839	302.2962	-0.37328	0.185981	0.044742	0.999413
ENSG00000138166	10.02642	-0.94371	0.470296	0.044789	0.999413
ENSG00000160932	102.6326	-0.86054	0.428909	0.04482	0.999413
ENSG00000167768	8.719783	-1.52293	0.759298	0.044887	0.999413
ENSG00000110318	5.45991	-1.39895	0.697526	0.0449	0.999413
ENSG00000066117	10.4374	-1.02057	0.509344	0.045102	0.999413
ENSG00000214212	13.7484	-1.31245	0.65512	0.045138	0.999413
ENSG00000268355	1.485407	-1.75028	0.873672	0.045138	0.999413
ENSG00000010361	15.87539	-0.63843	0.318986	0.045345	0.999413
ENSG00000255491	1.496534	-2.39035	1.194316	0.045345	0.999413
ENSG00000198189	91.14426	-0.65891	0.329314	0.04541	0.999413
ENSG00000258798	1.654488	-1.99689	0.999603	0.045751	0.999413
ENSG00000167703	22.28764	-1.37746	0.689585	0.045769	0.999413
ENSG00000111275	58.50388	-0.7518	0.376721	0.045972	0.999413

ENSG00000165168	267.604	-0.71156	0.357409	0.046493	0.999413
ENSG00000101220	39.1856	-0.60836	0.30566	0.046556	0.999413
ENSG00000144935	1.842775	-1.92358	0.966477	0.046558	0.999413
ENSG00000075223	4.121616	-2.08251	1.047232	0.046747	0.999413
ENSG00000002933	10.09975	-1.51513	0.762163	0.046819	0.999413
ENSG00000198223	21.80049	-1.39656	0.702825	0.046915	0.999413
ENSG00000111666	65.82214	-0.74747	0.376215	0.046943	0.999413
ENSG00000284951	1.378235	-2.75573	1.387067	0.046952	0.999413
ENSG00000105520	9.579815	-1.3981	0.704128	0.047081	0.999413
ENSG00000124523	15.96619	-0.70529	0.35573	0.047407	0.999413
ENSG00000071967	34.35257	-0.91682	0.462522	0.047455	0.999413
ENSG00000166211	1.061685	-3.10476	1.569024	0.047841	0.999413
ENSG00000065833	95.30545	-0.73416	0.371424	0.048087	0.999413
ENSG00000110077	142.3978	-1.31854	0.66715	0.048113	0.999413
ENSG00000135677	140.1781	-0.78762	0.398851	0.048301	0.999413
ENSG00000233578	1.111388	-2.8506	1.444576	0.04846	0.999413
ENSG00000062716	205.1088	-0.70647	0.358198	0.048578	0.999413

ENSG00000122644	21.8197	-0.89197	0.452402	0.048652	0.999413
ENSG00000142089	494.8122	-0.66024	0.335125	0.048824	0.999413
ENSG00000116514	35.86672	-0.56638	0.28774	0.049024	0.999413
ENSG00000140406	10.90472	-0.74913	0.38097	0.049257	0.999413
ENSG00000082146	292.8046	-0.35301	0.179696	0.049472	0.999413
ENSG00000256576	1.817212	-1.95128	0.993729	0.049577	0.999413
ENSG00000226706	5.365526	-1.08897	0.554973	0.049739	0.999413
ENSG00000235082	1.442301	-2.00504	1.022317	0.049848	0.999413
ENSG00000171425	6.416329	-0.82458	0.420475	0.049871	0.999413

The 'log2foldchange' indicates the fold change in gene expression between the two groups, calculated as the log2 ratio of the basemean in the PCa group relative to the control group. A positive log2foldchange signifies upregulation (increased expression in the cancer group), while a negative log2foldchange indicates downregulation. The 'basemean' signifies the mean of normalized counts for a particular gene across all the samples in the dataset, representing an average level of gene expression. This combines information from both the PCa and control groups. lfcSe: lfcSe stands for "Internal Sample-wise Coefficient of Variation Standard Error." The 'lfcSE' provides an estimate of the reliability of the log2foldchange for a specific gene, with a lower value indicating increased reliability. The 'p-value adjust' refers to the adjustment of raw p-values to account for multiple hypothesis testing, using methods such as the Benjamini-Hochberg or to adjust for false discovery rate (FDR). Padj: P value adjust.

Table 29. Details of the cases in the validation cohort (206 PCa and 77 non-cancer cases) for differentially expressed miRNA between PCa and non-cancer.

PCa (n=208)			Non-Cancer (n=77)
PPPP044	GPB114	pppp154	B01P0243B
PPPP049	GPB135	pppp157	B01P0537B
PPPP050	GPB149	pppp164	B01P0573
PPPP052	GPB175	pppp168	B01p0603A
PPPP055	GPB178	pppp171	B01P0622A
PPPP057	GPB203	pppp174	B01P0636A
PPPP058	GPB230	pppp175	B01P0659A
PPPP059	GPB231	pppp176	GPB218
PPPP060	GPB260	pppp177	GPB258
PPPP070	pppp020	pppp178	ICBC004
PPPP079	pppp023	pppp181	ICBC005
PPPP087	pppp033	pppp183	pppp017
PPPP089	pppp034	pppp184	pppp049
PPPP097	pppp035	pppp185	pppp105
PPPP114	pppp038	pppp186	pppp139
PPPP128	pppp039	pppp216	pppp212
PPPP130	pppp043	pppp223	pppp219
PPPP132	pppp045	pppp224	pppp257
PPPP135	pppp047	pppp225	pppp267
PPPP136	pppp051	pppp226	pppp272
PPPP137	pppp053	pppp227	pppp279
PPPP138	pppp056	pppp228	pppp280
PPPP140	pppp061	pppp229	pppp282
PPPP144	pppp063	pppp230	pppp283

PPPP146	pppp064	pppp240	pppp292
PPPP149	pppp065	pppp244	pppp294
PPPP150	pppp066	pppp246	pppp296
PPPP151	pppp067	pppp248	pppp299
PPPP154	pppp073	pppp249	pppp305
PPPP156	pppp074	pppp250	pppp306
PPPP159	pppp077	pppp252	pppp308
PPPP160	pppp081	pppp254	pppp310
PPPP161	pppp082	pppp256	pppp312
PPPP163	pppp083	pppp263	pppp316
PPPP165	pppp090	pppp264	pppp320
PPPP166	pppp091	pppp265	pppp326
PPPP167	pppp093	pppp268	pppp328
PPPP169	pppp096	pppp269	pppp329
PPPP170	pppp098	pppp270	pppp330
PPPP173	pppp100	pppp271	pppp331
PPPP179	pppp101	pppp274	pppp332
PPPP180	pppp102	pppp278	pppp338
PPPP182	pppp103	pppp281	pppp340
PPPP189	pppp104	pppp286	pppp341
PPPP191	pppp106	pppp287	pppp342
PPPP192	pppp107	pppp289	pppp343
PPPP193	pppp108	pppp290	pppp346
PPPP194	pppp110	pppp291	pppp350
PPPP196	pppp112	pppp293	pppp355
PPPP197	pppp113	pppp295	pppp361
PPPP199	pppp115	pppp297	1064

PPPP200	pppp116	pppp298	1065
PPPP201	pppp117	pppp301	1066
PPPP202	pppp120	pppp307	1067
PPPP203	pppp121	pppp309	1069
PPPP204	pppp122	pppp311	1070
PPPP205	pppp123	pppp314	1073
PPPP206	pppp124	pppp315	1074
PPPP207	pppp126	pppp317	1047A
PPPP208	pppp127	pppp321	1049A
PPPP209	pppp129	pppp323	1050A
PPPP210	pppp131	pppp324	CT01
PPPP213	pppp134	pppp325	CT28
PPPP215	pppp142	pppp333	CT29
PPPP217	pppp147	pppp337	CT30
PPPP218	pppp148	pppp344	PPPP036
PPPP220	pppp152	pppp347	PPPP046
PPPP222	pppp154	pppp348	PPPP048
		pppp351	PPPP068
		pppp352	PPPP069
		pppp353	PPPP088
		pppp356	PPPP092
			PPPP143
			PPPP162
			PPPP211
			PPPP259
			PPPP262

PCa: prostate cancer.

Table 30. Differential expressions in platelet mRNAs between aggressive and latent PCa patients by internal control gene miR23, miR548, U6 and UniSP6.

control probes	Highly expressed in latent PCa	*P* value	Highly expressed in aggressive PCa	*P* value
miR23	miR190	0.004	miR1306	0.047
			miR28	0.02535
			miR548	0.0449
miR548			Let7a	0.0106
			miR1306	0.0332
			miR191	0.0405
			miR195	0.0041
			miR23	0.0453
			miR28	0.0061
			miR342	0.008
			miR370	0.0183
			miR380	0.0385
			miR532	0.0266
			miR627	0.0441
			miR652	0.0386
			miR664	0.0261
			miR744	0.0164
U6*	-			
UniSP6	N/A		N/A	

The results from U6 were discarded due to its unstable expression in both groups (p=0.01) which may cause false-positive results. The results from U6 group were labelled as '-'. There is no differentially expressed miRNA found in the group of UnisSP6 (NA).

Results of white blood cell contamination in platelet sample from 2-step centrifugation

From 06/10/2016 to 07/01/2021, 40 platelet samples were collected by other group members and me for further RNA extraction and sequencing. The details of samples and the results of WBC contamination were shown in Table 31. The study revealed an average of 12-26 WBCs per one million platelets in the RNA sequencing samples collected for this project. Out of the 40 cases examined, 25 did not show any evidence of WBC contamination due to the absence of WBC checks during platelet collection. Due to the limited quantity and quality of the provided platelet RNAs, we selected samples without WBC contamination to meet the requirements for RNA sequencing.

Table 31. The results of WBC contamination in the 40 cases for platelet RNA sequencing.

ID	WBC count under a microscope	WBC contamination rate
PPPP017	N/A	N/A
PPPP047	N/A	N/A
PPPP049	N/A	N/A
PPPP053	N/A	N/A
PPPP056	N/A	N/A
PPPP063	N/A	N/A
PPPP067	N/A	N/A
PPPP074	N/A	N/A
PPPP122	N/A	N/A
PPPP123	N/A	N/A
PPPP127	N/A	N/A
PPPP139	N/A	N/A
PPPP141	N/A	N/A
PPPP153	N/A	N/A
PPPP156	N/A	N/A
PPPP164	N/A	N/A
PPPP170	N/A	N/A
PPPP178	N/A	N/A
PPPP216	N/A	N/A
PPPP257	N/A	N/A
PPPP267	N/A	N/A
PPPP272	N/A	N/A

PPPP278	N/A	N/A
PPPP279	N/A	N/A
PPPP294	N/A	N/A
PPPP308	0	0
PPPP310	51-100	28-56
PPPP316	21-50	11-28
PPPP329	11-20	6-11
PPPP338	11-20	6-11
PPPP341	51-100	28-56
PPPP342	21-50	11-28
PPPP343	11-20	6-11
PPPP344	21-50	11-28
PPPP347	21-50	11-28
PPPP348	11-20	6-11
PPPP350	51-100	28-56
PPPP355	11-20	6-11
PPPP356	1-10	1-6
PPPP361	51-100	28-56
average		12-26

The WBC contamination rate was shown as WBCs per one million platelets. WBC: white blood cell, N/A: not available.

Table 32. Results of the 47 cases' platelet count and platelet recovery (%) per 0.5ml by the two-step centrifugation.

	ID	Platelet count	Platelet recovery (%)
1	PPPP415	1575000	1.1
2	PPPP416	6362500	4.2
3	PPPP417	2505000	1.7
4	PPPP418	2325000	1.6
5	PPPP419	325000	0.2
6	CPM1 008	3377500	2.3
7	CPM1 009	2480000	1.7
8	CPM1 010	1890000	1.3
9	CPM1 011	2175000	1.5
10	CPM1 012	16950000	11.3
11	PPPP420	3725000	2.5
12	CPM1 014	7675000	5.1
13	CPM1 015	5525000	3.7
14	CPM1 016	8275000	5.5
15	PPPP440	5566667	3.7
16	PPPP441	7400000	4.9
17	PPPP442	3200000	2.1
18	PPPP443	9366667	6.2
19	PPPP444	9600000	6.4
20	PPPP445	15700000	10.5
21	PPPP446	1596667	1.1
22	PPPP447	556667	0.4
23	PPPP448	1480000	1.0

24	CPM1 065	1263333	0.8
25	CPM1 066	2233333	1.5
26	CPM1 067	1090000	0.7
27	CPM1 071	2665000	1.8
28	CPM1 073	1420000	1.0
29	CPM1 028	1190000	0.8
30	CPM1 076	1330000	0.9
31	CPM1 077	2213333	1.5
32	CPM1 019	1613333	1.1
33	CPM1 011	4100000	2.7
34	PPPP433	6833333	4.6
35	CPM1 055	430000	0.3
36	CPM1 059	1220000	0.8
37	CPM1 060	3333333	2.2
38	CPM1 050	2936667	2.0
39	CPM1 049	3920000	2.6
40	CPM1 048	833333.3	0.6
41	CPM1 047	6033333	4.0
42	CPM1 046	750000	0.5
43	PPPP437	31333333	20.9
44	PPPP438	1.89E+08	126
45	PPPP439	1.17E+08	78
46	CPM1-062	68333333	45.6
47	CPM1-065	15700000	10.5
average		12476738	8.3

The average platelet recovery of the 2-step centrifugation is 8.32% as well as 12476738 platelets collected per 0.5 ml. CPM1 011 and CPM1 065 were used twice due to abundance.